

August 3, 2007 1:53 am

Release
4.1.1



Tutorials Manual

CHEMKIN[®] Software

RD0411-C20-000-001
July 2007

Licensing:

For licensing information, please contact Reaction Design at (858) 550-1920 (USA) or licensing@ReactionDesign.com.

Technical Support:

Reaction Design provides an allotment of technical support to its Licensees free of charge. To request technical support, please include your license number along with input or output files, and any error messages pertaining to your question or problem. Requests may be directed in the following manner: E-mail: support@ReactionDesign.com, Fax: (858) 550-1925, Phone: (858) 550-1920.

Additional technical support hours may also be purchased. Please contact Reaction Design for the hourly rates.

Copyright:

Copyright© 2007 Reaction Design. All rights reserved. No part of this book may be reproduced in any form or by any means without express written permission from Reaction Design.

Trademark:

CHEMKIN® and REACTION DESIGN® are registered trademarks of Reaction Design in the United States and other countries.

AURORA, CONP, CRESLAF, EQUIL, EQUILIB, KINetics, MODEL FUELS CONSORTIUM, OPPDIF, OVEND, PARAMETER STUDY FACILITY, PARTICLE TRACKING MODULE, PASR, PLUG, PREMIX, SENKIN, SHOCK, SPIN, SURFACE CHEMKIN, SURFTHERM, TRANSPORT, TWAFFER, TWOPNT are all trademarks of Reaction Design or Sandia National Laboratories. All other trademarks are the property of their respective holders.

Limitation of Warranty:

The software is provided "as is" by Reaction Design, without warranty of any kind including, without limitation, any warranty against infringement of third party property rights, fitness or merchantability, or fitness for a particular purpose, even if Reaction Design has been informed of such purpose. Furthermore, Reaction Design does not warrant, guarantee, or make any representations regarding the use or the results of the use, of the software or documentation in terms of correctness, accuracy, reliability or otherwise. No agent of Reaction Design is authorized to alter or exceed the warranty obligations of Reaction Design as set forth herein. Any liability of Reaction Design, its officers, agents or employees with respect to the software or the performance thereof under any warranty, contract, negligence, strict liability, vicarious liability or other theory will be limited exclusively to product replacement or, if replacement is inadequate as a remedy or in Reaction Design's opinion impractical, to a credit of amounts paid to Reaction Design for the license of the software.

Literature Citation for CHEMKIN:

CHEMKIN 4.1.1 should be cited as:

R. J. Kee, F. M. Rupley, J. A. Miller, M. E. Coltrin, J. F. Grcar, E. Meeks, H. K. Moffat, A. E. Lutz, G. Dixon-Lewis, M. D. Smooke, J. Warnatz, G. H. Evans, R. S. Larson, R. E. Mitchell, L. R. Petzold, W. C. Reynolds, M. Caracotsios, W. E. Stewart, P. Glarborg, C. Wang, C. L. McLellan, O. Adigun, W. G. Houf, C. P. Chou, S. F. Miller, P. Ho, P. D. Young, D. J. Young, D. W. Hodgson, M. V. Petrova, and K. V. Pudukkham, CHEMKIN Release 4.1.1, Reaction Design, San Diego, CA (2007).

Table of Contents

1	Introduction.....	13
2	Combustion in Gas-phase Processes.....	17
2.1	Equilibrium	17
2.1.1	Adiabatic Flame Temperature	17
2.2	Using Equivalence Ratio.....	18
2.2.1	Example: Propane in Air.....	19
2.2.2	Example: Stoichiometric Products	21
2.3	Ignition, Flames and Flammability.....	22
2.3.1	Steady-state Gas-phase Combustion	22
2.3.2	Autoignition for H_2 /Air	24
2.3.3	Ignition-delay Times for Propane Autoignition	27
2.3.4	Burner-stabilized Flame.....	32
2.3.5	Flame Speed of Stoichiometric Methane/Air Premixed Flame	36
2.3.6	Parameter Study: Varying Equivalence Ratio of Propane/Air Flame.....	39
2.3.7	Hydrogen/Air Flame	46
2.4	Internal Combustion Engine.....	49
2.4.1	Homogeneous Charge Compression Ignition (HCCI) Engine.....	49
2.5	Simulating a Shock-tube Experiment	55
2.5.1	Shock-heated Air (Shock)	55
2.6	Combustion in Complex Flows	57
2.6.1	Gas Turbine Network.....	57
2.6.2	Jet Flame Network	60
2.6.3	Partially Stirred Reactor for Methane/Air	64
2.6.4	Side Inlet on a Plug Flow Reactor	69
2.6.5	Co-flowing Non-premixed CH_4 /Air Flame.....	72
2.7	Particle Tracking Module	78
2.7.1	Soot Formation and Growth in a JSR/PFR Reactor	78
2.8	Chemistry Sets.....	85
2.8.1	Hydrogen/Air	85
2.8.2	Methane/Air	86
2.8.3	NO_x and CH_4 , C_2H_4 , C_2H_6 , C_3H_6 , and C_3H_8	87
2.8.4	Propane/Air.....	87
2.8.5	Ethylene/Air Combustion and Soot Formation and Growth.....	87
3	Catalytic Processes	91
3.1	Catalytic Combustors, Converters and Aftertreatment	91
3.1.1	Two-Stage Catalytic Combustor	91

3.1.2	<i>Engine Exhaust Aftertreatment with a Transient Inlet Flow</i>	101
3.2	Parameter Studies.....	108
3.2.1	<i>Parameter Study Facility for Surface Chemistry Analysis</i>	108
3.3	Chemistry Sets.....	112
3.3.1	<i>Methane Oxidation on Pt</i>	112
3.3.2	<i>Pt/Rh Three-way Catalyst</i>	113
4	Materials Problems.....	115
4.1	Chemical Vapor Deposition.....	115
4.1.1	<i>Equilibrium Analysis of Chlorosilane CVD</i>	116
4.1.2	<i>PSR Analysis of Steady-state Thermal CVD</i>	118
4.1.3	<i>Approximations for a Cylindrical Channel Flow</i>	122
4.1.4	<i>Deposition in a Rotating Disk Reactor</i>	126
4.1.5	<i>Trichlorosilane CVD in Planar Channel Flow Reactor</i>	131
4.2	Atomic Layer Deposition (ALD).....	134
4.2.1	<i>Time-dependent Simulations of ALD Process</i>	135
4.3	Plasma Etching.....	141
4.3.1	<i>Steady-state Chlorine Plasma</i>	141
4.3.2	<i>Spacial Chlorine Plasma PFR with Power Profile</i>	145
4.3.3	<i>Fluorocarbon Plasma Etching of Silicon Dioxide</i>	149
4.4	Chemistry Sets.....	154
4.4.1	<i>Silicon Nitride CVD from Silicon Tetrafluoride and Ammonia</i>	154
4.4.2	<i>Silicon Deposition from Silane</i>	155
4.4.3	<i>Silicon Deposition from Trichlorosilane</i>	155
4.4.4	<i>Alumina ALD</i>	156
4.4.5	<i>Chlorine Plasma</i>	158
4.4.6	<i>Fluorocarbon Plasma with SiO₂ Etch Products</i>	159
5	Chemical Mechanism Analysis.....	161
5.1	Mechanism Analyzer.....	161
5.1.1	<i>Background Information</i>	162
5.1.2	<i>Reaction Mechanism for Diamond CVD</i>	164
	Index.....	177

List of Tables

1-1	Reactor Models Used in Sample Problems.....	14
2-1	Reactant Mole Fractions Sum to 1.0.....	19
2-2	Relative Moles Normalized So Mole Fractions Sum to 1.0.....	19
2-3	N ₂ as Added Diluent	20
2-4	N ₂ as Component of Oxidizer	20
2-5	Determining Stoichiometric Products	21
2-6	Initial Temperatures and Ignition Times	30
2-7	Test Engine Specifications.....	50
2-8	Composition of Initial Gas Mixture.....	51
2-9	Components in Fuel and Oxidizer Streams.....	70
2-10	Properties of the Co-flowing Jets	73
3-1	Excerpt of Data Representing Engine-out Test Measurements.....	103

List of Figures

2-1	Adiabatic Flame Temperatures—Hydrogen/Air Mixture.....	18
2-2	Steady-state Gas-phase Combustion—Hydrogen/Air Temperatures	23
2-3	Steady-state Gas-phase Combustion—Molar Conversions	24
2-4	Autoignition for Hydrogen/Air—Temperature Profile	26
2-5	Autoignition for Hydrogen/Air—Mole Fractions	26
2-6	Autoignition for Hydrogen/Air—Sensitivity Coefficients.....	27
2-7	Temperature and OH Mole Fraction Profiles as a Function of Time.....	30
2-8	Example of Doubled Temperature Inflection and OH Concentration Peak.....	31
2-9	Ignition Based on Varying Criteria.....	31
2-10	Ignition Times vs. Inverse of Temperature (Semi-log)	32
2-11	Burner-stabilized Flame—Experimental Gas Temperature Profile	35
2-12	Burner-stabilized Flame—Mole Fractions	35
2-13	Flame Speed—Temperature Profile Panel	36
2-14	C1_ Flame Speed—Reactor Physical Property	37
2-15	Flame Speed—Axial Velocity vs. Distance	39
2-16	Flame Speed—Temperature vs. Distance	39
2-17	Panel for Setup of Parameter Studies.....	41
2-18	Parameter Shown in Blue After Parameter Setup is Complete.....	42
2-19	Parameter Study Run.....	43
2-20	Post-Processor Options after Running Parameter Studies	44
2-21	Flame Speed Calculated Values as a Function of Equivalence Ratio	45

2-22	Final Temperature as a Function of Equivalence Ratio	46
2-23	Hydrogen/Air Flame—Temperature vs. Axial Distance.....	48
2-24	Hydrogen/Air Flame—Mole Fractions	48
2-25	Hydrogen/Air Flame—Temperature Sensitivity to Reaction Rates	49
2-26	Hydrogen/Air Flame—Temperature Sensitivity to Heats of Formation	49
2-27	IC Engine Icon.....	50
2-28	C1_ IC Engine—Reactor Physical Property for HCCI Woschni Heat Loss model.....	52
2-29	HCCI Engine—EGR Temperature Comparison.....	53
2-30	HCCI Engine—EGR Pressure Comparison	54
2-31	HCCI Engine—EGR Heat Loss Comparison	55
2-32	Nitrogen Atom Reaction in CHEMKIN Format	56
2-33	Shock Tube Experiment—NO Mole Fraction	57
2-34	Gas Turbine Network—Schematic	58
2-35	Gas Turbine Network—Diagram View	58
2-36	Gas Turbine Network—Temperature Comparisons	59
2-37	Gas Turbine Network—CO and NO Comparisons	59
2-38	Jet Flame Network—Diagram View	61
2-39	Jet Flame Network—Temperature Distribution	62
2-40	Jet Flame Network—CO Distribution	63
2-41	Jet Flame Network—NO Distribution	64
2-42	Jet Flame Network—Mole Fractions	64
2-43	PaSR Methane/Air—Temperature Comparison.....	67
2-44	PaSR Methane/Air—Temperature Variance Comparison.....	68
2-45	PaSR Methane/Air—CO Comparison	68
2-46	PaSR Methane/Air—Select the Import File Format.....	69
2-47	PaSR Methane/Air—PDF(T) Comparison.....	69
2-48	Illustration of the System to be Modeled.....	70
2-49	Total Flow Growing Directly as a Result of Side Inlet Flow.....	71

2-50	Peaking of NO Concentration Dependent on Temperature in a PFR with an Approximated Mixing Region.	72
2-51	Confined Co-flowing Annular Jet Configuration.	73
2-52	Preferences Panel Showing the Display User Routine Options Is Enabled.....	74
2-53	Get Initial Solution Profile from User Routine Check box.....	75
2-54	Visualization of Full Computational Domain Can Be Acquired by Selecting Proper Reflect Contour Data Option in the Chemkin Post-Processor Panel.	76
2-55	Contour Plot Window Showing the Pull-down List Selections of the Insert Menu.....	77
2-56	Colorbar Property Panel.....	77
2-57	Final 3-D Temperature Contours of the Entire Physical Domain with Vertical Contour Legend (Colorbar).....	78
2-58	A schematic of the JSR/PFR reactor configuration used by Marr ²³	79
2-59	Diagram View of the CHEMKIN 4.1 Project Used to Simulate the JSR/PFR Experiment	80
2-60	Specifying Particle Tracking Module Parameters and Initial Conditions of Particle Size Moments in the Reactor	80
2-61	Surface Area Fraction of the Particle Material Must Be Set to Zero in the Material-specific Data Tab. The Default Value of Surface Area Fraction Is One.	81
2-62	Dispersed Phase Tab for Specifying Particle Size Moments in Inlet Streams	81
2-63	Tolerances for Particle Size Moments Can Be Given Explicitly in the Solver Window	81
2-64	Comparisons of Mole Fraction Profiles of Selected Gas Phase Species Inside the PFR for the 1630K and F = 2.2 Case of the C ₂ H ₄ /O ₂ /N ₂ JSR/PFR Experiment by Marr ²³ . Symbols: data; Solid lines: predictions with HACA and PAH condensation growth mechanisms	83
2-65	Comparisons of Soot Mass Concentration Profiles Inside the PFR for the 1630K and F = 2.2 Case of the C ₂ H ₄ /O ₂ /N ₂ JSR/PFR Experiment by Marr ²³ . Symbols: data; Solid line: prediction with both HACA and PAH condensation growth mechanisms; Dash-dot line: prediction with HACA growth mechanism only	84
2-66	Comparison of Contributions of Different Soot Mass Growth Mechanisms by Using the Rate-Of-Production Analysis... 84	
2-67	The Particle Diameter Evolution Inside the PFR Predicted by the Present Soot Module for the 1630K and F = 2.2 case of the C ₂ H ₄ /O ₂ /N ₂ JSR/PFR Experiment by Marr ²³ (see p. 78)	85
3-1	Turbine Flow Capacity.....	92
3-2	Two-Stage Catalytic Combustor—Diagram View	95
3-3	Catalytic Pre-combustor (C1_)—Honeycomb Monolith, Catalyst sub-tab	95
3-4	Catalytic Pre-combustor (C1_)—Honeycomb Monolith, Honeycomb sub-tab	96
3-5	Homogeneous Stage Combustor (C3_)—Reactor Physical Property	96
3-6	Two Stage Catalytic Combustor—Excess_Air_Dilution (Cluster 4) Output Results	97

3-7	Two Stage Catalytic Combustor—Temperature Comparison	98
3-8	Two Stage Catalytic Combustor—Pressure Comparison	99
3-9	Two Stage Catalytic Combustor—CH ₄ Comparison	99
3-10	Two Stage Catalytic Combustor—CO Comparison	100
3-11	Two Stage Catalytic Combustor—NO Comparison	100
3-12	Sample USRINLET Subroutine for User-Defined Transient Inlet Conditions.....	104
3-13	Engine Exhaust Aftertreatment—Molar Conversion Rates	107
3-14	Engine Exhaust Aftertreatment—Mole Fractions	107
3-15	Engine Exhaust Aftertreatment—Gas Temperatures.....	108
3-16	Setting Up a Parameter Study for Sticking Coefficients vs. Predicted Temperature Profiles	110
3-17	Varying Rate Constants of Reactions 1 and 6.	111
4-1	Chlorosilane CVD—Equilibrium Calculations.....	117
4-2	Chlorosilane CVD—Mole Fractions.....	118
4-3	Steady-state Thermal CVD—Deposition Rate vs. SiF ₄ Mole Fraction.....	120
4-4	Steady-state Thermal CVD—ROP Comparison.....	121
4-5	Steady-state Thermal CVD—Growth Rates.....	121
4-6	Steady-state Thermal CVD—Site Fractions.....	122
4-7	Cylindrical Channel Flow—Shear-flow Simulation of SiF ₄ Mole Fractions	124
4-8	Cylindrical Channel Flow—SiF ₄ Mole Fractions Comparison	125
4-9	Cylindrical Channel Flow—Deposition Rates Comparison	126
4-10	Cylindrical Channel Flow—Axial Gas Velocities Comparison	126
4-11	Deposition in a Rotating Disk—Gas Velocity Components	128
4-12	Deposition in a Rotating Disk—Mole Fractions	129
4-13	Deposition in a Rotating Disk—Si Atom Concentrations.....	130
4-14	Deposition in a Rotating Disk—Experimental Data	130
4-15	Trichlorosilane CVD—Gas Temperatures vs. Axial and Radial Distance	132
4-16	Trichlorosilane CVD—Trichlorosilane Mole Fraction	133
4-17	Trichlorosilane CVD—Silicon Deposition Rate.....	133

4-18	Trichlorosilane CVD—Mole Fractions	134
4-19	Time-dependent ALD Simulations—PSR, Total Flow Rates vs. Time	138
4-20	Time-dependent ALD Simulations—TMA Contour Plot	138
4-21	Time-dependent ALD Simulations—O Mole Fraction	139
4-22	Time-dependent ALD Simulations—Stagnation-flow Site Fractions	139
4-23	Time-dependent ALD Simulations—O Mole Fractions Comparison	140
4-24	Time-dependent ALD Simulations—Deposition Thickness Comparison	140
4-25	Steady-state Chlorine Plasma—Electron Temperatures vs. Power.....	143
4-26	Steady-state Chlorine Plasma—Mole Fractions.....	143
4-27	Steady-state Chlorine Plasma—Cl and Cl ₂ Mole Fractions	144
4-28	Steady-state Chlorine Plasma—ROP Analysis	144
4-29	Spacial Chlorine Plasma—Plasma Power vs. Distance.....	146
4-30	Spacial Chlorine Plasma—Electron Mole Fraction.....	147
4-31	Spacial Chlorine Plasma—Cl Mole Fraction	147
4-32	Spacial Chlorine Plasma—Cl ⁺ and Cl ₂ ⁺ Mole Fractions	148
4-33	Spacial Chlorine Plasma—Electron Temperature.....	148
4-34	Fluorocarbon Plasma Etching of Silicon Dioxide—SiO ₂ Etch Rates Variations.....	151
4-35	Fluorocarbon Plasma Etching of Silicon Dioxide—10 Highest Mole Fractions.....	151
4-36	Fluorocarbon Plasma Etching of Silicon Dioxide—Positive Ion Mole Fractions.....	152
4-37	Fluorocarbon Plasma Etching of Silicon Dioxide—Surface Site Fractions	153
4-38	Fluorocarbon Plasma Etching of Silicon Dioxide—Highest ROP.....	153

1 Introduction

The CHEMKIN® software is designed for modeling many chemically reacting flow configurations. This manual consists of tutorials that illustrate how to use the CHEMKIN Reactor Models to address a variety of problems. The tutorials generally represent realistic situations that might be encountered by practicing scientists or engineers. They have been chosen to demonstrate the wide range of software capabilities, and the different ways CHEMKIN can be used.

In this manual, we address three major categories of chemically-reacting flow problems: Combustion problems are covered in [Chapter 2](#), Catalysis in [Chapter 3](#), and Materials Processing in [Chapter 4](#). Methods for analyzing chemical reaction mechanism are covered in [Chapter 5](#). In many cases, the same reactor models are used for simulations in different categories of problems. [Table 1-1](#) lists the tutorials in this manual along with a cross-reference to the Reactor Models employed in that tutorial.



Before working with the tutorials in this manual, we recommend that users first review [Getting Started with CHEMKIN](#) to become familiar with the operation of the CHEMKIN Interface and the available Reactor Models.

The files for the sample problems have been copied to a location specified by the user during the CHEMKIN installation. On a Windows machine, the default location is `%userprofile%\chemkin\samples41`. On a UNIX machine, the default location is `$HOME/chemkin/samples41`. The sample-problem files have a uniform naming convention based on the relevant Reactor Model name combined with a descriptor for that specific system. For example, a project file called `plasma_psr__chlorine.ckprj` uses the Plasma PSR Reactor Model, and involves chlorine chemistry. The data files used for a given sample are located in subdirectories of the `samples41` directory. For

the example project mentioned above, the corresponding chemistry and profile files (if used) would be located in the *samples41\plasma_psr_chlorine* directory. Sample problems involving multiple models or networks of reactors are treated as separate groups.

In the interest of keeping computational times reasonable, the sample problems generally do not include any of the larger chemical reaction mechanisms that are often used in combustion and plasma research. Some of the mechanisms are included only for the purposes of illustration, and should not be used for scientific research or engineering projects without consulting the current scientific literature.

Table 1-1 Reactor Models Used in Sample Problems

<i>Tutorial</i>	<i>Reactor Models Used</i>
2.1.1 Adiabatic Flame Temperature	Equilibrium Calculation
2.3.1 Steady-state Gas-phase Combustion	Perfectly Stirred Reactor
2.3.2 Autoignition for H ₂ /Air	Close Homogeneous Batch Reactor
2.3.3 Ignition-delay Times for Propane Autoignition	Perfectly Stirred Reactor
2.3.4 Burner-stabilized Flame	Premixed Burner-stabilized Flame
2.3.5 Flame Speed of Stoichiometric Methane/Air Premixed Flame	Premixed Flame-speed Calculation
2.3.6 Parameter Study: Varying Equivalence Ratio of Propane/Air Flame	Premixed Flame-speed Calculation
2.3.7 Hydrogen/Air Flame	Opposed-flow Flame
2.4.1 Homogeneous Charge Compression Ignition (HCCI) Engine	Internal Combustion Engine
2.5.1 Shock-heated Air (Shock)	Normal Incident Shock
2.6.1 Gas Turbine Network	Perfectly Stirred Reactor Plug Flow Reactor
2.6.2 Jet Flame Network	Perfectly Stirred Reactor
2.6.3 Partially Stirred Reactor for Methane/Air	Partially Stirred Reactor
2.6.4 Side Inlet on a Plug Flow Reactor	Plug Flow Reactor
2.6.5 Co-flowing Non-premixed CH ₄ /Air Flame	Cylindrical Shear Flow Reactor
2.7.1 Soot Formation and Growth in a JSR/PFR Reactor	Perfectly Stirred Reactor Plug Flow Reactor
3.1.1 Two-Stage Catalytic Combustor	Perfectly Stirred Reactor Plug Flow Reactor Honeycomb Reactor

Table 1-1 Reactor Models Used in Sample Problems (Continued)

<i>Tutorial</i>	<i>Reactor Models Used</i>
3.1.2 Engine Exhaust Aftertreatment with a Transient Inlet Flow	Perfectly Stirred Reactor
3.2.1 Parameter Study Facility for Surface Chemistry Analysis	Honeycomb Catalytic Reactor
4.1.1 Equilibrium Analysis of Chlorosilane CVD	Equilibrium
4.1.2 PSR Analysis of Steady-state Thermal CVD	Plasma Perfectly Stirred Reactor
4.1.3 Approximations for a Cylindrical Channel Flow	Plasma Perfectly Stirred Reactor Plug Flow Reactor Cylindrical Shear Flow
4.1.4 Deposition in a Rotating Disk Reactor	Rotating Disk CVD Reactor
4.1.5 Trichlorosilane CVD in Planar Channel Flow Reactor	Planar Shear Flow
4.2.1 Time-dependent Simulations of ALD Process	Perfectly Stirred Reactor Stagnation Flow CVD Reactor
4.3.1 Steady-state Chlorine Plasma	Plasma Perfectly Stirred Reactor
4.3.2 Spatial Chlorine Plasma PFR with Power Profile	Plasma Plug Flow Reactor
4.3.3 Fluorocarbon Plasma Etching of Silicon Dioxide	Plasma Perfectly Stirred Reactor
5.1.2 Reaction Mechanism for Diamond CVD	Mechanism Analyzer

2 Combustion in Gas-phase Processes

2.1 Equilibrium

2.1.1 Adiabatic Flame Temperature

2.1.1.1 Project Description

This user tutorial presents the use of a gas-phase equilibrium calculation to determine the adiabatic flame temperature for the hydrogen/air system. The adiabatic flame temperature is a measure of the maximum temperature that could be reached by combusting a particular gas mixture under a specific set of conditions. In a real system which includes heat losses, chemical kinetic and/or mass transport limitations, the flame temperature is likely to be lower than the adiabatic flame temperature.

2.1.1.2 Project Setup

The project file is called ***equilibrium__gas.ckprj***. The data files used for this sample are located in the ***samples41\equilibrium\gas directory***. This reactor diagram consists of a single equilibrium reactor.

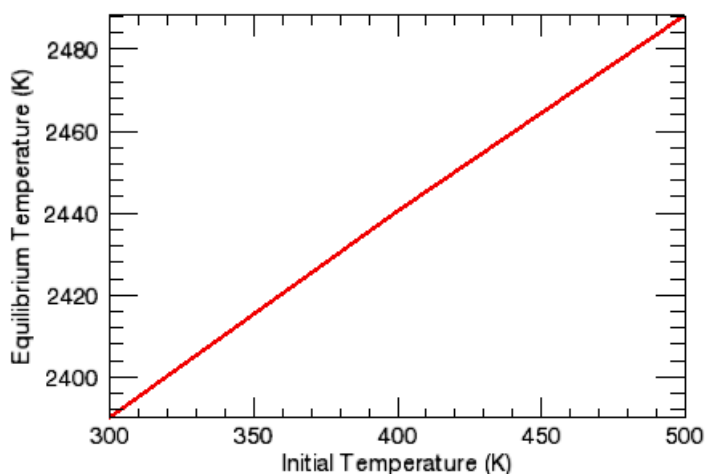
The equilibrium calculation only needs a list of species with their thermodynamic data. There is no need for a reaction list. For this sample problem, the chemistry input file includes only 3 elements: H, O and N; and 9 species: H₂, H, O₂, O, OH, HO₂, H₂O, N₂, and H₂O₂. It is important to include all likely radical species as well as stable species in the product list so as to obtain an accurate flame temperature prediction. For equilibrium calculations generally, it is better to include many unimportant species than to leave out species that may turn out to be important.

Setting up this problem first involves the C1 Equilibrium panel. The problem type (constant pressure and enthalpy), initial temperature (300 K) and pressure (1 atm) are entered on the Reactor Physical Properties tab. An estimated solution temperature of 2000 K is used to help ensure that the solution obtained is for an ignited gas rather than the unburned state. The presence of an estimated solution temperature is often unnecessary for equilibrium simulations but required when a trivial secondary solution may exist. The starting composition is entered on the Reactant sub-tab of the Species-specific Data tab. The reactant mixture defines the initial state, which provides the initial moles of chemical elements and the initial energy of the system. The Continuations panel is used to specify two additional simulations with increasing initial temperatures.

2.1.1.3 Project Results

Figure 2-1 shows the equilibrium temperatures from these simulations, which represent the adiabatic flame temperatures for a hydrogen/air mixture with a H/O ratio of 2.0. The temperatures are on the order of ~2400 K, and thus clearly correspond to the combusted gas. As expected, these adiabatic flame temperatures increase with increasing initial gas temperature.

Figure 2-1 Adiabatic Flame Temperatures—Hydrogen/Air Mixture



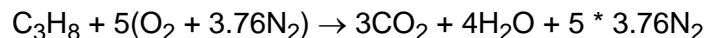
2.2 Using Equivalence Ratio

Many properties of combustion processes strongly depend on the stoichiometry of the combustion mixture. The parameter used most frequently to describe the stoichiometry of the mixture is the equivalence ratio, ϕ . CHEMKIN gives the user an option of describing the initial mixture composition by either listing all of the reactant species and their respective mole or mass fractions, or identifying fuel, oxidizer and complete-combustion (stoichiometric) product species, the mole fraction of any

additional species (such as an inert like Ar or N₂) and the equivalence ratio. Examples of the use of the equivalence ratio can be found in [Section 2.3.1](#), Steady-state Gas-phase Combustion, and [Section 2.3.6](#), Parameter Study: Varying Equivalence Ratio of Propane/Air Flame.

2.2.1 Example: Propane in Air

Stoichiometric equation for propane in air combustion:



Here, the equivalence ratio, ϕ , is defined as the ratio of the actual fuel/oxidizer ratio to the fuel/oxidizer ratio in the stoichiometric equation, as follows:

$$\phi = \frac{X_{\text{C}_3\text{H}_8}/X_{\text{O}_2}}{(X_{\text{C}_3\text{H}_8}/X_{\text{O}_2})_{\text{stoich}}} = 5(X_{\text{C}_3\text{H}_8}/X_{\text{O}_2})$$

CHEMKIN is able to interpret all of the input formats as illustrated in [Tables 2-1](#) to [2-4](#):

Table 2-1 Reactant Mole Fractions Sum to 1.0

	<i>Name</i>	<i>Mole Fraction</i>
Reactant	C ₃ H ₈	0.04
Reactant	O ₂	0.202
Reactant	N ₂	0.758

Table 2-2 Relative Moles Normalized So Mole Fractions Sum to 1.0

	<i>Name</i>	<i>Mole Fraction</i>
Reactant	C ₃ H ₈	0.2
Reactant	O ₂	1
Reactant	N ₂	3.76

Note that in [Table 2-2](#), the relative moles given will be normalized such that the total mole fractions sum to 1.0. However, it is often more convenient to enter relative moles, as described in [Tables 2-3](#) and [2-4](#).

Table 2-3 N₂ as Added Diluent

<i>Equivalence ratio = 1</i>		
	<i>Name</i>	<i>Mole Fraction</i>
Fuel	C ₃ H ₈	1.0
Oxidizer	O ₂	1.0
Added Species	N ₂	0.758
Complete-combustion Product	H ₂ O	
Complete-combustion Product	CO ₂	

Table 2-4 N₂ as Component of Oxidizer

<i>Equivalence ratio = 1</i>		
	<i>Name</i>	<i>Mole Fraction</i>
Fuel	C ₃ H ₈	1.0
Oxidizer	O ₂	1.0
Oxidizer	N ₂	3.76
Complete-combustion Product	H ₂ O	
Complete-combustion Product	CO ₂	
Complete-combustion Product	N ₂	

Note that in the second case ([Tables 2-3](#) and [2-4](#)), N₂ can be considered as either an added diluent ([Table 2-3](#)), or a component of the oxidizer, i.e., air ([Table 2-4](#)). If it is considered part of the oxidizer then it must be included in the complete-combustion products list. Also, the oxidizer composition can be given in relative moles or in mole fractions that sum to one (relative moles will subsequently be normalized to sum to 1.0). If using the equivalence ratio input format ([Tables 2-3](#) and [2-4](#)), the mole fraction of fuel is relative to the total number of moles of fuel and the mole fraction of oxidizer is relative to the total number of moles of oxidizer, they will equal to unity unless more than one species is given for each field of fuel and/or oxidizer. However, the “added species” mole fractions are relative to the total number of moles of the reactants, thus the total mole fraction of added species should not sum up to unity.

In general, the equivalence ratio is a good parameter for quantification of mixture stoichiometry for combustion of hydrocarbon fuels (composed only of hydrogen and carbon atoms) in air or in oxygen. However, one has to be careful when applying ϕ to describe fuel stoichiometry for oxygenates (oxygen is chemically bound to the fuel molecule) as well as other non-traditional fuels and oxidizers. Because the definition of the equivalence ratio does not properly account for the oxygen that might be chemically bound in the fuel, it might not be a useful parameter for some fuels.¹

When trying to determine the Complete-combustion or Stoichiometric Products for such fuels, one must remember that a species can be a saturated Stoichiometric Product if and only if the valence orbitals of all of its constituent atoms are filled. That is, if the oxidation numbers of all of the atoms in a given product species sum up to zero.

2.2.2 Example: Stoichiometric Products

Table 2-5 Determining Stoichiometric Products

<i>Element</i>	<i>Oxidation number</i>
C	+4
H	+1
O	-2
N	0
Ar	0

The oxidation numbers of the atoms in CO_2 sum up to $(+4) + 2 * (-2) = 0$ and in H_2O they sum up to $(-2) + 2 * (+1) = 0$ as well, thus CO_2 and H_2O are Stoichiometric Products. However, oxidation numbers of the atoms in O_2 do not sum up to zero $(-2 + -2 = -4)$, thus O_2 can not be entered as a Stoichiometric Product.^{2,3}

1. C. J. Mueller, M. P. B. Musculus, L. M. Pickett, W. J. Pitz, C. K. Westbrook. "The Oxygen Ratio: A Fuel-Independent Measure of Mixture Stoichiometry", *30th International Symposium on Combustion* (2004).
2. D. W. Oxtoby, H. P. Gillis, and N. H. Nachtrieb, *Principles of Modern Chemistry*, Thompson Learning, Inc. (2002).
3. S. S. Zumdahl, *Chemistry*. D.C. Heath and Company, Lexington, Massachusetts (1989).

2.3 Ignition, Flames and Flammability

2.3.1 Steady-state Gas-phase Combustion

2.3.1.1 Project Description

This user tutorial presents the simulation of the steady-state combustion of a mixture of hydrogen, nitrogen, and oxygen in a perfectly-stirred reactor at atmospheric pressure. This project uses the chemistry set for hydrogen combustion, described in [Section 2.8.1](#). This project demonstrates the use of equivalence ratio for specifying the starting gas mixture, as well as the use of a continuation to alter the equivalence ratio and add sensitivity calculations for a few species.

2.3.1.2 Project Setup

The project file is called *psr_gas.ckprj*. The data files used for this sample are located in the *samples41\psr\gas directory*. This reactor diagram contains one gas inlet and one perfectly stirred reactor model.

Many of the important parameters for this simulation are input on the C1_PSR panel. On the Reactor Physical Properties tab, the Problem Type is first set to Solve Gas Energy Equation, and the Steady State Solver is chosen. The residence time of the gas in the PSR (0.03 milliseconds), the estimated gas temperature (1700 K), system pressure (1 atm) and volume (67.4 cm³) are also set on this panel. No value is input for the Heat Loss, so the system will be treated as adiabatic. The Species-specific Properties tab provides an input field for an estimate of the gas composition to help the solver converge on a solution. In the current case, no solution estimates are supplied for the species fractions, so an equilibrium calculation will be performed at 1700 K with the reactant mixture to determine the initial estimates for them. These initial estimates are used as the starting point for the iterations that converge to the steady-state conditions.

Parameters pertaining to the incoming gas are input on the C1_Inlet1 panel. In this case, the Stream Property Data tab only has the value of 298 K for the inlet temperature. The gas residence time and reactor volume are input on the Reactor Physical Properties tab of the C1_PSR panel, such that including a flow rate here would over-specify the problem. The Equivalence Ratio box is checked at the top of the Species-specific Properties tab of the C1_Inlet1 panel, and a value for the fuel/air equivalence ratio of 1.0 is supplied. As defined on the Fuel Mixture sub-tab, the fuel is composed of 80% H₂ and 20% N₂. Likewise, on the Oxidizer Mixture sub-tab, the oxidizer is defined as 79% N₂ and 21% O₂ (air). Use of the equivalence-ratio form of input requires that the user specify the products of complete combustion for the Fuel

and Oxidizer specified. This is defined on the Complete-Combustion Products sub-tab. In this case, the product species are H_2O and N_2 , where N_2 is included (because it is part of the fuel and oxidizer mixtures). Note that all of the elements contained in the fuel and oxidizer species must also appear in the product species.

For this example, there are no inputs on the Basic tab of the Solver panel. We use the default settings, in which the application first solves a fixed-temperature problem and then uses the results of this solution as the initial guess to solve the full problem including the energy equation. On the Advanced tab of the Solver panel, the minimum bounds of species fractions have been specified as smaller than the default, to aid in convergence to a physical solution.

On the Continuations panel, 8 additional simulations are specified where the equivalence ratio is gradually changed. There are no inputs on the Output Control panels for this problem, since default output options will be used.

2.3.1.3

Project Results

Figure 2-2 shows the steady-state temperatures for the combusting hydrogen/air/nitrogen mixture. In this case, the temperature peaks at a fuel/air equivalence ratio or about 1.25. As shown by the molar conversions in *Figure 2-3*, neither the fuel nor the oxidizer is completely consumed in this combustor, as a result of the PSR residence time.



To get the plot in *Figure 2-3*, be sure to select the “molar_conversion” in the Select Results panel when the Post-Processor is first launched.

Figure 2-2

Steady-state Gas-phase Combustion—Hydrogen/Air Temperatures

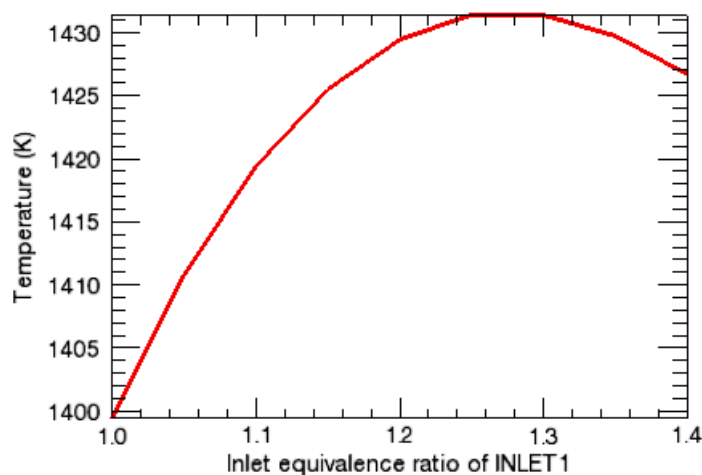
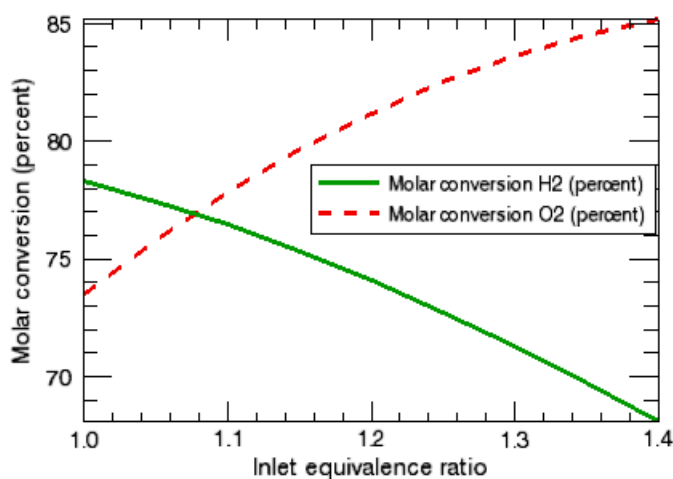


Figure 2-3 Steady-state Gas-phase Combustion—Molar Conversions



2.3.2 Autoignition for H₂/Air

2.3.2.1 Project Description

This user tutorial presents a transient simulation of the spontaneous ignition of a stoichiometric hydrogen/air mixture at constant pressure. This project uses the chemistry set for hydrogen combustion described in [Section 2.8.1](#). Here we are interested in determining the ignition time under a specified set of initial pressure and temperature conditions, assuming no heat loss to the environment (adiabatic conditions). In addition, we would like to determine which reactions contribute most to the CHEMKIN results, using sensitivity analysis. The system is a closed or batch process, so there is no flow of mass into or out of the reactor.

2.3.2.2 Project Setup

The project file is called ***closed_homogeneous_transient.ckprj***. The data files used for this sample are located in the ***samples41\closed_homogeneous\transient*** directory. This reactor diagram contains only one closed homogeneous reactor.

On the Reactor Physical Properties tab of the C1_Closed Homogeneous panel, first the problem type is selected as Constrain Pressure And Solve Energy Equation simulation (the default). The initial temperature (1000 K) is then input, along with the pressure (1 atm). A volume is not specified as it is not important for the results of this simulation, so the default value of 1 cm³ will be used for the initial volume. Since this is a closed homogeneous system, the results in terms of species fraction and temperature will be the same, regardless of the volume value. If surface chemistry were included, the volume-to-surface ratio would be important, but in this case it is gas only. On the Reactant Species sub-tab, the starting gas mixture is given in relative moles as 2.0 H₂, 1.0 O₂, and 3.76 N₂. Writing it this way makes it easy to see that the

O_2/N_2 ratio matches the composition of air, and that the fuel/air ratio is stoichiometric (two H_2 per one O_2). The **Normalize** button will set the mole fractions so that they sum to one, although this is optional, since the normalization will also occur automatically within the program.

On the Basic tab of the Solver panel, the end time of the simulation is set to 0.0002 sec. The Time Interval for Printing is set to 0.0001 sec, which will minimize the size of the text output file. This is only an issue because all reaction sensitivities are being printed, which would result in a very large text file. In contrast, the Time Interval for Saving Data is set to 1E-6 sec, which will provide the time-resolution needed to study ignition phenomena using the Graphical Post-Processor. The text output file lists a value for the ignition time near the end of the file.

On the Output Control panel, the criterion for Ignition Delay is specified using a Temperature Delta of 400 K. This means that ignition will be registered when the temperature reaches a value of 400 K above the initial temperature.

On the Output Control panel, the checkbox for All A-factor Sensitivity has been marked. This results in sensitivities being calculated for all species and all reactions, saved in the XML Solution File, and printed in the output file. This option should be used with care, as the computation time and solution-file sizes increase as a higher power of the size of the reaction mechanism. Except in the case of a very small reaction mechanism, such as the one being used in the sample problem, it is better to use the Species Sensitivity and ROP panel to request that these quantities be output only for a few species of highest interest. Including a value for the Threshold for Species Sensitivity that is higher than the default value of 0.001 will also help keep the amount of information to a manageable level.

There are no Continuations used for this problem.

2.3.2.3

Project Results

Figure 2-4 shows the temperature profile as a function of time for this problem. At the end of this simulation, the temperature is still rising; if it is run much longer, the temperature increases another ~300 K, nearing the adiabatic flame temperature. Although not shown, the volume in this constant-pressure system shows a corresponding increase at ignition. The text output file lists a value for the ignition time of 1.7263E-04 sec, where ignition is defined as the time at which the gas reaches a temperature of 1400 K. *Figure 2-5* shows a close-up of species mole fractions as a function of time. Note that zooming in on the x-axis shows the expected increase in radical species and the product at ignition, along with a decrease in hydrogen and oxygen reactants.

Figure 2-4 Autoignition for Hydrogen/Air—Temperature Profile

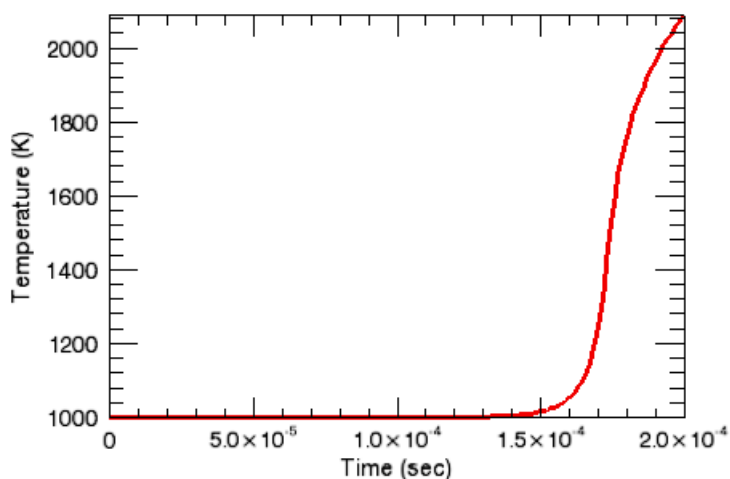


Figure 2-5 Autoignition for Hydrogen/Air—Mole Fractions

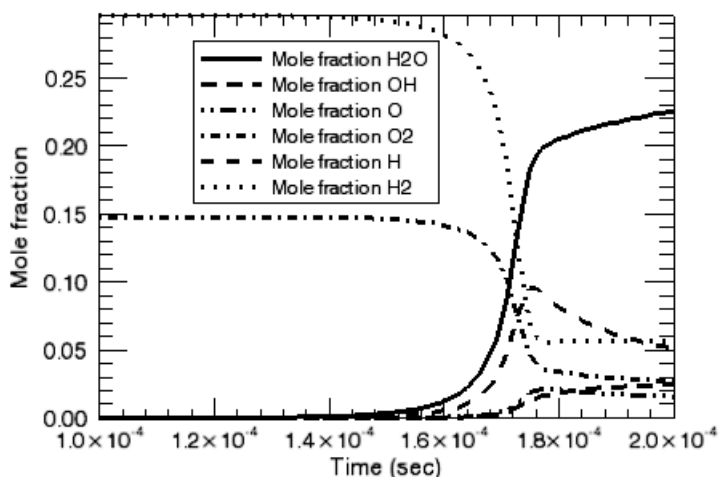
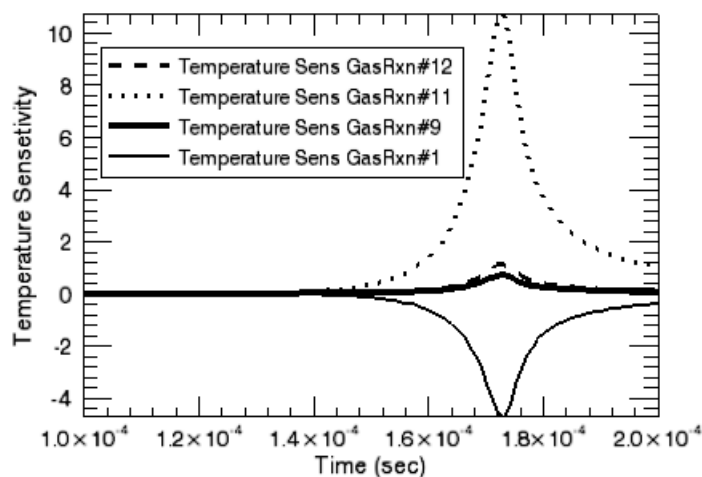


Figure 2-6 shows normalized sensitivity coefficients as a function of time for the four reactions that have the largest effect on the gas temperature. As one might expect, the largest sensitivity occurs near the time of ignition, when the most rapid change in temperature is taking place. The results also show that the dominant reaction for determining the temperature during ignition is the exothermic radical-recombination reaction #11: $\text{O} + \text{OH} \Leftrightarrow \text{O}_2 + \text{H}$. The sensitivity coefficient for this reaction is positive, indicating that increasing the rate of this reaction will lead to a higher temperature (more heat production). In contrast, the sensitivity coefficient for reaction #1 is large and negative, indicating that increasing the rate of this reaction will lead to a lower temperature (less heat production).

Figure 2-6 Autoignition for Hydrogen/Air—Sensitivity Coefficients



2.3.3 Ignition-delay Times for Propane Autoignition

2.3.3.1 Project Description

This user tutorial presents an ignition-delay time calculation for the homogeneous, isobaric, adiabatic combustion of propane in air. The ignition times are computed using two distinct definitions. Discrepancies between results are presented.

Premixed combustion technology is well established in the gas turbine industry. One of the major concerns of such technology, however, is avoiding the autoignition phenomenon to protect combustor components as well as to limit levels of pollutant emissions. Numerical predictions of the ignition time can be very useful in understanding the autoignition parameters, which can be important for the automotive and turbine industries. Chemical kineticists can also benefit from predicting ignition times. Work in validation and testing of detailed mechanisms as well as reduction of detailed mechanisms often requires analyzing ignition times. One of the better-known validation techniques for detailed chemical kinetic mechanisms consists of comparing computational predictions of the ignition-delay times to shock-tube experiments^{4, 5, 6}. Such comparisons can provide a good understanding of the underlying chemistry, since the 0-D computations are free from transport effects.

4. Reaction and Ignition Delay Times in Oxidation of Propane, B.F. Mayers and E.R. Bartle, AIAA Journal, V.7, No10, p.1862
5. Validation of Detailed Reaction Mechanisms for Detonation Simulation, E. Schultz and J. Sheperd, Explosion Dynamics Laboratory Report FM99-5, California Institute of Technology, Pasadena, CA, February 8, 2000
6. A Small Detailed Chemical-Kinetic Mechanism for Hydrocarbon Combustion, M.V. Petrova and F.A. Williams, Combustion and Flame, Volume 144, Issue 3, February 2006, p. 526

There are various ways of defining the ignition time, experimentally as well as computationally, for combustion applications. For example, it is often defined as the time at which either the maximum or onset of certain species concentrations is reached, the time at which a specified rate of increase of temperature occurs, the time at which luminous radiant output from the system is first observed, etc. The reported experimental data can vary greatly, depending on which definition was used in the experiments^{5, 7}. Thus, it is often useful to select which ignition-delay time definition should be used in numerical computations. CHEMKIN 4.1 allows the user such flexibility. For example, in CHEMKIN's homogeneous, perfectly-stirred reactor, the ignition time can be defined to be the time during which the maximum amount of heat is released during a combustion process (as indicated by the inflection point in the temperature profile), as well as the time of the maximum of a certain species concentration chosen by the user. CHEMKIN 4.1 further allows the user to input his/her specific definition of the ignition time via the Ignition Criterion User Routine.

2.3.3.2

Project Setup

The project file is called ***closed_homogeneous_ignition_delay.ckprj***. The data files used for this sample are located in the ***samples41\closed_homogeneous\ttransient\ignition_delay*** directory. This sample uses the mechanism and thermodynamic data from the University of California, San Diego^{6, 8}. This reactor diagram contains only one closed homogeneous reactor.

Open the project file. On the Reactor Physical Properties tab of the C1_Closed Homogeneous panel, the problem type is selected as a constant-pressure simulation where the energy equation will be solved (the default). The initial temperature (1000 K) is then input, along with the pressure (1 atm). A volume is not specified as it is not important for the results of this simulation, so the default value of 1 cm³ will be used for the initial volume. Since this is an isobaric closed homogeneous system, the results in terms of species fraction and temperature will be the same, regardless of the volume value. If surface chemistry were included, the volume-to-surface ratio would be important, but in this case only gas-phase chemistry is present. On the Reactant Species sub-tab, the starting gas mixture is given as 0.02 C₃H₈, 0.05 O₂, and 0.93 Ar. These rather dilute conditions are representative of shock-tube experimental conditions.

-
7. Combustion Theory, Second Edition, F.A. Williams, Addison-Wesley Publishing Company, The Advanced Book Program, Redwood City, CA, 1985
 8. <http://maemail.ucsd.edu/combustion/cermech/>

On the Basic tab of the Solver panel, the End Time of the simulation is set to 0.4 sec. It is important to check the resulting output file after the run is complete to make sure that the End Time is large enough to allow for ignition to occur. If no ignition time is provided at the end of the output file, ignition has not yet occurred and the End Time of the simulation should be adjusted. The Solver Maximum Step Time is set at 1e-6 sec. It is important to make sure that this number is small enough to produce smooth temperature and species profiles. If the profiles are rough, numerous wrong “ignition time” values (based on the numerical and not actual inflection points and peaks) might be printed at the end of the output file. The Time Interval is set at 0.4 sec for Printing and the Time Interval for Saving Data is set to 0.1 sec, which minimizes both the size of the text output file and the computational time. Since only the ignition delay times are of interest here, we do not need most of the CHEMKIN output.

On the Output Control tab, on the Ignition Delay sub-tab, the Temperature Inflection Point box is checked as well as Species Maximum Fraction, representing computational ignition time criteria. Species Maximum Fraction is set to the OH species. This means the ignition time will be computed based on the maximum of the OH concentration. The user can choose any species from the pull-down menu. The ignition time will also be computed at the point where the rate of change of temperature with respect to time is the largest (Temperature Inflection Point criteria). The user can choose any or all of the definitions of ignition times provided by CHEMKIN.

It is of interest to run the same problem, but vary the initial temperature in order to demonstrate ignition time dependence on temperature as well as its dependence on the chosen ignition time criteria. For this purpose CHEMKIN'S Parameter Study Facility is used. For each Parameter Study, the initial Temperature as well as the End Time, the Solver Maximum Time Step and Time Intervals for Printing and Saving Data are changed. The latter three parameters are changed to reflect the fact that ignition occurs faster at higher initial temperatures and thus less time is needed to obtain an ignition time. The Solver Maximum Time Step is refined accordingly. Please refer to [Chapter 3](#) of [Getting Started with CHEMKIN](#) for guidance in setting up a Parameter Study.

Once the project is run, the ignition times (based on peak OH concentration and temperature inflection point) for the three runs are printed in the text output files, stored in the **IgnitionTimeSample_<date>_<time>** folder, contained in your working directory. You can look at the output files by clicking on **Click to View Results** under **Run Results** in the Running Parameter Study window.

2.3.3.3 Project Results

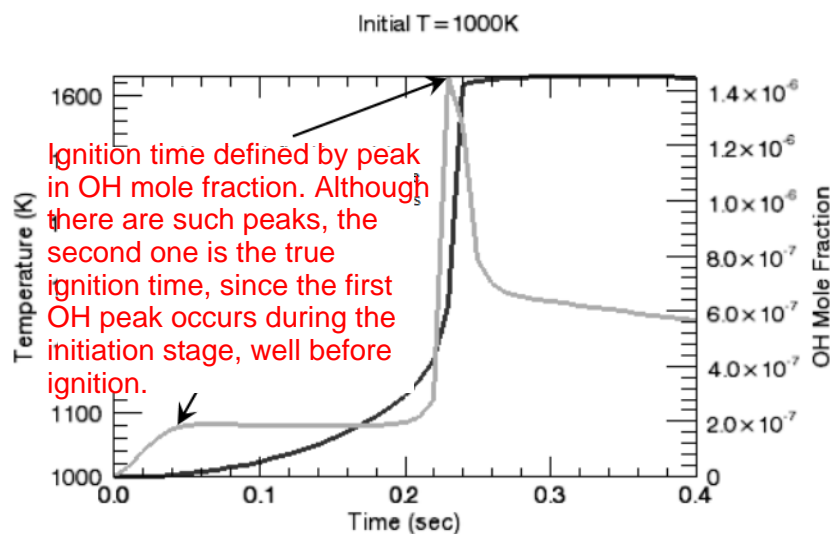
[Table 2-6](#) lists the initial temperatures as well as ignition times based on temperature inflection and OH concentration maximum for each run. The ignition times based on the two criteria differ more and more with increasing initial temperature. Looking at temperature and OH mole fraction profiles will give the user better insight as to how the ignition times are obtained.

Table 2-6 Initial Temperatures and Ignition Times

<i>T</i> [K]	<i>Ignition time</i> [sec]	
	<i>T inflection</i>	<i>OH max</i>
1000	0.2317	0.2321
1500	4.63E-04	5.02E-04
2500	2.34E-06	9.64E-06

[Figure 2-7](#) shows OH mole fraction and temperature profiles as a function of time obtained with CHEMKIN's Graphical Post-Processor. The dark line is the temperature profile and the light line is the OH mole fraction. There is an obvious spike in OH mole fraction at the time of ignition, which in this lower-temperature case corresponds very nicely to the maximum rate of change of the temperature (the inflection point). This is also a good example of how one should be careful when interpreting numerical results for ignition times. In this example, CHEMKIN produces two numbers for ignition times for the OH mole fraction peak. Only one of these numbers represents the ignition time.

Figure 2-7 Temperature and OH Mole Fraction Profiles as a Function of Time



Although the plot in [Figure 2-8](#), obtained with the Graphical Post-Processor, also shows two peaks for the OH concentration profile, because the temperature is decreasing during the first peak, CHEMKIN recognizes the first OH peak is not the true Ignition time and gives only one value (the correct one) for the delay time defined as the peak concentration of OH radicals. The dark line is the temperature profile and the light line is the OH mole fraction.

Figure 2-8 Example of Doubled Temperature Inflection and OH Concentration Peak

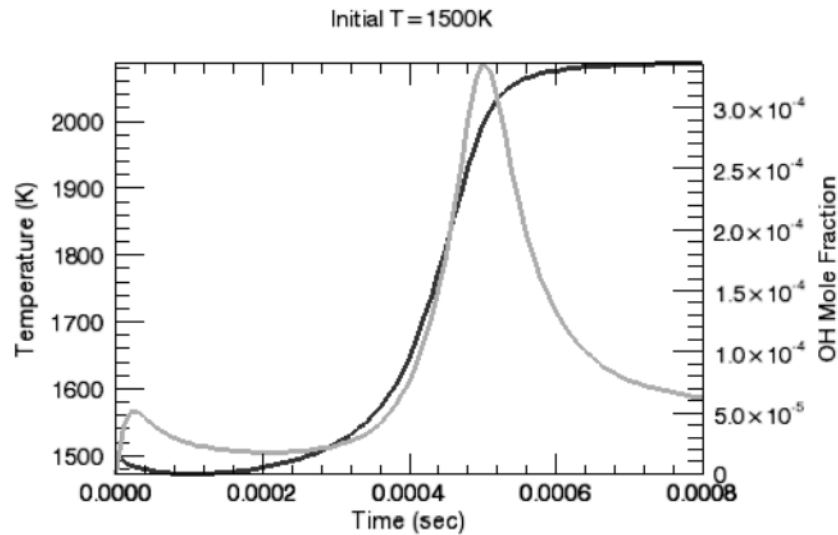
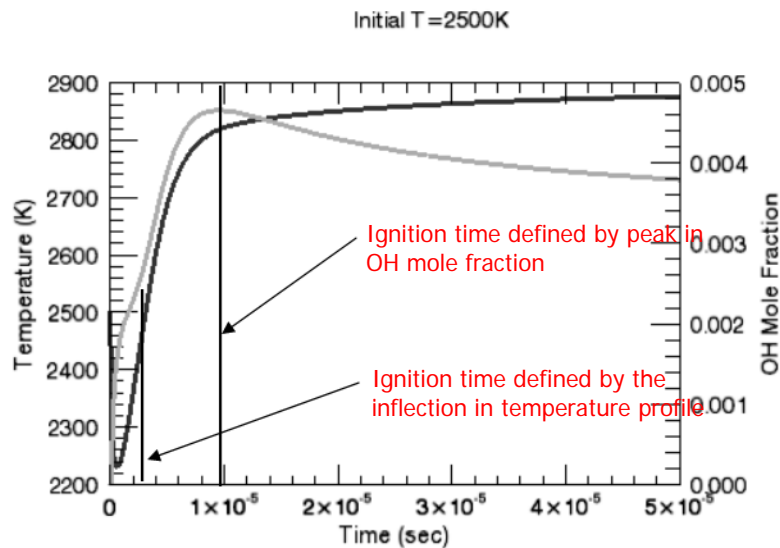


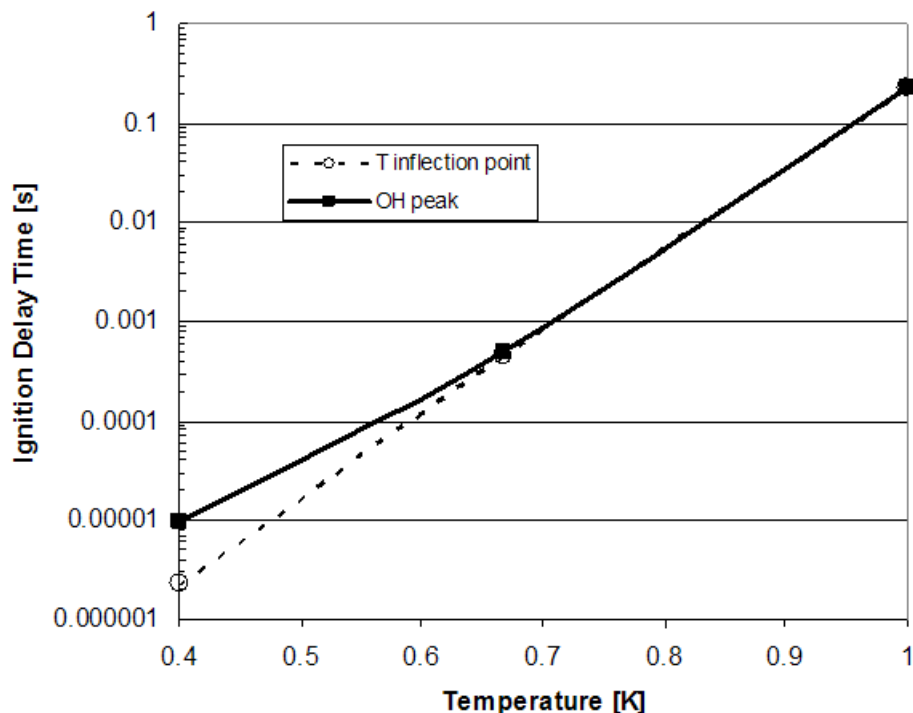
Figure 2-9 Ignition Based on Varying Criteria



In [Figure 2-9](#), there is an obvious difference (about a factor of four) between the ignition time values as defined by the two chosen criteria. This plot demonstrates why one should be mindful of ignition time definitions used in computations. The dark line is the temperature profile and the light line is the OH mole fraction.

Finally the ignition times vs. the inverse of temperature, are shown in [Figure 2-10](#) on a semi-log plot. Here the difference between the two ignition time definitions is obvious.

Figure 2-10 Ignition Times vs. Inverse of Temperature (Semi-log)



2.3.4 Burner-stabilized Flame

2.3.4.1 Project Description

This user tutorial presents a simulation of a burner-stabilized laminar premixed flame of hydrogen and air at low pressure. This project uses the chemistry set for hydrogen combustion described in [Section 2.8.1](#). Burner-stabilized laminar premixed flames are often used to study chemical kinetics in a combustion environment. Such flames are effectively one-dimensional and can be made very steady, facilitating detailed experimental measurements of temperature and species profiles. Also, laminar flame speed is often used to characterize the combustion of various fuel-oxidizer combinations. Therefore, the ability to model chemical kinetics and transport

processes in these flames is critical to interpreting flame experiments and to understanding the combustion process itself. Examples of the use of flame modeling to interpret experimental observations and to verify combustion chemistry and pollution formation can be found in Miller, et al.⁹

2.3.4.2 Project Setup

The project file is called ***pre-mixed_burner__burner_stabilized.ckprj***. The data files used for this sample are located in the ***samples41\pre-mixed_burner\burner_stabilized*** directory. This reactor model is simple and contains only one gas inlet and one premixed-burner reactor.

On the Reactor Physical Properties tab of the C1_ Pre-Mixed Burner panel, the problem type is selected as Fix Gas Temperature because a measured temperature profile is used rather than computing the gas temperatures from the energy equation. For these laminar flames, the gas temperatures are often obtained from experiment rather than by solving an energy conservation equation. This is because there can be significant heat losses to the external environment, which are unknown or difficult to model. For cases where the heat losses are known or negligible, the user can solve a burner-stabilized flame problem in which the temperatures are determined from the energy conservation equation. Even if the energy equation is to be solved for the temperatures, the iteration converges more reliably if the species profiles are first computed using a fixed temperature profile. In any case, the user needs to input an estimate of the temperature profile. For this example, a temperature profile called ***pre-mixed_burner__burner_stabilized_TPRO.ckprf*** is input on the Reactor Physical Properties tab and only the species transport equations are solved using the temperature as a constraint. The system pressure (25 Torr) is also input on this panel, along with the choice of Mixture-averaged Transport and the use of the Correction Velocity Formalism.

The Ending Axial Position (10 cm) for the simulation is input on the Initial Grid Properties tab of the C1_ Pre-Mixed Burner panel, along with a number of parameters concerning the gridding of the problem. A few of the grid parameters have been changed from the default values. The pre-mixed burner reactor model has adaptive gridding. The initial simulations are therefore done on a very coarse mesh that may have as few as five or six points. After obtaining a solution on the coarse mesh, new

9. J. A. Miller, R. E. Mitchell, M. D. Smooke, and R. J. Kee, in *Proceedings of the Nineteenth Symposium (International) on Combustion*, The Combustion Institute, Pittsburgh, Pennsylvania, 1982, p. 181. J. A. Miller, M. D. Smooke, R. M. Green, and R. J. Kee, *Combustion Science and Technology* **34**:149 (1983). J. A. Miller, M. C. Branch, W. J. McLean, D. W. Chandler, M. D. Smooke, and R. J. Kee, in *Proceedings of the Twentieth Symposium (International) on Combustion*, The Combustion Institute, Pittsburgh, Pennsylvania, 1985, p. 673.

mesh points are added in regions where the solution or its gradients change rapidly. The initial guess for the solution on the finer mesh is obtained by interpolating the coarse mesh solution. This procedure continues until no new mesh points are needed to resolve the solution to the degree specified by the user.

The simulation also needs a starting estimate of the solution from which to begin its iteration. This estimate is given in terms of a reaction zone in which the reactants change from their unreacted values (the unburned composition) to the products. Intermediate species are assumed to have a Gaussian profile that peaks in the center of the reaction zone with the width such that the profile is at 1/10 of its peak value at the edges of the reaction zone. The user provides estimates for the location and thickness of this reaction zone on the Initial Grid Properties tab of the C1_ Pre-Mixed Burner panel.

Starting estimates for the gas composition in various parts of the flame are input on the Species-specific Properties tab of the C1_ Pre-Mixed Burner panel. The species on the Intermediate Fraction tab are generally short-lived radical species, or species that are expected to be present throughout the flame. The species on the Product Fraction sub-tab are those expected to be present in the fully burned state. If no product species estimates are given, an equilibrium composition will be used for the product estimate. Within the reaction zone the model uses straight lines between the initial and final values for both the reactants and products. On the cold side of the reaction zone the reactant species profiles are flat at the unburned values. On the hot side, the product species are flat at the estimated product values. Note that any given species can be both a reactant and a product species. For example, the nitrogen in an air flame will be both a reactant and a product, while the excess fuel in a rich flame will also be both a reactant and a product.

Parameters pertaining to the incoming gas are input on the C1_Inlet1 panel. The input mass flow rate ($4.6 \text{ mg cm}^{-2}\text{sec}^{-1}$), which corresponds to an experimental value, is the only input on the Stream Properties Data tab. The composition of the fuel-rich input gas (28% H_2 , 9% O_2 and 63% Ar) is input on the Species-specific Data tab of the C1_Inlet1 panel. The Solver panel has some inputs where the default settings are being replaced. There are no inputs on the Output Control or Continuations panels for this project.

2.3.4.3

Project Results

[Figure 2-11](#) shows the experimental gas temperature profile as a function of distance imposed on the simulation. The gas composition in [Figure 2-12](#) exhibits the expected behavior of the primary combustion species as a function of distance above the burner, with most of the oxygen reacting away within the first 2 cm. At the larger

distances, some of the H atoms recombine to form molecular hydrogen. This would not have been important in a fuel-poor flame, but does occur in this fuel-rich situation. An inspection of the text file shows that the simulation now has 33 grid points, a significant increase from the initial six. The grid is more dense at the lower distances, as needed to resolve the more rapid changes in chemical composition and temperature occurring in that region.

Figure 2-11 Burner-stabilized Flame—Experimental Gas Temperature Profile

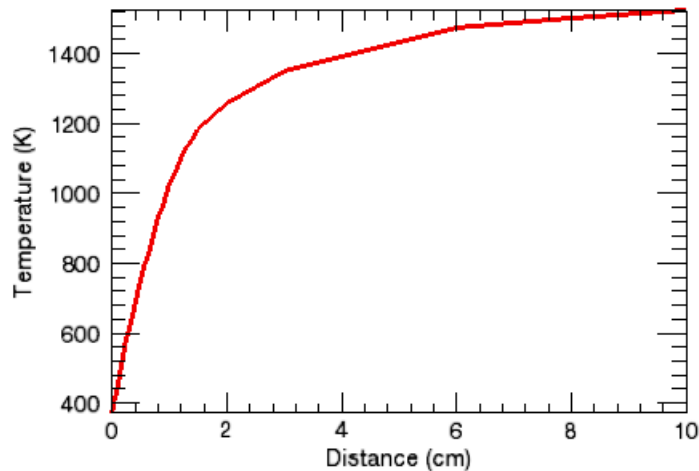
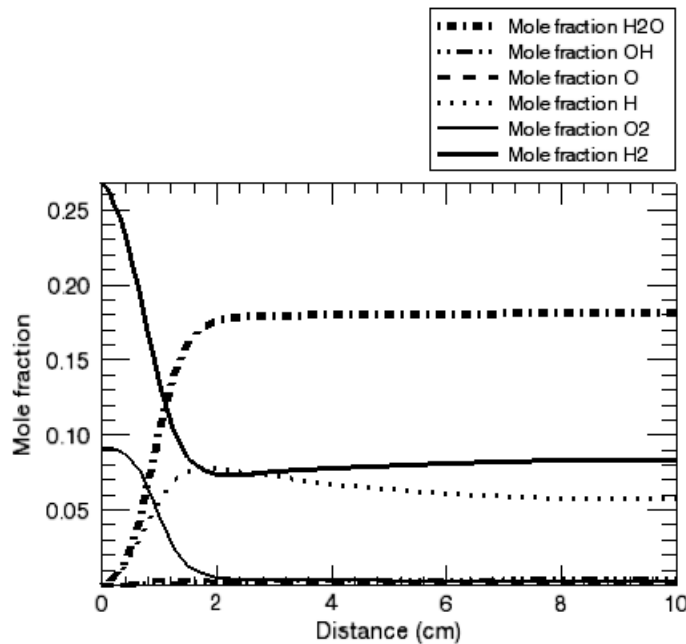


Figure 2-12 Burner-stabilized Flame—Mole Fractions



2.3.5 Flame Speed of Stoichiometric Methane/Air Premixed Flame

2.3.5.1 Problem description

In this tutorial we seek to determine the laminar flame speed and structure of an adiabatic, atmospheric-pressure, freely propagating, stoichiometric methane-air flame.

2.3.5.2 Problem Setup

The project file for this tutorial is called *flame_speed_freely_propagating.ckprj* and is located in the *samples41* directory. Since we are not interested in NO_x formation here, we use a skeletal methane-air combustion mechanism to speed up the calculation. As long as it contains all essential steps for methane oxidation under the desired conditions, the skeletal mechanism should yield adequate results.

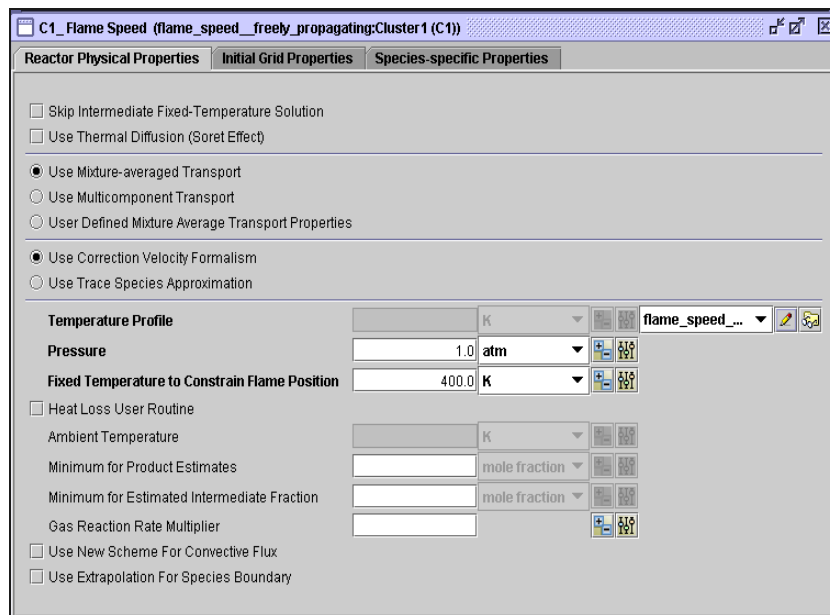
For freely propagating flame problems, properties of the fresh gas mixture are entered in two different panels. Composition of the unburned methane-air mixture should be provided on the Species-specific Properties tab of the C1_Inlet1 panel and the initial guess of the mass flow rate on the Stream Properties Data tab. The unburned gas temperature, however, should be given as the first data point of the estimated temperature profile (see [Figure 2-13](#)). The temperature profile is located on the Reactor Physical Properties tab of C1_Flame Speed panel (see [Figure 2-14](#)).

Figure 2-13 Flame Speed—Temperature Profile Panel

Distance	Temperature
0.0	298.0
0.03	300.0
0.05	400.0
0.06	766.0
0.07	1512.0
0.08	1892.0
0.09	2000.0
0.1	2030.0
0.2	2111.0
0.3	2188.0

Figure 2-14

C1_ Flame Speed—Reactor Physical Property



The pressure is also entered in the corresponding field on this tab. Since the freely propagating flame problem can be difficult to solve, we follow a “proven strategy” to set up and run the problem and provide as much assistance to the numerical solver as possible to ensure a converged final solution with adequate accuracy.

First, we need to pin the flame down to establish a flame-fixed coordinate system by explicitly assigning the gas temperature at one grid point in the computational domain. The fixed temperature should be unique and must lie between the minimum and the maximum temperatures of the problem. The entry for the fixed temperature is located in the Reactor Physical Properties tab as shown in [Figure 2-14](#). Initial guesses for temperature and species profiles and mass flow rate are also needed to run the problem. A good initial temperature profile is important as it can improve the convergence rate of freely propagating flame calculations. The temperature values used in the profile, except the first point, are estimates so they need not to be precise. The shape of the initial temperature profile, however, should closely resemble the actual temperature profile across the premixed flame. Since we have fixed the temperature at a point in the domain, we can easily situate the flame front and make it consistent with the guessed species profiles. The convergence rate normally is not very sensitive to the initial guess of mass flow rate but a good mass flow rate guess can be very helpful when the equivalence-ratio is close to the flammability limit. Note that the mixing zone width is larger than the initial domain. This is fine as these parameters have relatively little physical meaning, but we find that more spread-out guesses are often more likely to lead to convergence than narrow ones.

To compute an accurate flame speed, it is important to have the boundaries sufficiently far from the flame itself so that there is negligible diffusion of heat and mass through the boundary. However, we normally start with an initial run with only a few grid points and a computational domain just wide enough to encompass the flame, i.e., not necessarily the entire domain. We must make sure that a grid point corresponding to the fixed temperature is included in this initial grid, otherwise we lose the anchor of our flame-fixed coordinate system. In addition, we want to relax both gradient and curvature grid adaptation controls by setting their values close to one, meaning that relatively little mesh adaptation will be required on the first pass.

Note that the values for these two grid adaptation controls must be less than or equal to one. The solver will not perform any grid adaptation if both parameters are set to one. Once we obtain an initial solution, we will then expand the domain while reducing/tightening the gradient and curvature controls by using continuation runs (use the Continuations panel). We have to repeat this process until the temperature and species slopes at the boundaries are close to zero and both gradient and curvature controls are at least 0.5 or less.

2.3.5.3

Project Results

Solutions from the last continuation (solution number 3) are shown in [Figure 2-15](#) and [Figure 2-16](#). The fact that the burned gas temperature of 2234 K ([Figure 2-16](#)) is within 3 K of the adiabatic flame temperature indicates that the final solution is an accurate one. The laminar flame speed by definition is the relative speed between the unburned gas mixture and the flame front. Since the coordinate system is fixed to the flame, all velocity solutions are actually relative velocities with respect to the flame front. Accordingly, the flame speed should be the velocity solution at the point where temperature and composition are the same as the unburned gas mixture. But, before we can conclude that velocity value is the laminar flame speed, we must check the gradients of gas temperature and major species to make sure those values are nearly zero at both boundaries. If there is any non-zero gradient at the boundaries, we will need to extend the domain farther to ensure that the assumed adiabatic and zero-diffusive-flux conditions are being maintained.

The species and temperature gradients at both boundaries are seen to be sufficiently small so there is no appreciable loss of mass or energy through the boundaries. The flame speed can be found to be 41.01 cm/sec by looking at the head of the “V” column of the last solution in the text printout. The laminar flame speed measured by Egolfopolous *et al.*¹⁰ or the stoichiometric methane-air flame at one atmosphere is 36.53 cm/sec. The discrepancy may be due to the simplified kinetics used in the simulation or to potential non-adiabatic conditions in the experimental measurement.

Figure 2-15 Flame Speed—Axial Velocity vs. Distance

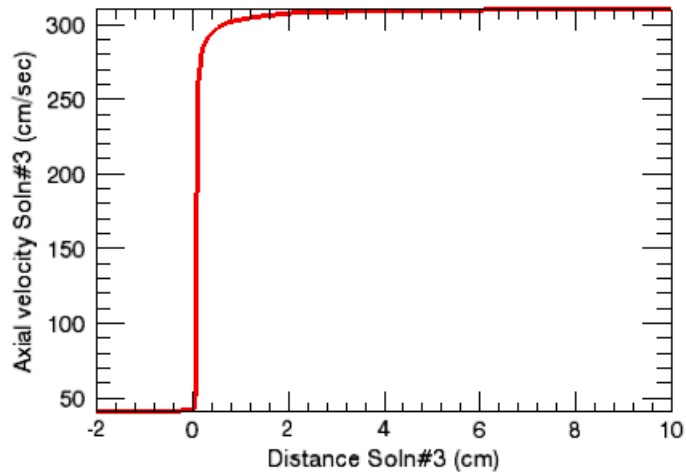
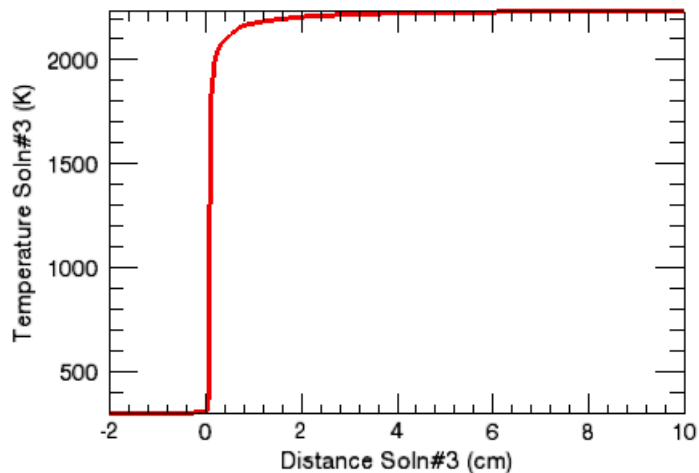


Figure 2-16 Flame Speed—Temperature vs. Distance



2.3.6 Parameter Study: Varying Equivalence Ratio of Propane/Air Flame

2.3.6.1 Project Description

This tutorial illustrates some of the features of the new Parameter Study Facility as applied to flame speed calculations of laminar, premixed flames of propane-air at atmospheric pressure. Parameter studies can be used to specify a range of values as inputs for one or more parameters. This results in several simulations being

10. F.N. Egolfopolous *et al.*, *Proceedings of Combustion Institute* vol. 23 p. 471 (1988).

performed, with each run using a different specified value of the parameter, but otherwise retaining the values for other model inputs. The Parameter Study Facility provides an intuitive setup of the problem, combined with features in the Post-Processor specifically targeted for the parameter studies to better visualize the output.

Parameter studies can be used for several purposes:

- ✓ To study the impact of varying inputs of operating conditions such as pressure or stream properties such as concentrations.
- ✓ To analyze the sensitivity of output to reaction rate parameters and transport properties, and to analyze the impact of uncertain parameters.
- ✓ To study the effect of varying domain size and grid resolution.


The Parameter Study Facility allows several parameters to vary simultaneously. This might be useful, for instance, in analyzing the impact of certain reaction rate parameters for different pressures or concentrations.

In this tutorial, simulations are performed with equivalence ratio as the varied parameter. The behavior of flames in fuel-lean and fuel-rich systems are of interest in several applications such as engine combustion. The problem uses the chemistry set described in [Section 2.8](#). The project file is named ***flame_speed__parameter_study.ckprj***. The data files for this project are located in the *samples41\flame_speed\parametric_study* directory.

2.3.6.2

Project Setup

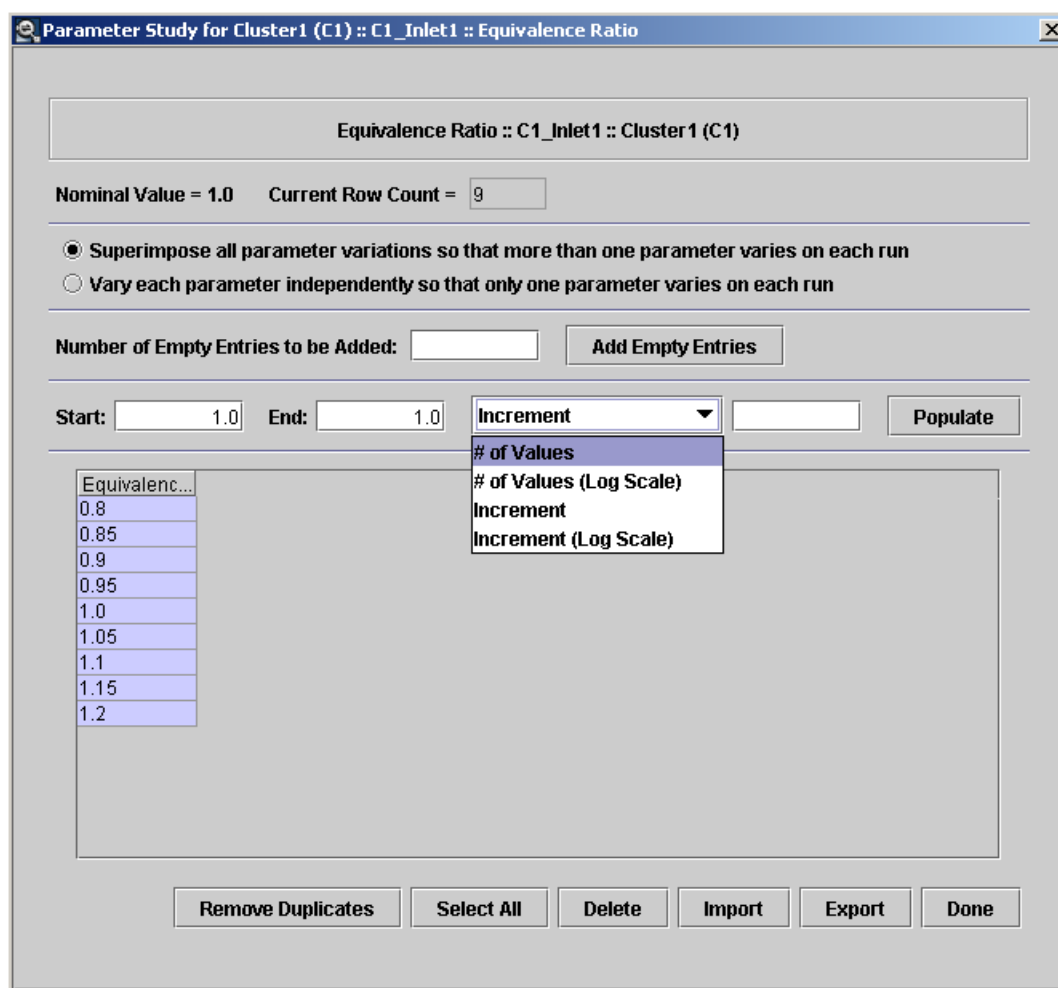
Most of the inputs are conceptually similar to the tutorial on flame speed calculation of methane/air flame in [Section 2.3.5](#). On the Reactor Physical Properties panel, the pressure is specified as 1 atm. Mixture-averaged transport properties are used, with correction velocity formulation. The length of the domain is 2 cm. On the inlet panel, the reactant concentrations are specified in terms of equivalence ratio. The equivalence ratio is a measure of the fuel/oxidizer ratio, as compared with the stoichiometric value (explained further in [Section 2.2](#)). The fuel consists of pure propane, while the oxidizer consists of air. The stoichiometric products from combustion must be specified; however, the composition of the products need not be specified, since CHEMKIN determines it.

The base equivalence ratio is defined as 1.0. To set up the parameter study based on equivalence ratio, the adjacent  icon is selected, and the window shown in [Figure 2-17](#) appears. The parameter study can be populated by entering the Start and End value for the equivalence ratio, and selecting one of 4 options from the dropdown menu for the appropriate distribution of values between the beginning and end value specified, as shown below in [Figure 2-17](#). In this tutorial, 9 values have been selected to provide a range of equivalence ratios of 0.8 – 1.2.

- To modify one of the values, double-click it.
- To delete a value, select it and press the **Delete** button.
- Add a value by pressing the **Populate** button.
- To clear the entire study, press the **Clear** button.

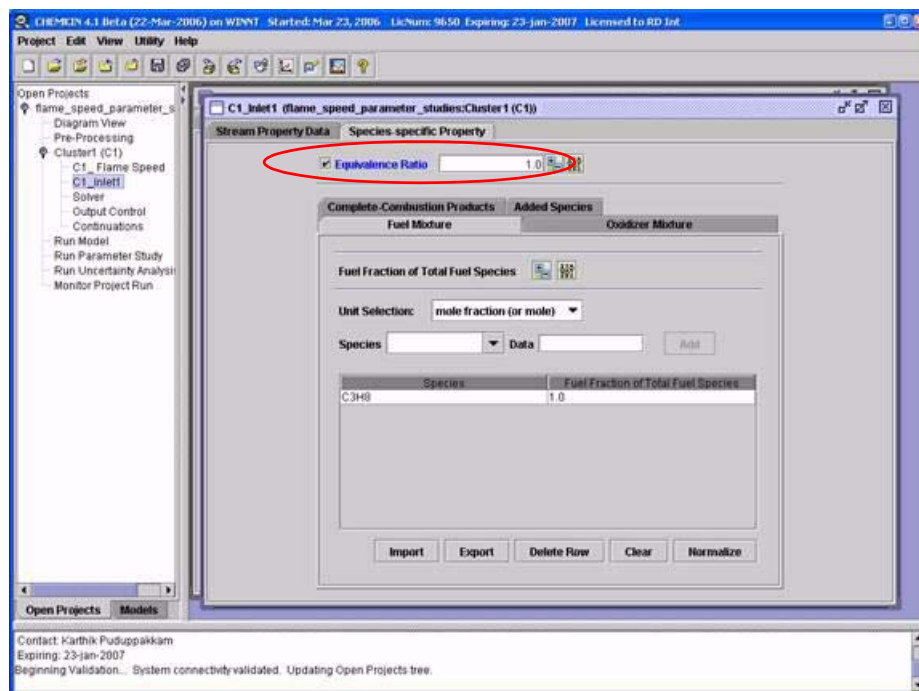
Once the setup is filled out, click the **Done** button to complete the setup.

Figure 2-17 Panel for Setup of Parameter Studies



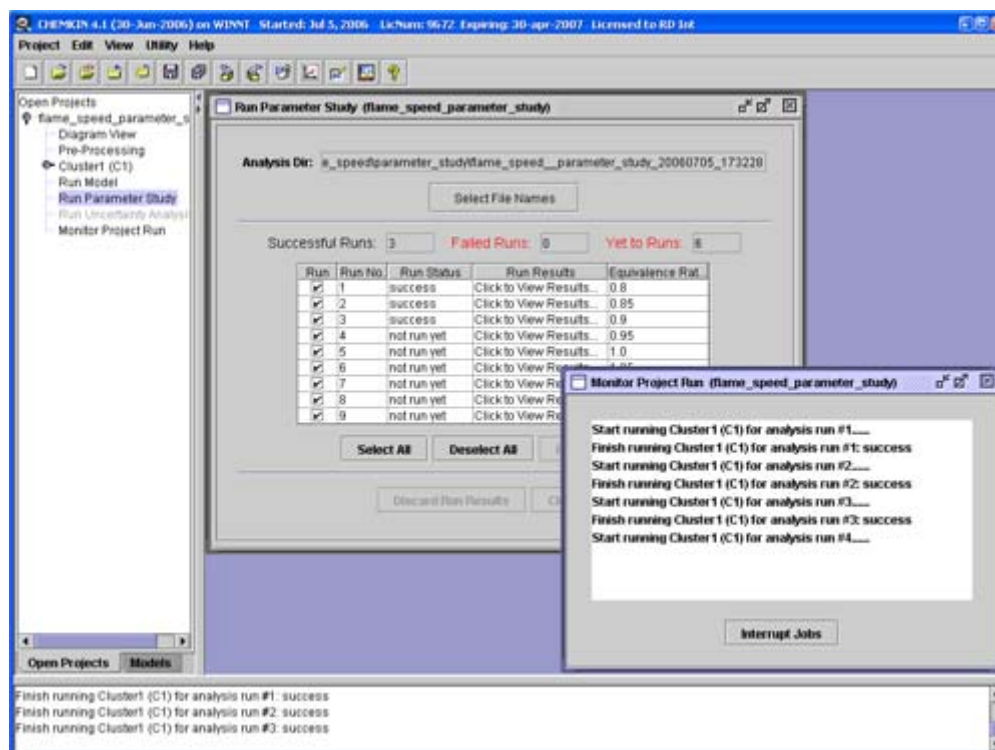
After the specification of the inputs for the parameter study, the parameter would appear in blue, as shown below in [Figure 2-18](#). This shows that the setup of the parameter study is complete for that parameter. Several parameters can be varied at the same time, if desired.

Figure 2-18 Parameter Shown in Blue After Parameter Setup is Complete



Once the setup is done, to run the parameter study, choose the Run Parameter Study panel from the project tree. After clicking the **Run Parameter Study** button, the upper window shown in [Figure 2-19](#), appears. The graphical User Interface gives the option of choosing which cases to run. For choosing all runs, press **Select All**, and for running the model, press **Run Selected**. While the model is running, the lower window in [Figure 2-19](#) shows the status of the runs. After the runs are finished, if the user wants to access the output file, the Run Parameter Study window in [Figure 2-19](#) has buttons for **Click to View Results** for each of the runs. Results can be post-processed after the runs are finished (from the same Run Parameter Study window shown in [Figure 2-19](#)).

Figure 2-19 Parameter Study Run

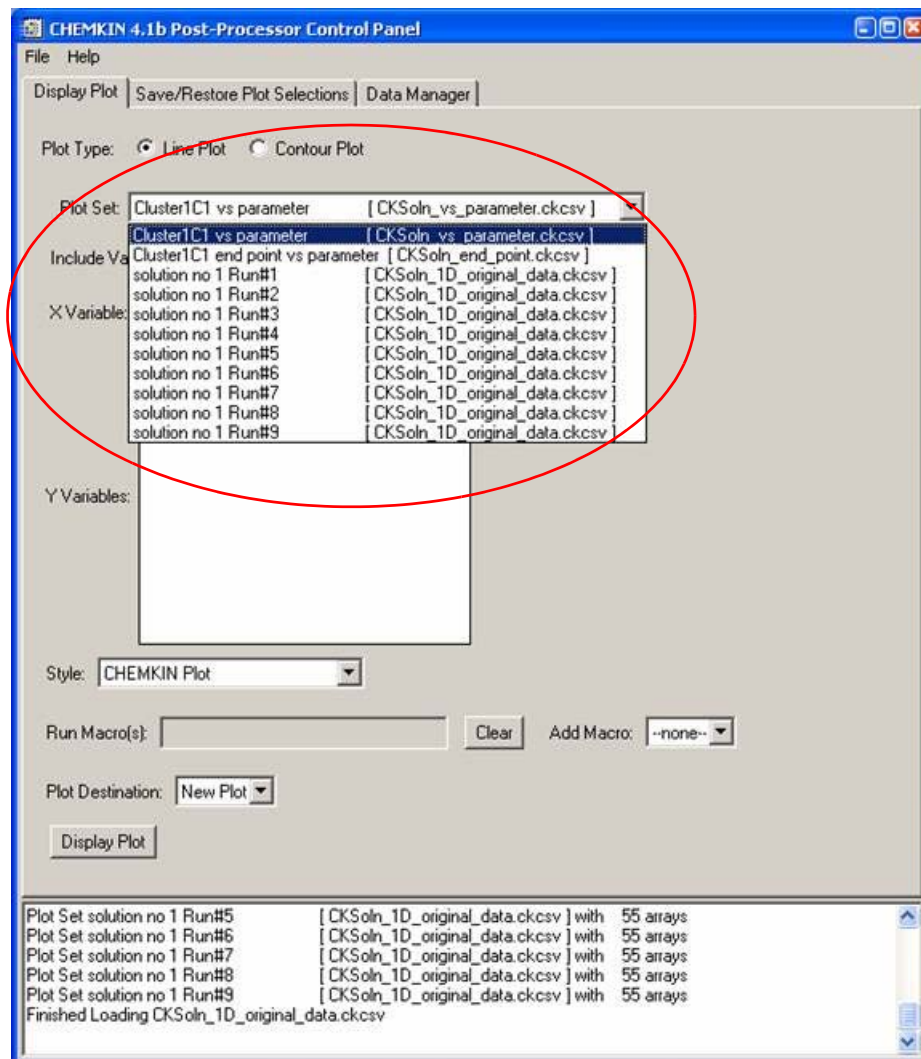


2.3.6.3

Project Results

After running the parameter studies, several additional post-processing options are available. By selecting the Line plot from **Plot Type** in the Post-Processor, options appear for accessing the calculated results as shown in [Figure 2-20](#). The first and second options are exclusive to parameter studies.

Figure 2-20 Post-Processor Options after Running Parameter Studies



2.3.6.3.1

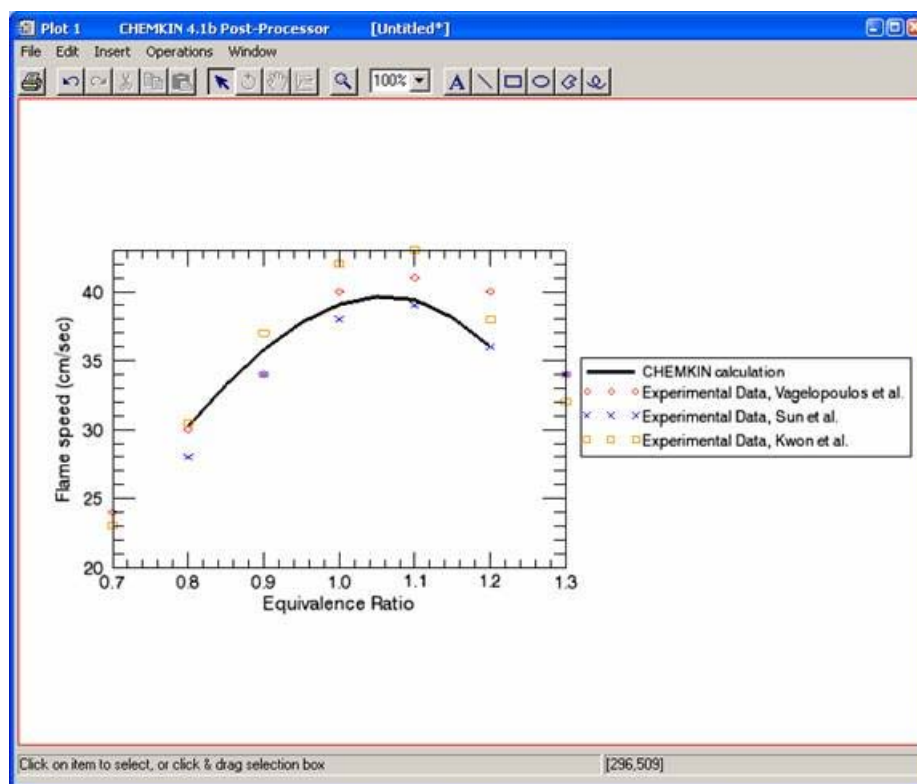
Cluster vs parameter

The first option, the **Cluster1C1 vs parameter** option, gives the output of most interest for this problem, i.e., the flame speed, as a function of equivalence ratio. The flame speed is not shown as an option for single runs, since it is just one data point. However, for parameter studies, flame speed is a characteristic that can be plotted, and is shown in [Figure 2-21](#).

The calculated flame speeds are compared with some experimental data^{11,12,13} in [Figure 2-21](#). This figure shows that the flame speed peaks at a stoichiometric ratio slightly larger than 1. The calculated values seem consistent with experimental data over the range of equivalence ratios simulated.

11. C.M. Vagelopoulos and F.N. Egolfopoulos, Proc. Combust. Inst. 27 (1998) 513.
12. C.J. Sun, C.J. Sung, L. He and C.K. Law, Combust. Flame 118 (1999) 108.
13. S. Kwon, L.K. Tseng and G.M. Faeth, Combust. Flame 90 (1992) 230.

Figure 2-21 Flame Speed Calculated Values as a Function of Equivalence Ratio

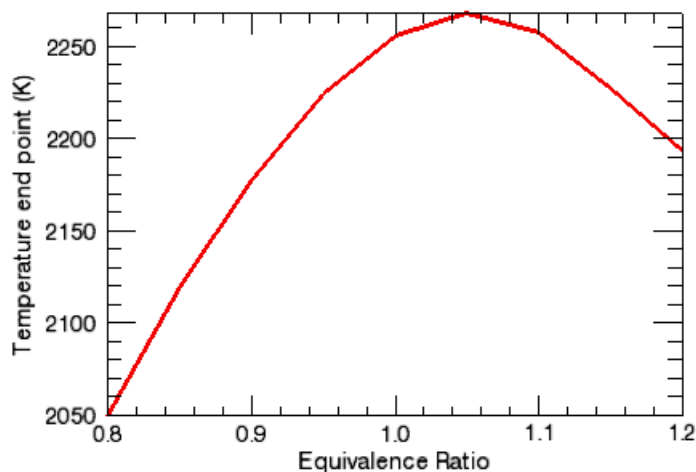


2.3.6.3.2

Cluster endpoint vs parameter

The second option in the Plot Set, i.e., **Cluster1C1 end point vs parameter**, gives values at the end of the domain for outputs such as temperature and composition, as a function of equivalence ratio. This utility is useful when assessing the impact of the parameter being studied on calculated output characteristics. [Figure 2-22](#) shows an example of temperature end point as a function of equivalence ratio. This utility would be helpful in several other models too, for instance, to study outlet concentration from a PSR with residence time as the parameter. The solutions for runs 1-9 have information on each of the individual runs, including profiles of temperature and species. Contour plots can also be made with the parameter that changes as the X-variable.

Figure 2-22 Final Temperature as a Function of Equivalence Ratio



2.3.7 Hydrogen/Air Flame

2.3.7.1 Project Description

This user tutorial presents a simulation of opposed flow diffusion flame of hydrogen and air at low pressure. This project uses the chemistry set for hydrogen combustion described in [Section 2.8.1](#). The opposed-flow geometry makes an attractive experimental configuration, because the flames are flat, allowing for detailed study of the flame chemistry and structure. The two or three-dimensional flow is reduced mathematically to one dimension. This problem uses cylindrical coordinates where one stream contains fuel and the other oxidizer. It also demonstrates the use of sensitivity analysis for reaction rates and species heats of formation. The latter analysis is useful for evaluating the effects of thermochemical parameters that may have been estimated, or have high uncertainties.

2.3.7.2 Project Setup

The project file is called ***opposed-flow_flame_h2_air.ckprj***. The data files used for this sample are located in the ***samples41\opposed-flow_flameh2_air*** directory. This reactor diagram contains two gas inlets and one Opposed-flow Flame Reactor.

On the Reactor Physical Properties tab of the C1_ Opposed-flow Flame panel, the problem type of Solve Gas Energy Equation is selected. Here, the use of Mixture-averaged Transport properties is also selected, as is the choice of a plateau-shaped, rather than a linear, profile for the starting guess used in the simulation. An optional value for the maximum temperature to be used in the initial profile is provided to help convergence.

On the Initial Grid Properties tab of the C1_ Opposed-flow Flame panel, the use of cylindrical geometry is selected for this problem, and the axial length of the simulation (2 cm) is input. In this reactor model, the fuel always enters the system at the origin, and the oxidizer inlet is located at the Ending Axial Position. The opposed-flow reactor model uses adaptive gridding, and in this case, the spacing of the 14 initial grid points have been specified by use of a profile file, ***opposed-flow_flame_h2_air.ckprf***. There are 4 optional parameters on this panel that provide input for the adaptive gridding, two of which have values that we have input to override the defaults. The simulation also needs a starting estimate of the solution from which to begin its iteration, and the Estimated Center Position and Estimated (reaction) Zone Width help specify that. The gas composition giving the expected combustion products that are input on the Product Fraction sub-tab of the Species-specific Data tab on the C1_ Opposed-flow Flame panel are also part of the initial guess.

The gas inlet panels are named to reflect their function. The inlet gas velocities (100 cm sec^{-1}) are input on the Stream-specific Data tabs of the Fuel and Oxidizer panels, along with inlet gas temperatures (300 K). The inlet gas compositions, pure hydrogen and pure air, are input on the Reactant Fraction sub-tab of the Species-specific Properties tab of the Fuel and Oxidizer panels, respectively.

On the Solver panel, there are a number of inputs on the Basic and Advanced tabs to override the default values and assist convergence. On the Output Control tab of the Output Control panel, boxes are checked to request that sensitivity calculations be done for all variables with respect to both reaction-rate A factors and species heats of formation. On the Species Sensitivity tab, three species are listed as being Output Species. The A-factor Sensitivity and Heat of Formation check boxes for these species do not need to be checked here, because they are already covered by the request for All A-factor sensitivities on the Output Control tab, but this redundancy does no harm. There are no inputs on the Cluster Properties or Continuations panels for this project.

2.3.7.3

Project Results

Figure 2-23 shows the gas temperature from the simulation as a function of axial distance. The flame is located on the fuel side of the stagnation plane, which is a result of using hydrogen as the fuel. Most fuels require more air than fuel by mass, so the diffusion flame usually sits on the oxidizer side of the stagnation plane. In a stoichiometric mixture, the fuel usually diffuses through the stagnation plane to establish the flame. For H_2 however, more fuel is required than air. The mole fractions in *Figure 2-24* for the major species show that the flame sits on the fuel side of the stagnation plane in this case. An inspection of the text file shows that the simulation now has 45 grid points, a significant increase from the initial 14 grid points.

Figure 2-23 Hydrogen/Air Flame—Temperature vs. Axial Distance

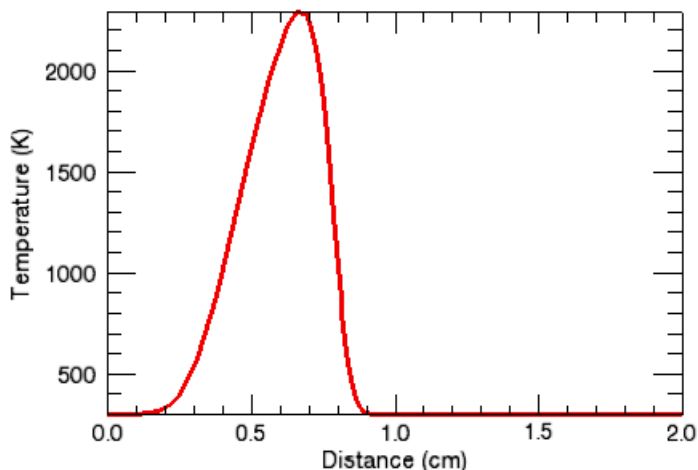


Figure 2-24 Hydrogen/Air Flame—Mole Fractions

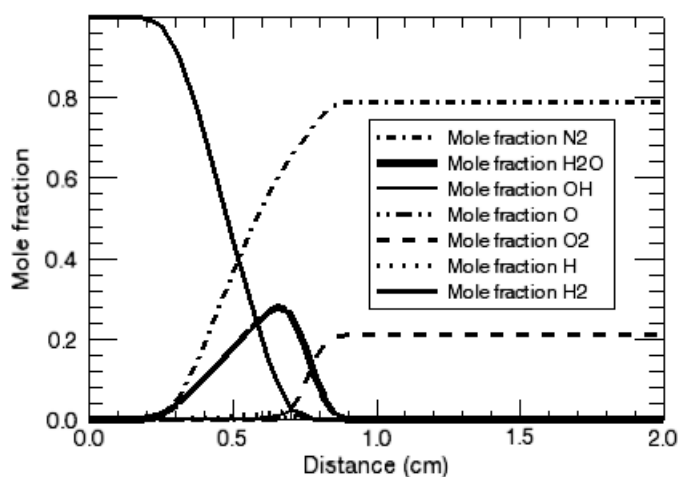


Figure 2-25 shows the normalized sensitivity coefficients as a function of distance for the five reactions with the largest temperature sensitivities. Reaction #1, $\text{H} + \text{O}_2 + \text{M} = \text{HO}_2 + \text{M}$, has both the most positive and most negative values. Increasing the rate of this reaction would increase the temperature on the fuel side, and decrease it at the oxidizer side of the flame. *Figure 2-26* shows the sensitivity coefficients as a function of distance for the five species with the largest temperature sensitivities for heats of formation. The temperature is most sensitive to the heat of formation of H_2O , which makes sense as this is the primary product species.

Figure 2-25 Hydrogen/Air Flame—Temperature Sensitivity to Reaction Rates

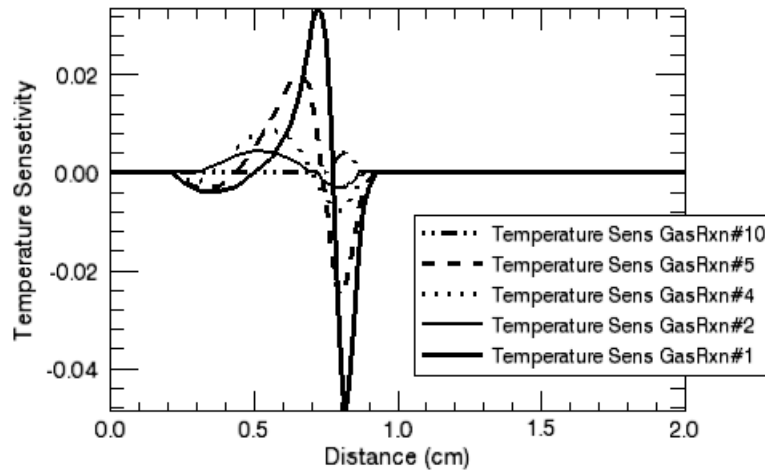
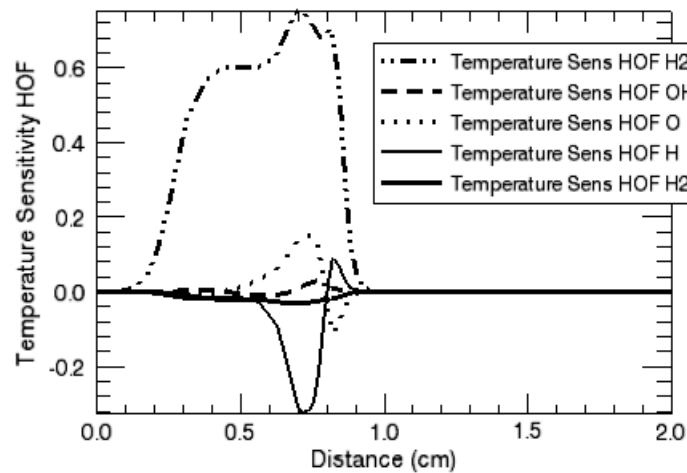


Figure 2-26 Hydrogen/Air Flame—Temperature Sensitivity to Heats of Formation



2.4 Internal Combustion Engine

2.4.1 Homogeneous Charge Compression Ignition (HCCI) Engine

2.4.1.1 Problem Description

Homogeneous Charge Compression Ignition, or HCCI, is a relatively new combustion process for internal combustion engines. The main appeal of the HCCI engine is the great potential for lowering emissions and improving fuel economy.

For this problem, we have some data from a single-cylinder HCCI test engine and would like to use the single-zone IC engine model to simulate the same HCCI process. We would also like to find out how sensitive the solutions are to the heat loss at cylinder wall.

The HCCI engine for this problem runs on natural gas, a mixture of CH_4 , C_2H_6 and C_3H_8 , with exhaust gas recirculation (EGR). The use of EGR can provide some ignition control and CO_2 from the exhaust gas can keep combustion temperature low due to its relatively large heat capacity. Specifications of the test engine that are related to our model setup are given in [Table 2-7](#).

Table 2-7 Test Engine Specifications

<i>Parameter</i>	<i>Setting</i>
Compression ratio	16.5
Cylinder clearance volume	103.3 cm ³
Engine speed	1000 rpm
Connecting rod to crank radius ratio	3.714286
Cylinder bore diameter	12.065 cm

2.4.1.2

Problem Setup

CHEMKIN has a pre-defined model for HCCI engine simulations. The model is called the Closed Internal Combustion Engine Simulator and we can select it either by drag-and-dropping or by double-clicking on the reactor icon (see [Figure 2-27](#)).

Figure 2-27

IC Engine Icon



The next step is to define the chemistry set, or combustion mechanism, for our HCCI simulation. Since methane is the main component of natural gas, we can use GRI Mech 3.0, as described in section [Section 2.8.2](#), to describe the combustion process. Once we successfully complete the pre-processor step, we can start to fill out the Reactor Properties (or C1_ IC Engine) panel with the engine specifications listed in [Table 2-7](#).

Since the HCCI model is for a closed system, the simulation is only valid within the time period when both intake and exhaust valves are closed. We need to find out when the intake valve is closed and use the gas properties at that moment as the initial conditions for our HCCI engine simulation. As a convention, engine events are expressed in crank rotation angle relative to the top dead center (TDC). The intake

valve close (IVC) time of our test engine is 142 degrees (crank angle) before TDC (BTDC). Accordingly, we should set our simulation starting crank angle to -142 degrees. We let the simulation run for 0.043 sec or for 257 degrees crank angle to 115 degrees after TDC. The gas mixture pressure and temperature at IVC are 107911 Pa (or 1.065 atm) and 447 K, respectively. The composition of the initial gas mixture is a combination of natural gas, air, and EGR gas and is given in [Table 2-8](#).

Table 2-8 Composition of Initial Gas Mixture

<i>Species</i>	<i>Mole Fraction</i>
CH4	0.0350
C2H6	0.0018
C3H8	0.0012
O2	0.1824
CO2	0.0326
H2O	0.0609
N2	0.6861

The project file for this HCCI engine simulation problem is called ***ic_engine_hcci_heat_loss_methane.ckprj*** and is located in the ***samples41*** directory. This project file actually contains two “sub-projects”: the *ic_engine_hcci_adiabatic* project assumes the cylinder is adiabatic and the other project, *ic_engine_hcci_heat_loss_woschni*, considers heat loss through the cylinder wall. By default CHEMKIN will append the new project to an existing project file if the name of the new project is different from the ones already saved in the file. Therefore, we can group similar projects into the same project file by saving those projects one by one to the same project filename.

Heat transfer between the gas mixture inside the cylinder and the cylinder wall can be specified on the Reactor Physical Properties panel. For the adiabatic case, no heat transfer occurs between the gas and the wall. We can simply leave the text box corresponding to the heat loss entry blank because the heat loss value is set to zero by default. For non-adiabatic cases, we have several ways to describe the heat loss to the wall: a constant heat transfer rate (positive for heat loss to environment), a piecewise heat transfer rate profile, a user subroutine, or a heat transfer correlation. Here we choose the heat-transfer correlation for our HCCI problem. We also apply the Woschni correction¹⁴ to get better estimates of gas velocity inside the cylinder.

14. J. B. Heywood, *Internal Combustion Engines Fundamentals*, McGraw-Hill Science/Engineering/Math, New York, 1988.

The parameters used in the heat-transfer correlation are shown in [Figure 2-28](#). Note that the parameters for heat-transfer correlation or Woschni correction must be given as a group. If any entry or parameter in the group is left blank, the entire group of parameters will be considered invalid and will be reset to their default values.

Figure 2-28 C1_ IC Engine—Reactor Physical Property for HCCI Woschni Heat Loss model

Parameter	Value	Unit
End Time	0.043	sec
Engine Crank Revolutions		
Engine Compression Ratio	16.5	
Engine Cylinder Clearance Volume	103.3	cm ³
Engine Cylinder Displacement Volume		cm ³
Engine Connecting Rod to Crank Radius Ratio	3.714286	
Engine Speed	1000.0	rpm
Starting Crank Angle	-142.0	degrees
Temperature	447.0	K
Pressure	1.065	atm
Heat Loss		cal/sec
Heat Transfer Correlation		
Coefficient a	0.035	
Coefficient b	0.71	
Coefficient c	0.0	
Chamber Bore Diameter	12.065	cm
Wall Temperature	400.0	K
Heat Loss User Routine		
Prandtl Number		
Woschni Correlation of Average Cylinder Gas Velocity		
Coefficient C11	2.28	
Coefficient C12	0.308	
Coefficient C2	3.24	cm/sec-K
Ratio of Swirl Velocity to Mean Piston Speed	0.0	
Use Initial Conditions as Reference	<input type="checkbox"/>	
Wall Heat Transfer Coefficient		cal/cm ² -K-sec
Wall Thermal Mass		cal/K
Gas Reaction Rate Multiplier		

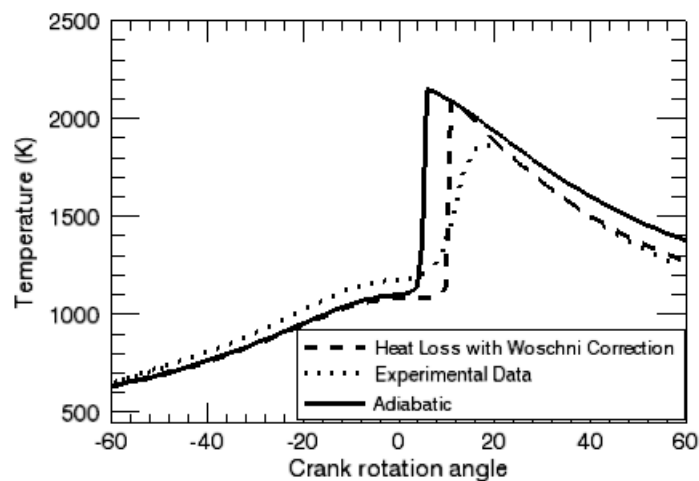
2.4.1.3

Project Results

After simulations of both projects are successfully completed, we can launch the CHEMKIN Post-Processor from the Run Model panel of one the projects. We can load the solutions from the other project by using the **File > Open** menu option. The experimental data are saved in text data files and can be imported via the **File > Import** menu option.

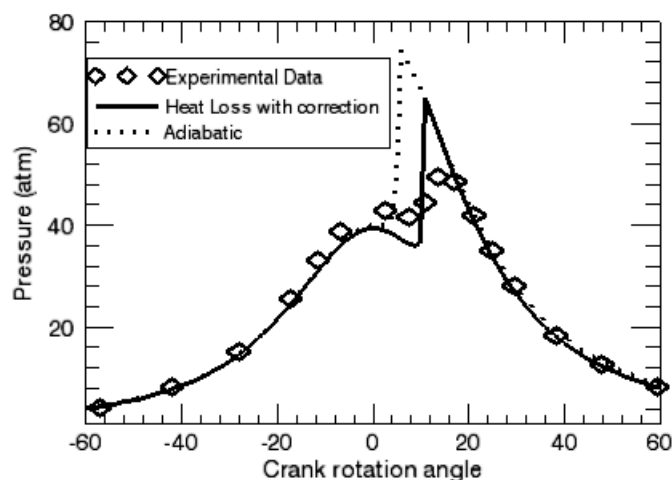
The temperature solutions are shown in [Figure 2-29](#). We mentioned earlier, crank_rotation_angle = 0 is the TDC. We notice that the measured gas temperature before ignition is higher than the one predicted by the adiabatic model. If the measurement was done correctly, this could mean that a small portion of fuel starts burning before TDC and our models fail to capture this phenomenon. The ignition time predicted by the adiabatic model is about 5 degrees earlier than those obtained by experiment and by the non-adiabatic model. The temperature solution from the non-adiabatic model generally agrees with the measurement. Both models predict stronger ignition in the cylinder as indicated by the sharp increases in the temperature profiles. The weaker ignition shown by the experimental data is likely due to temperature variation inside the real cylinder. Although gas composition is homogeneous throughout the cylinder, gas temperature in the core region can be different from that in the boundary layer. The temperature difference can be large if heat loss at the cylinder wall is large. If the gas mixture of the hot core region ignites first, the mean temperature inside the cylinder will not jump as sharply as predicted by the models.

Figure 2-29 HCCI Engine—EGR Temperature Comparison



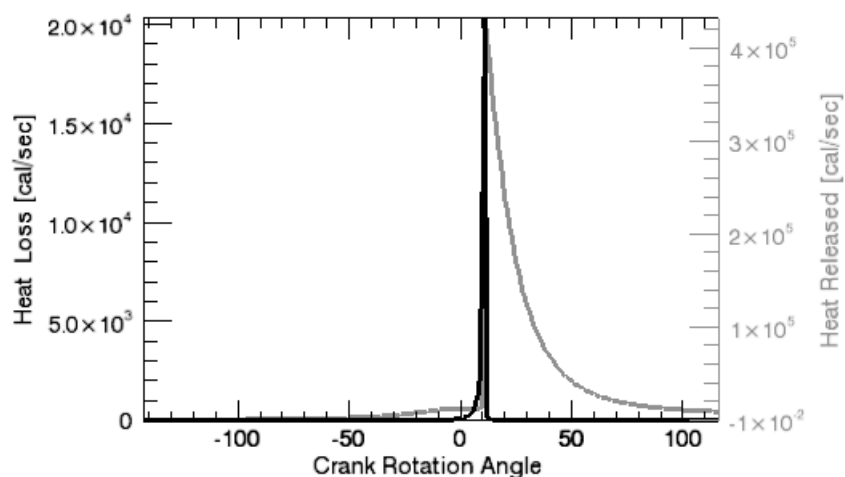
[Figure 2-30](#) gives the comparisons of the measurement and the predictions. In general, the profiles show similar trends as observed in the temperature profiles except that the pressure results are less sensitive to heat loss.

Figure 2-30 HCCI Engine—EGR Pressure Comparison



We can examine the heat-release rate profile for the timing and the magnitude of heat generated by combustion. Since the temperature profile predicted by the non-adiabatic model is in good agreement with the measurement, we can “reverse-engineer” to determine how much thermal energy is dissipated to the environment, i.e., the heat loss rate, during the combustion/expansion period. The heat-release rate and the heat loss rate profiles predicted by the non-adiabatic model are shown in [Figure 2-31](#). Since the solution file provides the heat production rate (`heat_gas_rxn`, you must change the units from $\text{erg}/\text{cm}^3\text{-sec}$ to $\text{cal}/\text{sec}\text{-cm}^3$) instead of the heat-release rate (`heat_loss_rate`, cal/sec), we need to export the solutions to a text file and use a utility program such as Microsoft Excel to obtain the heat release rate (= heat production rate \times volume). We then import the manipulated text data file back to the Post-Processor to get the plot in [Figure 2-31](#). Note that the heat-release profile usually contains narrow spikes. If we want to calculate the total heat-release from the heat release rate profile, we must make sure the profile has enough time resolution to reduce numerical error.

Figure 2-31 HCCI Engine—EGR Heat Loss Comparison



2.5 Simulating a Shock-tube Experiment

Mechanism development often involves analyzing experimental data to understand the chemical reactions and extract rate parameters. Shock tube experiments are often used to obtain chemical kinetic data at high temperatures, which is especially relevant to combustion modeling.

2.5.1 Shock-heated Air (Shock)

2.5.1.1 Problem Description

Shock tube experiments are commonly used to study reaction paths and to measure reaction rates at elevated temperatures. We can apply the Normal Shock Reactor Model to validate the reaction mechanism or kinetic parameters derived from such experiments.

In this tutorial, we want to reproduce one of the shock tube experiments done by Camac and Feinberg.¹⁵ Camac and Feinberg measured the production rates of nitric oxide (NO) in shock-heated air over the temperature range of 2300 K to 6000 K. They also assembled a reaction mechanism with kinetic parameters derived from their experimental results. The reaction $N_2 + M = N + N + M$ in their mechanism has a different temperature dependency when the third body is a nitrogen atom (N). To properly incorporate different temperature dependencies for different third bodies, we exclude N from participating as a third body in the original reaction, i.e., the effective

15. M. Camac and R.M. Feinberg, Proceedings of Combustion Institute, vol. 11, p. 137-145 (1967).

third body efficiency for N is set to zero. And we add a new reaction $N_2 + N = N + N + N$ to explicitly address the different temperature dependence of nitrogen atom as the third body. [Figure 2-32](#) shows these two reactions in CHEMKIN format.

Figure 2-32 Nitrogen Atom Reaction in CHEMKIN Format

```

N2+M=N+N+M          1.92E17  -0.5  224900.
N2/2.5/ N/0/
N2+N=N+N+N          4.1E22   -1.5  224900.

```

2.5.1.2 Problem Setup

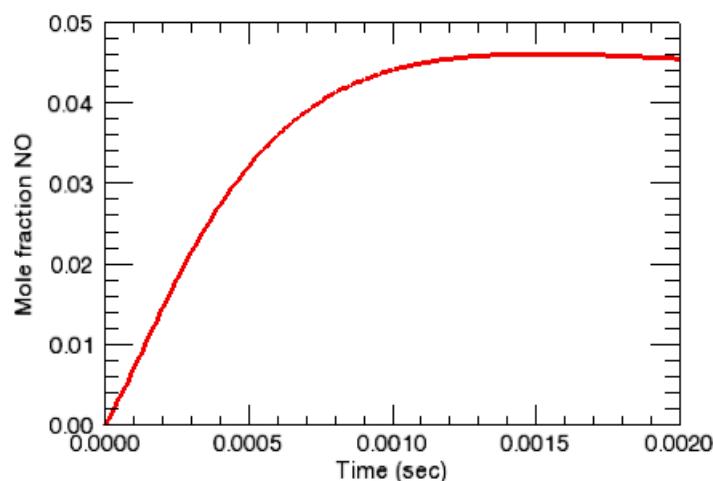
Setting up a shock tube model requires information from the corresponding experiment. In addition to the conditions of the initial (unshocked) gas mixture, we will need to provide information on the diameter of the shock tube, the viscosity of the gas at 300 K, and the velocity of the incident shock. If we do not know the shock velocity from the experiment, we can estimate it by using the Equilibrium Reactor Model with the Chapman-Jouguet detonation option. The shock tube diameter and the gas viscosity at 300 K are only required when the boundary-layer correction is used in the shock simulation.

The project file, *incident_shock_normal_air.ckprj*, is stored in the *samples41* directory and the air dissociation mechanism by Camac and Feinberg is located in the associated working directory.

2.5.1.3 Project Results

The NO mole fraction behind the incident shock is shown in [Figure 2-33](#) as a function of time. The NO mole fraction profile rapidly rises to a peak value then gradually falls back to its equilibrium level. Reasons for the greater-than-equilibrium peak NO concentration can be found in the paper by Camac and Feinberg and references therein. The predicted peak NO mole fraction is 0.04609 and is in good agreement with the measured and the computed data by Camac and Feinberg.

Figure 2-33 Shock Tube Experiment—NO Mole Fraction



2.6 Combustion in Complex Flows

2.6.1 Gas Turbine Network

2.6.1.1 Problem description

This tutorial utilizes a PSR-PFR network to predict NO_x emission from a gas turbine combustor.

2.6.1.2 Problem setup

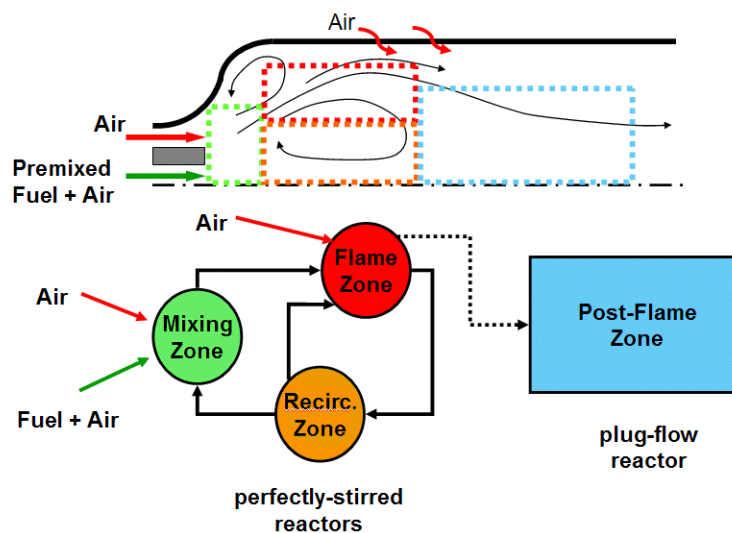
A PSR network or a hybrid PSR-PFR network is commonly used to simulate mixing and flow characteristics of a gas turbine combustor.^{16,17} This reactor network approach can greatly reduce the computational burden yet provide reasonable solutions for a complicated combustion process. However, constructing such a reactor network is rather empirical. Slight changes in combustor operating conditions often lead to a new reactor network configuration with a different number of reactors and connectivity. To speed up the time-consuming trial-and-error process, the CHEMKIN Interface provides a Diagram View that facilitates building and modification of a reactor network. A gas turbine reactor network is shown in [Figure 2-35](#). Typically, a gas turbine reactor network consists of a flame/ignition zone, a recirculation zone, and a post-flame zone. However, depending on how the fuel and oxidizer are delivered and the complexity of the flow field, additional reactors and inlets may be needed to properly represent the combustor. The reactor network shown in

16. A. Bhargava et al., *J of Engineering for Gas Turbines and Power* **122**:405-411 (2000).

17. T. Rutar and P.C. Malte, *J of Engineering for Gas Turbines and Power* **124**:776-783 (2002).

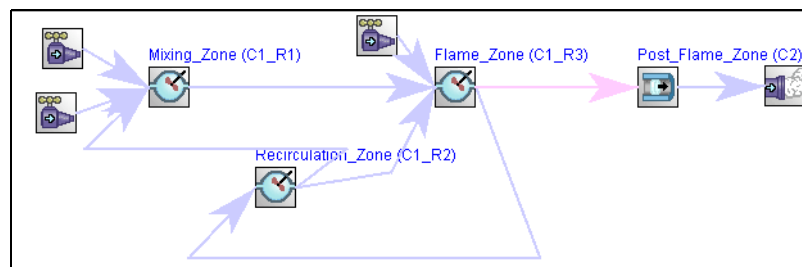
[Figure 2-35](#) has two reactor network clusters. The first cluster represents the region around the flame in the combustor and the second cluster uses a single PFR for the post-flame region between the flame and turbine inlet. We set the first PSR as the mixing zone because the fuel stream is partially premixed. A flame zone PSR is directly connected to the mixing zone and is followed by a recirculation zone for back mixing of hot combusted gas. The solutions of the through flow from the flame zone (the last reactor of cluster number 1) are automatically fed to the post-flame zone (the second cluster) as indicated by the gray line. [Figure 2-34](#) shows the reactor configuration that will be modelled.

Figure 2-34 Gas Turbine Network—Schematic



The project file, *reactor_network_gas_turbine.ckprj*, can be found in the **samples41** directory. The reaction mechanism for methane-air combustion is the GRI Mech 3.0, as described in [Section 2.8.2](#).

Figure 2-35 Gas Turbine Network—Diagram View



2.6.1.3 Project Results

The solutions from the reactor network are shown in [Figure 2-36](#) and [Figure 2-37](#). The temperature solutions in [Figure 2-36](#) indicate that the gas mixture ignites in the third reactor (flame zone) and the temperature continues to increase in the second reactor (recirculation zone) where part of the recycled CO is consumed. Gas temperature increases slightly in the post-flame region (the second cluster) as remaining CO is converted to CO₂ in the hot flue gas (see [Figure 2-37](#)).

The NO profiles are also given in [Figure 2-37](#). As we expected, NO level continues to rise in the post-flame region mainly due to the thermal NO formation.

Figure 2-36 Gas Turbine Network—Temperature Comparisons

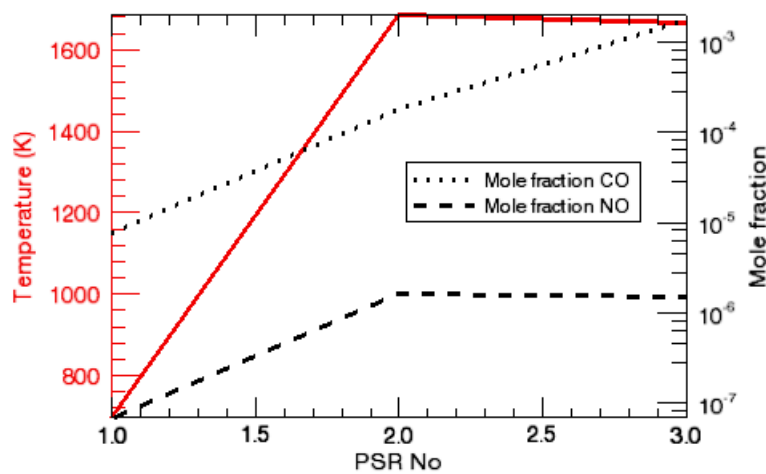
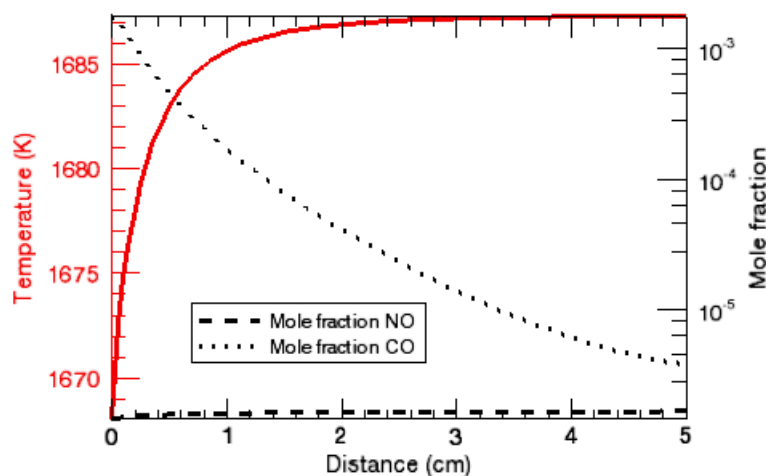


Figure 2-37 Gas Turbine Network—CO and NO Comparisons



2.6.2 Jet Flame Network

2.6.2.1 Problem Description

This user tutorial describes the mechanics of constructing a PSR (perfectly stirred reactor) cluster to represent a non-premixed jet flame.

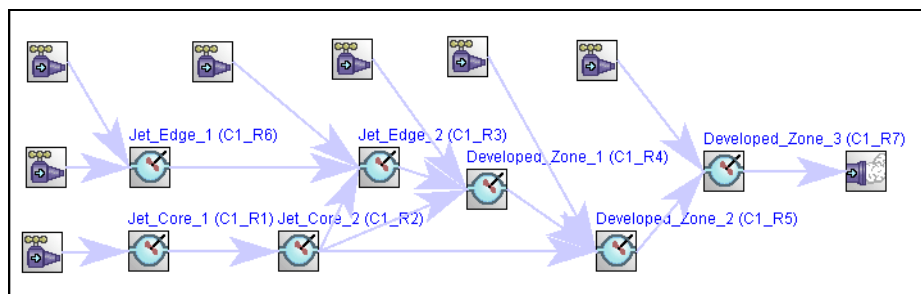
Often, chemical kinetics is either omitted entirely or greatly reduced to make CFD simulations possible for chemically reactive flow systems. When pollutant emissions are to be predicted, the assumption of local chemical equilibrium is not appropriate and the utilization of detailed reaction mechanism is needed. For example, the characteristic chemical time scale of NO is much larger than that of a typical flame species and is compatible to the characteristic time scale, or residence time, of the flow system. Consequently, the local NO concentration level is far from its equilibrium value and depends on the chemical state, the age, and the history of the gas mixture. For simple flow fields, the exit concentration of the species of interest can be obtained by simply integrating its production rates along streaklines (or streaktubes). In this case, the detailed reaction mechanism is used to calculate production rates according to local chemical states and can be a component of the post-processing utility. However, this approach is not suitable for complex flow fields as strong mixing actions and re-circulations make tracking streaklines difficult. Building a reactor network from “cold” CFD solutions is a plausible approach under this situation as it can utilize the detailed reaction mechanism while preserving some key fluid dynamic features that are important to emission predictions such as the residence time. Discussions on how to identify the reactors and their connectivity are beyond the scope of this tutorial. General guidelines on deriving reactor networks from CFD solutions can be found in papers done by Bhargava *et al.*¹⁶ (see p. 57) and Faravelli *et al.*¹⁸

2.6.2.2 Problem Setup

For this problem, we assume that a seven-reactor network is derived from local gas composition and temperature solutions of a CH₄-air diffusion jet flame simulation. The residence times of these reactors and the connectivity and mass flow rates among them are also obtained from the velocity solutions of the CFD simulation. The PSR network representing the diffusion jet flame is given in [Figure 2-38](#).

18. Faravelli *et al.*, *Computers and Chemical Engineering* **25**:613-618 (2001).

Figure 2-38 Jet Flame Network—Diagram View



We use GRI Mech 3.0, as described in section [Section 2.8.2](#), for the gas phase reactions. Because we use PSR's in the network, no transport data is needed. The chemistry set file for this project, **reactor_network_jet_flame.cks**, is located in the working directory, **samples41reactor_networkjet_flame**. Since our reactor network model does not consider molecular transport processes, i.e., diffusion and thermal conduction, we cannot resolve the fine structure of the diffusion flame. The chemical state of each reactor in our model will be controlled by chemical kinetics, residence time, and compositions of gas mixtures entering the reactor, rather than by chemical kinetics and molecular diffusion of reactants as in a fully resolved diffusion flame.

The input parameters for properties of reactors and inlet streams can be found in the project file, **reactor_network_jet_flame.ckprj**, in the **samples41** directory. Since reactor and stream inputs are straightforward and are already described in previous tutorials, we will focus only on the new Recycling panel here.

The Recycling panel allows us to direct a certain fraction of exit mass flow from one reactor to other reactors in the network. The recycling fraction must be a non-negative number and the sum of recycling fractions from a reactor must equal to one to conserve mass.

If all exit mass flow from reactor n is going to reactor $n + 1$, we do not need to provide a value for the through-flow stream, i.e., the default through-flow “recycling” fraction is 1. For instance, the recycling stream Jet_Edge_2 to Developed_Zone_1 on the Recycling panel is actually a through-flow stream from reactor C1_R3 to reactor C1_R4 (see [Figure 2-38](#)). We can leave the text box blank and CHEMKIN will use the default value of 1 for the “recycling” fraction. For other recycling streams, there is no default value and a recycling fraction (between zero and one) must be provided in the text box.

2.6.2.3 Project Results

The solution plots of a reactor network are difficult to interpret because the reactor number does not necessarily correspond to its actual location in the flow field. In our case, reactor C1_R6 actually represents the outer edge of the fuel jet and should be physically located right next to the fuel jet nozzle in an upstream region. On the other hand, reactors C1_R5 and C1_R7 are the flame zone and the post-flame region, respectively, and are both located downstream from reactor C1_R6. Therefore, when we look at the solution plots as a function of the reactor number, we should ignore the sudden changes corresponding to reactor C1_R6.

The predicted temperature distribution is shown in [Figure 2-39](#). The adiabatic flame temperature of the stoichiometric CH₄-air mixture is also given on the plot for reference. We can see that reactors C1_R3, C1_R4, C1_R5, and C1_R7 have temperatures close to the adiabatic flame temperature, which is a good indication for the flame zone and post-flame region. The reactor temperature dropping when coming from reactor C1_R5 to reactor C1_R7 is appropriate, since C1_R7 is in the post-flame region. We can further confirm this speculation by checking the solutions of other variables. We also think the jet flame is slightly lifted from the fuel jet nozzle because the outer edge of the fuel jet (reactor C1_R6) stays at a relatively low temperature.

Figure 2-39 Jet Flame Network—Temperature Distribution

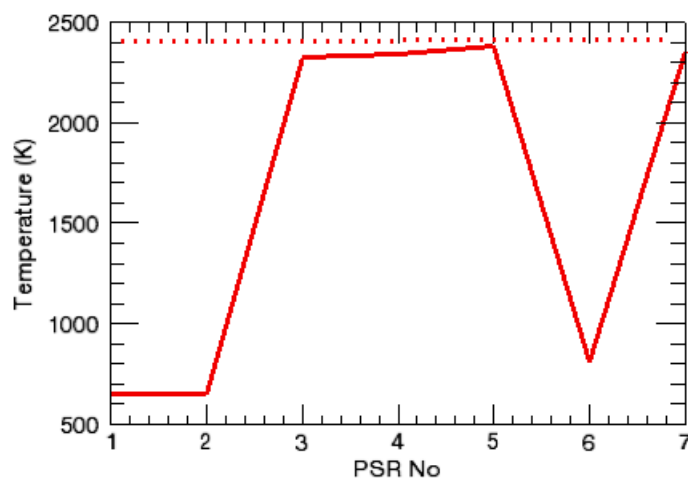
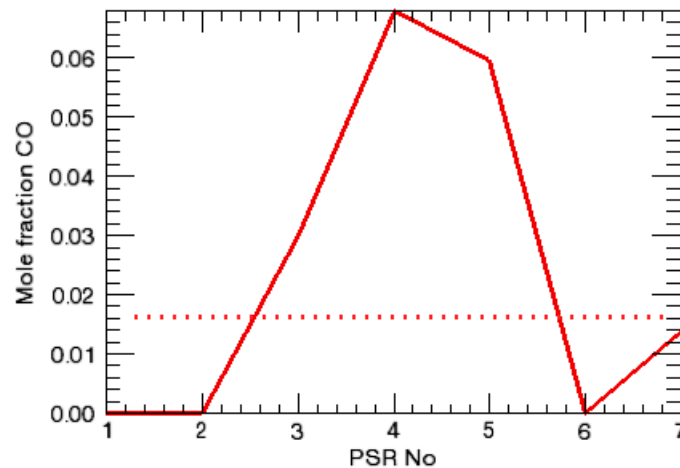


[Figure 2-40](#) gives the CO mole fraction distribution among the reactors. Again, the CO mole fraction at the adiabatic flame condition is provided to show where the combustion zone ends. The CO profile shows a spike starting from reactor C1_R3 to reactor C1_R7. We ignore reactor #6 because it does not connect either to reactor

C1_R5 or reactor C1_R7. This CO spike resembles the one we observe in a typical flame zone and makes us believe that the flame zone ends before reaching reactor C1_R7. The predicted CO mole fraction in reactor C1_R7 is also lower than its adiabatic flame value and is consistent with our observation for the post-flame region.

Figure 2-40 Jet Flame Network—CO Distribution



One of the advantages of using a reactor network is the ability to predict NO formation without running a full CFD calculation with detailed chemistry. The NO profile in [Figure 2-41](#) shows that NO starts to form in the flame zone (reactors C1_R3, C1_R4, and C1_R5) and continues to rise in the hot post-flame region (reactor C1_R7). We can find out which NO formation mechanism is responsible for the NO increase in the high temperature region. In the absence of fuel nitrogen, NO in our jet flame can be formed via prompt NO and thermal NO mechanisms.¹⁹ Since the prompt NO mechanism is characterized by the existence of radicals such as CH and HCN, we can plot the profiles of these radicals to find out the region where thermal NO is the dominant NO formation mechanism. From the profiles in [Figure 2-42](#), we can see that all prompt-NO-related radicals disappear in the post-flame region (reactor C1_R7). so we can conclude that thermal NO is the main NO formation mechanism in the hot post-flame region. The reactor model also shows that, unlike gas temperature and CO mole fraction, the “exit” NO mole fraction is far below its equilibrium value. This is in accord with the fact that the characteristic chemical time scale of NO is greater than the fluid mechanical time scale of our jet-flame system.

19. Miller and Bowman, *Prog. Energy Combust. Sci.*, **15**:287-338 (1989).

Figure 2-41 Jet Flame Network—NO Distribution

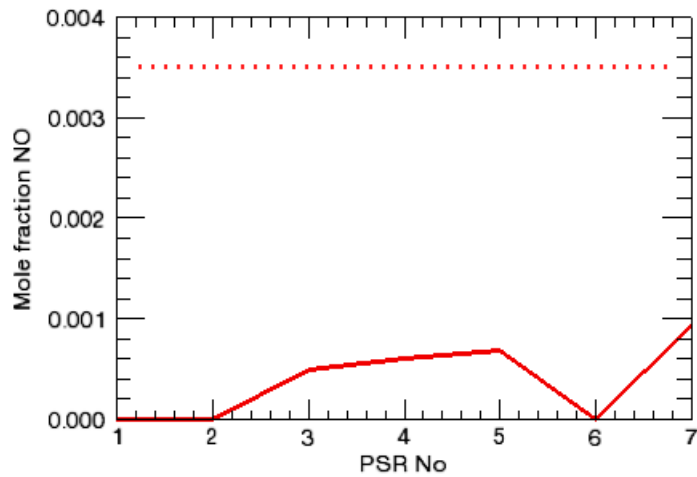
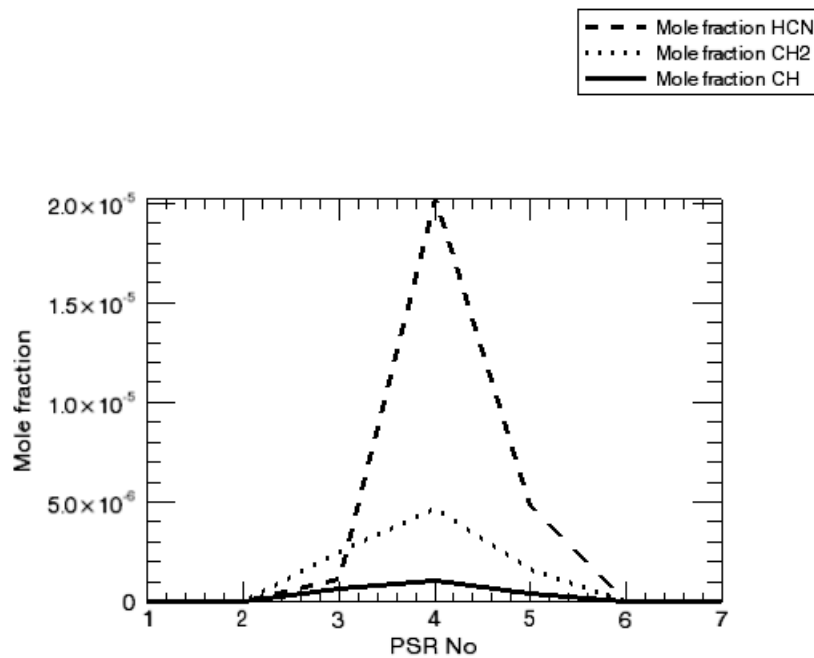


Figure 2-42 Jet Flame Network—Mole Fractions



2.6.3 Partially Stirred Reactor for Methane/Air

2.6.3.1 Problem description

In this tutorial, we want to explore effects of imperfect mixing on the exit flow condition from a premixed gas turbine combustor.

When chemical kinetics is the limiting factor of the reacting system under investigation, we would model the reactor as a perfectly stirred reactor (PSR). The perfect mixing of reactants and products inside a PSR is usually accomplished by using mixers or multiple-jet injections. However, a gas-turbine combustor normally does not have these mixing mechanisms and has to rely on fluid motions, i.e., large-scale eddies and turbulence, to provide the necessary mixing actions. Local turbulence is particularly important as it promotes micro-scale mixing among the gas species.

Although it is adequate in many cases to treat the gas-turbine combustor as a PSR,²⁰ this PSR approach does not always yield proper predictions for the combustor outlet condition. One of the factors that can cause the failure of a PSR approach is the interaction between the turbulence (micro-mixing) and chemical kinetics. If the turbulence is too weak to provide fast mixing among the gas species, the micro-mixing process will interfere with the chemical kinetics. In some cases, when the reactants (non-premixed cases) or the reactants and the products (premixed cases) fail to mix microscopically before they are blown out of the combustor, no combustion zone can be established inside the combustor. The partially stirred reactor (PaSR) model is a tool that can be used to assess the extent of turbulence-kinetics interaction in a gas-turbine combustor or to provide information on how turbulence intensity will affect the combustor.

2.6.3.2

Problem Setup

The project file for this sample problem is located in the **samples41** directory and is called **pasr_ch4_air.ckprj**. A skeletal methane/air combustion mechanism is used to speed the calculation, since we are interested in knowing whether combustion can be sustained inside the combustor by turbulence mixing.

Molecular mixing is important to this problem despite the fact that the fuel and air are premixed before entering the combustor. For premixed problems, good and fast mixing between the fresh reactants and the burned products is required to anchor the combustion zone inside the combustor. To provide a good starting point for the back mixing, we need to initialize the PaSR with the burned state. This is similar to starting a gas-turbine combustor with a pilot flame. We can use the equilibrium model or the steady state PSR model to obtain the burned state of the premixed fuel-air mixture. Effects of the initial condition on the solutions will be minimal once the simulation time passes the residence time of the combustor.

20. T. Rutar and P.C. Malte, *J of Engineering for Gas Turbines and Power*, **124**:776-783 (2002).

There are several model parameters that are unique to the PaSR model. First, we need to specify how the PaSR will treat chemical reactions. In the current case, we want to use finite rates defined by the reaction mechanism. Secondly, we have to select a Monte Carlo mixing model and define parameters for the mixing model. The choice of mixing model depends on how we “envision” the mixing process will behave in the combustor. In this case, we choose the modified Curl's model because we think turbulence eddies in our combustor have a relatively large size variation. The mixing time on our panel (0.0001 sec) is actually the mechanical time scale of the turbulence, or the large eddy turnover time. The “factor for mixing models” entry is the scaling factor between the mechanical and scalar time scales and is usually set to 2. We also need to specify the time step size for the Monte Carlo simulation. The time step size should be no greater than the mixing time scale. Finally, define the size of our PaSR simulation. The solution time profiles will be smoother if we use more statistical events, or particles, in the simulation. However, the run time and memory requirement also increase with the number of statistical events in the ensemble.

There are several solvers available for the PaSR model. Usually, we want to pick between the default DDASPK solver and the DVODE solver with backward differencing. The DDASPK solver is more reliable but more time consuming. Here we use the DVODE solver because the chemistry is simple.

In addition to providing the time profiles of the mean and root-mean-squared (rms) values of scalar variables, the PaSR model can generate probability density functions (pdf) of scalars in separate output data files. The pdf profile shows the instantaneous distribution of a scalar at the end of the simulation time. The shape of a pdf profile is a result of the turbulence-chemistry interaction. The pdf will become a delta function (a spike) if the PaSR behaves closely to a PSR. We can also use the pdf's to find out all possible states inside the combustor. Here we would like to examine the pdf of gas temperature at the end of the simulation time. We want the temperature pdf to have a resolution of 100 intervals, or number of bins. The Output Probability Distribution of Scalar tab of the Output Control panel provides the setup parameters for this pdf output, which is set with $T = 100$. The temperature pdf profile will be saved to a file called ***pdf_T.plt*** and we can import this file to the Post-Processor later.

We want to compare solutions from two cases with different mixing time scales so we can find out how turbulence intensity would affect our premixed combustor. The first case is a relatively strong mixing case with a mixing time of 0.1 msec. The weak mixing case will have a mixing time of 1 msec. After we finish running the first case, we have to rename the solution files, *XMLdata.zip* and *pdf_T.plt*, to ***XMLdata_0.1.zip***

and **pdf_T_0.1.plt**, respectively, so they will not be overwritten by the second run. To switch to the weak mixing case, we can simply go back to the Reactor Properties panel, C1_ PaSR, and increase the mixing time to 0.001 sec. We can then go to the Run Model panel, re-create the input file, and run the second case.

2.6.3.3 Project Results

The mean and rms gas temperature are shown in [Figure 2-43](#) and [Figure 2-44](#) for mixing times of 0.1 msec and 1 msec. The mean temperature profile of the strong mixing case (mixing time = 0.1 msec) indicates that a combustion zone is established inside the combustor and the outlet temperature is around 1800 K. On the other hand, the mean outlet temperature of the weak mixing case continues to drop because poor mixing between the fresh gas and the burned products fails to stabilize a combustion zone. The rms temperature profile of the weak turbulence case has a higher peak value than that of the strong mixing case. This large temperature variation indicates that part of the gas mixture inside the combustor does not burn in the weak mixing case. As most of the initial burned products get pushed out of the combustor, the statistics contain more and more non-burned events and the temperature variation starts to decrease consistently. Statistics of the strong mixing case are mainly made up of burning states so that the temperature variation is relatively small and stable. Similar trends are also shown by the mean CO mole fraction profiles in [Figure 2-45](#).

Figure 2-43 PaSR Methane/Air—Temperature Comparison

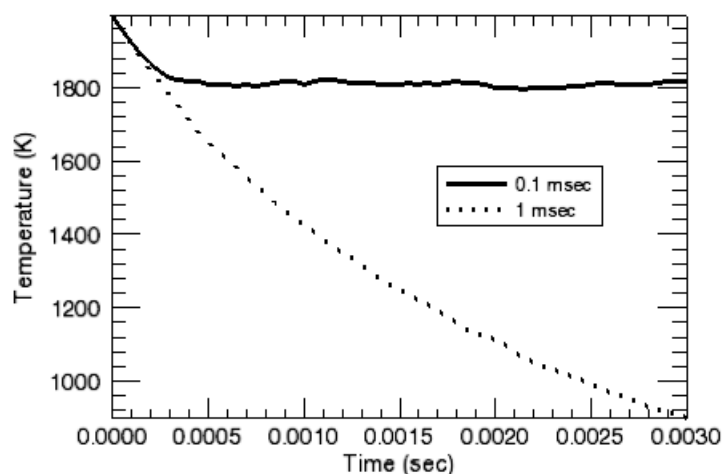


Figure 2-44 PaSR Methane/Air—Temperature Variance Comparison

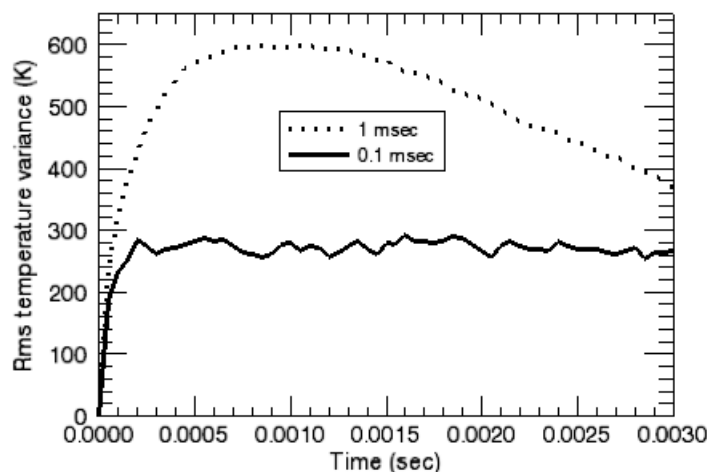
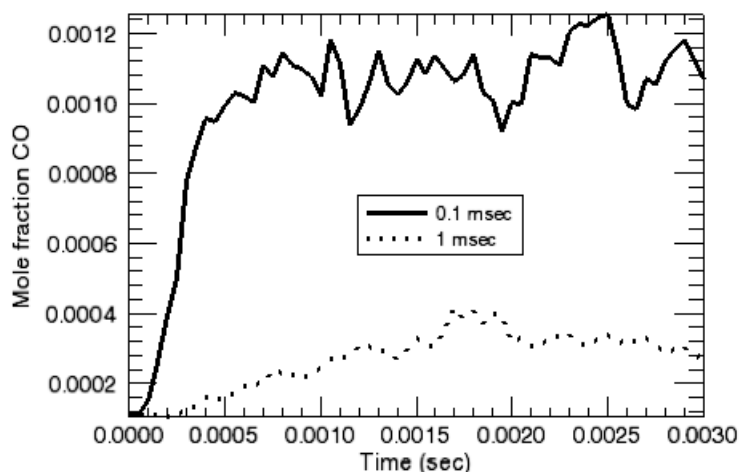


Figure 2-45 PaSR Methane/Air—CO Comparison



Since we requested the temperature pdf to be saved to a data file, we can view the pdf profile by importing it into the Post-Processor. To import the pdf profile generated by the PaSR, we use the **Import** command in the **File** menu of the CHEMKIN Post-Processor. After we select the data file, *pdf_T_0.1.plt*, we should instruct the Post-Processor to skip the first two lines of the text and to read the third line as column titles as shown in [Figure 2-46](#). We also need to set the column delimiter to “space”. We can repeat the same procedures for the second file containing the temperature pdf of the weak mixing case. Once we have both pdf’s imported to the Post-Processor, we can plot these two profiles together for easy comparisons. As shown in [Figure 2-47](#), the pdf of strong mixing case peaks around 2000 K with a small “tail” over temperatures slightly lower than the peak value. We can conclude that a stable combustion zone is established in the strong mixing combustor. The weak mixing case, however, has two peaks in its temperature pdf profile. A smaller peak is located

near 2000 K suggesting there is still some initially burned gas mixture left in the combustor. The large peak of the temperature pdf indicates the combustor most likely has a temperature of 500 K which is the temperature of the inlet gas mixture. Although there might be limited chemical reactions, the slow mixing process cannot sustain a combustion zone inside the combustor.

Figure 2-46 PaSR Methane/Air—Select the Import File Format

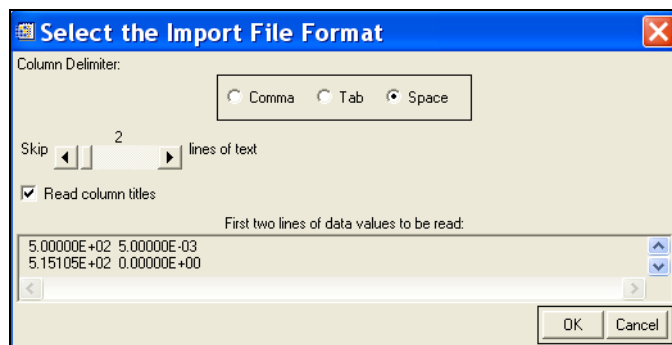
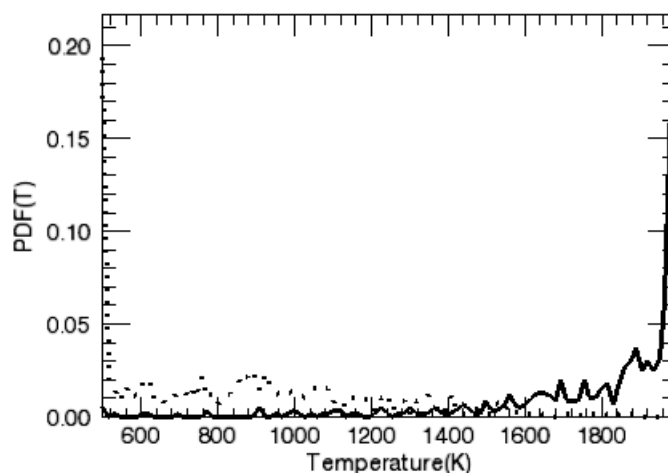


Figure 2-47 PaSR Methane/Air—PDF(T) Comparison



2.6.4 Side Inlet on a Plug Flow Reactor

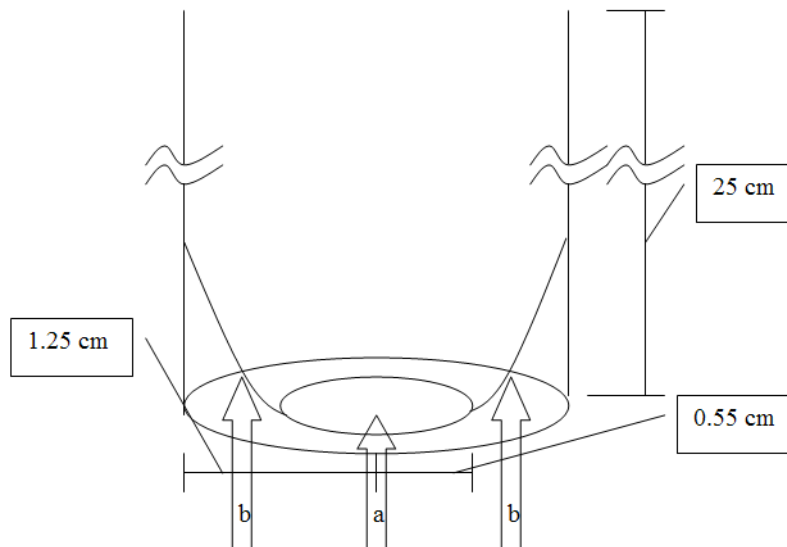
2.6.4.1 Project Description

This tutorial illustrates the use of the side inlet flow into a plug flow reactor, to approximate the effect of a mixing region on product composition. The chemistry used by this project is the Lawrence Livermore National Laboratory NO_x mechanism²¹. Ammonia as a product of a nitrogen fuel contributes to the production of NO in post-flame oxidation. This model predicts how a mixing region affects the production of NO in a high-temperature oxidizing region that is post-flame.

2.6.4.2 Project Setup

The project file is called *pfr_side_inlet_parameter_study.ckprj*. All data files are found in the *samples41\pfr\side_inlet_parameter_study* directory. The simulated model is based on a Lawrence Berkeley National Laboratory experimental setup²². Their report includes a description of a concentric tube, with the ammonia stream in the center, and the oxidizing stream around the edges, as illustrated in *Figure 2-48*.

Figure 2-48 Illustration of the System to be Modeled.



The two streams have the following composition:

Table 2-9 Components in Fuel and Oxidizer Streams

Component	Stream a (fuel)	Stream b (oxidizer)
N₂	0.974	0.88
CH₄	2.E-3	0
NH₃	6.E-4	0
O₂	0	0.08
H₂O	0	0.04

21. Marinov, N. M., Pitz, W. J., Westbrook, C. K., Hori, M., and Matsunaga, N. "An Experimental and Kinetic Calculation of the Promotion Effect of Hydrocarbons on the NO-NO₂ Conversion in a Flow Reactor", Proceedings of the Combustion Institute, Volume 27, pp. 389-396, 1998. (UCRL-JC-129372).

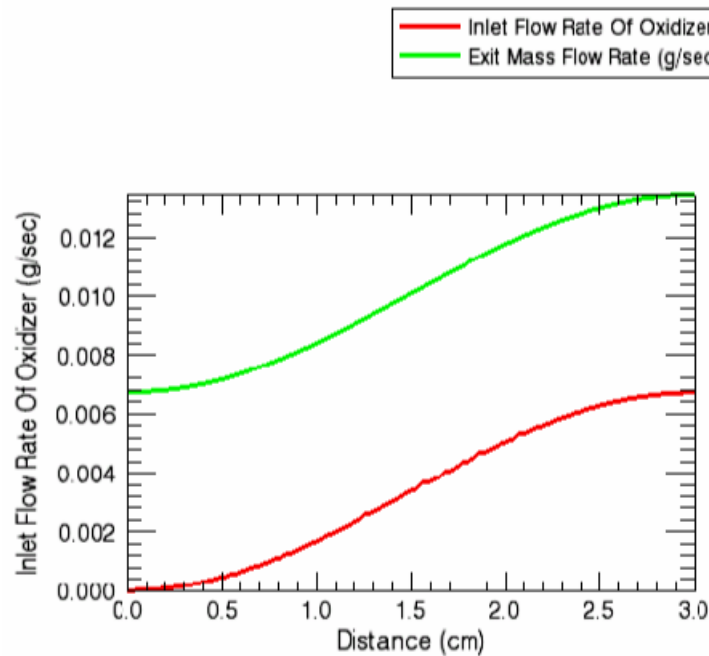
22. Grcar, J. F., Glarborg, P., Bell, J.B., Day, M. S., Loren, A., Jensen, A. D. "Effects of Mixing on Ammonia Oxidation in Combustion Environments at Intermediate Temperatures", Lawrence Berkeley National Laboratory report LBNL-54187.

A length of 3 cm in the mixing region is an estimate based on CFD calculations²² (see p. 70). The temperature of the gas was varied between the range of 1000 to 1500 K in a parameter study. The diameter profile and the flow rate profile vary in the 3-cm mixing region. The fuel and oxidizer streams have a 1:1 flow ratio, with their sum being a value of 2 l/min, which is 16.667 cm³/s for each stream. The oxidizer stream volumetric flow rate is brought up from zero to 16.6667 over the 3-cm mixing region.

2.6.4.3 Project Results

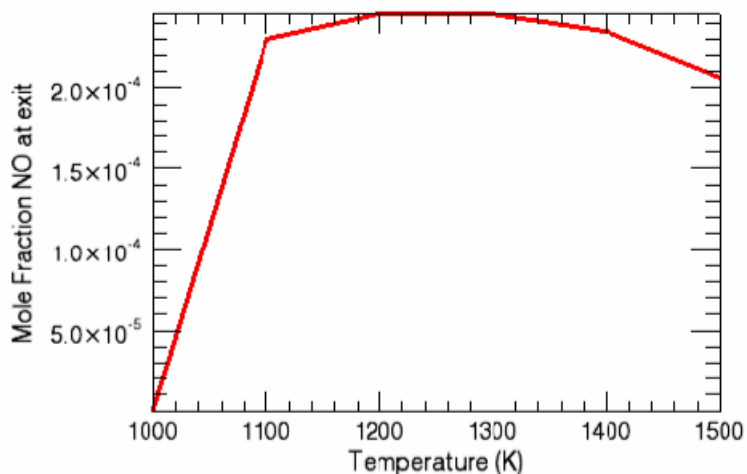
Figure 2-49 shows the increase in mass attributed to the effect of the side inlet flow.

Figure 2-49 Total Flow Growing Directly as a Result of Side Inlet Flow.



At the exit, the predicted NO concentration has a peak near 1250 K, similar to experimental results²².

Figure 2-50 Peaking of NO Concentration Dependent on Temperature in a PFR with an Approximated Mixing Region.



Mixing causes a drop in the peak of NO and a lowering shift in the corresponding temperature, similar to the results found in the report. The NO peak shift is attributed to the locations of the reactions in the mixing zone. At temperatures higher than 1300 K, reaction occurs quickly when the oxidizing stream is in low concentrations, thereby decreasing the amount of NO. When the temperature is in the 1200-1300-K range, the reactions occur later in the mixing zone, a location with more oxidizer and consequently more NO. At temperatures lower than 1200 K, the formation of NO is not favored, so the NO concentration drops off.

2.6.5 Co-flowing Non-premixed CH₄/Air Flame

2.6.5.1 Problem Description

By default, the cylindrical shear flow reactor model uses the uniform inlet and initial profile for all variables except axial velocity. The default inlet velocity profile is considered to be fully developed, i.e., parabolic. In this example, we will establish a co-annular flow inlet condition by using the user routine option to override the default inlet profiles. Properties of both jets are assumed to be uniform when they enter the reactor so there is a jump in the inlet profiles at the jet interface. A non-premixed flame will be established downstream as fuel and air are mixed due to diffusion. The co-flowing annular jet configuration is shown in [Figure 2-51](#) and properties of the inner (fuel) and the outer (air) jets are given in [Table 2-10](#). The outer wall is adiabatic.

Figure 2-51 Confined Co-flowing Annular Jet Configuration.

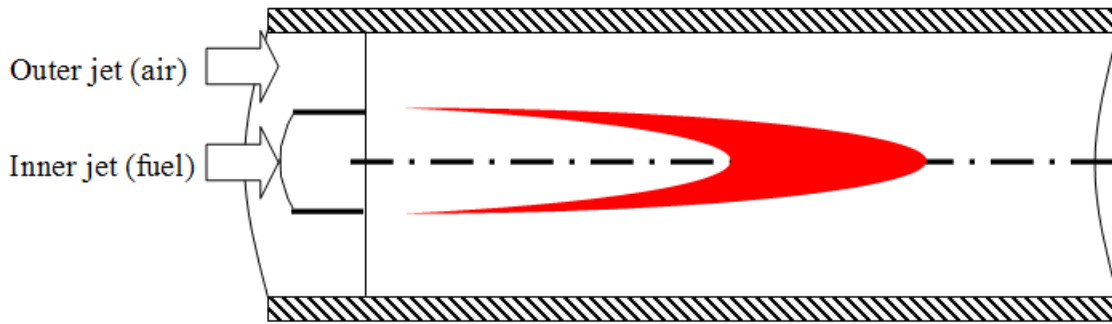


Table 2-10 Properties of the Co-flowing Jets

	<i>Inner Jet (Fuel)</i>	<i>Outer Jet (Air)</i>
Radius (cm)	0.8	4.0
Velocity (cm/sec)	10	25
Temperature (K)	600	1000
H2 Mass Fraction	0.05	0
CH4 Mass Fraction	0.45	0
O2 Mass Fraction	0	0.2329
N2 Mass Fraction	0.5	0.7671

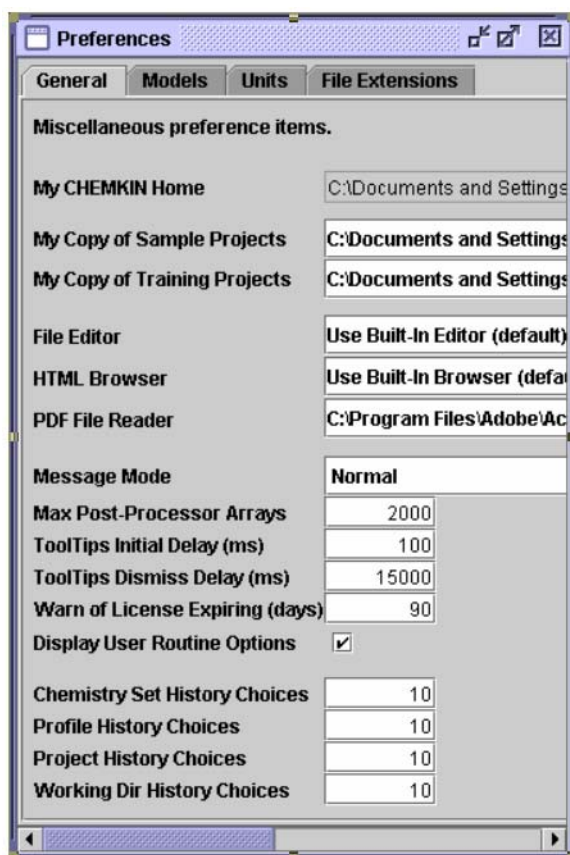
2.6.5.2

Problem Setup

The project file, *cylindrical_shear_flow_profile.ckprj*, is located in the *samples41* directory. The FORTRAN subroutine used to set up inlet profiles is called `CRUPROF` and can be found inside the user routine file *crslaf_user_routines.f* in the *user_routines* directory. The GRI Mech 3.0, described in [Section 2.8.2](#), is used for the gas phase combustion chemistry. No surface chemistry mechanism is needed because the outer wall is chemically inert.

The user routine options are not shown in the graphical User Interface by default. To make these options available from the User Interface, the Display User Routine Options box in the Preferences panel must be checked. [Figure 2-52](#) shows a typical Preferences panel and the Display User Routine Options is located near the bottom of the panel.

Figure 2-52 Preferences Panel Showing the Display User Routine Options Is Enabled.



Once the Display User Routine Options is enabled, the Get Solution Profile from User Routine option will become available when the Reactor Physical Property panel is opened. The check box for the Get Solution Profile from User Routine option is located near the bottom of the Reactor Physical Property panel as shown in [Figure 2-53](#). Once the box is checked, the reactor model will use the initial profiles defined by the `CRUPROF` subroutine instead of the default ones. The other way to activate the `CRUPROF` subroutine is by including the keyword `UPROF` in the reactor model input file `cylindrical_shear_flow__profile.inp`. In addition to the user routine option, other reactor parameters such as the number of grid points in the radial direction, reactor pressure, reactor radius (radius of the outer pipe wall), and ending axial position, must be specified in this panel.

The inlet velocity and temperature are entered in the Stream Property Data panel. These two inlet parameters are required even though their values will be overridden by the user routine later. Note that the cylindrical shear flow reactor model will set the outer wall temperature to the inlet stream temperature when the wall is not chemically active (no surface chemistry). If the inlet temperature given in the Stream Property Data panel is different from that of the outer jet (as defined in the user profile routine CRUPROF), a thermal boundary layer will be developed next to the outer wall.

Figure 2-53 Get Initial Solution Profile from User Routine Check box.

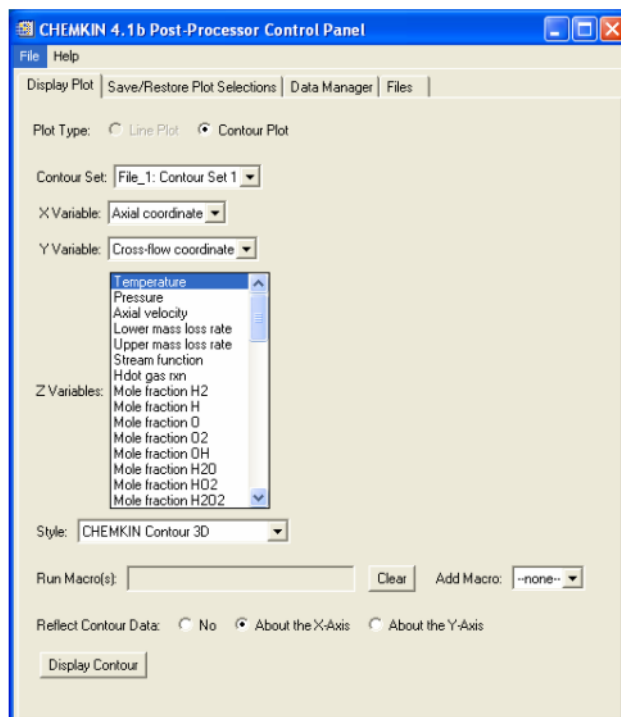
The screenshot shows the 'C1_Cylindrical Shear Flow' reactor model settings. The 'Basic' tab is active, displaying the following parameters:

- Number of Grid Points:** 51.0
- Stretch Parameter for Non-uniform Grid:** 1.0
- Ending Axial Position:** 5.0 cm
- Boundary Layer Thickness:** cm
- Reactor Radius:** 4.0 cm
- Pressure:** 1.0 atm
- Reactor Type:**
 - Adiabatic Reactor
 - Heat Flux Per Unit Area (cal/cm²-s)
 - Surface Temperature (K)
 - Spline-fit Surface Temperature Profile (K)
 - Heat Transfer Coefficient (cal/cm²-K)
- Ambient Temperature:** K
- Ramp-up Distance for Surface Temperature:** cm
- Transport Model:**
 - Use Mixture-averaged Transport
 - Use Multicomponent Transport
 - User Defined Mixture Average Transport Properties
- Other Options:**
 - Use Thermal Diffusion (Soret Effect)
 - Use Correction Velocity Formalism
 - Acceleration of Gravity:** cm/sec²
 - Gas Reaction Rate Multiplier:**
 - Surface Reaction Rate Multiplier:**
 - Get Initial Solution Profile from User Routine

2.6.5.3 Project Results

After the simulation has completed successfully, contour plots of solution variables can be visualized in the CHEMKIN Post-Processor. Since this is an axisymmetric problem, the reactor model only solves the top half of the flow domain. To visualize the solutions of the entire physical domain, we can have the CHEMKIN Post-Processor reconstruct contours in the bottom half of the physical domain by “mirroring” the contours with respect to the x-axis. This operation is activated by selecting About the X-Axis under the Reflect Contour Data option, as shown in [Figure 2-54](#).

Figure 2-54 Visualization of Full Computational Domain Can Be Acquired by Selecting Proper Reflect Contour Data Option in the Chemkin Post-Processor Panel.



Once the 3-D contour plot of the full computational domain is displayed in a new plot window, we can add a colorbar to label the contours. We first select the 3-D contour plot to be labeled by right-clicking the mouse over the plot. Then, we click on the **Insert** button on the menu bar to make the pull-down list available (see [Figure 2-55](#)). Select **Colorbar** to insert a contour level legend. By default, the colorbar is horizontal and is shown at the middle lower area of the plot. We can customize the colorbar by adjusting the colorbar properties. Double-clicking on the colorbar will open the Colorbar property panel. We will change Orientation from Horizontal to Vertical, set the Text show to True, and type **Temperature (K)** in the text field next to the Title. [Figure 2-56](#) shows the final look of the Colorbar property panel after all the changes. The contour plot will be updated as changes in the Colorbar property panel are made so we do not need to close the property panel. Finally, we can re-position the colorbar on the plot by dragging it with the right mouse button pressed. The finished 3-D temperature contour plot is shown in [Figure 2-57](#). We can print the contour plot directly to a printer or copy-and-paste it to a document.

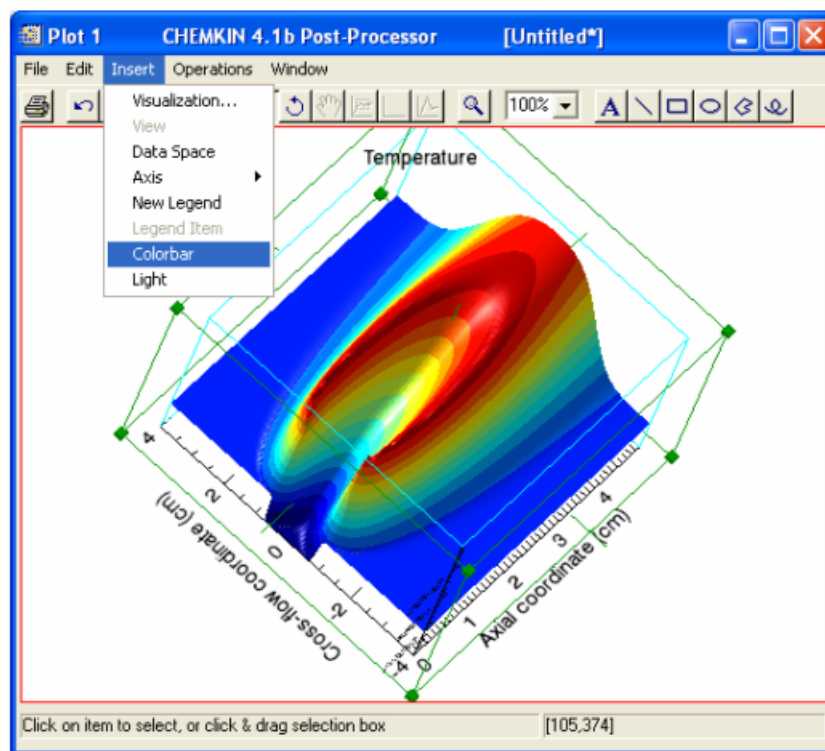
Figure 2-55 Contour Plot Window Showing the Pull-down List Selections of the **Insert** Menu.

Figure 2-56 Colorbar Property Panel.

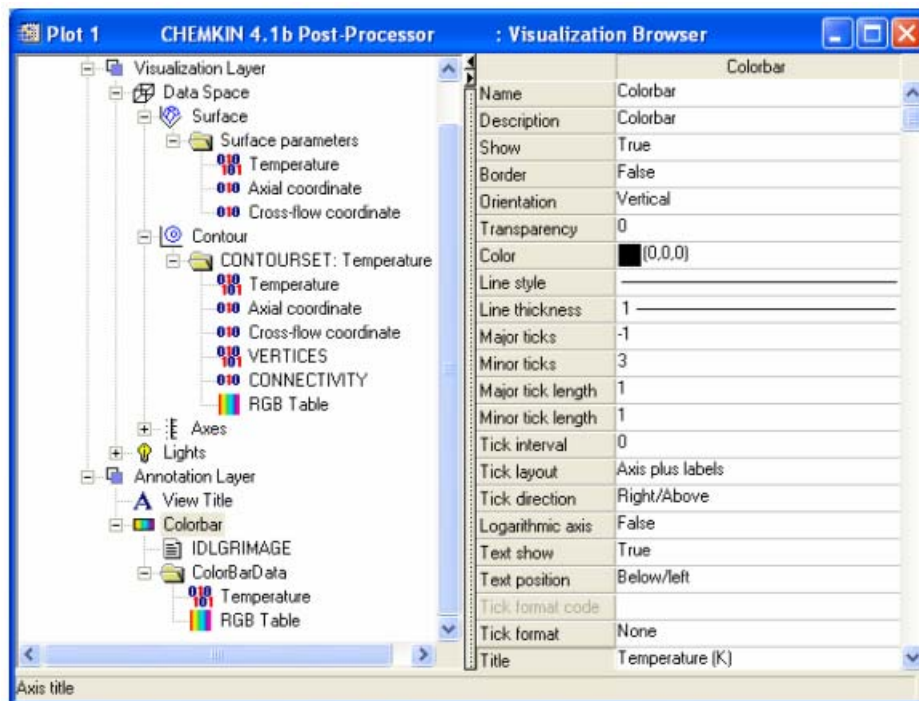
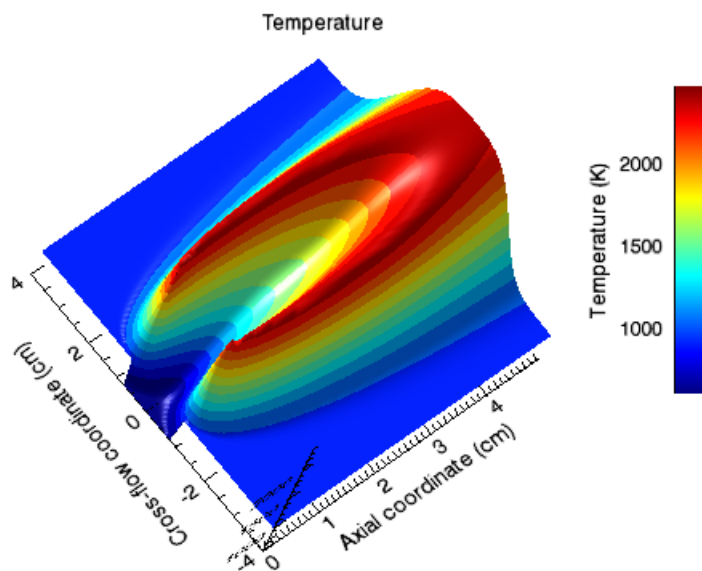


Figure 2-57 Final 3-D Temperature Contours of the Entire Physical Domain with Vertical Contour Legend (Colorbar).



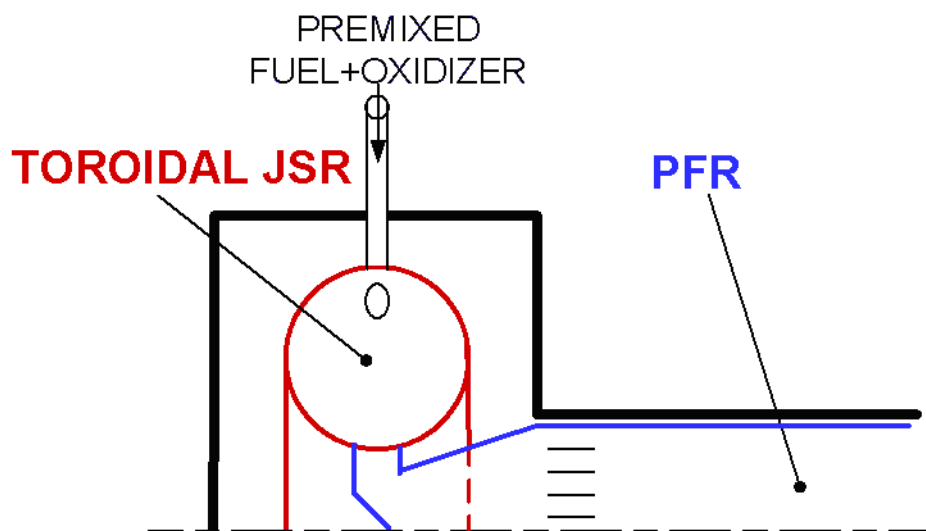
2.7 Particle Tracking Module

2.7.1 Soot Formation and Growth in a JSR/PFR Reactor

The JSR/PFR system developed at MIT²³ provides a good platform for kinetic studies of soot formation and growth because, under the JSR and PFR conditions, the influence of mass diffusion on gas phase species profiles is minimized. The JSR serves as the pre-heat and flame zones of a premixed flame and the PFR is used to simulate the postflame region. From the prospect of model simulation, the JSR/PFR implementation greatly reduces the complexity of the numerical process as well as the run time. A schematic of the JSR/PFR configuration is shown in [Figure 2-58](#).

As an example to assess the performance of the Particle Tracking Module, modified PSR and PFR models are employed to simulate one of the premixed $C_2H_4/O_2/N_2$ experiments by Marr²³. The experimental data include mole fractions of major gas-phase species and PAH's and soot mass concentration at various locations inside the PFR. Therefore, this data set is useful not only to validate the Particle Tracking Module but to provide insights on the kinetics of nucleation and soot growth surface reactions used to simulate the experiment.

23. J.A. Marr, PhD. Thesis, Dept. of Chemical Engineering, MIT (1993).

Figure 2-58 A schematic of the JSR/PFR reactor configuration used by Marr²³

2.7.1.1

Problem Setup

The CHEMKIN project file for this tutorial is named ***reactor_network_soot_JSRRPFR.ckprj*** and is located in the ***samples41*** directory. The reaction mechanisms for ethylene/air combustion and soot formation and growth are described in [Section 2.8](#).

The JSR/PFR experiment shown in [Figure 2-58](#) can be modeled by one PSR and two PFR's in series. The first PSR is for the upstream (or flame zone) JSR, the following PFR is to model the transition piece between JSR and PFR in the experimental setup, and the last PFR is for the postflame PFR where measurement was performed. The main purpose of the transition PFR is to allow the JSR exhaust to cool down from 1630K to 1620K before entering the test section. The diagram view of this three-reactor network is given in [Figure 2-59](#). Since the Particle Tracking Module is activated by special keywords in surface reaction mechanism, all soot simulations will need both gas phase and surface chemistry input files. Once the chemistry files have been pre-processed, the Dispersed Phase tab will appear in the Reactor Physical Properties panel as shown in [Figure 2-60](#). Most parameters for the Particle Tracking Module can be assigned in this Dispersed Phase tab. Initial conditions of the particle size moments can also be specified here. The initial size moments can be constructed from particle number density alone. Additional particle size information such as particle mass density or particle volume fraction can also be specified. Because the dispersed phase does not exist on the reactor wall, the surface area fraction of the particle material must be set to zero in the Material-specific Data tab (see [Figure 2-61](#)). Here, we set Carbon to 0.0 and Wall to 1.0. (Parameters for all materials can be specified on the Reactor Physical Properties tab.)

If particles exist in the inlet streams, their size moments can be provided in the Dispersed Phase tab of the Stream Properties panel. *Figure 2-62* shows the Dispersed Phase tab for inlet streams.

The values of high particle-size moments can become very large so sometimes the absolute tolerance suitable for species mass fractions might not work well for those high moments. Therefore, the Particle Tracking Module allows the tolerances for size moments solutions to be given explicitly for the steady state PSR model. The tolerances for particle size moments can be specified in the Solver window, as shown in *Figure 2-63*.

Once all model parameters, initial/guess conditions and inlet stream properties are set, the JSR/PFR simulation can be launched from the Run Model window like any other CHEMKIN project.

Figure 2-59 Diagram View of the CHEMKIN 4.1 Project Used to Simulate the JSR/PFR Experiment

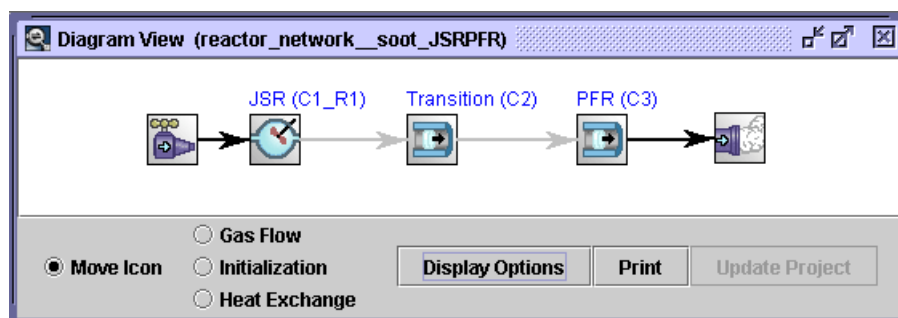


Figure 2-60 Specifying Particle Tracking Module Parameters and Initial Conditions of Particle Size Moments in the Reactor

Property	Value	Units
Number of Moments	3.0	
Minimum Particle Density	100.0	#/cm ³
Critical Particle Class		
Minimum Particle Class		
Exclude Coagulation of Particles	<input type="checkbox"/>	
Coagulation Collision Regime		
Coagulation Collision Efficiency		
Initial Particle Number Density		#/cm ³
Initial Particle Volume Fraction		cm ³ /cm ³
Initial Particle Mass Density		g/cm ³

Figure 2-61 Surface Area Fraction of the Particle Material Must Be Set to Zero in the Material-specific Data Tab. The Default Value of Surface Area Fraction Is One.

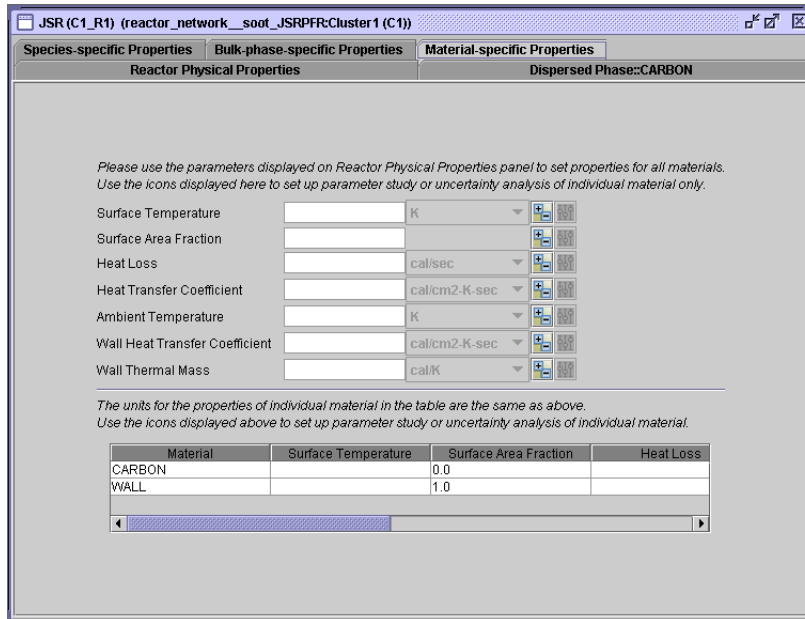


Figure 2-62 Dispersed Phase Tab for Specifying Particle Size Moments in Inlet Streams

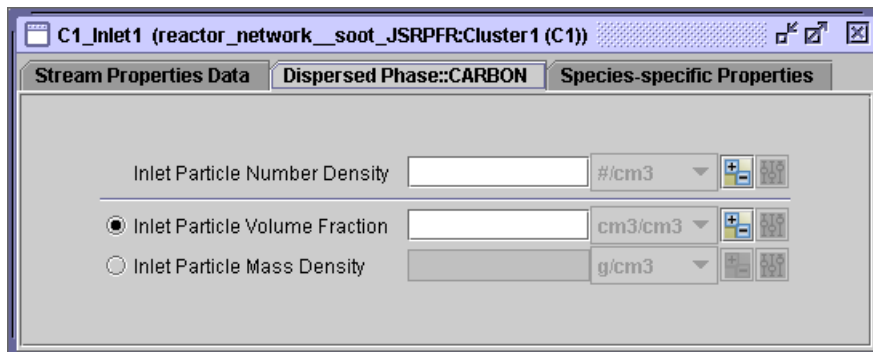
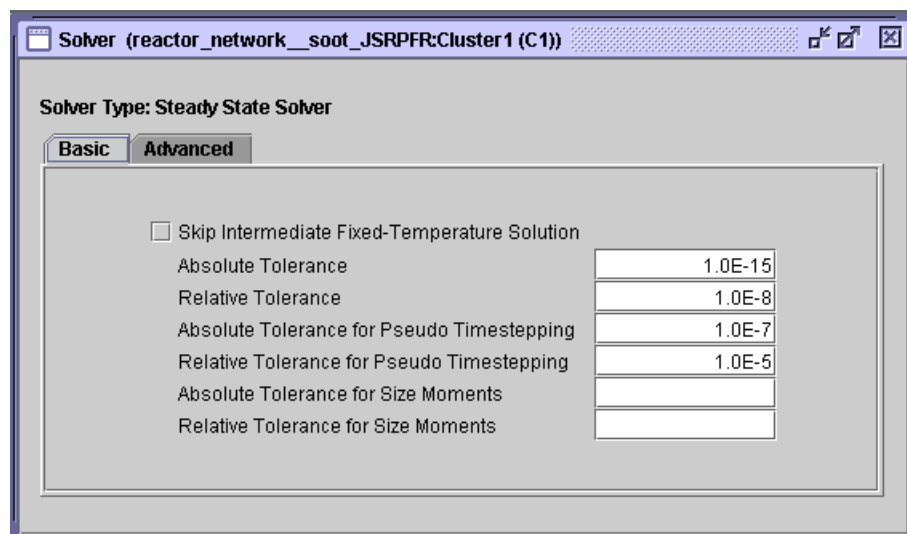


Figure 2-63 Tolerances for Particle Size Moments Can Be Given Explicitly in the Solver Window



2.7.1.2 Project Results

Two simulations, one with both H-abstraction-C₂H₂-addition (HACA) and PAH condensation growth reactions and the other with HACA growth reactions only, are performed so that contributions of either soot mass growth mechanism can be identified.

Results of the $T_{\text{JSR}} = 1630\text{K}$ and $\Phi = 2.2$ case are presented in [Figure 2-64](#) and [Figure 2-66](#). As can be seen from these figures, predictions obtained by the Particle Tracking Module are in good agreements with experimental data. The Particle Tracking Module in general slightly underpredicts gas-phase species. There are many factors that can contribute to the discrepancies shown in the figures. For example, Marr did not provide details composition and temperature of the inlet gas mixture to the JSR. Since the temperature of the JSR is maintained by adjusting the N₂ fraction in the inlet gas stream, uncertainties in inlet condition, reactor heat loss, and reactor residence time will surely affect the simulation results in the PFR section behind the JSR.

Comparison of the predicted and measured soot mass concentration profiles in the PFR is presented in [Figure 2-65](#). While the HACA-only mechanism shows an excellent agreement with the data at the PFR inlet, the slope of the soot mass profile predicted by the HACA-only mechanism (dash-dot line) is much smaller than that of the experimental profile. This is an indication that the HACA growth mechanism alone gives a too-slow soot mass growth rate in the post-flame region. Since the present soot model underpredicts C₂H₂ mole fraction in the PFR ([Figure 2-64](#)), it is possible that the lower C₂H₂ concentration leads to lower HACA soot mass growth rate. It is also possible that another growth mechanism, possibly PAH condensation, might contribute equally to soot mass growth under this condition. The soot mass growth rate predicted by the HACA + PAH mechanism (solid line), on the other hand, shows a much better agreement to the experimental data that the HACA only mechanism does. Since the sticking coefficients of all the PAH considered here are within the range suggested by Marr²³, the PAH contribution to soot mass growth should be reasonably predicted by the model. However, the HACA + PAH mechanism does overpredict the soot mass density at the PFR inlet. Note that experimental data indicate that soot mass density increases by about $4 \times 10^{-8} \text{ gm/cm}^3$ for the first 5 mini-seconds in the PFR. Since the residence time in the JSR is about 5 mini-seconds and the temperature in JSR is only 10K higher than that of PFR, the soot mass density at the PFR inlet should be higher than the measured value. Of course, this assessment is based on the assumption that soot particles start to grow once they are created inside the JSR.

Figure 2-66 compares the contributions of HACA and PAH condensation to soot mass growth by using the Rate-Of-Production (ROP) analysis. PAH condensation accounts for about one-third of the soot mass growth. Note that PAH condensation reactions also contribute to part of the HACA growth by eliminating some H atoms on soot particle surface. The pure HACA growth effect is indicated by the dash-dot line of *Figure 2-65*.

The evolution of average soot particle diameter inside the PFR is shown in *Figure 2-67*. The soot particle diameter increase along the plug flow reactor due to particle coagulation and mass growth. Note that the average particle diameter actually drops a little near the PFR entrance. This signifies that soot nucleation is still occurring as the gas mixture entering the PFR.

Figure 2-64

Comparisons of Mole Fraction Profiles of Selected Gas Phase Species Inside the PFR for the 1630K and $\Phi = 2.2$ Case of the $C_2H_4/O_2/N_2$ JSR/PFR Experiment by Marr²³. Symbols: data; Solid lines: predictions with HACA and PAH condensation growth mechanisms

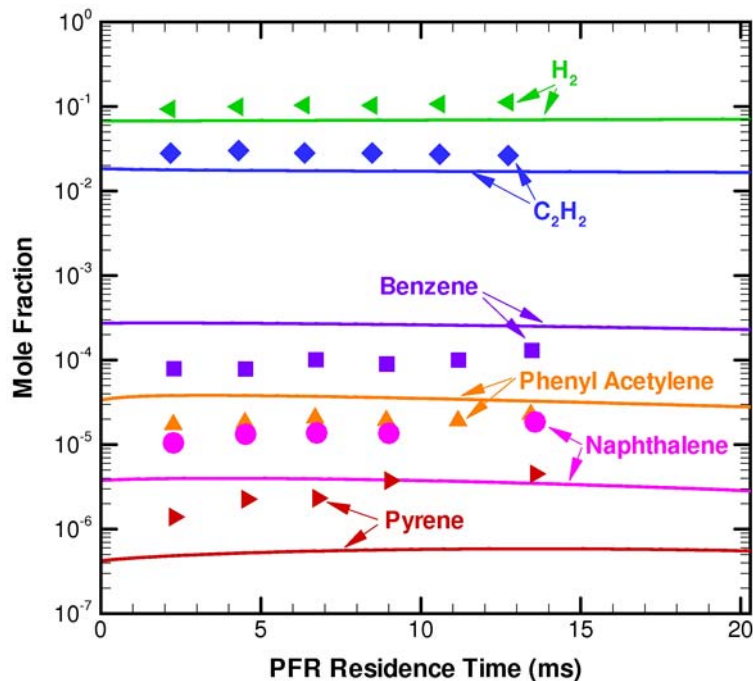


Figure 2-65

Comparisons of Soot Mass Concentration Profiles Inside the PFR for the 1630K and $\Phi = 2.2$ Case of the $C_2H_4/O_2/N_2$ JSR/PFR Experiment by Marr²³. Symbols: data; Solid line: prediction with both HACA and PAH condensation growth mechanisms; Dash-dot line: prediction with HACA growth mechanism only

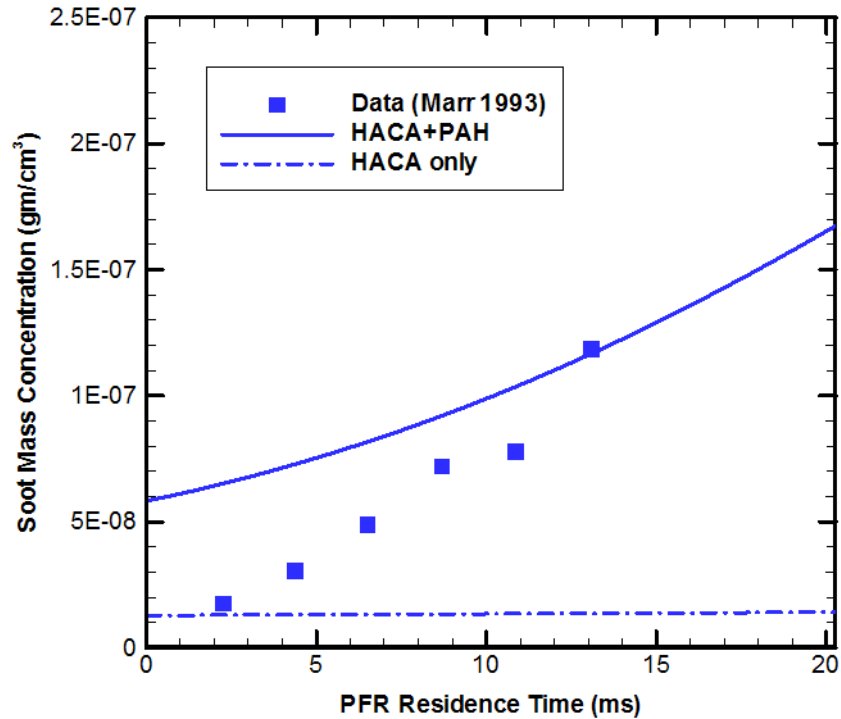


Figure 2-66

Comparison of Contributions of Different Soot Mass Growth Mechanisms by Using the Rate-Of-Production Analysis

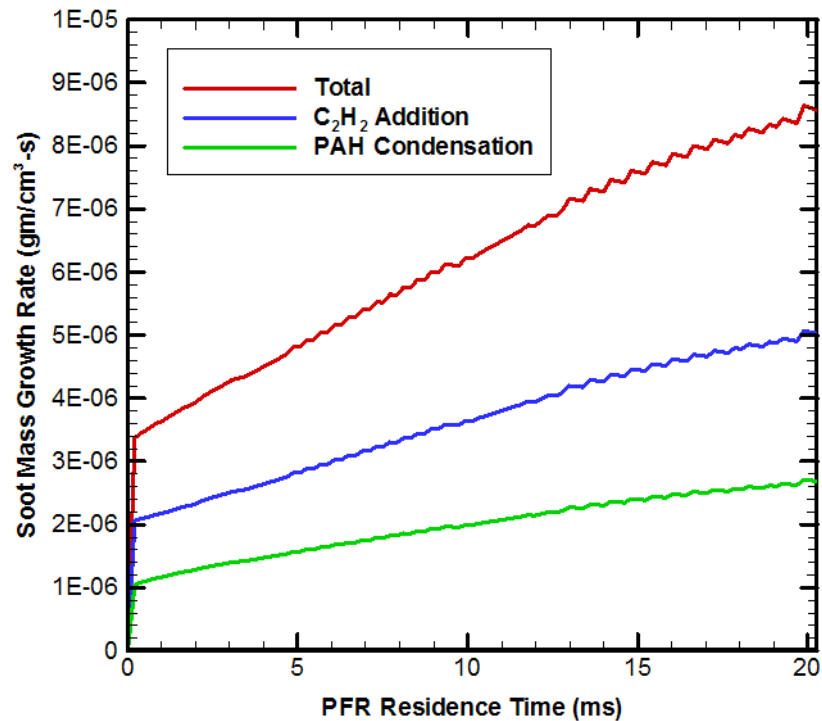
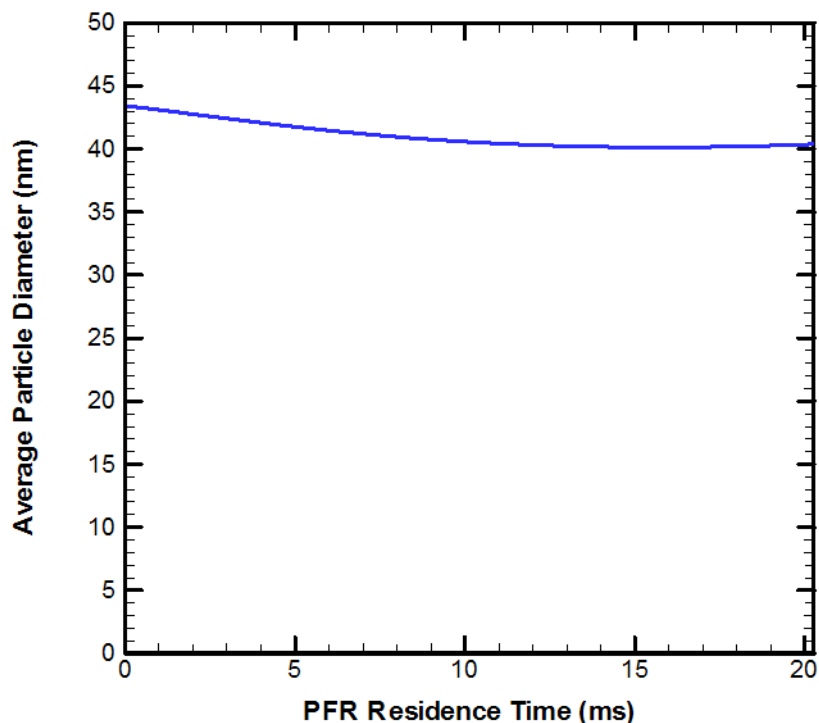


Figure 2-67

The Particle Diameter Evolution Inside the PFR Predicted by the Present Soot Module for the 1630K and $\Phi = 2.2$ case of the $C_2H_4/O_2/N_2$ JSR/PFR Experiment by Marr²³ (see p. 78)



2.8 Chemistry Sets

In this section we provide a brief description of and references for the chemistry mechanisms employed in [Chapter 2](#).

2.8.1 Hydrogen/Air

The chemistry sets used to describe the combustion of hydrogen in air are provided for the purposes of illustration only. These are slight variations of early work done at Sandia National Laboratories, and are out-of-date. The gas-phase kinetics input files are relatively simple. They generally contain 3 elements H, O and N or Ar, and 9 gas-phase species: H_2 , H, O_2 , O, OH, H_2O , HO_2 , H_2O_2 and N_2 or Ar, with about 18-20 reactions. Nitrogen is generally present as N_2 only, where it does not participate in any chemical reactions (i.e., NO formation is not included). Pressure dependencies for reaction rates are not explicitly treated, although there are enhanced collision efficiencies for some reactions.

2.8.2 Methane/Air

Two somewhat different chemistry sets are used in the user tutorials to describe the combustion of methane in air or oxygen. One is the full version of GRImech 3.0,²⁴ which includes the reactions leading to NO_x formation. The other is a smaller reaction mechanism, which is used for the purposes of illustration in cases where reducing computation time is helpful.

2.8.2.1 GRImech 3.0

GRImech version 3.0 is a relatively well-tested reaction mechanism that was developed under the auspices of the Gas Research Institute. This reaction mechanism, consisting of gas-phase chemistry, thermodynamic, and transport data files, is provided as one of the default chemistry sets in CHEMKIN 4 in the system data folder. A detailed description of the development and extensive validation of this mechanism is available.

The gas-phase kinetics input file contains 5 elements, C, H, O, N and Ar, 53 chemical species, and 325 reactions. The reaction mechanism describes the combustion of methane and smaller species such as hydrogen, as well as the formation of nitrogen oxide pollutants. Most of the reactions are reversible; only a small number of irreversible reactions are included. Many of the reactions have explicit descriptions of their pressure-dependencies, using the Troe formulation and including enhanced collision efficiencies for particular species.

2.8.2.2 Reduced Mechanism

This smaller reaction mechanism is from early work at Sandia National Laboratories and is given for purposes of illustration only. The gas-phase kinetics input file contains 4 elements, C, H, O, and N, 17 chemical species, and 58 reversible reactions. The reaction mechanism describes the combustion of methane and smaller species such as hydrogen, but nitrogen is present as N₂ only, and does not participate in any chemical reactions. There is no explicit treatment of pressure-dependencies for reaction rates, although there are enhanced collision efficiencies for some reactions.

24. <http://www.me.berkeley.edu/gri-mech/>.

2.8.3 NOx and CH₄, C₂H₄, C₂H₆, C₃H₆, and C₃H₈

This reaction mechanism is made available by Lawrence-Livermore National Labs. The gas-phase kinetics input file contains 5 elements, Ar, C, H, O, and N, 126 chemical species, and 638 reversible reactions. The chemical kinetic mechanism was validated to describe the promotion effect of hydrocarbons (methane, ethane, ethene, propene and propane) on NO to NO₂ conversion in an atmospheric flow reactor. The NO level was 20 ppm and the hydrocarbon level was 50 ppm. The flow reactor temperature ranged from 600 to 1100 K.

2.8.4 Propane/Air

This mechanism is the result of work at the Center for Energy Research (CER), University of California, San Diego. It consists of 46 species and 235 reactions. The elements constituting the species are N, H, C, O, Ar, and He. The thermodynamic and transport data in this chemistry set are included from the same source. All reactions are reversible, and some of the reactions include pressure-dependencies on the rate constant using the Troe formulation (see [Equation 3-27](#) in the *CHEMKIN Theory Manual*). Enhanced collision efficiencies are used for some reactions. The references for the reaction rate parameters as well as for thermodynamic and transport data can be obtained from the CER website:

<http://maemail.ucsd.edu/combustion/cermech/>

2.8.5 Ethylene/Air Combustion and Soot Formation and Growth

2.8.5.1 Combustion Mechanism and Soot Nucleation Reaction

The C₂H₄-air combustion mechanism of Appel et al.²⁵ is used in the simulation. This reaction mechanism consists of 101 species and 543 reactions which include PAH growth reactions up to pyrene, A4.

According to Frenklach and coworkers^{25,26}, soot particles are created by the dimerization of pyrene molecules. However, the Particle Tracking Module does allow multiple inception paths as suggested by Marr²³ (see p. 78). The kinetic parameters of the soot nucleation reaction are derived by matching the nucleation-only soot mass concentration prediction at PFR inlet to the measurement.

```
(S1) 2A4=>32C(B)+20H(S)+28.72(S) 2.00E08 0.5 0.0
```

25. J. Appel, H. Bockhorn, and M. Frenklach, *Combust. and Flame*, **121**:122-136 (2000).

26. M. Frenklach and H. Wang, in *Soot Formation in Combustion: Mechanisms and Models*, H. Bockhorn (Ed.), Springer-Verlag, pp. 165-192 (1994).

The A-factor computed from the collision frequency between A4 molecules is of the order of 10^{12} and is much larger than the one used in the above nucleation reaction.

2.8.5.2

Soot Mass Growth Reactions

One of the advantages of the Particle Tracking Module is that soot mass growth and oxidation reactions can be provided as regular surface reactions. For example, the H-Abstraction-C₂H₂-Addition (HACA) soot growth sequence proposed by Frenklach and coworkers^{25,26} can be given as:

(S2)	H+H(S)=>(S)+H2	4.20E13	0.0	13000.0
(S3)	H2+(S)=>H(S)+H	3.90E12	0.0	9320.0
(S4)	H+(S)=>H(S)	2.00E13	0.0	0.0
(S5)	H(S)+OH=>H2O+(S)	1.00E10	0.734	1430.0
(S6)	H2O+(S)=>OH+H(S)	3.68E08	1.139	17100.0
(S7)	C2H2+(S)=>H(S)+2C(B)+H	8.00E07	1.56	3800.0

It is easy to see that each sweep of the HACA growth sequence will increase the soot particles by two classes.

Marr²³ (see p. 78) suggested that PAH condensation on the soot particle surface can have significant contribution to soot mass growth in post flame zone. He also found from his experimental study that the collision efficiency of PAH condensation is of the order of 0.1. Since a description on how PAH species interact with a soot particle is not readily available, the PAH condensation reactions used in the simulation are purely hypothetical. Only condensations of major PAH species in the gas mechanism are considered. The reaction orders are determined by fitting the experimental data while keeping the sticking coefficients within the order of 0.1. Basically, the PAH condensation reactions used here are designed to increase soot particle mass in two ways: they grow the soot particle by the addition of PAH species and they remove some H atoms (H(S)) on the soot particle surface so that the more effective soot growth reaction, C₂H₂ addition (S7), can proceed at a greater rate.

(S8)	$A1+6H(S) \Rightarrow 6C(B)+6(S)+6H_2$ FORD/H(S) 1.0/ FORD/(S) 1.0/ DCOL/2.46E-8/ STICK	0.2	0.0	0.0
(S9)	$A1C_2H+6H(S) \Rightarrow 8C(B)+6(S)+6H_2$ FORD/H(S) 2.0/ DCOL/2.46E-8/ STICK	0.21	0.0	0.0
(S10)	$A_2+16H(S) \Rightarrow 10C(B)+16(S)+12H_2$ FORD/H(S) 2.0/ DCOL/4.92E-8/ STICK	0.1	0.0	0.0
(S11)	$A_2R_5+16H(S) \Rightarrow 10C(B)+16(S)+11H_2+C_2H_2O.1$ FORD/H(S) 2.0/ DCOL/4.92E-8/ STICK		0.0	0.0
(S12)	$A_3+20H(S) \Rightarrow 14C(B)+20(S)+15H_2$ FORD/H(S) 2.0/ DCOL/4.92E-8/ STICK	0.1	0.0	0.0
(S13)	$A_4+20H(S) \Rightarrow 16C(B)+20(S)+15H_2$ FORD/H(S) 2.0/ DCOL/4.92E-8/ STICK	0.1	0.0	0.0

Expressing the soot growth sequence as a chain of surface reactions has other advantages. As part of surface mechanism, it is easy to check for the conservation of elements and to perform sensitivity analysis and optimization to these reactions. If information about certain reactions, such as PAH condensation, is available from surface-science experiments, utilization of such information would be straightforward.

2.8.5.3 Soot Oxidation Reaction

Once soot particles are created in the flame zone, they start interacting with the surrounding gas mixture and with one another. Therefore, if oxidizers such as O, OH, and O₂ are available in the gas mixture, the soot particles are also subjected to oxidation. Neoh et al.²⁷ found that the most effective soot oxidizer in the flame zone is OH and determined that the collision efficiency (or sticking coefficient) for the OH oxidation reaction is 0.13. For simplicity, the current mechanism only includes soot oxidation due to OH:



27. K.G. Neoh, J.B. Howard, and A.F. Sarofim, in *Particulate Carbon Formation During Combustion*, D.C. Siegla and G.W. Smith (Eds.), Plenum Publishing Corp., pp. 261-282 (1981).

3 Catalytic Processes

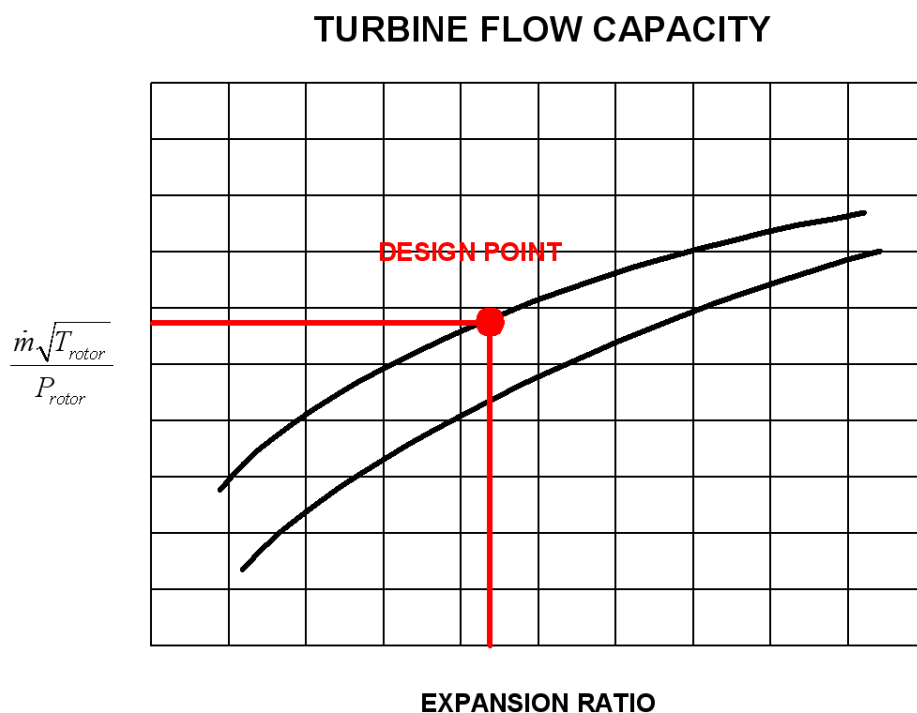
3.1 Catalytic Combustors, Converters and Aftertreatment

3.1.1 Two-Stage Catalytic Combustor

3.1.1.1 Problem description

For this problem, we need to design a virtually zero-NO_x combustor for a sub-scale test unit of our micro-turbine system. This new combustor must also match several gas turbine inlet specifications to optimize the overall system performance under full-load, steady-state operation. A typical gas turbine flow capacity chart is shown in [Figure 3-1](#). The combustor-related design specifications normally include total mass flow rate of the gas turbine system and the turbine rotor inlet temperature, TRIT.

Figure 3-1 Turbine Flow Capacity



The basic rule for minimizing NO_x emissions from a gas turbine combustor is to keep the gas temperature low by operating the combustor under ultra-lean conditions. However, if the fuel-air ratio gets too low, the combustor will run into flame stability problems. We decide to work around the flame stability issue with the implementation of a catalytic combustor. A catalytic combustor produces essentially no NO_x and can convert very lean fuel-air mixtures at relatively low temperatures. There are some disadvantages of a catalytic combustor, though. For instance, the honeycomb monolith introduces a large pressure drop and the thermal mass of the honeycomb material can slow down the catalytic combustor's response to changes in operating conditions. The precious metals used as catalysts are usually very expensive (Pt \$870/oz, Pd \$230/oz) and, to prolong the lifetime of the catalyst, the maximum operating temperature is much lower for catalytic combustors than for homogeneous (gas-phase only) combustors. To raise the catalytic combustor exit gas temperature (< 1200 K) to the desired TRIT (~1475 K), a second stage combustor must be added and it has to be a homogeneous combustor. We expect that almost all NO_x emission from this two-stage combustor system will come from the homogeneous combustor. Fortunately, the gas mixture entering the homogeneous combustor is already at an elevated temperature, we can try to push the fuel-air ratio as lean as possible to minimize NO_x generation without getting into flame stability issues. If the exit temperature of the second combustor becomes too high for the turbine rotor, a third stage can be added to cool the gas down with excess air.

3.1.1.2 Problem Setup

The CHEMKIN project file for this tutorial problem is called ***reactor_network_two_stage_catalytic_combustor.ckprj*** located in the default sample directory. We are going to use methane as the main fuel in our micro-turbine combustor system, so we choose GRI Mech 3.0, as described in section [Section 2.8.2](#), to handle the gas phase combustion and, for the catalytic combustion, the surface reaction mechanism developed by Deutschmann *et al.*²⁸ for methane oxidation on platinum catalyst, as described in section [Section 3.3.1](#), is employed. The chemistry set, ***reactor_network_two_stage_catalytic_combustor.cks***, which includes the gas phase (GRI methane oxidation mechanism) and surface (Deutschmann's methane/platinum catalytic oxidation mechanism) reactions can be found in the working directory ***samples\reactor_network\two_stage_catalytic_combustor***. Since we will use only the perfectly stirred reactor (PSR) and plug flow reactor (PFR) in our model, we do not need any transport data.

Before building a model for our combustor system, we need to find out all the important parameters of the system. The total mass flow rate of our sub-scale micro-turbine system has to match the gas-turbine design point, which, in our case, is 980 g/sec. Since this designed flow rate is too large to be handled by a single combustor, we divide the flow evenly into 6 identical combustor units in parallel and merge them before entering the gas turbine. We set the mass flow rate of each catalytic combustor to 127 g/sec so that there is about 21.5% (or 35 g/sec) excess air per combustor for liner cooling and downstream dilution. Methane and compressed air are pre-mixed before entering the catalytic combustor. We keep the fuel-air mixture very lean so it will not ignite before reaching the catalytic combustor. The gas temperature and pressure at the inlet of the catalytic combustor are 715 K and 3.75 atm, respectively. The inlet gas temperature is higher than that of a homogeneous combustor. We have to use a higher inlet gas temperature to ensure a light-off (or surface ignition) on the catalyst surface. Note that we could lower the inlet temperature if a palladium-based catalyst were used or if a small amount of hydrogen were added to the fuel. However, at this point, we consider methane as the only fuel component.

The catalytic combustor is 10 cm in diameter and 10 cm long. It consists of a metal outer liner providing structure support and a honeycomb monolith core. The catalyst is coated on all internal surfaces of the monolith. The cell density of the honeycomb monolith we selected is 400 cpsi (cells per square-inch) and the cell wall thickness is 0.18 mm. The pressure drop across the monolith is determined to be 0.064 psi/cm for the given flow rate. 5.2 grams of platinum are wash-coated onto the internal surfaces

28. Deutschmann *et al.*, *Proceedings of Combustion Institute*, **26**:1747-1754 (1996).

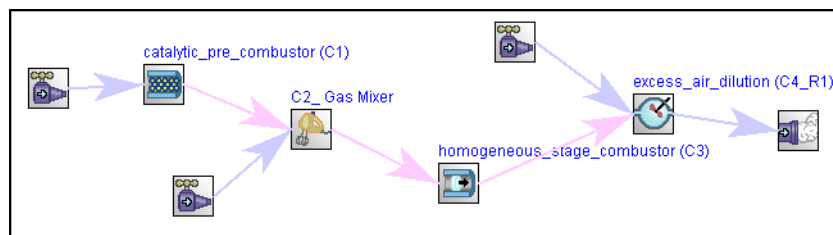
of the honeycomb monolith. The metal surface area is $189 \text{ m}^2/\text{g}$ and the metal dispersion is 70%. Based on the inlet stream properties, mass flow rate, and the geometry of the honeycomb monolith, we find that the inlet velocity of the catalytic combustor should be 1200 cm/sec.

Since we want to make the catalyst last longer to reduce operating costs, we need to keep the catalyst surface below its maximum operating temperature. Theoretically the maximum surface temperature in the catalytic combustor should not exceed the adiabatic flame temperature of the inlet gas mixture. In other words, we can determine the maximum equivalence ratio of the fuel-air mixture entering the catalytic combustor by comparing the adiabatic flame temperatures against the maximum catalyst operating temperature. The adiabatic flame temperature of a given equivalence ratio can be easily obtained by using CHEMKIN's Equilibrium Reactor Model. Of course, the minimum equivalence ratio of the inlet fuel-air mixture is the one below which no light-off is observed on the catalyst surface. Accordingly, we set the equivalence ratio to 0.185.

With all the basic information defined, we are ready to build a simple reactor network model for our two-stage combustor system. We choose the Honeycomb Monolith Reactor Model to represent the first-stage catalytic combustor and a Plug Flow Reactor Model for the second-stage homogeneous combustor. Since all of the initial fuel is expected to be consumed by the catalytic combustor, we have to inject additional fuel to the second-stage homogeneous combustor. To achieve this, we need to add a gas mixer between the Honeycomb Monolith Reactor and the Plug Flow Reactor in our reactor network model. A fourth reactor, which can be either a PSR or a PFR, is added after the PFR (the homogeneous combustor) to simulate the post-flame flow in transition to the gas turbine and to allow the introduction of excess air to cool down the flue gas if needed. [Figure 3-2](#) shows the “diagram” of our combustor system model that comprises four reactor clusters. We will run these clusters in sequence.

Temperatures of both the additional fuel and the excess air are assumed to be the same as the inlet temperature of the catalytic combustor. The mass flow rate of excess air is the difference between the design flow rate of the gas turbine and the exit mass flow rate of the homogeneous combustor. The amount of fuel added to the homogeneous combustor should be able to raise the gas temperature high enough so that, after excess air dilution, the gas temperature can still meet the required TRIT. After a few iterations, we find the additional fuel mass flow rate is 1.5 g/sec.

Figure 3-2 Two-Stage Catalytic Combustor—Diagram View



Now we can further set up our combustor system model by providing proper information on each input panel. The catalyst properties and the honeycomb monolith geometry are entered on two special sub-tabs (please see [Figure 3-3](#) and [Figure 3-4](#)). To find these two special sub-tabs, go to the Honeycomb Monolith Reactor's Catalytic Pre-combustor (C1_) panel and click on the Honeycomb Monolith tab.

Figure 3-3 Catalytic Pre-combustor (C1_)—Honeycomb Monolith, Catalyst sub-tab

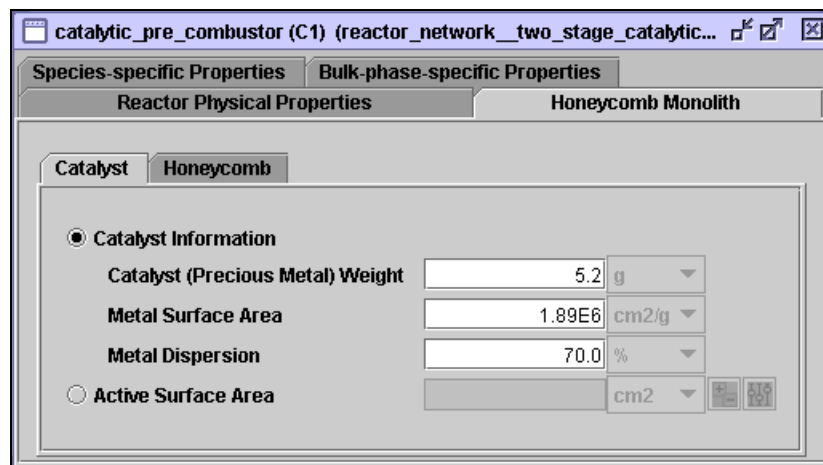
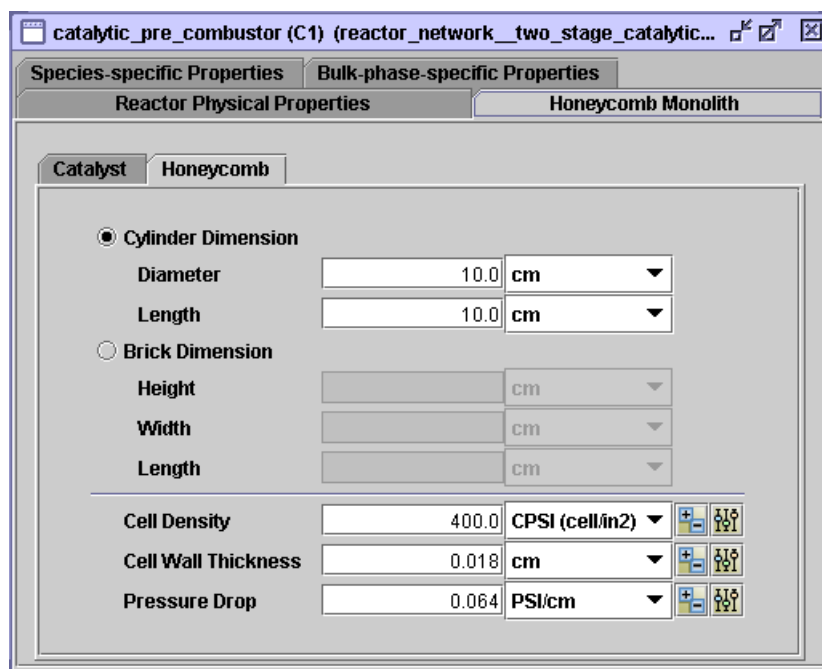
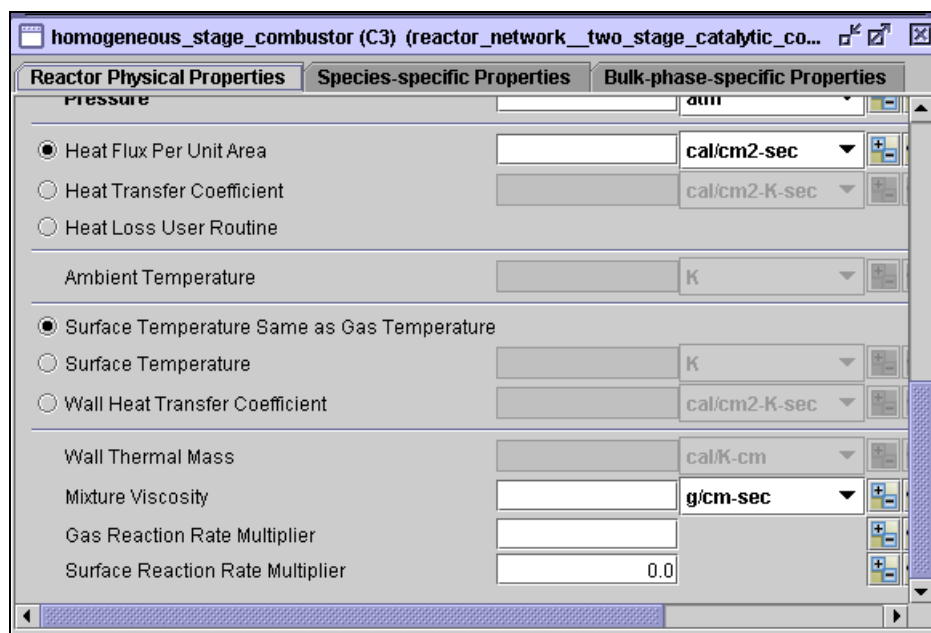


Figure 3-4 Catalytic Pre-combustor (C1_)—Honeycomb Monolith, Honeycomb sub-tab



Since there is no surface reaction in the homogeneous combustor and the post-flame mixer, we need to turn the surface chemistry calculations off in our reactor models. There are several methods to make the models ignore the surface chemistry. Here we choose to set the surface reaction rate multiplier to 0.0, using the parameter at the bottom of the Reactor Physical Property tab as shown in [Figure 3-5](#).

Figure 3-5 Homogeneous Stage Combustor (C3_)—Reactor Physical Property



3.1.1.3 Project Results

We have to run the reactor clusters in order because calculations of later clusters require information from the solution of the previous cluster. After finishing all four cluster runs, we want to see if the predicted mass flow rate and gas temperature at the exit of the last (fourth) reactor cluster match the gas turbine design point targets. The predicted mass flow rate of each combustor system, which is 1/6 of the total mass flow rate, and the turbine rotor inlet temperature can be found from the output file from the last cluster run (see [Figure 3-4](#)).

Figure 3-6 Two Stage Catalytic Combustor—Excess_Air_Dilution (Cluster 4) Output Results

```

RESIDENCE TIME                2.0000E-03  SEC
MASS FLOW RATE                1.6344E+02  GM/SEC
PRESSURE                      3.706      ATM
MASS DENSITY                  8.9762E-04  GM/CM^3
VOLUME                        364.2      CM^3
TOTAL MASS                    0.3269     G
TOTAL SURFACE AREA            0.000     CM^2
TOTAL SURFACE TO VOLUME RATIO 0.000     CM-1
GAS CHEM HEAT PRODUCTION     2.4787E-02  CAL/S/CM^3
TEMPERATURE (INLET: C4_Inlet1) 715.0000  K
TEMPERATURE (INLET: homogeneous_stage_combustor_(C3)_to_excess_air_dilution_(C4_R1)) 1604.8422  K
TEMPERATURE                   1432.      K
SURF TEMP, CATALYST           1431.7645  K (same as gas temp)
HEAT LOSS, CATALYST           0.000     CAL/SEC
SURF CHEM HEAT PRODUCTION,
    CATALYST                   0.0000E+00  CAL/S/CM^2

EXIT  GAS PHASE MOLE FRACTIONS

H2      = 2.4346E-07      H      = 6.4653E-09      O      = 1.2176E-06
O2      = 0.1415        OH      = 4.3865E-05      H2O    = 6.1973E-02
HO2     = 1.7456E-07    H2O2   = 2.1733E-08      C      = 2.7748E-29
CH      = 6.2309E-26    CH2    = 1.7516E-21      CH2(S) = 2.3901E-23
CH3     = 3.4262E-20    CH4    = 7.9325E-20      CO     = 6.7181E-07
CO2     = 3.0997E-02    HCO    = 1.5364E-17      CH2O   = 5.5756E-19
CH2OH   = 4.0071E-24    CH3O   = 1.5159E-23      CH3OH  = 2.8979E-20
C2H     = 5.2478E-24    C2H2   = 5.7414E-19      C2H3   = 2.3233E-27
C2H4    = 5.5634E-25    C2H5   = -1.1224E-29      C2H6   = -8.3607E-28
HCCO    = 7.2071E-23    CH2CO  = 6.2675E-20      HCCOH  = 1.3396E-16
N       = 1.6142E-15    NH     = 1.6120E-15      NH2    = 1.1668E-14
NH3     = 1.9345E-13    NNH    = 2.5381E-14      NO     = 2.1733E-07
NO2     = 2.7833E-09    N2O    = 2.8628E-07      HNO    = 6.8928E-14
CN      = 1.0318E-19    HCN    = 3.2286E-14      H2CN   = 1.6808E-23
HCNN    = 7.8380E-28    HCNO   = 3.0547E-12      HOCN   = 7.9809E-13
HNCO    = 1.0060E-12    NCO    = 4.7661E-15      N2     = 0.7655
AR      = 0.000        C3H7   = 4.0541E-34      C3H8   = 3.6879E-31
CH2CHO  = 4.1871E-27    CH3CHO = 2.0225E-26

Volatile Organic Compounds (ppm): 4.8914E-06
Unburned Hydrocarbons (ppm): 1.2637E-12

SURFACE SITE FRACTIONS IN SURFACE PHASE, PT_SURFACE
Site density = 2.7063E-09 mole/cm^2
Standard State Site density = 2.7063E-09 mole/cm^2
Rate of change of site density = 0.000 mole/(cm^2*sec)

PT(S)    = 9.0909E-02      H(S)    = 9.0909E-02      H2O(S)  = 9.0909E-02
OH(S)    = 9.0909E-02      CO(S)   = 9.0909E-02      CO2(S)  = 9.0909E-02
CH3(S)   = 9.0909E-02      CH2(S)s = 9.0909E-02      CH(S)   = 9.0909E-02
C(S)     = 9.0909E-02      O(S)    = 9.0909E-02

BULK PHASE MOLE FRACTIONS AND ACTIVITIES IN BULK PHASE, PT_BULK
Linear growth rate of this bulk phase = 0.000 cm/sec
Total growth rate of this bulk phase = 0.000 gm/sec
Density of the bulk phase = -1.000 gm/cm^3
Average molecular weight of bulk phase = 195.1 gm/mole

```

Species Name	Mole_frac	Activity	Density (gm/cm ³)	-----Growth Rate-----			
				mole/(cm ² *sec)	gm/(cm ² *sec)	cm/sec	(microns/hr)
PT(B)	= 1.000	1.000	-1.000	0.000	0.000	0.000	0.000

The predicted mass flow rate for each combustor is 163.4 g/sec so the total mass flow rate is 980.4 g/sec (= 6*163.4). The predicted exit gas temperature, TRIT, is 1433.4 K. Both values are very close to the targets. Since our goal is a zero-NO_x combustor, we want to find out NO, NO₂, and N₂O emissions from our new combustor. The solution shows the mole fractions of NO, NO₂, and N₂O are 0.22 ppm, 0.003 ppm, and 0.27 ppm, respectively. All these concentrations are below 1 ppm and are not detectable by instruments. Before we can say a job well done, we need to check on CO and UHC (unburned hydrocarbon) emissions as well. Sometimes CO and UHC concentrations increase when we try to minimize NO_x formation. Our model indicates our combustor has sub-ppm CO emission (0.66 ppm) and essentially no UHC.

We are also interested in knowing how the gas temperature varies inside the combustor system and whether the maximum temperature inside the catalytic combustor exceeds its safe operating temperature. We can use the CHEMKIN Post-Processor to obtain profiles along the two-stage combustor for quick visual confirmation. We only need to load solutions of the first (catalytic combustor) and the third (homogeneous combustor) clusters into the CHEMKIN Post-Processor because the other two clusters yield a single solution point each. The “axial” profiles of gas temperature, pressure, and mole fractions for CH₄, CO and NO are shown in the following figures.

Figure 3-7 Two Stage Catalytic Combustor—Temperature Comparison

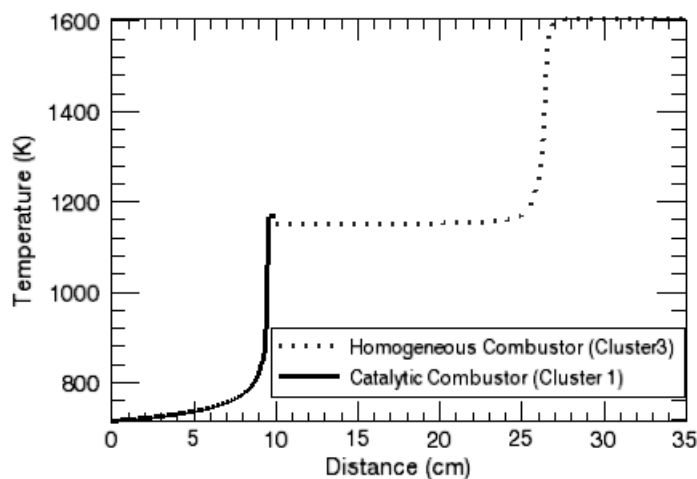


Figure 3-8 Two Stage Catalytic Combustor—Pressure Comparison

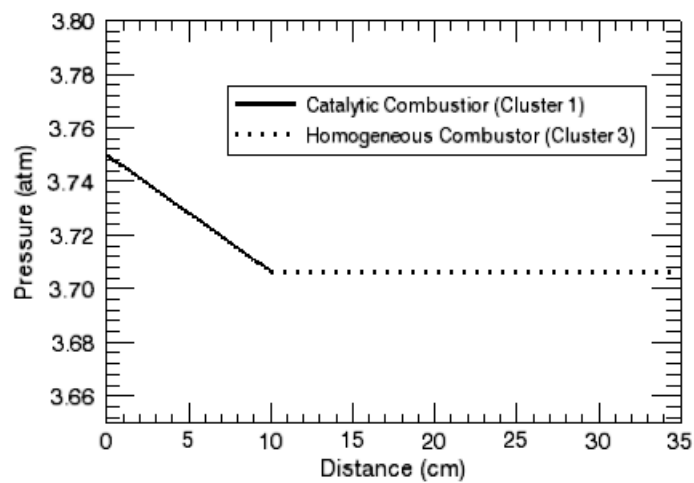
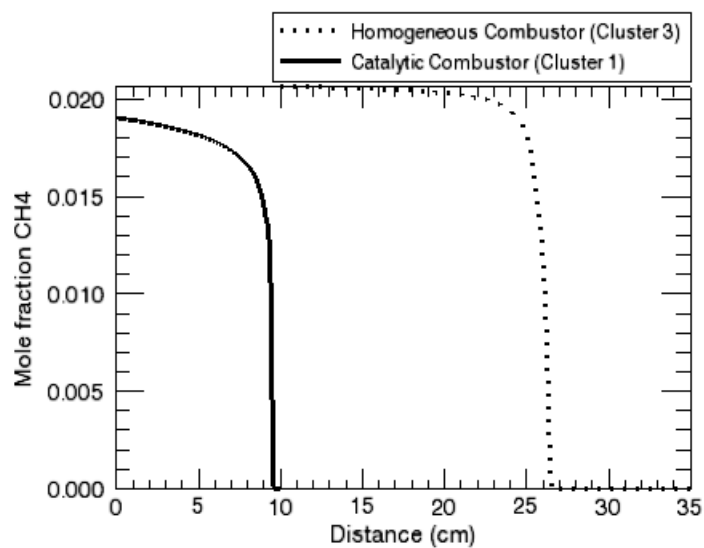
Figure 3-9 Two Stage Catalytic Combustor—CH₄ Comparison

Figure 3-10 Two Stage Catalytic Combustor—CO Comparison

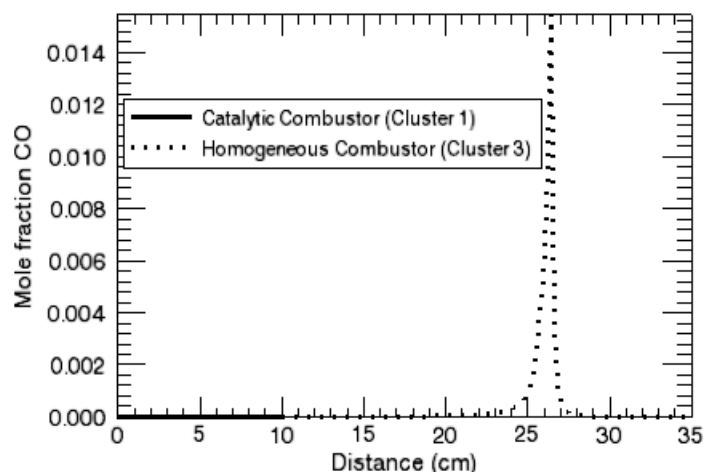
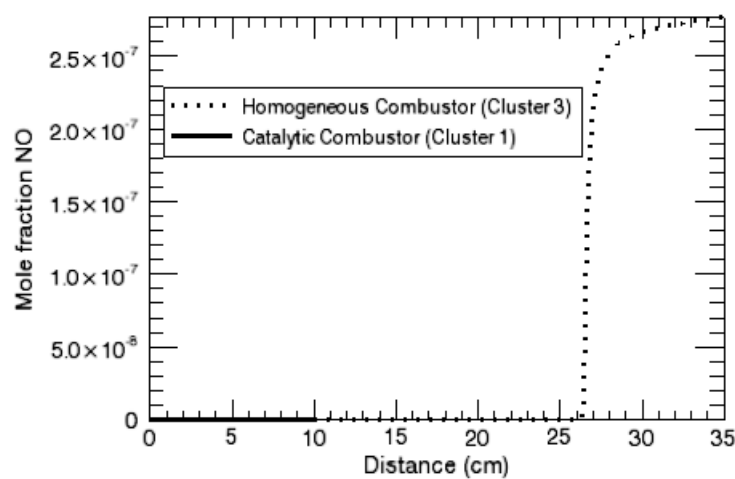


Figure 3-11 Two Stage Catalytic Combustor—NO Comparison



The temperature profile ([Figure 3-7](#)) indicates that the gas temperature is increased in two steps. The catalytic combustor has a lower operating temperature and only raises the gas temperature to about 1100 K. The homogeneous combustor, which can operate at higher temperatures, further raises the gas temperature to more than 1600 K before the excess air cools the gas mixture down to the target TRIT at about 1450 K. The CO profile ([Figure 3-10](#)) has a spike inside the homogeneous combustor corresponding to the gas-phase ignition and all CO generated is later consumed in the post-flame region. The model also predicts that NO_x is formed after gas-phase ignition and, unlike CO, its concentration continues to grow in the post flame region.

Note that this project only addresses the limitation posted by chemical kinetics. Mass transport, i.e., diffusion and turbulence mixing, can become the limiting factor in determining the performance of this gas combustor system. At high pressure, species transport between the bulk gas and the active surface can be the rate-limiting factor for the catalytic combustor. Poor molecular diffusion at high pressure could also affect the homogeneous combustor. When the mixing between injected fuel and oxygen in the hot gas slows down, the ignition distance becomes longer and could even cause flame-out in the homogeneous combustor. The tutorial in [Section 2.6.3](#) addresses some of these issues.

3.1.2 Engine Exhaust Aftertreatment with a Transient Inlet Flow

3.1.2.1 Project Description

This user tutorial demonstrates a user-defined subroutine that defines transient inlet conditions for engine exhaust aftertreatment. In this sample, the engine-out conditions as a function of time are stored in a tab-delimited text file. A user subroutine is defined to read the contents of this file and then, at every time point during the simulation, the user routine provides the inlet composition, temperature, and flow rate to the PSR model. The reactor being modeled is an approximation of a 3-way catalytic converter, designed to convert NO_x , CO, and un-burned hydrocarbons (UHCs) through catalytic surface reactions on a platinum/rhodium catalyst. For this sample, gas-phase chemistry is neglected in order to focus on the surface conversion reactions. This sample routine is already compiled and linked into the standard installation, so it can be run from the CHEMKIN Interface without the need for a FORTRAN compiler. Modifying the behavior of the sample user routine being used requires access to an appropriate FORTRAN compiler on the computer where CHEMKIN is installed, but changing the numerical values of the input data does not.

3.1.2.2 Project Setup

The project file is called ***psr__aftertreatment.ckprj***. Catalytic conversions of NO_x , CO, and UHCs are modelled by the Pt/Rh three-way catalyst surface mechanism described in [Section 3.3.2](#). The data files used for this sample are located in the ***samples\psr\aftertreatment*** directory. This reactor diagram contains only one gas inlet and one perfectly-stirred reactor model. The sample user subroutine that is used to define the inlet is provided in the standard CHEMKIN installation location, in the ***user_routines*** sub-directory. The FORTRAN subroutine is named `USRINLET` and is included in the file *aurora_user_routines.f*. The subroutine is discussed in more detail below.



Before running this sample problem from the CHEMKIN Interface, the Display User Routines box on the General tab of the User Preferences panel must be checked.

3.1.2.2.1

Reactor and Inlet Settings

On the Reactor Physical Property tab of the C1_ PSR panel, first the problem type is selected as Solve Gas Energy Equation with the Transient Solver. In this case, the reactor volume is the void volume in the converter honeycomb or porous media, estimated here as 1400 cm³ for the entire length of the converter. Similarly, the reactive (internal) surface area within the converter is estimated based on the void geometry to be 59000 cm². No residence time is input because the volume and flow rates are specified. The initial temperature (296.15 K) is input, along with the pressure (1 atm), and the fact that the system is treated as adiabatic (no heat loss).

On the Species-specific Properties tab of the C1_ PSR panel, the initial conditions of the converter system, prior to the exhaust gas flowing through the system, are assumed to be air and are input on the Initial Gas Fraction sub-tab. The surface site fractions are estimated based on initial tests of the mechanism. Often choosing the initial guess for the site fractions can be difficult and may require some trial and error to obtain convergence at the first time step. In this case, O(S) is assumed to dominate the platinum portion of the catalyst and CO(S1) the rhodium portion. These site species are set to 1.0 on the Surface Fraction sub-tab to provide the initial conditions for the catalyst surface.

The gas inlet has been given a name that reflects its function, **engineout**. On the Stream Property Data tab of the engineout panel, the Use Inlet User Routine button is selected, which indicates that information about the gas inlet composition, flow rate and temperatures should be obtained from the user inlet routine. The user routine pre-packaged with CHEMKIN reads a text file. The name of this file, **engineout.txt**, is set in the FORTRAN subroutine. The inlet conditions, some of which are shown in [Table 3-1](#), are representative of measurements that might be taken during an engine test, where engine load and therefore exhaust flow rates and composition vary as a function of time. In this case, mole fractions for only a few species are provided (CO, NO, UHCs, and O₂). We will assume that the balance of the gas can be represented by N₂ and that C₃H₆ will chemically represent the UHCs. On this panel, the box is also checked to indicate that flow rates are given in volumetric flow units, rather than mass flow units.

On the Basic tab of the Solver panel, the end time of the simulation is set to 100 sec. Although the input data file extends to longer times, this is sufficient for this demonstration. The maximum Solver Time Step is set to 1 msec, the Time Interval for Printing the solution to the text output file is set to 10 sec, and the Time Interval for Saving Data is set to 1 sec. There are no inputs on the Output Control or Continuations panels for this problem.

Table 3-1 Excerpt of Data Representing Engine-out Test Measurements

<i>Time(s)</i>	<i>InletT(C)</i>	<i>Flow(SLM)</i>	<i>C_{3xx}(ppm)</i>	<i>CO(ppm)</i>	<i>CO₂(ppm)</i>	<i>NO_x(ppm)</i>	<i>O₂(ppm)</i>
0	23.9	87.08	924	4341	22764	38	127856
0.5	25	85.49	1238	23557	49535	127	77187
1	20.1	27.15	1369	36212	66499	126	50914
1.5	22.6	81.89	1267	37984	80793	118	28314
2	39.1	81.2	1176	29212	95735	92	14359
2.5	66.2	83.17	1016	18119	104492	89	9577
3	88.2	86	999	10391	110148	108	7744
3.5	111.3	87.08	912	5786	111276	101	13012
4	125.4	85.42	877	3663	112346	111	8645
4.5	141.2	82.53	843	2532	111864	104	11867
5	163	81.1	808	1967	111803	110	16508
5.5	175.2	82.43	681	1619	111685	101	12255
6	189.8	85.28	756	2224	110433	119	15728
6.5	208.9	87.06	825	6022	108765	207	7865
7	218.2	86.12	825	11532	107414	366	12835
7.5	230.6	83.34	732	9837	105707	440	20696
8	244.3	81.27	857	5259	102752	446	24211
8.5	251.6	193	957	2823	100132	381	28629
9	272.1	374.28	991	2942	99228	354	28534
9.5	297.4	479.67	864	2355	101356	331	28906
10	313.6	483.61	851	1514	103822	309	29511
10.5	333.2	431.87	796	1343	105570	276	23807
11	347	388.16	788	1251	106826	241	26600
11.5	349.6	344.94	868	910	106112	207	26409

3.1.2.2.2

Details of the User Routine

The subroutine for the user-defined inlet is reproduced in [Figure 3-12](#). The data in [Table 3-1](#) has units of parts-per-million for species composition, standard liters per minute for flow rate, and degrees Celsius for temperature, which are not the standard units used by the CHEMKIN software. The user routine must therefore perform necessary conversions before providing the data to the PSR program executable. It is also responsible for interpolating between data points for each time value needed during the time integration. At each time step during the transient simulation, the PSR program will call `USRINLET`. Parameters needed by the `USRINLET` subroutine are passed in through integer and real workspace arrays called `IINWRK` and `RINWRK`, respectively. The comments at the top of the code explain what parameters are stored in these arrays.

The sample `USRINLET` code in [Figure 3-12](#) reads in data from a file on the first call, as determined when the time is equal to the starting time of the simulation. In this section, the routine uses the CHEMKIN library routine `CKCOMP` to find the location of a given species name in the gas-phase species array (`KNAMES`). Conversion from Celsius to Kelvin and from parts-per-million to mole fraction are performed as the data is read and stored on the first call. On subsequent calls, the data is accessed from memory (stored in a FORTRAN common block), and values are interpolated for the specified simulation time. The interpolation uses the CHEMKIN GAS-PHASE KINETICS library routine `CKBSEC` to linearly interpolate between the data points. Before returning, the routine converts the flow rate from standard liters per minute (slm) to standard cubic centimeters per minute (scm). Note that the routine could have been written to return mass flow rate in units of g/sec. In this case, however, CHEMKIN Interface inputs tell the program to expect user-defined flow rates in units of scm.

Figure 3-12

Sample `USRINLET` Subroutine for User-Defined Transient Inlet Conditions

```

      SUBROUTINE USRINLET (LIUIN, IINWRK, LRUIN, RINWRK, INAME, KNAMES,
      1      FLRT, TINL, TEIN, XIN)
C This is a USER SUBROUTINE for defining Inlet properties
C as an arbitrary function of time.
C Use of this subroutine is controlled by the PSR program
C keyword, USRIN, as described in the CHEMKIN Input Manual.
C
C The subroutine USRINLET is used to supply values of
C   FLRT - Real scalar, Mass flow rate in g/s
C           (or if SCCM are the preferred units,
C           use keyword LFPSC in addition to USRIN)
C   TINL - Real scalar, Inlet temperature (K)
C   TEIN - Real scalar, Inlet electron temperature (K)
C   XIN(*) - Real array, Gas-phase reactant composition of
C             the inlet (mole fraction);
C             The length of this array is *exactly* KKGAS,
C             the number of gas-phase species in the problem.
C and the user may set the Integer flag
C   IINWRK(1) - if 0, inlet parameter setting was successful,
C             else, there was a problem, so discontinue calculations
C
C Given the following data:
C
C   LIUIN - Integer scalar, length of some Integer workspace

```



```

C      IINWRK(*) - Integer workspace array, containing
C      IINWRK(2), LOUT - if positive, the unit number of an open output file
C      IINWRK(3), IPSR - PSR index number
C      IINWRK(4), IINL - Index number of an Inlet of IPSR
C      IINWRK(5), KKGAS- Gas-phase species count
C      IINWRK(6), LENRGY-If 0, then inlet temperature TINL is fixed,
C                          else TINL must be supplied here
C      IINWRK(7), LENRGE-If 0, then inlet electron temperature TEIN is fixed,
C                          else TEIN must be supplied here
C
C      LRUIN - Integer scalar, length of some Real workspace
C      RINWRK(*) - Real workspace array, containing
C      RINWRK(1), TSTART - Initial time (sec.) of calculation
C      RINWRK(2), TIM - Current time (sec.)
C
C      INAME - Character-string Inlet name
C      K NAMES- Character-string array, Gas-phase species names
C*****
C      IMPLICIT DOUBLE PRECISION (A-H, O-Z), INTEGER (I-N)
C      PARAMETER (PATM = 1.01325D6,TSTD=273.15)
C      Variables passed in from calling routine
C      DIMENSION IINWRK(LIUIIN), RINWRK(LRUIN)
C      CHARACTER*16 INAME, K NAMES(*)
C      Arrays returned by this user routine
C      DIMENSION XIN(*)
C      Local variables:
C      CHARACTER*80 MYFILE
C      PARAMETER (MYFILE = 'engineout.txt',LUNIT=33,
1          MXPTS=10000,MXSPEC=6)
C      Local storage space for variables
C      CHARACTER*16 MYSPEC(MXSPEC)
C      CHARACTER*80 HEADER
C      LOGICAL LENRGY,LENRGE
C      DIMENSION PPM(MXSPEC)
C      COMMON/USRINL1/ MAPSP(MXSPEC),NPTS
C      COMMON/USRINL2/ TIMEPT(MXPTS),SLMPT(MXPTS),XINPT(MXPTS),
1          TPT(MXPTS)
C      set error flag
C      IINWRK(1) = 0
C      set local variables from workspace data provided
C      LOUT = IINWRK(2)
C      IPSR = IINWRK(3)
C      IINL = IINWRK(4)
C      KKGAS= IINWRK(5)
C      LENRGY=IINWRK(6).GT.0
C      LENRGE=IINWRK(7).GT.0
C
C      TSTART=RINWRK(1)
C      TIME =RINWRK(2)
C
C      Initialize returned variables
C      FLRT = 0.0
C      TINL = 298.
C      TEIN = 298.
C      DO K = 1, KKGAS
C          XIN(K) = 0.0
C      ENDDO
C
C      First time in, read in all the points so we don't have to do
C      IO on each call. Interpolate from saved points thereafter
C      IF (TIME .EQ. TSTART) THEN
C          Open and read the time-date file
C          Store points in arrays for access/interpolation at later times
C          IOS = 0
C          OPEN(LUNIT, FILE=MYFILE, FORM='FORMATTED', STATUS='OLD',
1              IOSTAT=IOS)
C      Check that file open was successful, if not return with error
C      IF (IOS .NE. 0) GO TO 1000
C
C      Map input species to CHEMKIN names and find indices
C      MYSPEC(1) = 'C3H6'
C      MYSPEC(2) = 'CO'
C      MYSPEC(3) = 'CO2'
C      MYSPEC(4) = 'NO'
C      MYSPEC(5) = 'O2'
C      MYSPEC(6) = 'N2'
C      DO MYK = 1, MXSPEC
C          CALL CKCOMP(MYSPEC(MYK),KNAMES,KKGAS,INDX)
C          IF (INDX .GT. 0 .AND. INDX .LE. KKGAS) THEN
C              MAPSP(MYK) = INDX
C          ENDDIF

```

```

      ENDDO
C      Read in the arrays of available information
C      In this case file format is as follows:
C      Time(s),T(C),Flrt(SLM), C3H6(ppm),CO(ppm),CO2(ppm),NO(ppm),O2(ppm)
      READ(LUNIT, 'A', END=800, ERR=1000) HEADER
      NPTS = 0
      ZERO = 0.0
      DO I = 1, MXPTS
        READ(LUNIT, *, END=800, ERR=1000)
1       TIMEPT(I),TCELS,SLM,(PPM(K),K=1,MXSPEC-1)
        NPTS = NPTS + 1
        TPT(I) = TCELS + 273.15
        SLMPT(I) = SLM
        XSUM = 0.0
        DO MYK = 1, MXSPEC-1
          XINPT(I,MYK) = PPM(MYK) * 1.E-6
          XSUM = XSUM + XINPT(I,MYK)
        ENDDO
C       Set fraction of N2 = 1 minus the sum of others
        XREM = 1.0-XSUM
        XINPT(I,MXSPEC) = MAX(XREM,ZERO)
C       Note: if XSUM > 0.0, AURORA will normalize so that sum = 1
      ENDDO
800    CONTINUE
      IF (NPTS .EQ. 0) GO TO 1000
      CLOSE(LUNIT)
    ENDF
C
C      Interpolate data for input time and perform units conversions
      XSUM = 0.0
      DO MYK = 1, MXSPEC-1
        XIN(MAPSP(MYK)) = CKBSEC(NPTS,TIME,TIMEPT,XINPT(1,MYK))
        XSUM = XSUM + XIN(MAPSP(MYK))
      ENDDO
      XREM = 1.0-XSUM
      XIN(MAPSP(MXSPEC)) = MAX(XREM, ZERO)
      SLM = CKBSEC(NPTS,TIME,TIMEPT,SLMPT)
C      Convert from SLM to SCCM
      FLRT = SLM * 1000.
      IF (LENRGY) THEN
C        Set the gas inlet temperature
        TINL = CKBSEC(NPTS,TIME,TIMEPT,TPT)
      ENDF
      IF (LENRGE) THEN
C        Set the electron inlet temperature
        TEIN = TINL
      ENDF
      RETURN
C
1000  CONTINUE
      IF (IOS .NE. 0) THEN
        WRITE (LOUT, *) ' ERROR...OPEN failure on inlet data file'
      ELSE
        WRITE (LOUT, *) ' ERROR...READ failure on inlet data file'
      ENDIF
      CLOSE (LUNIT)
      IINWRK(1) = 1
C
      RETURN
      END

```

3.1.2.3

Project Results

Figure 3-13 shows molar conversions for C_3H_6 , CO, NO as a function of time. The effectiveness of conversion can also be viewed by comparing the inlet mole fraction to the outlet mole fractions, as shown in *Figure 3-14* for C_3H_6 . These figures clearly show that C_3H_6 and CO are converted more effectively than NO under these conditions. Early in the simulation, the conversion rates are low for all of these species. Although at $t = 0$, the calculated molar conversion is 100%, this is simply due to setting the initial conditions in the reactor to pure air, which determines the initial

exit flow. At certain times the calculated conversion rates for CO and NO actually go negative. This results from the fact that CO and NO can be formed on the surface and thus can be “produced” as the state of the surface changes. [Figure 3-15](#) shows inlet and exit gas temperatures as a function of time. Temperatures show that the gas heats up relative to the inlet gas due to exothermic surface reactions. The catalyst does not become effective until it reaches a temperature above about 600 K, which is consistent with the work by Chatterjee et al.²⁹

Figure 3-13 Engine Exhaust Aftertreatment—Molar Conversion Rates

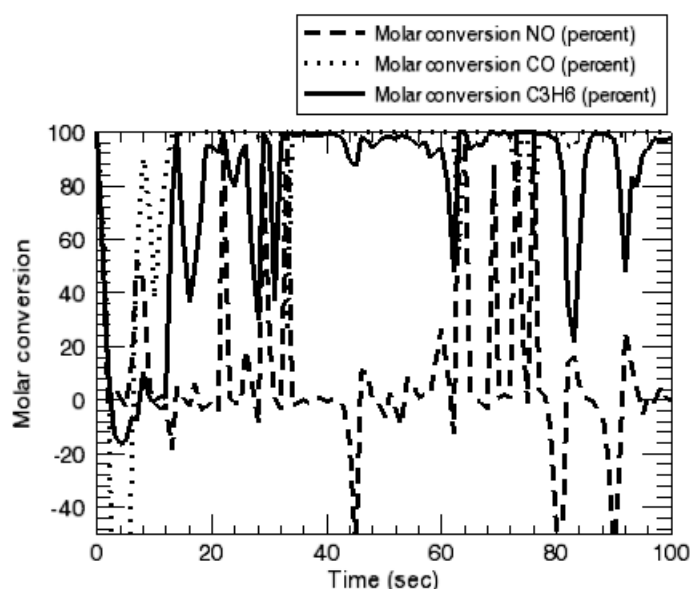
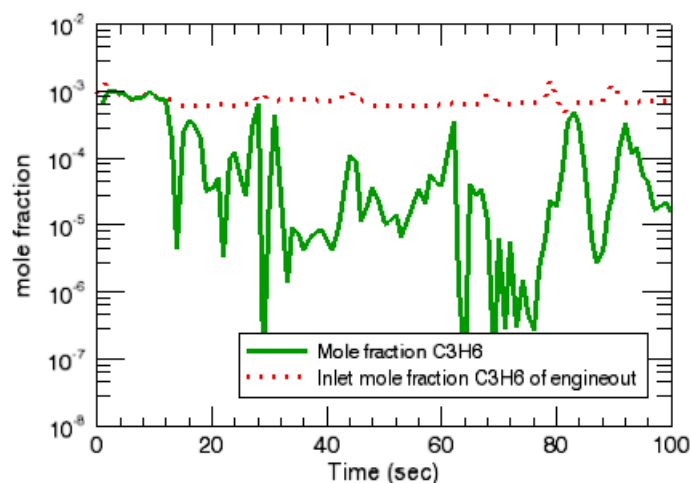
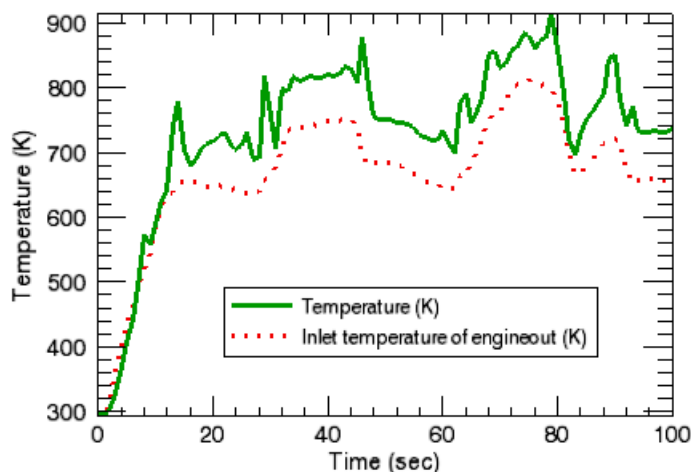


Figure 3-14 Engine Exhaust Aftertreatment—Mole Fractions



29. D. Chatterjee, O. Deutschmann and J. Warnatz, “Detailed Surface Reaction Mechanism in a Three-way Catalyst,” *Faraday Discussions*, **119**:371-384 (2001).

Figure 3-15 Engine Exhaust Aftertreatment—Gas Temperatures



3.2 Parameter Studies

3.2.1 Parameter Study Facility for Surface Chemistry Analysis

The science of surface chemistry has undergone rapid development in recent years, and there is a trend towards use of more detailed “microkinetic” models, especially in the field of catalysis. However, compared with gas-phase combustion problems, surface reaction mechanisms often contain larger uncertainties in reaction rate coefficients that must often be estimated by semi-empirical methods. For this reason, and because there are variabilities in the catalyst definition, it is often necessary to adjust kinetic parameters to model a specific catalytic system. Thus it is of interest to see how uncertainties that exist in surface mechanisms affect predicted modeling results. Performing a parameter study, which varies key reactions in the system, is one way to analyze these effects.

In this tutorial, we apply a parameter study to investigate the effects of a reaction rate coefficient for a catalytic oxidation problem. The associated project file is called ***honeycomb_monolith_reaction_rate_param_study.ckprj***. The chemistry-set files used for this sample problem are located in the ***ParameterStudy*** folder of your CHEMKIN ***samples*** directory. For the gas-phase kinetics, we employ the GRI gas-phase mechanism and thermodynamic data for methane combustion. For the catalytic surface-chemistry that describes the oxidation of methane on a platinum catalyst, we use the surface chemistry mechanism reported by Chou, et al.³⁰ In this example’s reactor model, we focus on the first stage (Honeycomb Catalytic Reactor) of the Two-stage Catalytic Combustor Sample (***reactor_network_two_stage_catalytic_combustor.ckprj***).

3.2.1.1 Determining Influential Reactions with Sensitivity Analysis

We are first interested in identifying those surface reactions that will be the most influential to our output parameters of interest for the conditions in this sample. Since this is a catalytic combustion case, where the catalytic stage serves to preheat the gas, the reactor temperature is of interest. We therefore first run a sensitivity analysis in order to determine the sensitivity of Temperature to the Arrhenius pre-exponential factors (A-factors) of the various reaction-rate constants. In order to accomplish this, first open the **Mechanism_ParameterStudy** project and pre-process the chemistry set. Then look at the nominal case, which is set up in the Reactor and Inlet panels and which can be run from the Run Model node on the project tree.

Follow the steps below to run the sensitivity analysis.

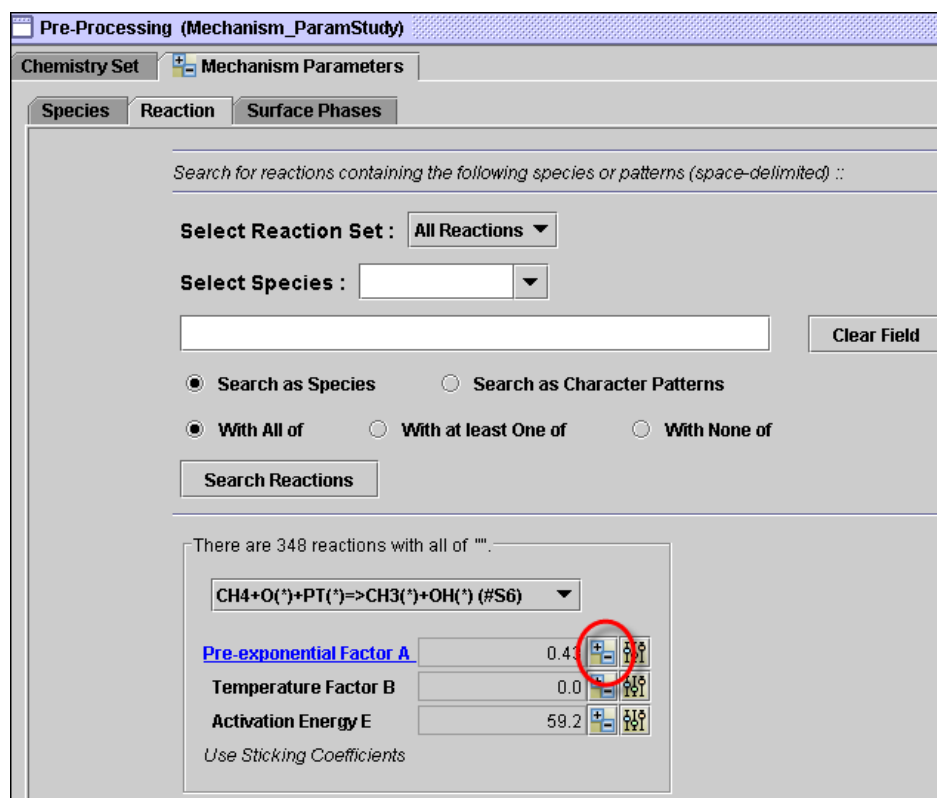
1. Double-click on the Output Control in the Open Projects tree.
2. On the Output Control tab under the Basic tab, select Temperature A-factor Sensitivity.
3. Open the Run Model panel and click the **Run** button.
4. Once the run has completed successfully, post-process the solution.
5. In the Select Results to Load from Solution File panel, check the Rxn Sens box for temperature. Then click **OK** to proceed to the Post-Processor.
6. In the Post-Processor control panel, use the Plot Set pull-down menu to select "sensitivity for solution no1".
7. Select Distance for the X Variable and all of the surface reaction sensitivities that are listed for Y Variables (hold down the <Ctrl> key while clicking, in order to select multiple variables).
8. Click on Display Plot.

From the plot results, you should see that Surface reactions #1, ($O_2 + 2PT(*) \rightarrow O(*) + O(*)$) and #6, ($CH_4 + O(*) + PT(*) \rightarrow CH_3(*) + OH(*)$), are particularly important in determining the resulting temperature. In the case of both of these reactions, the A-factors are actually sticking coefficients as indicated by the keyword `STICK` in the surface-chemistry file.

30. C.-P. Chou, J.-Y. Chen, G. H. Evans and W. S. Winters, *Combustion Science and Technology*, **150**:27 (2000).

It is now of interest to vary the sticking coefficients for these rates one by one, and see how such variations will affect predicted temperature profiles in the reactor. A Parameter Study has already been set up to do this in the **Mechanism_ParameterStudy** project. To see how this is done, go to the Mechanism Parameters tab in the Pre-processing panel. On the Reaction sub-tab, select COMBUST (which is the name of our surface material, so we're selecting reactions related to this material only) from the pull-down menu of the Select Reaction Set and click on the Search Reactions button. The first reaction to show up in the pull-down window under the Search Reactions button is highlighted in blue, indicating that a parameter study has been set up for this reaction rate constant. Click on the **Setup Parameter Study** button next to the Pre-exponential Factor A value for this reaction to view the Parameter Study Setup.

Figure 3-16 Setting Up a Parameter Study for Sticking Coefficients vs. Predicted Temperature Profiles



3.2.1.2 Viewing Results with the Post-Processor

Run the Parameter Study by selecting all of the runs in the Run Parameter Study window and clicking the **Post-Process** button. Once in the Post-Processor control panel, select Line Plot for Plot Type. Under Plot Set, select Solution no 1. Ctrl-click all of the temperature profiles for each of the Parameter Study runs as the Y Variables. Click on Display Plot.

Figure 3-17 Varying Rate Constants of Reactions 1 and 6.

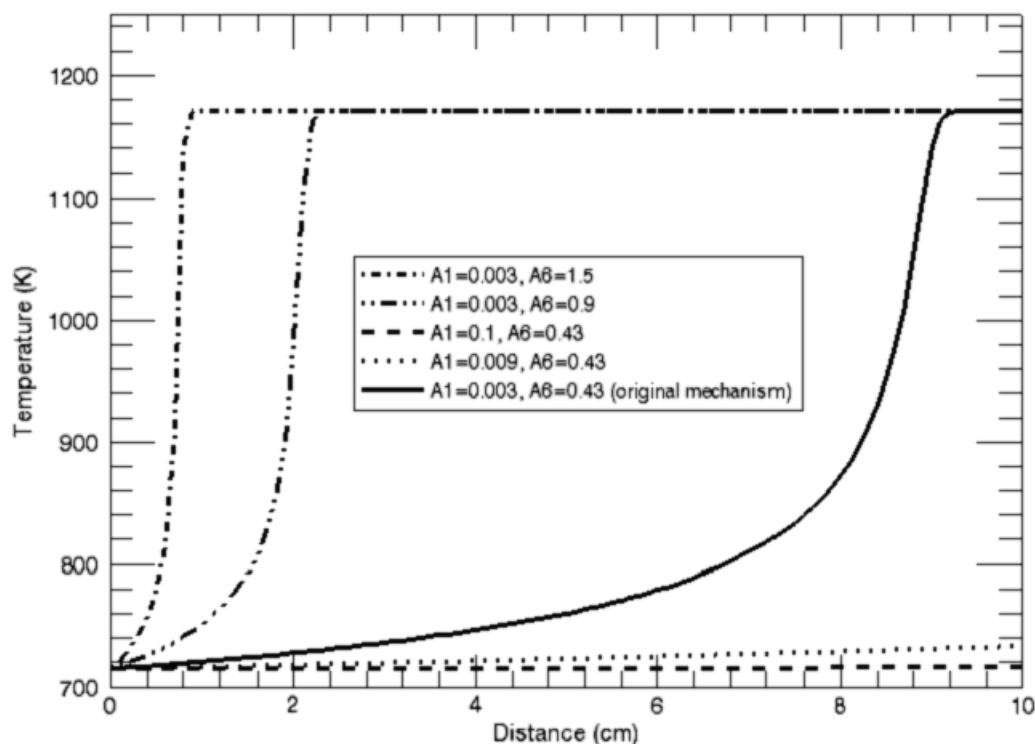


Figure 3-17 demonstrates the results of the Parameter Study displayed by the CHEMKIN post-processor. The results clearly indicate that if we keep the sticking coefficient of reaction 1 constant, and increase the sticking coefficient for reaction 6, the ignition occurs much sooner and the maximum combustion temperature is reached almost as soon as the reactants enter the catalytic reactor. This makes sense, because reaction 6, $\text{CH}_4 + \text{O}^* + \text{PT}^* \rightarrow \text{CH}_3^* + \text{OH}^*$, is a branching reaction that liberates radicals CH_3 and OH , thus rapidly increasing the radical pool that in turn is responsible for catalytic light-off. On the other hand, increasing the sticking probability of the $\text{O}_2 + 2\text{PT}^* \rightarrow \text{O}^* + \text{O}^*$ reaction delays ignition probably because it is competing with the adsorption of CH_4 on open sites.

3.3 Chemistry Sets

In this section, we discuss briefly the chemistry sets used in [Chapter 3](#) and provide references for further study.

3.3.1 Methane Oxidation on Pt

Two projects in this chapter involve methane oxidation on a platinum surface. This demonstrates that the gas-phase mechanism does not need to align to a particular surface mechanism by implementing two different surface mechanisms to describe the same surface process – methane oxidation on a platinum (Pt) surface.

The chemistry set of the two-stage catalytic combustor project ([Section 3.1.1](#)) uses a slightly altered version of the surface mechanism published by Deutschmann et al.²⁸ (see p. 93) in 1996 and put into CHEMKIN format by L. Raja. A different surface mechanism developed by Chou et al.³⁰ (see p. 109) in 2000 is employed by the Parameter Study Facility for the surface chemistry analysis project ([Section 3.2.1](#)).

If gas-phase reactions are expected to be important, any reaction mechanism describing the gas-phase kinetics for methane oxidation chemistry can be used, but Pt needs to be added to the element list. In both projects, an altered version of the GRImech 3.0 is provided as an example. In the case of a simulation where it is known that gas-phase chemistry is not important, a simple gas-phase chemistry input file can be used that only defines the elements and species that are included in the SURFACE KINETICS input file.

The SURFACE KINETICS input file for Duetschmann's mechanism describes chemistry occurring on one material called CATALYST that has one site type called PT_SURFACE. The PT(B) bulk material is defined, but does not participate in any reactions, as neither etching or deposition of platinum occurs in this system. The surface site can be occupied by any of 11 surface species, where PT(S) is the open platinum site, and the other surface species represent H, C or O atoms, CO, CO₂ or H₂O molecules, OH, CH₃, CH₂, or CH radicals adsorbed on the platinum surface atom. Note that GRImech has already used the symbol CH₂(S) to represent gas-phase methylene radicals in the singlet electronic state, such that adsorbed methylene radicals have been given the symbol CH₂(S)s. Thermochemical data for surface species are included in the surface kinetics input file, and have been defined using PT(S) as the reference point. There are 22 surface reactions, some reversible and some irreversible. These reactions include simple and dissociative adsorption reactions, as

well as simple and associative desorption reactions, plus reactions between adsorbed species. Some reactions are described in terms of sticking coefficients, a few reactions have reaction-order overrides, and in two cases, the activation energy for an adsorption reaction varies with surface coverage.

The surface mechanism published by Chou et al. in 2000 describes the oxidation of methane on the surface of a supported platinum catalyst under fuel-lean conditions. The surface reactions take place on the PT_POLY surface phase (site type) of the material. Bulk species PT(B) and surface species PT(*) represent the platinum atom covered by a surface species and the bare surface platinum atom (or open surface site), respectively. There are 9 other surface species that can exist on the platinum surface (H, C, O, CO, H₂O, OH, CH₃, CH₂, and CH), and their thermodynamic data are provided in the SURFACE KINETICS input file. Since definitions of these surface species (given as part of their thermochemical data) do not contain a platinum atom, the PT(B) bulk species in Chou's mechanism must participate in some of the surface reactions so that these reactions are balanced. The conservation of platinum atom is important because, as a catalyst, platinum should not be created or consumed by the surface reactions. Chou's surface mechanism consists of 23 irreversible reactions. These reactions describe simple and dissociative adsorption of reactants, simple and associative desorption of products, and reactions between adsorbed species. Some adsorption rates are given in terms of sticking coefficients.

3.3.2 Pt/Rh Three-way Catalyst

This chemistry set describes several processes that occur on a platinum/rhodium “three-way” catalyst. These processes are: the oxidation of unburned hydrocarbons (represented by C₃H₆) on Pt, the reduction of NO on Pt, the reduction of NO on Rh, and the oxidation of CO on Rh. This reaction mechanism is based on the published work of Chatterjee, *et al.*³¹ in 2001. This reaction mechanism was developed for a surface made of 75% Pt and 25% Rh, and should be considered valid only for this composition. In particular, the coverage dependent activation energies have been scaled for that Pt/Rh ratio.

Gas-phase kinetics is ignored in this chemistry set. The GAS-PHASE KINETICS input file, therefore, includes 6 elements: O, H, C, N, Rh and Pt; 9 species: O₂, C₃H₆, H₂, H₂O, CO₂, CO, NO, NO₂, and N₂; and no reactions.

31. D. Chatterjee, O. Deutschmann and J. Warnatz, “Detailed Surface Reaction Mechanism in a Three-way Catalyst”, *Faraday Discussions*, **119**:371-384 (2001).

The SURFACE KINETICS input file describes chemistry occurring on one material called 3WAYCATALYST that has two site types each representing one of the metals, called PLATINUM and RHODIUM. The PLATINUM site can be occupied by any of 18 surface species, of which Pt(S) is the open site, and one of which, the C3H6(S) species, occupies two sites. The RHODIUM site has simpler chemistry with only 5 surface species, of which Rh(S1) is the open site. Thermochemical data are provided for some of the surface species, but others have placeholder values. All surface reactions are irreversible, such that none of the thermochemical data are used to obtain rates for reverse reactions. The PLATINUM site in this reaction mechanism has a site density of $2.04\text{E-}9 \text{ moles} \cdot \text{cm}^{-2}$, which is close to the number of $2.717\text{E-}9 \text{ moles} \cdot \text{cm}^{-2}$ that is obtained from the density and molecular weight of solid platinum. This indicates that the creators of this mechanism chose to describe some of the effects of the high-surface-area nature of the catalyst material by increasing the site density, rather than by increasing the effective surface area for chemistry. This aspect should be kept in mind in applying this mechanism to other systems.

The oxidation of C_3H_6 (or UHCs) on platinum is described in 47 irreversible reactions that include simple and dissociative adsorptions, simple and associative desorptions, plus reactions between adsorbed species. The latter include decomposition of adsorbed hydrocarbon species by hydrogen transfer to Pt(S) species, as well as various oxidation reactions for adsorbed hydrocarbon species ranging from a global description of C3H5(S) oxidation to more step-wise oxidation reactions for other hydrocarbon fragments. NO reduction on platinum is described in 5 reactions, while NO reduction and CO oxidation on rhodium are described in another 9 reactions, each involving adsorptions, desorptions and reactions among adsorbed species. Some reactions are described in terms of sticking coefficients, a few reactions have reaction-order overrides, and in several cases, the activation energy for a reaction varies quite strongly with the extent of coverage of the surface by one or more species.

4 Materials Problems

4.1 Chemical Vapor Deposition

A number of CHEMKIN Reactor Models can be used for CVD simulations. Thermal CVD processes generally involve furnaces or heated surfaces. Simulations of CVD processes, therefore, often treat the temperature of the reactor or deposition surfaces a fixed, experimentally determined input parameter, rather than a quantity that is obtained by solving an energy equation. The surface temperature is usually assumed to be equal to the temperature of the adjacent gas, except for processes performed at very low pressures. Many CVD processes also have fairly long run times compared with startup and end-of-process transients, such that a steady-state simulation is often a good representation of a CVD process.

Generally, a low-dimensional simulation, such as an Equilibrium calculation or a PSR simulation, will be used to assess the chemistry, and possibly to simplify a reaction mechanism before using it in higher-dimensional simulations. A multiple-phase equilibrium calculation can be used to determine the maximum possible deposition rate for a certain gas mixture, pressure and temperature. In a PSR simulation of a CVD process, the assumption is made that the chemical kinetics are rate limiting rather than mass transport effects or the inlet reagent supply rate. Higher dimensional simulations allow evaluation of the relative effects of chemical kinetics and mass transport. The reactor models in the CHEMKIN software can be used to simulate a number of reactor geometries used for CVD. The Plug Flow Reactor and Cylindrical Shear Flow Reactor Models can be used to model tube-furnace CVD systems, while the Planar Shear Flow Reactor can be used to model horizontal flow CVD systems. The Stagnation Flow Reactor Model can simulate a vertical showerhead system, while the Rotating Disk Reactor Model is for reactors in which high-speed rotation of

the plate dominates the gas flow field. There are also specialized models (available from the Utilities menu in the CHEMKIN Interface) for the thermal analysis and modeling of the multi-wafer batch low-pressure CVD furnaces used in the fabrication of microelectronic devices.

4.1.1 Equilibrium Analysis of Chlorosilane CVD

4.1.1.1 Project Description

This user tutorial presents a multi-phase equilibrium calculation of the Si-Cl-H system. A constant pressure and temperature equilibrium calculation gives the maximum amount of solid product that could be formed in the absence of kinetic or transport limitations. This can be a valuable screening tool in choosing operating conditions for a CVD process. In this case, adding HCl to a mixture of SiCl_3H , H_2 , and solid silicon alters the Si/Cl ratio in the system enough to change the equilibrium composition from one that would result in deposition of more solid Si, to one that would result in etching.

4.1.1.2 Project Setup

The project file is called ***equilibrium__siclh_cvd.ckprj***. The data files used for this sample are located in the ***samples\equilibrium\siclh_cvd*** directory. This diagram contains only one Equilibrium calculator.

The equilibrium calculation only needs a list of species with their thermodynamic data; a reaction list is not needed. It is important to include all likely radical species as well as the desired and undesired product species in the calculation. It is generally better to include some unimportant species than to leave out ones that turns out to be important. The *chem.inp* file includes 3 elements and 22 gas-phase species and no reactions. This file contains more species than the trichlorosilane CVD chemistry set described in [Section 4.4.3](#). In the interest of completeness, a number of species such as SiH_4 or atomic Cl were added that are not expected to be important at standard CVD conditions, but that might be more important under different conditions. The *surf.inp* file includes only solid silicon in the bulk (condensed) phase.

Setting up this problem first involves the C1_ Equilibrium panel. The problem type, temperature (1400 K) and pressure (1 atm) are entered on the Reactor Physical Property tab. The starting composition is entered on the Reactant Species tab. Starting with a molecular mixture will give the same equilibrium composition as starting with elemental Si, H, and Cl with the same Si/Cl and H/Cl ratios. The Continuations panel is used to specify three additional simulations where increasing amounts of HCl are added, replacing some of the hydrogen carrier gas. All components of the starting mixture have been re-entered, because the composition must be entered as a set.

4.1.1.3 Project Results

Figure 4-1 shows the initial and equilibrium amounts of solid silicon for an initial mixture of 10% (by volume) SiCl_3H in hydrogen with increasing amounts of HCl at 1 atm total pressure and 1400 K. With no added HCl, the equilibrium mole fraction of solid silicon is larger than the initial amount, indicating that this gas mixture is likely to result in the deposition of silicon. As the HCl content increases, the mole fraction of Si(B) expected at chemical equilibrium decreases below the initial mole fraction. This initial gas mixture is thus expected to result in etching, rather than deposition of Si under these conditions. This primarily results from the decreasing Si/Cl ratio in the system. As shown in *Figure 4-2*, the most prevalent gas-phase species at equilibrium are the hydrogen carrier gas and various chlorinated silicon species. Increasing the relative amount of Cl in the system favors the formation of these gas-phase species.

Figure 4-1 Chlorosilane CVD—Equilibrium Calculations

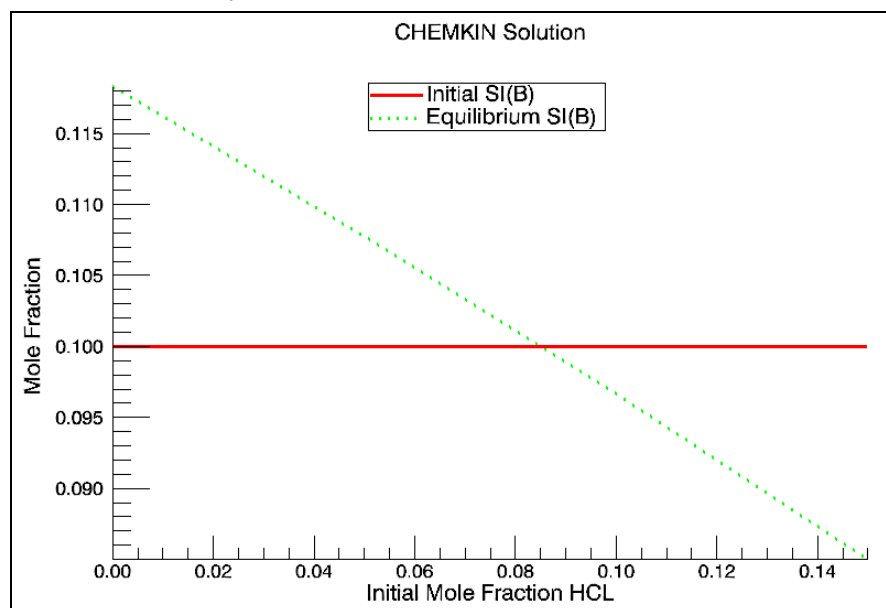
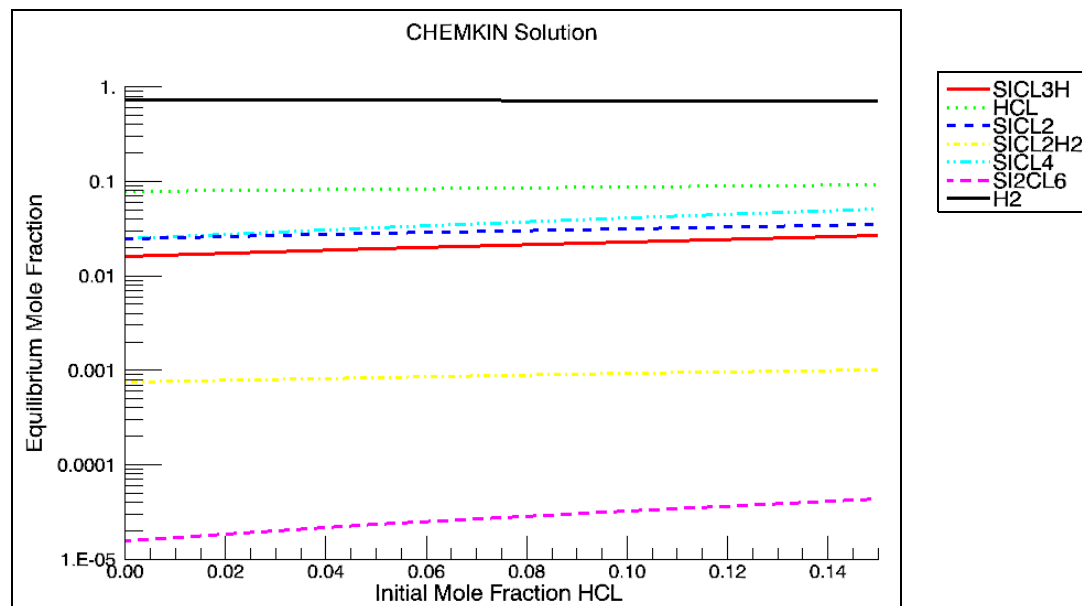


Figure 4-2

Chlorosilane CVD—Mole Fractions



4.1.2 PSR Analysis of Steady-state Thermal CVD

4.1.2.1 Project Description

This user tutorial presents a model for the CVD of silicon nitride in a steady-state PSR, using the chemistry set described in [Section 4.4.1](#). The process operates at a low pressure of 1.8 Torr, and a high temperature of 1440 C, which makes it reasonable to approximate this system as a PSR. In the PSR model, the CVD reactor is described using a volume, surface area, and gas flow rate. This is a fixed-temperature simulation that uses continuations to see the effects of changing the SiF₄/NH₃ ratio in the input gas. It also uses sensitivity and rate-of-production (ROP) options to analyze the chemistry occurring in the system.

4.1.2.2 Project Setup

The project file is called *psr_cvd.ckprj*. The data files used for this sample are located in the *samples\psr\cvd* directory. This reactor diagram contains only one inlet, one Perfectly Stirred Reactor, and an output Product icon.

The inlet flow rate (11300 sccm, standard cubic centimeters per minute) is input on the Stream Property Data tab of the Inlet Stream panel. The inlet gas composition is input on the Species-specific Property tab of the Inlet Stream panel.

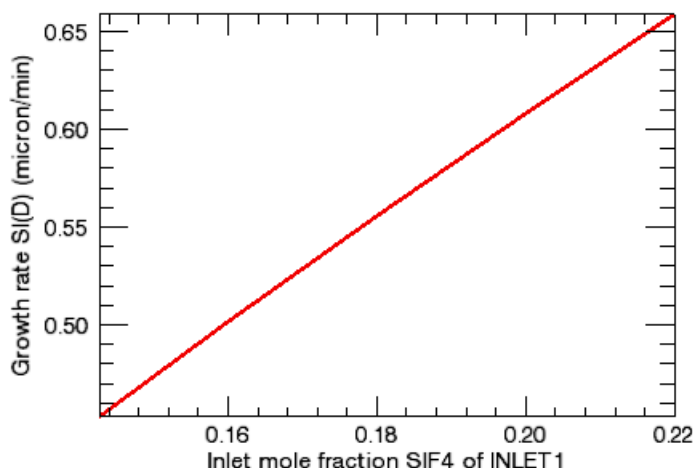
The constant reactor temperature (1440 C), pressure (2.368E-3 atm), volume, and internal surface area are input on the Reactor Physical Property tab of the (C1_) PSR panel. In this sample problem, no estimated gas mole fractions are input on the Initial Gas Fraction sub-tab of the Species-specific tab of the (C1_) PSR panel. This is not a restart problem, so the absence of a solution estimate for the gas-phase species causes the equilibrium composition to be calculated at 1713 K and used as a starting point for the iterations. However, solution estimates for the surface site concentrations and bulk phase activities are input on the corresponding sub-tabs of the Species-specific tab of the (C1_) PSR panel. The Bulk-phase-specific Data tab of the (C1_) PSR panel does not have input values because this is a deposition rather than an etching system.

The Output Control tab of the Output Control panel specifies that a threshold of 0.001 should be used for filtering A-factor sensitivities, while a threshold of 0.01 should be used for ROP. These are the default values in determining what gets printed in the output file and saved in the XML Solution File. The check box for indicating that growth rate sensitivities should be calculated and saved is on this tab, as are similar boxes to choose that sensitivities or ROP for all species should be calculated and stored. These latter options should be used with care for large mechanisms, as they can result in very large output and solution files. The Species Sensitivity and ROP tab allows the user to specify that sensitivities should be calculated and saved for only particular species, in this case HF, SiF₄ and NH₃. Also on this table are choices for printing ROP information for particular species in the output file. The Continuations panel has input specifying four more simulations to be done with increasing SiF₄/NH₃ ratios.

4.1.2.3 Project Results

Figure 4-3 shows that the predicted deposition rate increases with increasing SiF_4/NH_3 ratio, as expected under these conditions of excess ammonia. Although this particular plot shows the growth rate of Si(D), choosing to plot the growth rate of N(D), BULK1 or BULK2 would give essentially the same result.

Figure 4-3 Steady-state Thermal CVD—Deposition Rate vs. SiF_4 Mole Fraction



In studying a CVD system, it is often useful to know the relative importance of gas-phase and surface reactions. For this system, the model shows that very little gas-phase decomposition occurs under these conditions. *Figure 4-4* shows the total rates of production (ROPs) for SiF_4 and NH_3 due to gas-phase and surface reactions. In these cases, the negative numbers indicate that these are really loss rates rather than production rates. However, these results clearly show that surface reactions (rather than gas reactions) dominate the decomposition of these starting materials.

Sensitivity analysis gives complementary information to the ROP analysis. *Figure 4-5* shows the silicon nitride growth rate is most sensitive to surface reaction #2, which is the reaction of SiF_4 at the surface. *Figure 4-6* shows that the $\text{NH_NH}_2(\text{S})$ site fraction is much larger than the site fractions of the other surface species.

Figure 4-4 Steady-state Thermal CVD—ROP Comparison

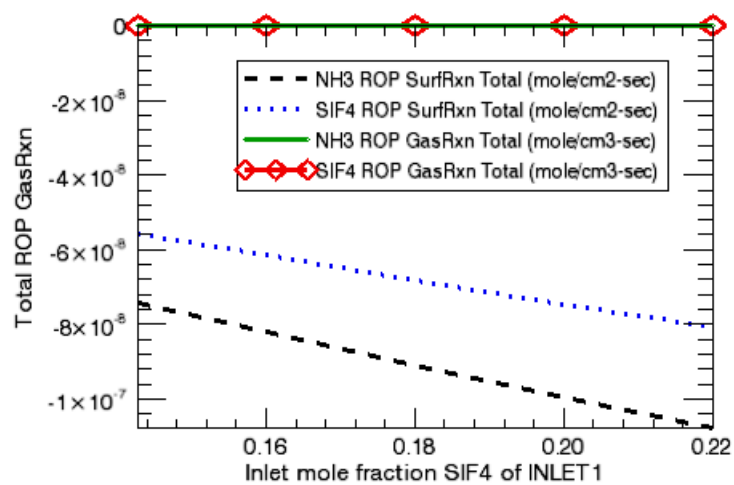


Figure 4-5 Steady-state Thermal CVD—Growth Rates

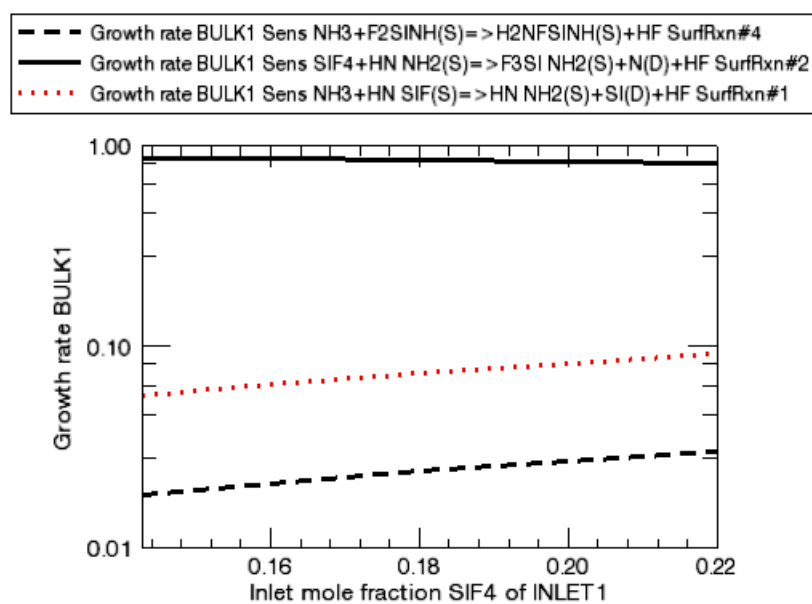
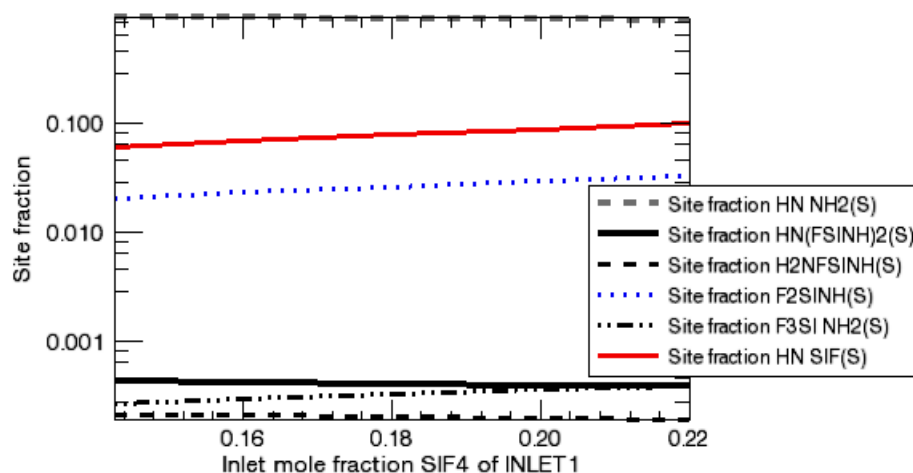


Figure 4-6 Steady-state Thermal CVD—Site Fractions



4.1.3 Approximations for a Cylindrical Channel Flow

4.1.3.1 Project Description

This user tutorial explores three ways of modeling steady-state CVD in a cylindrical flow reactor, and compares the results of the levels of approximation. This project uses the silicon nitride CVD chemistry set described in [Section 4.4.1](#). The three approximations used are, in order of increasing simplification, Cylindrical Shear-layer Flow Reactor, Plug Flow Reactor, and a series of Perfectly Stirred Reactors.

4.1.3.2 Project Setup

This project file is an example of a project that contains multiple sub-projects. It is called ***multiple_models_channel_flow_approximations.ckprj***. The data files used for this sample are located in the ***samples\multiple_models\channel_flow_approximations*** directory. The first reactor diagram contains one inlet and a network of 10 sequential PSRs. The other two reactor diagrams in this project are simple ones that contain only one inlet and either a Plug Flow or a Cylindrical Shear-Flow Reactor Model.

4.1.3.2.1 Cylindrical Shear-Flow Reactor

The properties of the inlet gas are described on the R1_IN1 panel. The inlet gas temperature and mass flow rate are input on the Stream Property Data tab. The mass flow rate is the maximum gas-phase velocity at the inlet. For this problem, which is in cylindrical coordinates, the average velocity equals one half of the maximum velocity of the assumed parabolic velocity profile. The composition of the inlet gas is input on the Species-specific Property tab of the R1_IN1 panel. This example uses mole fraction, but the user may choose to input these values in mass fractions instead.

Parameters describing the reactor geometry and wall temperature are entered on the Reactor Physical Property tab of the C1_ Cylindrical Shear Flow panel. The temperatures for the wall are input on this tab. In this case, the inlet gas temperature is equal to the wall temperature, so there is no need to provide transitioning parameters. The pressure, grid parameters, as well as the use of multicomponent diffusion and thermal diffusion (the Soret effect) are specified on this tab. To be consistent in our approximation to the Plug Flow as well as to the multiple PSR examples, the Boundary Layer Thickness has been set to 0.01 cm, to provide an initially flat velocity profile. The Species-specific Data tab allows the specification of initial guesses for the gas composition adjacent to the surface, which is not used in this example, as well as estimated values for the surface site fractions and bulk activities, which are provided. A good initial guess for these values is very helpful in attaining convergence.

No values are entered on the Solver panel; the default tolerance values are used. The Output Control panel has been used to specify that the text output file should have solution data printed every 1 cm.

4.1.3.2.2

Plug Flow Reactor

The properties of the inlet gas are described on the R1_IN1 panel. The inlet mass flow rate is input on the Stream Property Data tab. The composition of the inlet gas is input on the Species-specific Property tab of the R1_IN1 panel. This example uses mole fractions, but the user may choose to input these values in mass fractions instead.

Parameters describing the reactor geometry and gas temperature are entered on the Reactor Physical Property tab of the C1_ PFR panel. The problem type and pressure are also specified on this tab. The Species-specific Data tab allows the specification of initial guesses for the surface site fractions and bulk activities. No values are entered on the Solver panel, except to specify that the text output file should have solution data printed every 1 cm.

4.1.3.2.3

Perfectly-stirred Reactor Network

As for the other sub-projects, the properties of the inlet gas for the series PSR project are described on the R1_IN1 panel. The mass flow rate is input on the Stream Property Data tab. The composition of the inlet gas is input on the Species-specific Property tab of the R1_IN1 panel.

This sub-project contains a series of 10 identical PSR reactors, so in this case, the C1_Rx PSR (where $x = 1 - 10$) panels have no entries. Instead, the properties of these reactors are input on the C1 Cluster Properties panel. Cluster properties will apply to all PSRs in the cluster unless overridden in the individual reactor panels.

Parameters describing the problem type, reactor geometry, pressure, and gas temperature are entered on the Property for All Reactors tab of the Cluster Properties panel. The Species-specific Data for All Reactors tab allows the specification of initial guesses for the gas composition, which are not used in this example, as well as estimated values for the surface site fractions and bulk activities, which are used. A good initial guess for these values is very helpful in attaining convergence. There are no entries on the Solver, Output Control, or Continuations panels; all the default values are used.

4.1.3.3

Project Results

Figure 4-7 shows a contour plot of the SiF_4 mole fractions as a function of radial and axial position in the shear flow simulation. There is a minor degree of radial non-uniformity for this reactant species, as a result of chemical reactions consuming SiF_4 at the wall. *Figure 4-8* shows SiF_4 mole fraction as a function of axial distance for all three simulations. The mole fraction for the centerline is higher than that for the upper-wall in the shear-flow simulation, as expected, and these results bracket the results from the plug-flow and series-PSR simulations. Although not shown, the area-averaged value for the SiF_4 mole fraction from the shear-flow simulation agrees well with the results from the other two simulations.

Figure 4-7 Cylindrical Channel Flow—Shear-flow Simulation of SiF_4 Mole Fractions

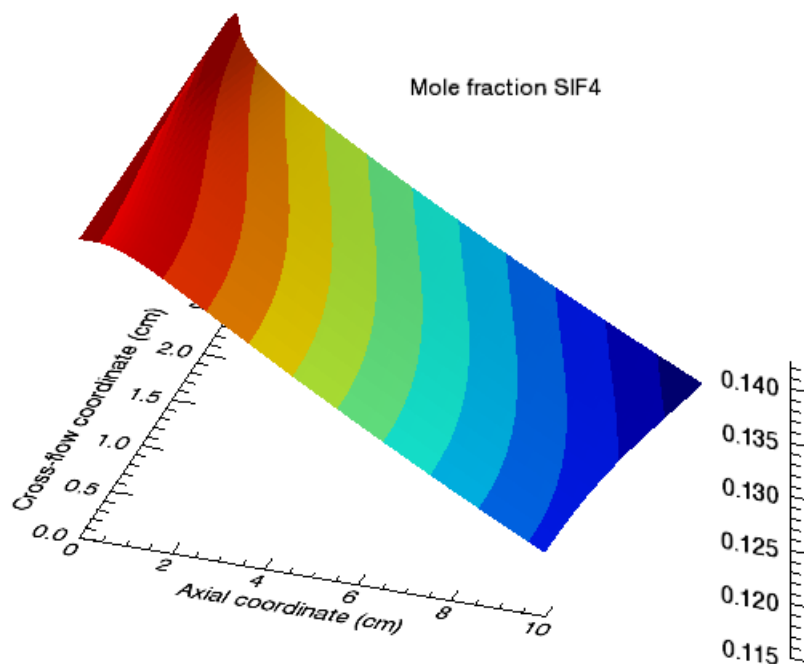


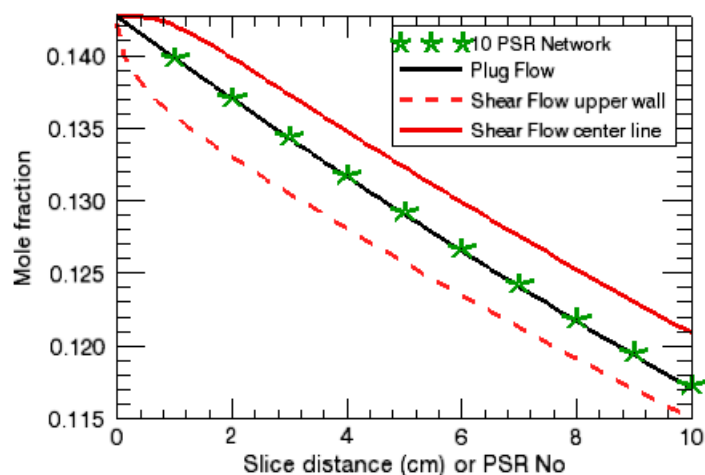
Figure 4-8 Cylindrical Channel Flow—SiF₄ Mole Fractions Comparison

Figure 4-9 shows the silicon nitride deposition rates from these three simulations. The predictions from the plug-flow and series-PSR simulations are nearly identical, with the shear-flow simulations results being somewhat lower. Although there is some differences in the axial gas velocities shown in *Figure 4-10* for the shear-flow and plug flow simulations, the difference in deposition rates mostly results from the lower reactant concentrations at the surface in the higher-dimensional simulations. The series of 10 PSR reactors and the Plug Flow simulations represent comparable levels of approximation to the channel flow. As the Plug Flow simulation actually runs faster, it would be the recommended reactor model to use in developing chemical mechanisms, or for exploring general trends for these conditions. However, the series-PSR approach has the advantage that it can approximate transient flow, as well as steady-state flow, in a channel. The deposition rate is affected by mass-transfer in this case, so the higher-dimensionality shear-flow simulations would be used for final mechanism adjustment and reactor design simulations.

Figure 4-9 Cylindrical Channel Flow—Deposition Rates Comparison

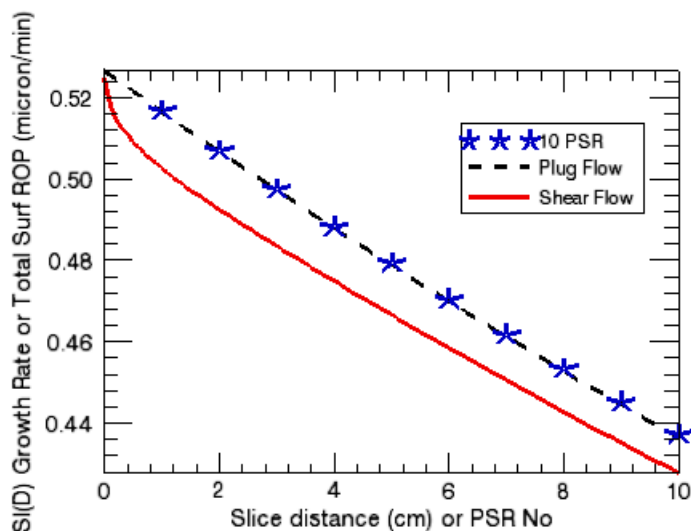
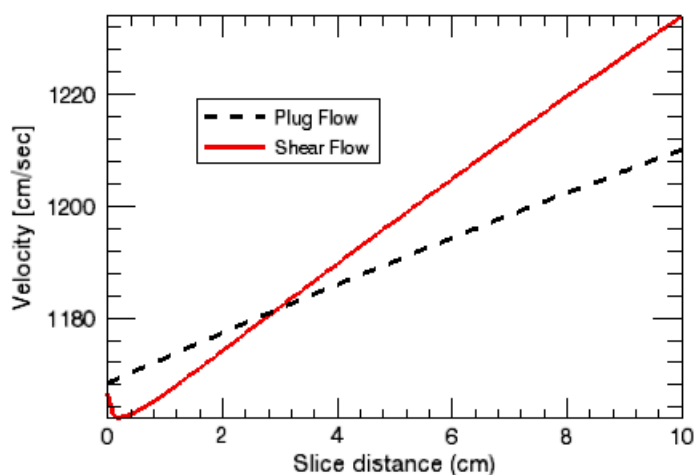


Figure 4-10 Cylindrical Channel Flow—Axial Gas Velocities Comparison



4.1.4 Deposition in a Rotating Disk Reactor

4.1.4.1 Project Description

This user tutorial presents a model for the CVD of silicon from silane in a steady-state rotating disk reactor using the chemistry set described in [Section 4.4.2](#). This is a fixed-surface temperature simulation that represents the experimental rotating-disk reactor used by Ho, Coltrin and Breiland,³⁴ (p. 155) with the conditions corresponding

to *Figure 4* in that paper. The inlet gas is a dilute mixture of silane in helium. The use of a helium carrier gas, rather than hydrogen, favors the gas-phase decomposition reactions of silane. For this case, a surface temperature of 923 K (650° C) is used. This example has two continuations, where the silane partial pressure is increased.

4.1.4.2 Project Setup

The project file is called *rotating_disk_sih4_cvd.ckprj*. The data files used for this sample are located in the *samples\rotating_disk\sih4_cvd* directory. This reactor diagram contains only one inlet and one rotating-disk CVD reactor.

The properties of the inlet gas are described on the C1_Inlet panel. The inlet gas temperature is input on the Stream Property Data tab. An inlet gas velocity is usually not entered for a steady-state rotating disk simulation, as it is calculated from the spin rate, pressure, and gas-properties, but the user may override this value on the Reactor Physical Property tab, Basic sub-tab, if desired. The composition of the inlet gas is input on the Species-specific Property tab of the C1_Inlet panel. Note that the mole fractions do not add up to one, as the partial pressures (in Torr) have actually been entered. This is permitted, as the program will normalize the gas composition internally if the user does not do so in the CHEMKIN Interface. The Continuations panel is used to input the new compositions of the reactant gas mixture for the second and third simulations in this sample project.

Parameters describing the reactor conditions are entered on the Reactor Physical Property tab, Basic sub-tab of the C1_Rotating Disk panel. The choice of a steady-state simulation solving the gas energy equation is entered here, as well as the use of multicomponent diffusion and thermal diffusion (the Soret effect). The temperature for the deposition surface (923 K), pressure (200 Torr), and disk rotation rate (450 rpm) are input on this tab. The other sub-tabs on the Reactor Physical Property tab are for options that are not used in this example. The Initial Grid Property tab of the Reactor Physical Property tab allows specification of the locations of the deposition surface ($x = 0$, default) and the end axial location where the gas enters (6.2 cm). Grid parameters are specified on this tab. This reactor model includes adaptive gridding, and the use of a relatively-low value for the initial number of grid points is recommended. The Species-specific Data tab allows the specification of initial guesses for the gas composition at the inlet, adjacent to the surface, or maximum mole fractions for intermediate species, none of which are used in this example. However, estimated values for the surface site fractions and bulk activity are provided. A good initial guess for these values can be very helpful in attaining convergence.

4.1.4.3 Project Results

Figure 4-11 shows the axial, radial and circumferential velocity components for the rotating disk reactor as a function of height above the surface. The deposition surface is at the origin, and the gas enters at $x = 6.2$ cm with an axial velocity of -12.4 cm/sec and zero radial and circumferential velocity components. As the gas approaches the rotating surface, the axial velocity initially increases slightly then decreases while the radial and circumferential velocity components increase. At the surface, the axial and radial velocity components are zero, and the circumferential velocity matches that of the disk (in radians/sec), as expected.

Figure 4-11 Deposition in a Rotating Disk—Gas Velocity Components

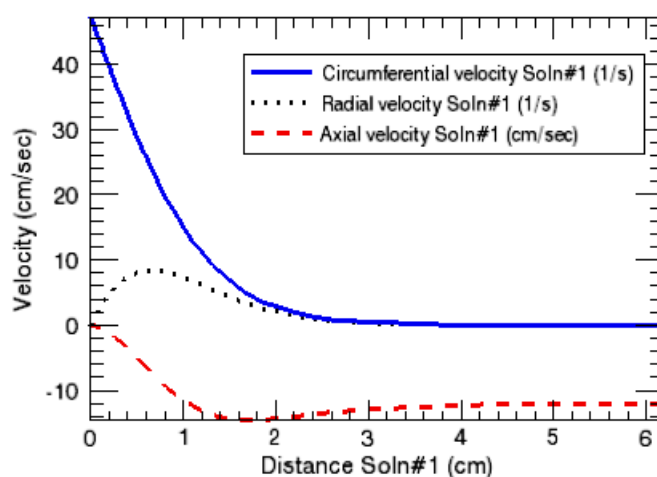


Figure 4-12 shows predicted mole fractions for the various silicon hydrogen species as a function of distance above the surface (the helium carrier gas is not included), again for the first simulation in the project. The composition at the grid point with largest x value is constrained to that of the inlet gas (silane and helium only). The other grid points show varying amounts of product and reactive intermediate species that are formed by gas-phase and surface reactions. Si atoms are present in very low amounts (mole fractions $\sim 10^{-12}$), but can easily be detected by laser-induced fluorescence techniques, so they are kept in the mechanism. You can choose concentration units for species composition in the Species/Variables tab of the Select Results to Load panel when the Post-Processor is first launched. This yields the results shown in *Figure 4-13*, illustrating that Si atom concentrations increase with increasing silane concentration, as expected. The profiles of the Si atom concentrations are shown as a function of distance above the surface for different starting silane partial pressures: #1 = 0.11 Torr, #2 = 0.34 Torr, #3 = 0.67 Torr. The curves in this figure suggest that the profiles might also be changing shape. This is confirmed in *Figure 4-14*, which was made by exporting the simulation results, normalizing and plotting experimental results from Ho, Coltrin and Breiland (see

Figure 4 of referenced paper)³⁴ (p. 155) in third party software. It shows that: a) Si atom profiles are experimentally observed to be narrower for higher silane concentrations, and b) this reaction mechanism reproduces this observation. Comparisons between the model and this experimental data set shown that the original reaction proposed for Si atom formation, the collisionally-induced decomposition of SiH₂, could not account for the experimental observations. Two other reactions, H₃SiSiH ↔ Si + SiH₄ and Si + Si₂H₆ ↔ H₃SiSiH + SiH₂, are instead the primary reactions involving Si atoms.

Figure 4-12 Deposition in a Rotating Disk—Mole Fractions

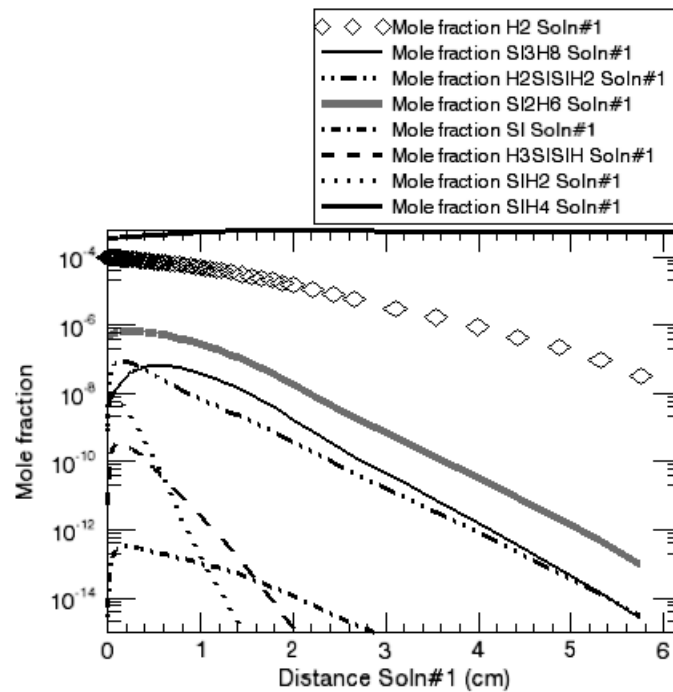


Figure 4-13 Deposition in a Rotating Disk—Si Atom Concentrations

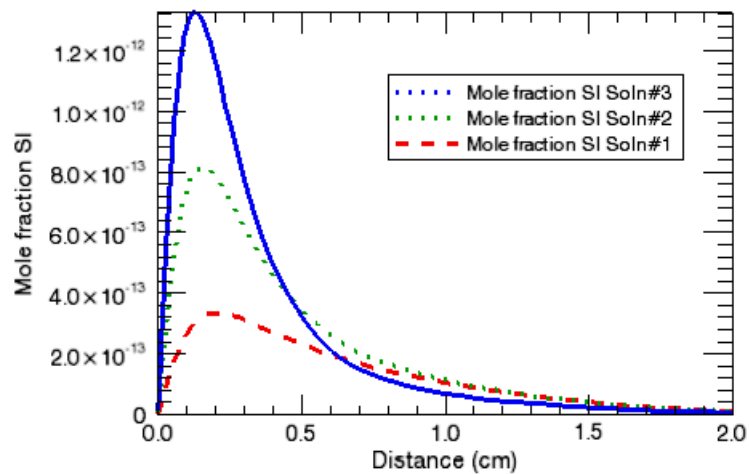
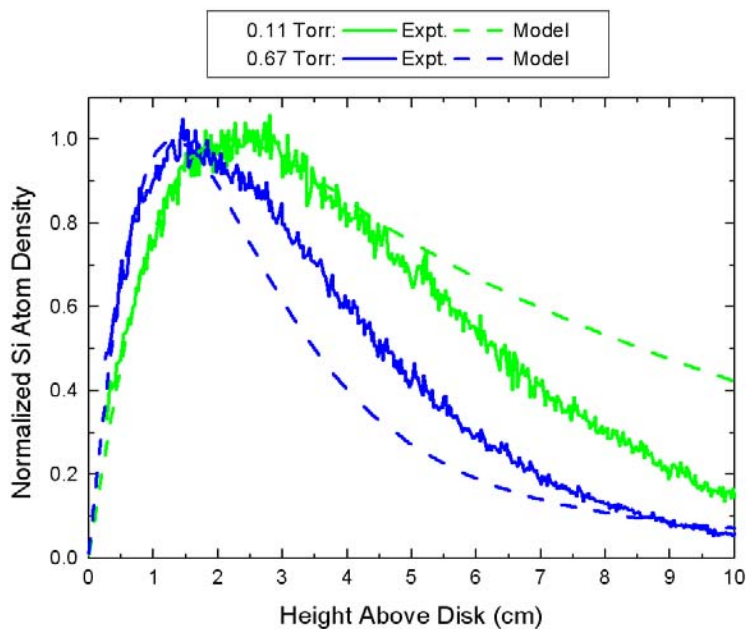


Figure 4-14 Deposition in a Rotating Disk—Experimental Data



4.1.5 Trichlorosilane CVD in Planar Channel Flow Reactor

4.1.5.1 Project Description

This user tutorial presents a model for the CVD of silicon in a steady-state planar shear-layer flow reactor using the chemistry set described in [Section 4.4.3](#). The process operates at atmospheric pressure, and a relatively high temperature (1398 K). This is a fixed-temperature simulation that represents a horizontal cross-flow reactor of the type used to deposit epitaxial silicon layers. In this case, the upper wall temperature is held at a temperature (773 K), which is significantly lower than the deposition substrate, but higher than the inlet gas temperature (623 K).

4.1.5.2 Project Setup

The project file is called *planar_shear_flow_tcs_cvd.ckprj*. The data files used for this sample are located in the *samples\planar_shear_flow\tcs_cvd* directory. The reactor diagram contains one inlet, one planar shear-flow reactor, and an outlet.

The properties of the inlet gas are described on the C1_Inlet panel. The inlet gas temperature and inlet gas velocity are input on the Stream Property Data tab. The Axial Velocity should be the maximum gas-phase velocity at the inlet. For this problem, which is in cartesian coordinates, the average velocity equals two-thirds of the maximum velocity of the parabolic velocity profile. The composition of the inlet gas is input on the Species-specific Property tab of the C1_Inlet panel.

Parameters describing the reactor geometry and wall temperatures are entered on the Reactor Physical Property tab of the C1_Planar Shear Flow panel. The temperatures for the upper wall and deposition surface (lower wall) are input on this tab, as well as an optional parameter specifying the distance over which the wall temperatures are smoothly transitioned from the inlet gas temperature to the desired wall temperature. The pressure, grid parameters, as well as the use of multicomponent diffusion and thermal diffusion (the Soret effect) are specified on this tab. The Species-specific Data tab allows the specification of initial guesses for the gas composition adjacent to the surface, which is not used in this example, as well as estimated values for the surface site fractions and bulk activities, which are provided. A good initial guess for these values is very helpful in attaining convergence.

On the Basic tab of the Solver panel, the text output file has been specified to have solution data printed every 1 cm along the channel.

4.1.5.3 Project Results

The gas temperatures in [Figure 4-15](#) show that the gas heats up substantially near the deposition surface, with the hot zone expanding with axial distance, as expected. The inlet gas temperature is lower than the upper wall temperature, such that the coolest gas lies in a region near to, but below the top wall. This cooler gas region is reflected in the trichlorosilane mole fraction contours shown in [Figure 4-16](#). Depletion as a result of chemical reaction causes the low SiCl_3H mole fractions near the lower wall, but thermal diffusion causes the heavier gas to move away from the upper wall. A simulation run without thermal diffusion gives uniform SiCl_3H mole fractions in the upper part of the reactor. [Figure 4-17](#) shows how the deposition rate of solid silicon varies as a function of axial distance. Initially, the deposition rate is quite high, but it drops rapidly as the SiCl_3H near the surface is depleted, indicating that the deposition process is transport limited in this system. [Figure 4-18](#) shows gas-phase mole fractions near the lower surface as a function of axial distance. The extent of SiCl_3H depletion and HCl formation is notably larger than the formation of the other silicon-chlorine species (SiCl_2 , SiCl_2H_2 and SiCl_4), which indicates that deposition of solid silicon is the dominant reaction pathway.

Figure 4-15 Trichlorosilane CVD—Gas Temperatures vs. Axial and Radial Distance

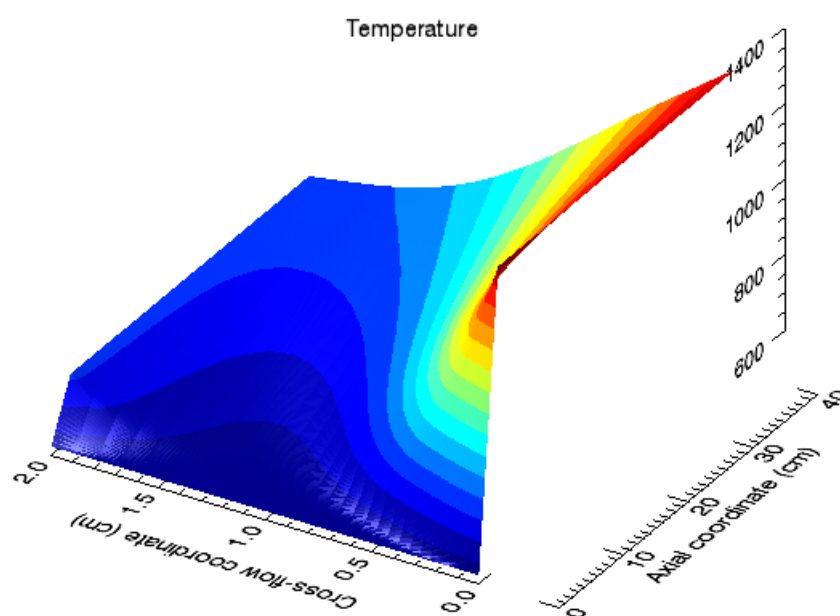


Figure 4-16 Trichlorosilane CVD—Trichlorosilane Mole Fraction

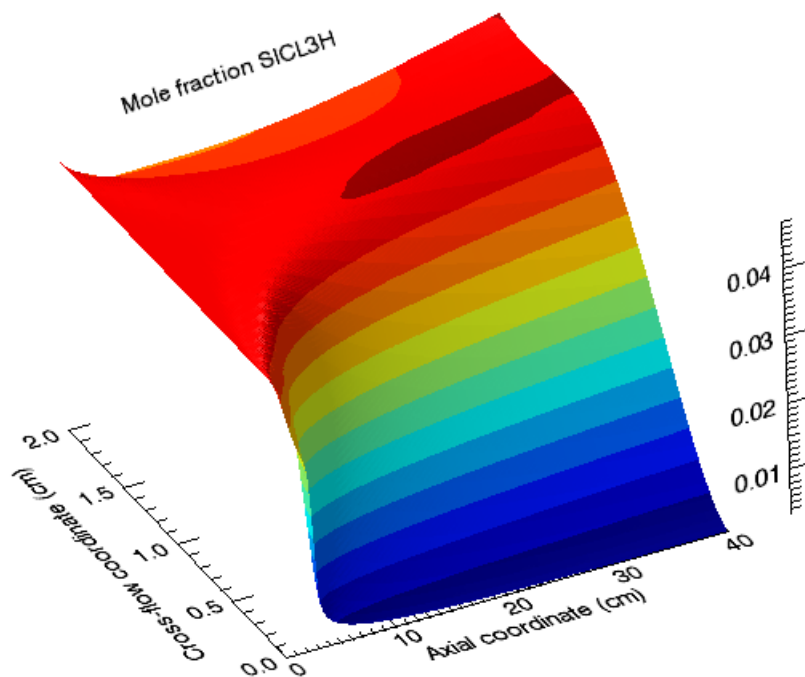


Figure 4-17 Trichlorosilane CVD—Silicon Deposition Rate

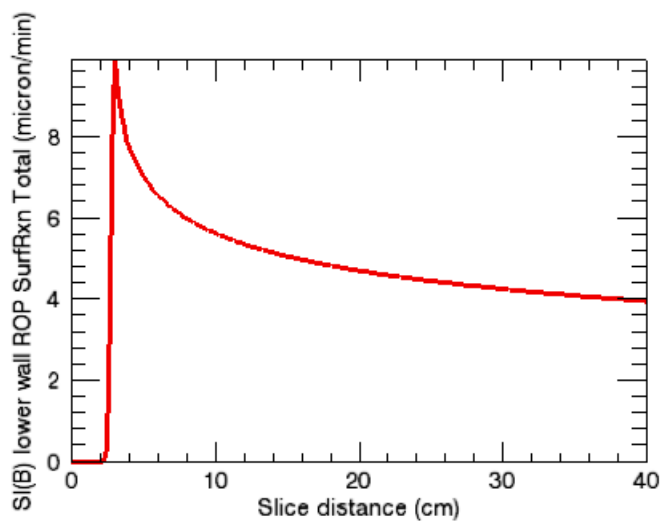
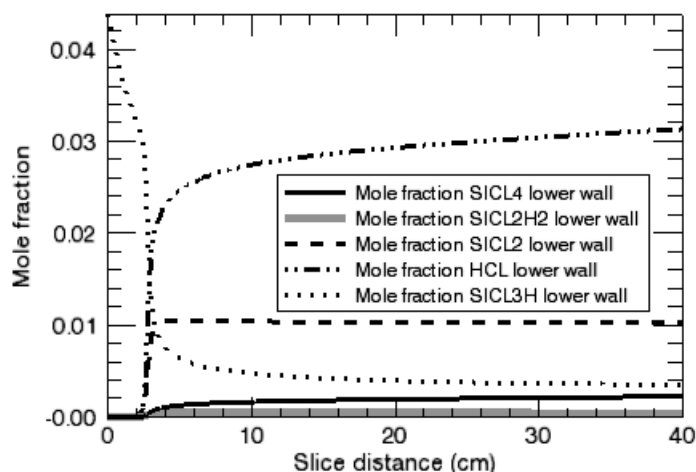


Figure 4-18 Trichlorosilane CVD—Mole Fractions



4.2 Atomic Layer Deposition (ALD)

The CHEMKIN software includes several reactor models that can be used for simulating ALD processes. ALD is a technique used to deposit thin films of solid materials in a very controlled manner, and differs from CVD primarily in that it is a transient process with the deposition surface being exposed to pulses of alternating gases. Ideally, the deposition chemistry in ALD is self-limiting, with growth occurring in a layer-by-layer manner and the deposition thickness being controlled only by the number of cycles. ALD is also called: ALE, Atomic Layer Epitaxy, NLD, Nano Layer Deposition, ALCVD, Atomic Layer Chemical Vapor Deposition, and AVD, Atomic Vapor Deposition. There are also plasma enhanced variations such as PENLD, Plasma Enhanced Nano Layer Deposition. It is a relatively new technology, having made the transition from the research lab to production in the last decade.

The transient models within the CHEMKIN software are useful for optimizing pulse sequences and thus minimizing cycle times in ALD. The major advantage of ALD over CVD is the improved control over the deposition process and more conformal deposition. The inherently lower deposition rates, however, lead to longer process times and higher costs. During a pulse, it is important that enough molecules react with all parts of the substrate to be coated. But many of the precursor materials are expensive. Thus one of the process optimization goals is to reduce the amount of precursor that flows through the reactor but does not react at the surface. Considering the effects of finite-rate kinetics for surface reactions can be an important part of such an optimization, as reactions do not always behave in an ideal manner.

4.2.1 Time-dependent Simulations of ALD Process

4.2.1.1 Project Description

This user tutorial demonstrates two ways of simulating a time-dependent ALD process. The transient Perfectly Stirred Reactor Model runs relatively quickly and is useful for developing and initial testing of the chemical reaction mechanism. The transient stagnation flow model more realistically simulates a production-scale shower-head ALD reactor by including mass-transport effects. The alumina ALD chemistry described in [Section 4.4.4](#) is used. The process operates at a pressure of 1 Torr, and a relatively low surface temperature (compared to CVD) of 450° C (723 K). This sample demonstrates four cycles of the flow sequence including: metalorganic precursor in argon; argon purge; ozone in oxygen and argon; and argon purge. The four cycles are sufficient, in this case, to characterize the process.

4.2.1.2 Project Setup

This project file is an example that contains multiple reactor models or sub-projects. It is called ***multiple_models_atomic_layer_deposition.ckprj***. The data files used for this sample are located in the ***samples\multiple_models_atomic_layer_deposition*** directory. The two reactor diagrams in this project each contain three gas inlets and either a Perfectly Stirred Reactor or a Stagnation-flow CVD Reactor Model.

In this project, the names of the gas inlets, and their corresponding input panels, have been changed away from the default names of R1_IN1, etc, to **METORG**, **OXIDIZER** and **PURGE**, which reflect the function of the gas flowing through the inlets. The listings of flow rate as a function of time for each gas-flow inlet are saved as time-dependent profile files:

- ✓ *SCCMPRO_METORG.ckprf*
- ✓ *SCCMPRO_OXIDIZER.ckprf*
- ✓ *SCCMPRO_PURGE.ckprf*

In this case, the profiles of total flow rates for each gas inlet are in volumetric flow units of sccm, but flow profiles can also be specified in mass flow units. The PSR and stagnation-flow models use the same flow-profile files.

Although both simulations run for the same length of process time, the stagnation flow simulation takes significantly more compute time to run, due to the inclusion of mass-transport effects.

4.2.1.2.1

Transient PSR

The names of the flow-profile files are designated on the Stream Property Data tab of each Gas Inlet panel. If a profile file already exists, it can be selected by browsing or by the pull-down menu, if it has already been accessed. The Edit button opens a panel that allows profile files to be edited or created. In this case, inlet temperatures are not specified on the Gas Inlet panel, as this is a fixed-gas temperature simulation. The composition of each reactant gas inlet is specified on the Species-specific Property panel of the corresponding Gas Inlet panel.

The choice of fixed gas temperature for this simulation is made with the Problem-type dropdown list on the Reactor Physical Property tab of the C1_ PSR panel. The gas temperature, pressure, volume and surface area (which are generally representative of ALD reactors) are also input here. In this case, the gas temperature for the PSR simulation was chosen to reproduce the degree of ozone decomposition to O atoms and match the deposition rate observed in the higher dimensional simulation. The surface temperature is different from the gas temperature, and it is also specified on the Reactor Physical Properties tab. On the Species-specific Data tab, the starting gas composition of pure argon is specified on the Initial Gas Fraction sub-tab, the starting surface composition of complete O(S) coverage is specified on the Surface Fraction sub-tab, and an activity of 1.0 specified for AL₂O₃(B) on the Bulk Activity sub-tab. These correspond to a reasonable starting condition where the substrate might have an initial oxide coating, and the system was purged with argon after loading. No entries are made on the other parts of this panel.

The end time of the transient simulation is specified on the Basic tab of the Solver panel, along with the solver step time, interval for saving the solution, and the interval for printing data to the diagnostic output file. No entries are needed on the Output Control or Continuations panels for this problem.

4.2.1.2.2

Transient Stagnation Flow Reactor

The names of the flow-profile files are designated on the Stream-property panel of each Gas Inlet panel. In this case, the gas energy equation is being solved, so inlet temperatures of 150° C (423 K) are input for each gas inlet. The composition of each reactant gas inlet is specified on the Species-specific Property tab of the corresponding Gas Inlet panel.

Choices to solve a transient problem, include the gas energy equation, use multicomponent diffusion but not the Soret effect, etc., are input in the Reactor Physical Property tab, Basic sub-tab of the C1_ Stagnation Flow panel. The process pressure and surface temperature are input on this sub-tab, along with the name of

file containing the initial guess for the gas temperatures as a function of height above the disk, and a cross sectional flow area used for translating volumetric flow rates to linear flow velocities. There are no entries on the other sub-tabs of the Reactor Physical Property tab.

The Initial Grid Property tab of the C1_ Stagnation Flow panel allows the input of the number of points in the grid of distance above the substrate, along with the ending axial distance. In transient simulations, the grid currently does not adapt as it does in steady-state stagnation flow simulations. Thus, a reasonably dense initial grid should be specified, and the adaptive gridding parameters are ignored. Note that the surface is defined as being at a coordinate value of $x = 0$, and the maximum distance of 1.2 cm is the location of the gas inlets (showerhead). In other words, the solution is given as a function of distance from the surface.

On the Species-specific Data tab of the C1_ Stagnation Flow panel, the starting gas composition of pure argon is specified on the Initial Gas Fraction sub-tab, the starting surface composition of complete O(S) coverage is specified on the Surface Fraction sub-tab and an activity of 1.0 specified for AL₂O₃(B) on the Bulk Activity sub-tab. These are the same as were used in the PSR simulation, and correspond to a reasonable starting condition where the substrate might have an initial oxide coating, and the system was purged with argon after loading. No entries are made on the other parts of this panel.

The end time of the transient simulation is specified on the Basic tab of the Solver panel, along with the interval for printing data to the output file and some tolerance parameters that have been relaxed from the default values. The Advanced tab of the Solver panel contains a time-step specification and a solver parameter that have been altered from the default values. No entries are made on the Output Control or Continuations panels for this problem.

4.2.1.3 Project Results

Figure 4-19 shows the gas pulses used in this example for the metal-organic and oxidizer gas inlets. The pure-argon purge gas pulses are not shown. The metal-organic gas pulses are considerably shorter than the oxidizer gas pulses, but appear to be sufficient. The contour plot of one TMA pulse from the stagnation-flow simulation in *Figure 4-20* clearly shows that the TMA is consumed at the surface only at the beginning of the pulse. By the end of the pulse, all the TMA flowing into the reactor is also flowing out again.

Figure 4-19 Time-dependent ALD Simulations—PSR, Total Flow Rates vs. Time

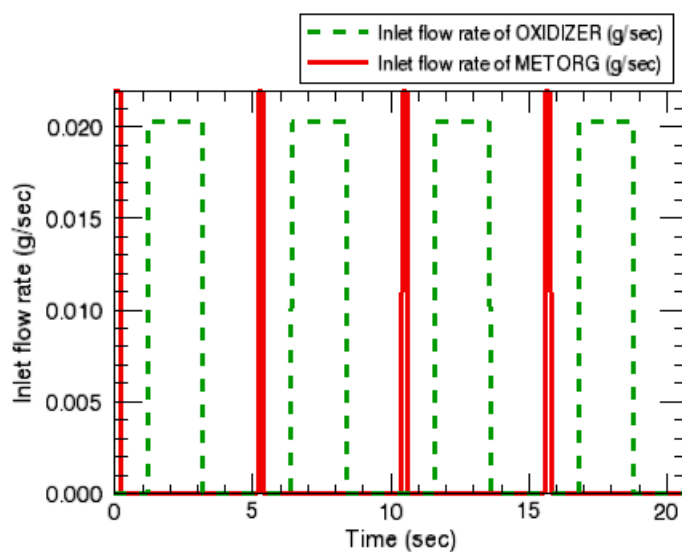
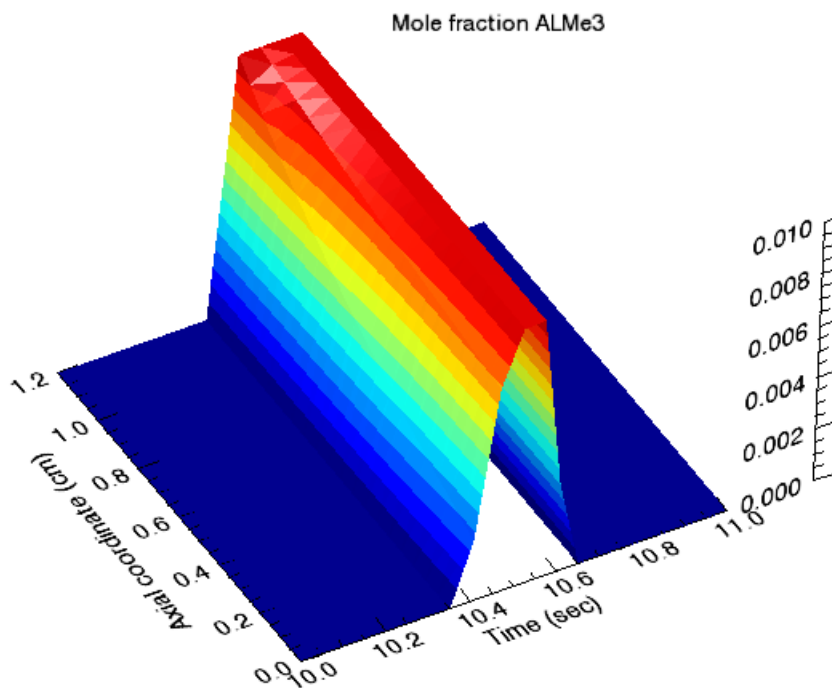


Figure 4-20 Time-dependent ALD Simulations—TMA Contour Plot



The chemistry that occurs during the oxidizer pulses is more complex. The contour plot of O atom mole fractions in [Figure 4-21](#) show how the O atoms are formed by gas-phase decomposition of ozone in the hotter regions of the gas, and then react away at the surface. The site fractions in [Figure 4-22](#) show that the methylated surface species, ALME2(S) and ALMEOALME(S), are not completely converted to O(S) during the oxidizer pulse. This probably results from the fact that the oxidation

occurs as two sequential steps and the kinetics are limiting the process. The O atom mole fractions in [Figure 4-23](#) shows that the O atoms are not being depleted at the surface in the stagnation flow simulations, which suggests a kinetic limitation, possibly resulting from the default reaction orders in this simple mechanism. The incomplete oxidation of the methylated surface species in turn leads to less than unity O(S) coverage at the beginning of the TMA pulse, which in turn leads to less efficient use of TMA and some notable differences between the first and subsequent pulses.

Figure 4-21 Time-dependent ALD Simulations—O Mole Fraction

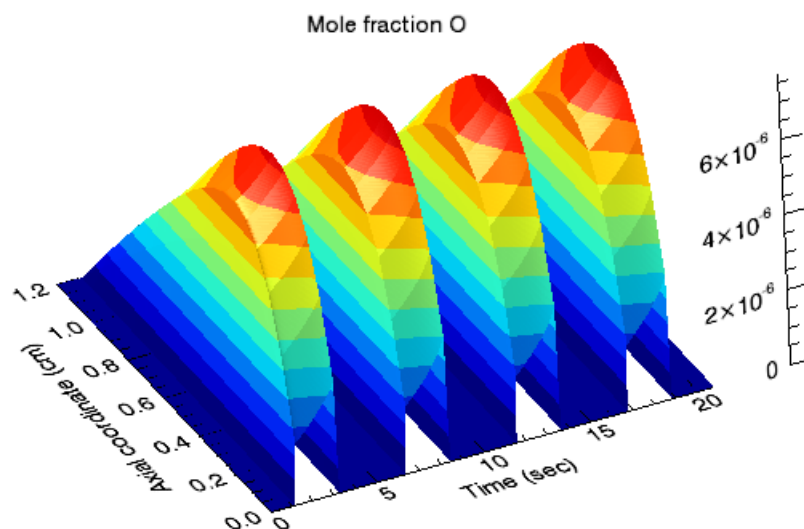


Figure 4-22 Time-dependent ALD Simulations—Stagnation-flow Site Fractions

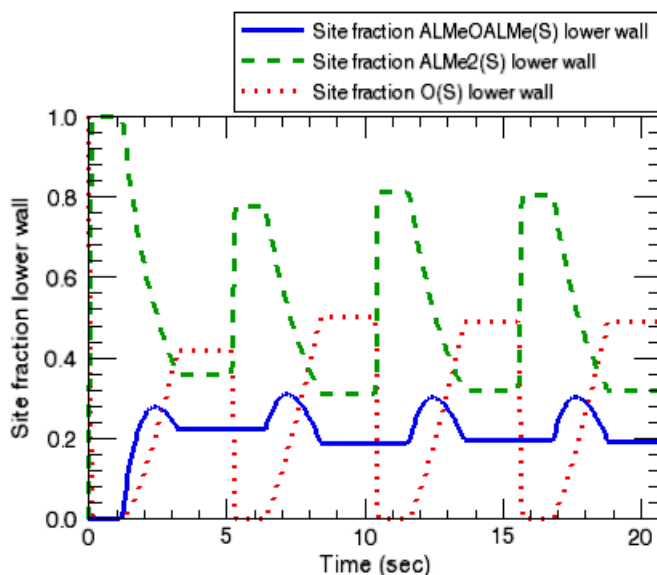
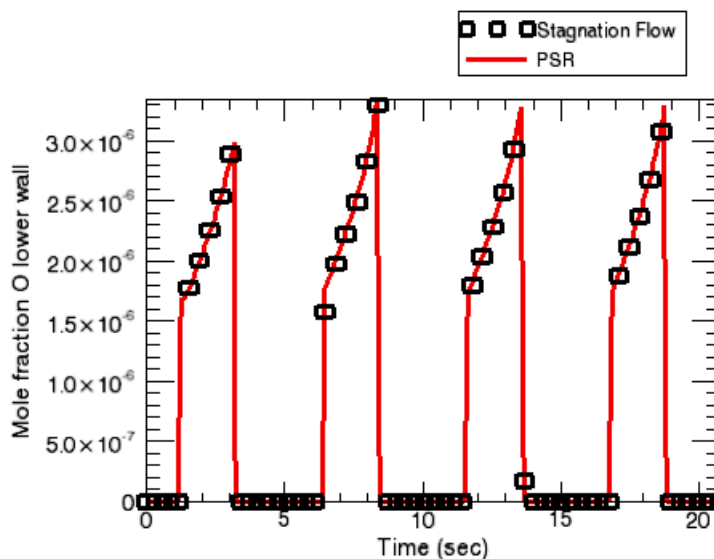
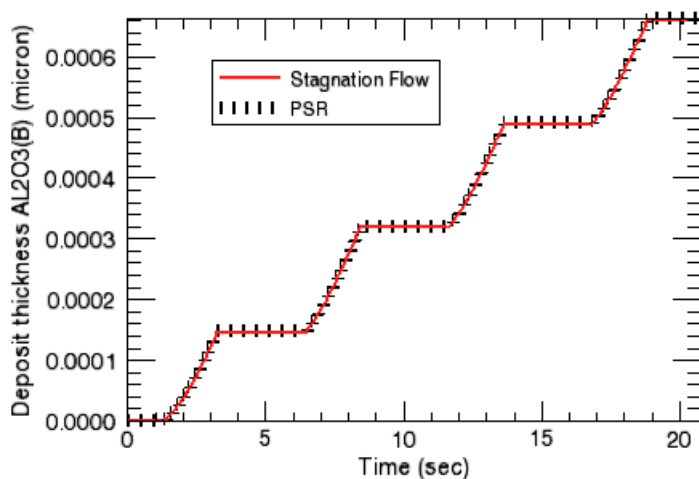


Figure 4-23 Time-dependent ALD Simulations—O Mole Fractions Comparison



The O atom mole fractions in [Figure 4-23](#) from the stagnation flow simulations agree well with those from the PSR simulations. Within the limits of this simple deposition chemistry, this directly leads to the good agreement for deposition thickness shown in [Figure 4-24](#). The agreement between the two models, in this case, results from the fitting of the gas-phase temperature in the PSR simulation to reproduce the O atom mole fractions in the higher-dimensional simulation. This kind of a calibration allows the faster-running PSR simulation to be used to quickly explore a wide range of pulse sequences and other experimental conditions of interest, before returning to higher-dimensional simulations for more careful study.

Figure 4-24 Time-dependent ALD Simulations—Deposition Thickness Comparison



4.3 Plasma Etching

The CHEMKIN software includes a number of special features for modeling plasmas, most of which are demonstrated in these examples. For treating non-equilibrium plasmas, the plasma models allow you to specify different temperatures for the neutral gas, electrons, ions, and surfaces. A gas-phase reaction rate can be designated to depend on the electron temperature rather than the default neutral gas temperature. An electron-impact reaction can also be designated to involve a specified energy loss per collision. This option is used to describe excitation energy losses for electrons in solving the electron energy equation, without explicitly defining each vibrationally or electronically excited-state as a separate species within the corresponding thermodynamic data. For surface reactions, ion-assisted reactions can have yields that depend on the ion energy. Such reactions can also be designated as Bohm reactions, which means that the ion flux is limited by the Bohm velocity of the ions, rather than by the ion's thermal speed. The implementation of the Bohm criterion is described in detail in [Section 8.5.3](#) of the *CHEMKIN Theory Manual*. This factor has been introduced to account for the fact that the ion interaction with the surface will be subject to transport limitations, such that a gradient near the walls in the ion density will occur. A zero-dimensional model cannot capture this effect, such that a Bohm-flux correction model is used.

4.3.1 Steady-state Chlorine Plasma

4.3.1.1 Project Description

This user tutorial provides an example of modeling a low-pressure plasma reactor as a steady-state Perfectly Stirred Reactor, using the chlorine plasma chemistry set described in [Figure 4.4.5](#). The plasma pressure is 5 mtorr and pure chlorine gas flows into the reactor at 35 sccm. The energy equation and the electron energy equation are solved, and a heat-transfer correlation is used to account for heat loss through the wall of the reactor.

4.3.1.2 Project Setup

The project file is called *plasma_psr__chlorine.ckprj*. The data files used for this sample are located in the *samples\plasma_psr__chlorine* directory. This reactor diagram contains one gas inlet, one plasma PSR, and one outlet.

The reactant gas mixture, which is pure Cl_2 in this case, is input on the Species-specific Property tab of the C1_Inlet1 panel. The initial guess for the steady-state gas composition, which is input on the Initial Gas Fraction subtab of the Species-specific Data tab of the C1_Plasma PSR panel, is quite important. A good initial guess (one that is close to the steady-state solution) will result in fast convergence, while a poor initial guess can at worst lead to failure of the simulation.

The Reactor Physical Property tab of the C1_Plasma PSR panel is where problem type and reactor parameters such as pressure, temperatures, volume, area, heat loss, and plasma power are entered. Solving the electron energy equation requires that an initial guess for the electron temperature be input on this tab, as well as an inlet electron temperature on the Stream Property tab of the C1_Inlet1 panel. The latter has no impact on the solution unless there are electrons in the inlet gas mixture. The Sheath Loss parameter describes the ion energy gained crossing the sheath and may be specified differently for each material in the system. On the Solver panel, skipping the intermediate fixed-temperature solution is usually more robust for plasma simulations than trying to solve it first.

4.3.1.3 Project Results

[Figure 4-25](#) shows the electron temperature as a function of power for this chlorine plasma. The electron temperature shows only small changes over the large variation in plasma power, since most of the power is transferred into ionization and dissociation rather than electron heating. However, as the plasma power drops the electron temperature rises as the plasma nears extinction, since there are fewer electrons and electron-driven events. The mole fractions of the electrons and positive ions, increase steadily with increasing plasma power, as shown in [Figure 4-26](#), but the chlorine negative ions show a maximum at intermediate powers. [Figure 4-27](#) shows that the net dissociation of molecular chlorine to atomic chlorine steadily increases with increasing plasma power, as expected.

Figure 4-25 Steady-state Chlorine Plasma—Electron Temperatures vs. Power

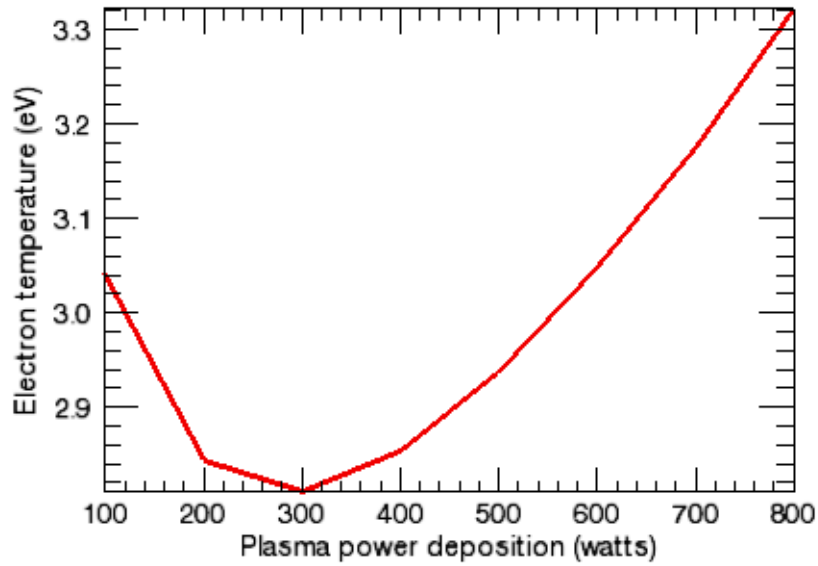


Figure 4-26 Steady-state Chlorine Plasma—Mole Fractions

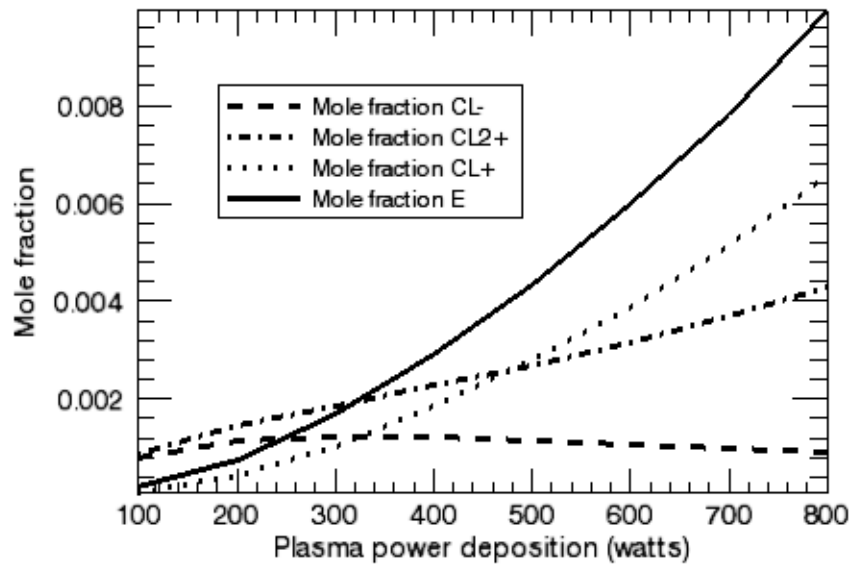


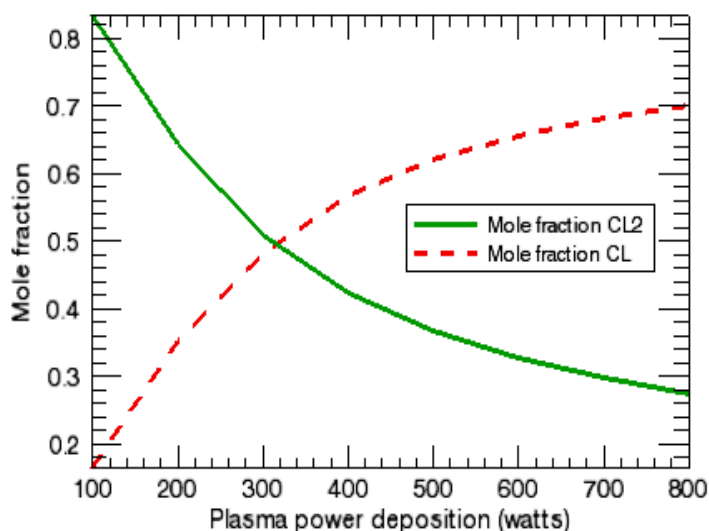
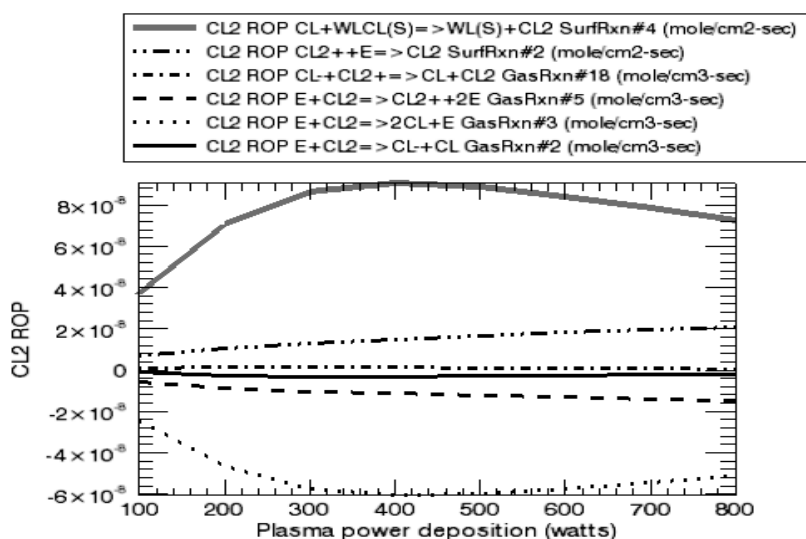
Figure 4-27 Steady-state Chlorine Plasma—Cl and Cl₂ Mole Fractions

Figure 4-28 shows a rate-of-production analysis for the input gas Cl₂. In this case, there are clear major and minor pathways. The primary reaction consuming molecular chlorine is gas-phase reaction #3, which is the electron-impact dissociation to two Cl atoms. Gas reactions #5 and 2, the electron-impact ionization and dissociative attachment reactions of Cl₂, respectively, are minor channels for Cl₂ consumption. The primary reaction producing Cl₂ is surface reaction #4, the reaction between gas-phase and adsorbed Cl atoms producing molecular chlorine in the gas phase. Gas reaction #18, the neutralization reaction between Cl⁻ and Cl₂⁺, and surface reaction #2, the neutralization of Cl₂⁺ on the wall, are minor channels for Cl₂ production.

Figure 4-28 Steady-state Chlorine Plasma—ROP Analysis



4.3.2 Spatial Chlorine Plasma PFR with Power Profile

4.3.2.1 Project Description

This user tutorial presents an example of a Plasma Plug Flow Reactor with a specified power versus distance profile. This feature might be used to model an experimental apparatus where the inductive coils providing the power are spaced unevenly. Alternatively, this could be used to model a system where there is a lower-power region where a probe is used that cannot operate in a high-plasma density region, or where a measurement window is located.

This example is for a plasma at a total pressure of one torr with pure chlorine gas flowing into the reactor at $35 \text{ cm}^3/\text{s}$, using the chlorine plasma chemistry set described in [Section 4.4.5](#). The electron energy equation is solved, and there is consideration of heat loss through the wall of the reactor. The area used for surface chemistry and heat loss corresponds to the physical walls of the tubular reactor.

4.3.2.2 Project Setup

The project file is called ***plasma_pfr_cl_power_profile.ckprj***. The data files used for this sample are located in the *samples\plasma_pfr\cl_power_profile* directory. This reactor diagram contains a gas inlet, a Plasma Plug Flow Reactor, and an outlet.

The reactant gas mixture is input on the Species-specific Property tab of the C1_Inlet1 panel. Although the input gas is actually pure Cl_2 , in order to have the plasma “light” in the simulation, we have modified the inlet gas to include a small amount of electrons and ions in the inlet gas.

The Reactor Physical Property tab of the C1_Plasma PFR panel is where problem type and reactor parameters such as pressure, temperatures, geometry, heat loss, and plasma power are entered. The value for the electron temperature input on the Reactor Physical Property tab of the C1_Plasma PFR panel is used as the inlet electron temperature. The plasma power profile can be entered by using the Profile tool or by selecting an existing profile file on the Reactor Physical Property tab of the C1_ panel. This is an alternative to entering a constant value for the Plasma Power Deposition parameter. The profile is entered as a list of pairs of numbers giving the power as a function of position. Values at intermediate points are straight-line interpolations of the two nearest specified values. Unphysically abrupt changes in the power profile can cause convergence problems in the simulation unless solver time steps are set accordingly. Note that the power deposition for a plug-flow reactor profile must be specified in per-distance units, as it will be integrated over the channel distance.

As a simulation that marches forward from the inlet state, this sample problem has no “initial guess” for the gas composition, but Surface Fractions are provided on the Species-specific Data tab of the C1_ Plasma PFR panel. These site fractions provide initial estimates for the surface state of the channel inlet. An initial pseudo-steady calculation will be performed to determine consistent surface state based on these estimates and the inlet gas composition, prior to the channel integration. The Sheath Loss parameter on the Material-specific Data tab of the C1_ Plasma PFR panel describes the ion energy gained crossing the sheath.

4.3.2.3 Project Results

Figure 4-29 shows the profile of electrical power deposited into the plasma as a function of distance down the Plug Flow Reactor. As expected, the mole fractions of the electrons and atomic chlorine, shown in *Figure 4-30* and *Figure 4-31*, respectively, generally follow the plasma power profile, with differing degrees of non-linearity. This is consistent with the fact that the Cl is created in the plasma by electron-impact dissociation of molecular chlorine. The mole fractions for the Cl^+ and Cl_2^+ ions, shown in *Figure 4-32* also follow the plasma power profile.

Figure 4-29 Spatial Chlorine Plasma—Plasma Power vs. Distance

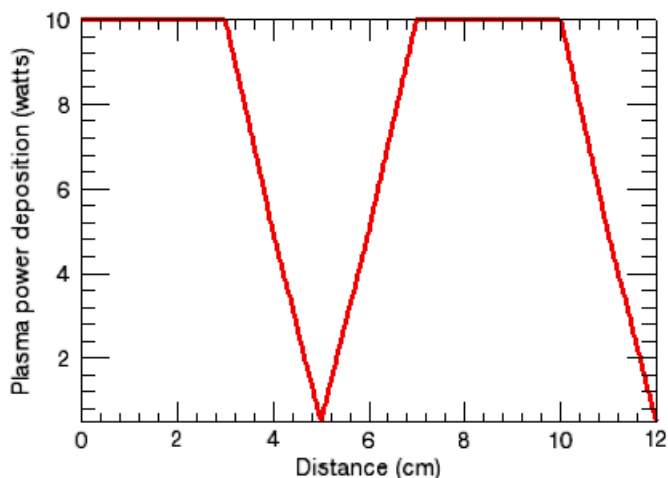


Figure 4-30 Spatial Chlorine Plasma—Electron Mole Fraction

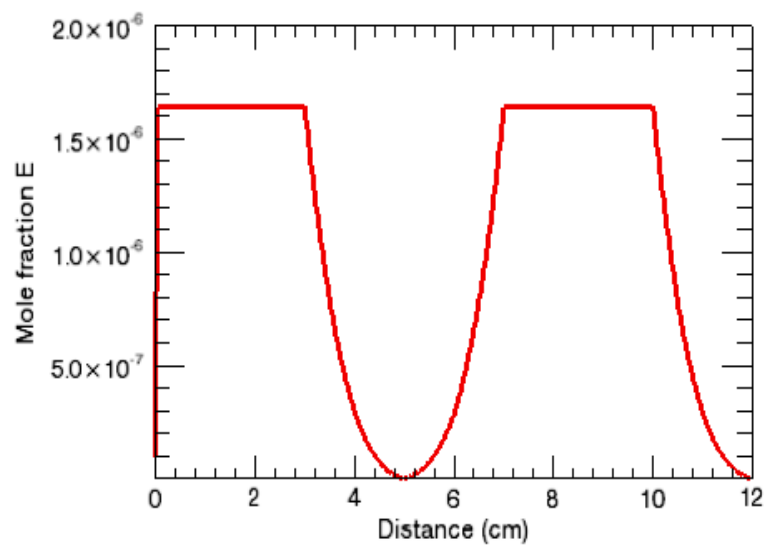


Figure 4-31 Spatial Chlorine Plasma—Cl Mole Fraction

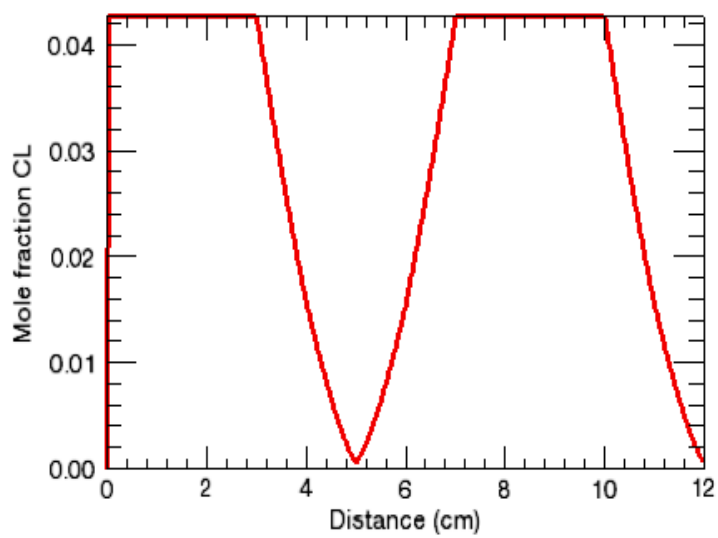
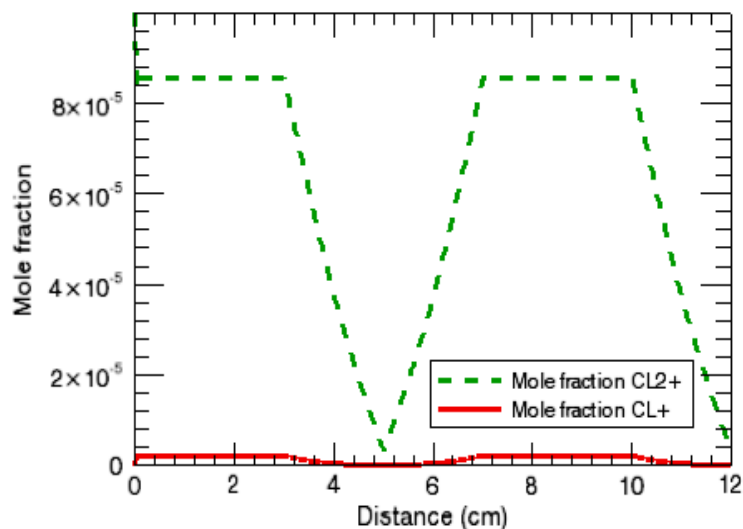
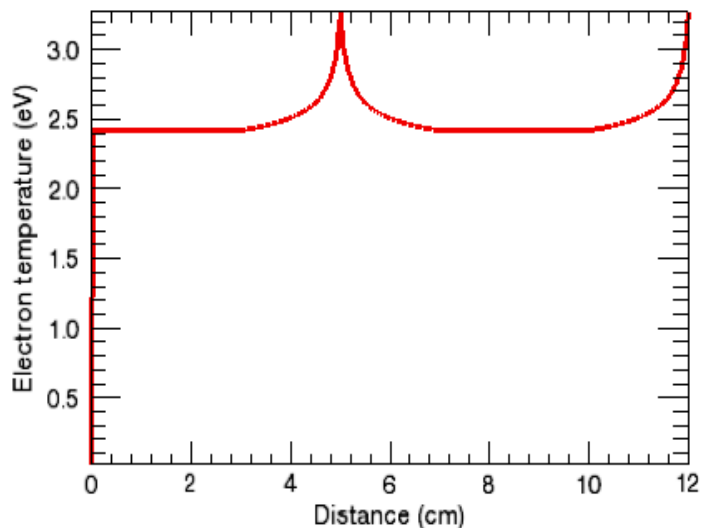


Figure 4-32 Spatial Chlorine Plasma—Cl⁺ and Cl₂⁺ Mole Fractions

The electron temperature rises somewhat in the lower-power regions of the reactor tube. This is consistent with the inverse trend between electron densities and electron temperatures seen at low power densities in [Section 4.3.1](#).

Figure 4-33 Spatial Chlorine Plasma—Electron Temperature



4.3.3 Fluorocarbon Plasma Etching of Silicon Dioxide

4.3.3.1 Project Description

This user tutorial is an example of modeling a low-pressure plasma reactor as a steady-state Perfectly Stirred Reactor, using the fluorocarbon plasma chemistry set described in [Section 4.4.6](#). This example is representative of a high-density plasma, with a plasma power of 3000 Watts and a pressure of 10 mtorr. Pure hexafluoroethane is the inlet gas. The energy equation and the electron energy equation are solved, and a heat-transfer correlation is used to account for heat loss through the wall of the reactor. This example illustrates the use of multiple materials, each with a different set of surface reactions, as well as the use of continuations with varying flow rate and ion impact energy.

4.3.3.2 Project Setup

The project file is called *plasma_psr__c2f6_etch.ckprj*. The data files used for this sample are located in the *samples\plasma_psr__c2f6_etch* directory. This reactor diagram contains a gas inlet and a plasma PSR.

The reactant gas mixture, which is pure C_2F_6 in this case, is input on the Species-specific Property tab of the C1_Inlet1 panel. The gas flow rate (30 sccm), inlet gas temperature and inlet electron temperature are input on the Stream Property tab of the R1_IN1 panel. The latter is required, but has little impact on the solution unless there are electrons in the input gas mixture.

The C1_Plasma PSR panel is where most of the parameters are input. The Reactor Physical Property tab allows selection of problem type, as well as places to enter parameters such as the plasma power, pressure (10 mTorr), volume, internal area, heat loss parameters, cross-section for electron momentum loss, and initial guesses for the electron, neutral, and ion temperatures. The Species-specific Data tab allows input of initial guesses for the steady-state gas composition, surface site fractions, and bulk activities, on the corresponding sub-tabs, as well as species-specific values for electron-momentum loss cross-sections. A good initial guess for the gas and surface compositions (one that is close to the steady-state solution) will result in fast convergence, while a poor initial guess can lead to failure of the simulation. The Bulk-phase -specific Data tab is used to indicate that all the bulk materials are being etched, which affects some of the equations. The Material-specific Properties tab is for specifying properties like surface temperature (if different from the neutral gas temperature), ion energy or bias power, Bohm factor, sheath energy loss factor, area fraction, or heat loss, either for all materials, or on a per-material basis. For this non-parameter-study problem, the bottom part of the panel is used to set up values that are dependent on the material. Material-independent properties can be set on the

Reactor Physical Properties panel. In this example, the `WAFER` is held at a temperature near room temperature (consistent with active cooling), while the `TOPWALL` is held at an elevated temperature (consistent with active heating), while the `SIDEWALL` temperature is allowed to float with the gas temperature (the default). A relatively high ion energy (in electron Volts) is specified for the `WAFER`, reflecting that this material substrate has an applied electrical bias, separate from the main power, for this system. The low ion energy for the `SIDEWALL` is consistent with the plasma self-bias, rather than active biasing of this surface. The `TOPWALL` has no ion energy specified, as no ion-energy dependent reactions occur on this material.

On the Solver panel, a number of parameters on both the Basic and Advanced tabs have been altered from the defaults in order to help get a good solution. Skipping the intermediate fixed-temperature solution is the default for plasma simulations and is recommended. The Output Control panel allows specification of whether sensitivities should be calculated and printed in the output and solution files, and whether ROPs should be printed and saved. In this case, sensitivities for temperature, growth (etch) rate, F atoms and SiF_4 will be calculated. ROPs for 6 species will be included. The Continuations panel specifies two continuations. First, the ion energy for the wafer is changed from 200 to 300 V, and the flow rate is increased from 30 to 50 sccm. Second, the flow rate is returned to the initial lower value, while leaving the ion energy at the higher value. In this example, the plasma power is entered on both continuation panels, although it is not changed. This is not necessary, but will not cause any problems and may serve as a useful reminder.

4.3.3.3 Project Results

In [Figure 4-34](#), the SiO_2 etch rates for variations of C_2F_6 flow rate and Wafer ion energy are: 1) 30 sccm, 200 V. 2) 50 sccm, 300 V. 3) 30 sccm, 300 V. This shows that oxide etch rates (negative growth rates) on the Wafer are much larger than those on the Sidewall, in accord with the higher ion energy for that material. Comparing solutions 1 and 3 shows that increasing the Wafer ion energy increases the etch rate, as expected. But comparing solutions 2 and 3 shows that increasing the reactant flow rate also increases the etch rate, indicating that the etching system may be reagent-supply limited. This is consistent with the results shown in [Figure 4-35](#), which shows the 10 neutral species with the highest mole fractions. C_2F_6 , the reactant species, does not appear, as it is mostly decomposed to smaller fragments in the plasma. The species with the highest mole fraction, F atoms, is a reactant fragment that can contribute to etching, as are CF and CF_3 , which are also present in relatively high concentrations. These species have higher mole fractions in solution 2, which has the highest flow rate, whereas etch-product species, such as CO and SiF_3 , have lower mole fractions at the shorter residence time. [Figure 4-36](#) shows that CF^+ is the most prevalent positive ion, with F^+ , CF_2^+ and CF_3^+ about a factor of 2 lower. There is less

F^+ than CF^+ , even though there is more F than CF, and the major pathways producing F^+ and CF^+ are ionization of F and CF, respectively. This reflects a higher rate for the CF ionization reaction than the F ionization reaction. Although not shown, the electron is the most prevalent negatively charged species, with CF_3^- roughly a factor of 6 lower. Negative ions stay in the body of the plasma and do not participate in reactions at the surface due to the presence of an electronegative sheath.

Figure 4-34 Fluorocarbon Plasma Etching of Silicon Dioxide— SiO_2 Etch Rates Variations

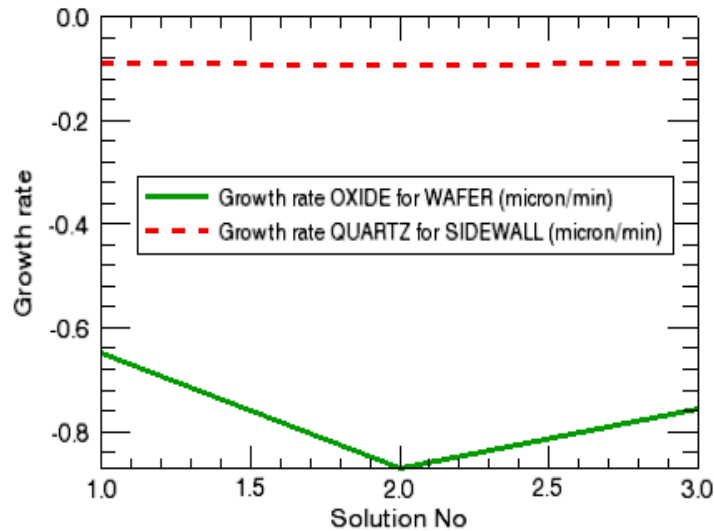


Figure 4-35 Fluorocarbon Plasma Etching of Silicon Dioxide—10 Highest Mole Fractions

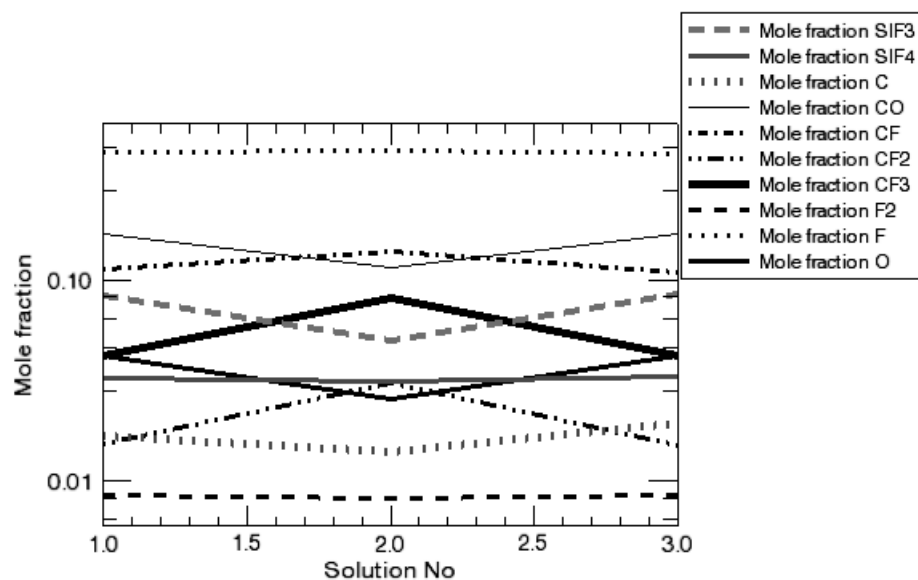
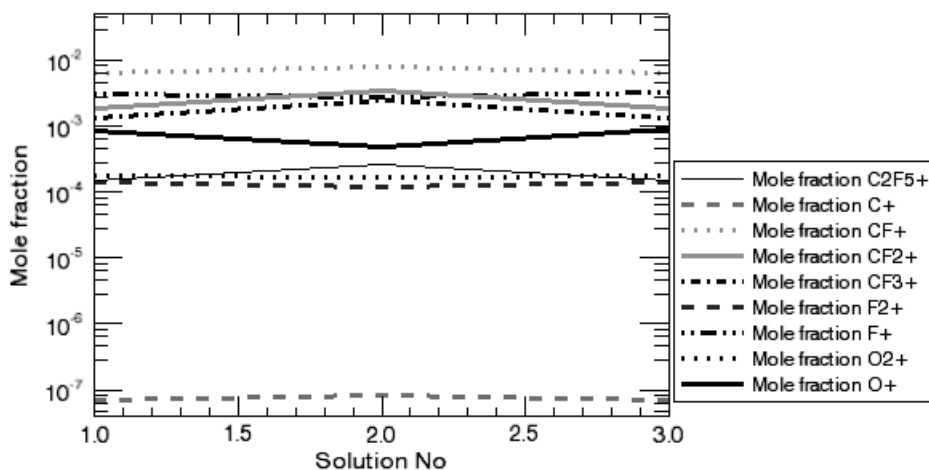


Figure 4-36 Fluorocarbon Plasma Etching of Silicon Dioxide—Positive Ion Mole Fractions



The surface site fractions shown in [Figure 4-37](#) show minor changes with conditions. Comparing solutions 1 and 3 shows that increasing the Wafer ion energy increases the fraction of open sites and decreases the fraction of fluorocarbon-covered sites. This is consistent with the increased ion energy causing an increase in yield for the ion-enhanced etching reactions. Comparing solutions 3 and 2 shows that increasing the C_2F_6 flow rate decreases the fraction of open sites and increases the fraction of fluorocarbon-covered sites. This is consistent with an increased supply of fluorocarbon radicals that can react with the open sites. [Figure 4-38](#) shows the 5 reactions with the largest contribution to the loss of silicon dioxide from the wafer. In order of decreasing importance, surface reactions 13, 14, 11, and 12 are etching of WSIO2_CF2(S) sites assisted by CF^+ , F^+ , CF_2^+ , and CF_3^+ , respectively. Reaction 5 is the F^+ ion-assisted etching reaction of the WSIO2_F2(S) site. These five reactions are responsible for most of the etching, but a number of other reactions contribute to the total etch rate.

Figure 4-37 Fluorocarbon Plasma Etching of Silicon Dioxide—Surface Site Fractions

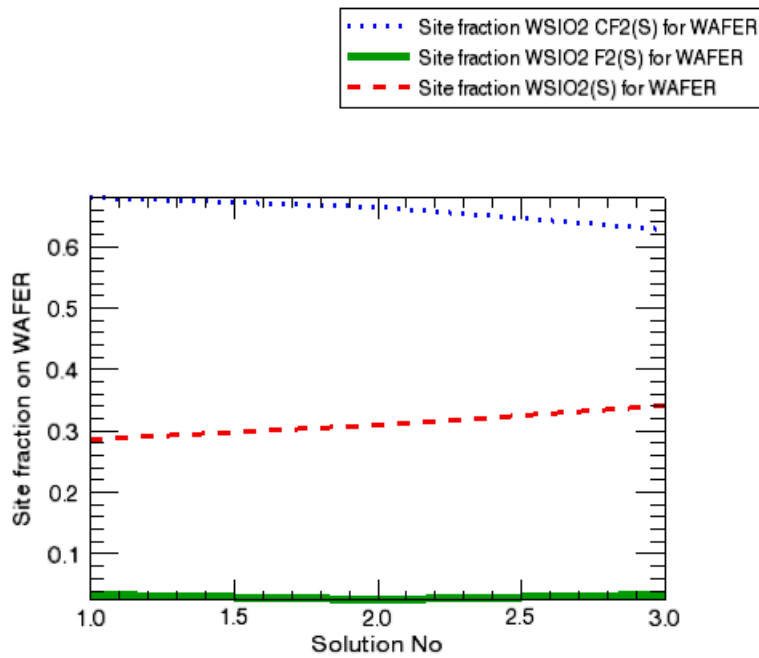
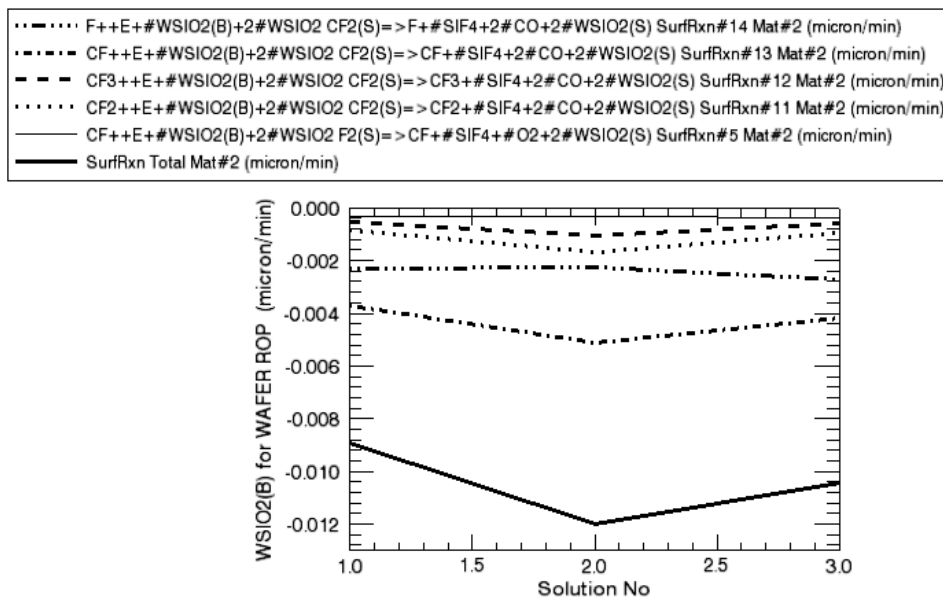


Figure 4-38 Fluorocarbon Plasma Etching of Silicon Dioxide—Highest ROP



4.4 Chemistry Sets

In this section, we describe in more detail the chemistry sets employed in the tutorials described in [Chapter 4](#).

4.4.1 Silicon Nitride CVD from Silicon Tetrafluoride and Ammonia

This chemistry set describes the deposition of silicon nitride (Si_3N_4) from a mixture of SiF_4 and NH_3 .³² This mechanism demonstrates one way of describing the deposition of a compound solid, but it should generally be considered as illustrative only and not as a source of kinetic data for Si_3N_4 deposition.

The *chem.inp* file includes 4 elements, 17 gas-phase species and 33 reactions. The first 27 of these reactions describe the pyrolysis of ammonia, and are taken from published models for ammonia oxidation and De-NOx.³³ The other 6 reactions describe SiF_4 decomposition and likely cross reactions between Si and N-containing species. Rate parameters were not available in the literature for these reactions, so the mechanism uses estimates based on bond strengths and analogies with related gas-phase reactions.

The *surf.inp* file defines six surface species in the Si_3N_4 surface phase and the Si_3N_4 solid, which is defined in terms of two bulk phases, Si(D) and N(D). The surface species all occupy more than one site, and have placeholder thermodynamic data. Six irreversible surface reactions are also defined in this file. The surface reactions are “lumped” reactions, meaning that they each represent several elementary steps that have been combined into one reaction. Rate parameters for these surface reactions were determined by fitting the model results to experimental deposition-rate data. The activation energies for the surface reactions are all zero, which reflects the limitations of the experimental data set used to derive the rate parameters. Although it is not immediately obvious, the surface species and reactions were designed to produce a bulk-phase stoichiometry of 3 Si to 4 N. The densities of bulk species has been defined to force the linear deposition rates of either Si(D) or N(D) match the experimentally observed deposition rate for Si_3N_4 . These reactions have zero for activation energies because they were fit to an experimental data set taken at one temperature. These rates would therefore not be likely to be valid at other temperatures.

32. M. E. Coltrin, P. Ho, Sandia National Laboratories, private communication.

33. J. A. Miller, M. D. Smooke, R. M. Green, and R. J. Kee, *Comb. Sci. Technol.* **34**:149 (1983).

4.4.2 Silicon Deposition from Silane

This chemistry set described the CVD of silicon from silane. This CVD system has been the subject of numerous studies, facilitated by the simplicity of the precursor molecule. This reaction mechanism was published by Coltrin and coworkers at Sandia National Laboratories in the last³⁴ of a series of papers. This mechanism has been validated with a variety of optical diagnostic measurements and deposition rate data in a variety of experimental reactor geometries.

The *chem.inp* file includes 3 elements (helium is used as a carrier gas), 9 gas-phase species, and 10 reversible gas-phase reactions. Many of the reactions are unimolecular decomposition reactions with explicit treatment of pressure dependent rate parameters. The most important reaction is the decomposition of SiH_4 to SiH_2 and H_2 . The other reactions include the reaction of SiH_2 with SiH_4 to form Si_2H_6 , which can then react again to form Si_3H_8 , or decompose to H_3SiSiH and H_2 . Other reactions involve interconversion between various silicon-hydride species, plus the formation of atomic silicon, which was one of the experimentally measured species. This mechanism was originally much larger, but over time, it was substantially reduced by the elimination of species and reactions deemed to be unimportant.

The *surf.inp* file includes two surface species, open Si sites and hydrogen covered silicon sites, plus solid silicon as a bulk species. There are 8 surface reactions, all written as irreversible reactions with placeholders for the thermodynamic data of the surface species. These reactions include the two-site dissociative adsorption of silane, disilane and trisilane, which form hydrogenated silicon sites, deposited bulk silicon, and H_2 . Collisions of Si atoms, SiH_2 , H_3SiSiH and H_2SiSiH_2 species with the surface result in deposition of bulk silicon and formation of gas-phase H_2 with unit probability. Adsorbed hydrogen is removed from the surface by the associative desorption of H_2 , where a coverage dependence parameter has been used to alter the default second-order dependence to the experimentally observed first order.

4.4.3 Silicon Deposition from Trichlorosilane

This chemistry set describes the deposition of silicon from trichlorosilane in a hydrogen carrier gas. This mechanism is built on a significant number of independently published chemical kinetic parameters, and is described in more detail in a publication by Ho, *et al.*³⁵

34. "Laser-Induced Fluorescence Measurements and Kinetic Analysis of Si Atom Formation in a Rotating Disk Chemical Deposition Reactor", P. Ho, M. E. Coltrin, W. G. Breiland, *J. Phys. Chem.* **98**: 10138 (1994), and references therein.

The *chem.inp* file includes 3 elements, 11 gas-phase species, and 9 reversible gas-phase reactions. The gas-phase reactions are reversible decomposition reactions of various chlorosilanes and chlorinated disilanes. These reactions cause the conversion of some of the initial chlorosilane starting material to these other gas-phase species, which can be significant because the less-chlorinated molecules have higher surface reactivities. These reactions are written as unimolecular decomposition reactions at their high-pressure limit, so this reaction mechanism would tend to overstate the importance of gas-phase chemistry if it were used at lower total pressures.

The *surf.inp* file has 3 surface species: open silicon surface sites, hydrogen-covered sites, and chlorine-covered sites, plus solid silicon as a bulk phase. There are 10 surface reactions, all written as irreversible reactions with placeholders for the thermodynamic data of the surface species. These reactions include the dissociative adsorption of SiCl_3H , SiCl_2H_2 and SiCl_4 , which result in the formation of deposited silicon and hydrogenated/chlorinated silicon surface species. These are “lumped reactions” to the extent that the initial adsorption event, plus the successive transfer of H and Cl atoms from the initially adsorbed Si to other surface Si atoms, are all described as one step. The physical interpretation of this “lumping” is that adsorption of the gas-phase species is assumed to be slow compared to subsequent transfer of H and Cl atoms on the surface. For a chemically balanced reaction, this is written as involving 4 open sites, which by default would make the reaction fourth order in open sites, so the coverage dependence option has been used to set the kinetics to a more reasonable first-order dependence. Other reactions include the dissociative adsorption and associative desorption of H_2 , HCl and SiCl_2 , plus the dissociative adsorption of HSiCl. In many cases, the rate parameters are based on experimental surface-science studies, in other cases they are the result of fitting a model to experimental silicon deposition rate data from a specific CVD reactor.

4.4.4 Alumina ALD

This chemistry set describes the atomic layer deposition (ALD) of alumina from trimethylaluminum (TMA) and ozone. This mechanism is deliberately simplistic for illustration purposes only. It demonstrates one way of describing the ALD of alumina, but it should generally be considered as illustrative only and not used as a source of

35. “Chemical Kinetics for Modeling Silicon Epitaxy from Chlorosilane”, P. Ho, A. Balakrishna, J. M. Chacin, A. Thilderkvist, B. Haas, and P. B. Comita, in “Fundamental Gas-Phase and Surface Chemistry of Vapor-Phase Materials Synthesis”, T. J. Mountziaris, M. D. Allendorf, K. F. Jensen, R. K. Ulrich, M. R. Zachariah, and M. Meyyappan, Editors, PV 98-23, p. 117-122, Proceedings of the 194th Meeting of the Electrochemical Society, 11/1-6/98, The Electrochemical Society Proceedings Series, Pennington, NJ (1999).

kinetic data for this process. This mechanism is designed to deposit stoichiometric alumina, with three oxygen atoms being deposited for each two aluminum atoms. If the goal of a simulation was to track the elemental make-up of a material with a wide range of possible compositions, the choice of surface species and reactions would have to be quite different.

The fact that the different chemicals are separately pulsed into the system, rather than being mixed in the gas, prevents many possible gas-phase reactions from occurring in this process. The gas-phase chemistry described in the *chem.inp* file has 5 elements: Al, C, H, O, and Ar; and 6 gas-phase species: AlMe_3 , O, O_2 , O_3 , C_2H_6 and Ar. There are only two gas phase reactions; the collisionally-induced decomposition of ozone and the reaction of O atoms with ozone to form molecular oxygen. The rate parameters are from Benson and Axworthy.³⁶ This mechanism does not include reactions for TMA decomposition because it was determined to be too slow at the temperatures of interest. But if such reactions were included, they would be listed in the same chemistry input file. The temporal separation of the gas mixtures is accounted for by omitting reactions between gas-phase species that would not be present in the reactor at the same time, such as reactions between TMA and O atoms. A reaction mechanism for alumina CVD, in contrast, would need to include all such reactions.

The surface chemistry described in the *surf.inp* file defines three surface species: O(S), ALME2(S) and ALMEOALME(S); where the last species occupies two surface sites, plus the bulk alumina AL₂O₃(B). There are only three surface reactions, each of which represents several elementary surface processes. The first surface reaction represents the dissociative adsorption of TMA on the oxygenated surface species O(S) to form the ALME2(S), combined with the recombination of two methyl groups and desorption of an ethane molecule. This reaction has been given a moderately high sticking coefficient of 0.1, and is written in terms of a half ethane molecule in order to have a balanced reaction that is first order in TMA. This reaction only occurs in the presence of TMA, and will terminate when all of the O(S) surface species have reacted. The second surface reaction describes gas-phase oxygen atoms reacting with the two ALME2(S) to form the ALMEOALME(S) species and a gas-phase ethane molecule. The third surface reaction describes an O atom reacting with the ALMEOALME(S) species to deposit AL₂O₃(B), regenerate O(S), and form gas-phase ethane, where fractional molecules are used to write balanced reactions. Oxygen atoms are expected to be very reactive, so these reactions have been given high sticking coefficients of 1.0. These reactions only occur in the presence of O atoms generated from ozone decomposition, and will terminate when all the methylated

36. S. W. Benson and A. E. Axworthy, Jr., *J. Chem. Phys.*, **26**:1718 (1957).

surface species have reacted. All the surface reactions are irreversible. As a result, the thermodynamic properties for surface species provide the elemental composition of the surface species, but the polynomial fitting parameters are merely placeholder values.

4.4.5 Chlorine Plasma

This chemistry set is for a pure chlorine plasma without surface etching reactions that is based on work published by Meeks and coworkers.^{37, 38}

The gas-phase chemistry in the chlorine plasma is relatively simple. The element list contains 3 elements: E (the electron), Cl and Si. Si does not actively participate in any chemical reactions, as it only appears in *surf.inp* in the composition of surface species on the wall material, but it still needs to be included in the element list in the GAS-PHASE KINETICS input file. The gas-phase species list contains seven species: Cl₂, Cl, Cl* (chlorine atoms in a metastable electronically excited state), Cl₂⁺, Cl⁺, Cl⁻ and E. The gas-phase reactions include electron collisions with Cl₂ leading to vibrational and electronic excitation, dissociation, ionization, and dissociative attachment. Electron reactions with Cl include electronic excitation into a number of excited states, including Cl* formation, and ionization. The gas-phase reaction mechanism also includes electron collisions with Cl⁻ leading to electron detachment, electron collisions with Cl* leading to ionization, and gas-phase neutralization of Cl⁻ with Cl⁺ and Cl₂⁺ ions. All the reactions are irreversible as is typical of non-thermal plasmas. In low-pressure plasmas, ionization and dissociation are balanced primarily by surface recombination reactions. The rates for the electron-impact reactions depend on the electron energy, rather than the neutral gas temperature.

The surface mechanism for reactions occurring on the reactor wall is also fairly simple. It only involves neutralization of Cl⁺ and Cl₂⁺ with electrons (subject to the Bohm criterion), de-excitation of Cl* and radical recombination reactions for Cl to Cl₂. The neutralization and de-excitation reactions are non-site specific, but the recombination reactions are described in terms of open and Cl covered sites. Although this example problem does not include surface etching reactions, surface recombination and neutralization reactions can be quite important in determining the

37. "Modeling of Plasma-Etch Processes Using Well Stirred Reactor Approximations and Including Complex Gas-Phase and Surface-Reactions", E. Meeks and J. W. Shon, *IEEE Transactions On Plasma Science*, **23**(#4):539-549 (1995).

38. "Effects of Atomic Chlorine Wall Recombination: Comparison of a Plasma Chemistry Model With Experiment," E. Meeks, J. W. Shon, Y. Ra, P. Jones, *JVSTA* **13**(#6):2884-2889 (1995).

overall composition of these kinds of low-pressure plasmas. All the surface reactions are irreversible. The thermodynamic properties for surface species, therefore, provide the elemental composition of the surface species, but the polynomial fitting parameters are considered placeholder values and are not used in the simulation.

4.4.6 Fluorocarbon Plasma with SiO₂ Etch Products

This chemistry set is for a fluorocarbon plasma (C₂F₆) used for etching silicon dioxide films, a process that is used in the fabrication of microelectronic and MEMS devices. The chemistry set includes detailed surface reactions, including multiple materials with different reaction sets. Although it is quite complex, this mechanism is actually a small, early version of a more complete mechanism developed by Meeks and coworkers for etching several fluorocarbon precursors. Detailed descriptions of the full mechanisms, including information on the sources of rate parameters, can be found in their publications.^{39, 40, 41}

The gas-phase chemistry described in the *chem.inp* file involves 6 elements, 36 species, of which there are 9 positive ions, 3 negative ions, the electron, and 23 neutral species. There are 149 gas-phase reactions. Of these, 75 are electron-impact reactions leading to dissociation, dissociative ionization, attachment, vibrational and electronic excitation. Such reactions are included for the starting reactant C₂F₆, dissociation fragments such as CF₃ and CF₂, as well as etching products such as O₂ and SiF₄. The electron-impact reactions are all irreversible, and the rates depend on the electron energy, rather than the neutral gas temperature. There are 22 irreversible reactions describing the neutralization between positive and negative ions in the gas phase. Such reactions have high A-factors and are not energy dependent. The remaining 46 reactions are reactions of neutral gas-phase species, mostly reversible, some with explicitly specified reverse reaction rates. Many of the reactions include the participation of new specific collision partners (M), and a number of the unimolecular decomposition/bimolecular recombination reactions have detailed descriptions of the pressure dependence of the rate parameters.

-
39. "Modeling the Plasma Chemistry of C₂F₆ and CHF₃ Etching of Silicon Dioxide, with Comparisons to Etch Rate and Diagnostic Data", P. Ho, J. E. Johannes, R. J. Buss, and E. Meeks, *J. Vac. Sci. Technol. A* **19**:2344 (2001).
 40. "Plasma Modeling", E. Meeks and P. Ho, Chapter 3 in "Advanced Plasma Processing Technologies", edited by R. J. Shul and S. J. Pearton, Springer-Verlag, Heidelberg, (2000).
 41. "Chemical Reaction Mechanisms for Modeling the Fluorocarbon Plasma Etch of Silicon Oxide and Related Materials", P. Ho, J. E. Johannes, R. J. Buss and E. Meeks, Sandia National Laboratories Technical Report No. SAND2001-1292.

The surface chemistry described in the surf.inp file involves three materials with different reaction sets. The different materials in the model correspond to different physical parts of a plasma reactor that are all exposed to the plasma, but are affected by the plasma in different ways. The material called `SIDEWALL` and the material called `WAFER` are both silicon dioxide. The wafer is expected to have an applied electrical bias, resulting in higher ion energies. It thus has a more extensive set of reactions, especially ion-enhanced chemical reactions that result in etching. Although both sets of reactions describe the chemical species in the plasma interacting with silicon dioxide, the mechanism description needs to have unique names for the two sets of materials, surface sites, surface species, and bulk species to allow for different reaction sets. The material `SIDEWALL` has a surface site called `GLASS` with species `SIO2(S)` and `SIO2_F2(S)`, and a bulk phase `QUARTZ` with a bulk species `SIO2(B)`. The material `WAFER` has a surface site called `AMOXIDE` (for amorphous oxide) with species `WSIO2(S)`, `WSIO2_F2(S)`, and `WSIO2_CF2(S)`, and a bulk phase `OXIDE` with a bulk species `WSIO2(B)`. In the species names, the (S) is a convention often used to indicate a surface species, the `_F2` and the `_CF2` indicate a surface silicon oxide site with two F atoms or a C atom and two F atoms bonded to it, respectively, and the (B) indicates a bulk species. All the surface reactions are irreversible. All ion-surface reactions are subject to the Bohm flux criterion.

There are 31 surface reactions for the material `WAFER`. First there is a reaction describing the spontaneous etching of silicon dioxide by F atoms, and a reaction describing the adsorption reaction of F atoms with an open-site surface species to form a fluorinated surface species. There are 5 reactions describing the ion-enhanced etching of SiO_2 from the fluorinated surface species, producing SiF_4 and O_2 as etch products, and regenerating the open `SIO2(S)` species. These reactions have yields (number of surface sites converted per ion) that depend on the ion energy, as well as overrides of the default order of the reaction. More details about these features are provided in the input manual. Next are reactions describing the adsorption of CF_x radicals to form the `WSIO2_CF2(S)` species, and 5 reactions describing the ion-enhanced etching of SiO_2 from the fluorocarbon-covered surface species, producing SiF_4 and CO as etch products, and regenerating the open `SIO2(S)` species. These reactions also have ion energy dependent yields and overrides of the default order of the reaction. There are 9 reactions describing ion-neutralization with electrons on the surface, plus 7 reactions describing the direct sputtering of SiO_2 by ions.

The reaction set for the material `SIDEWALL` is a 16 reaction subset of that for the material `WAFER`, but with the appropriate species names. The material called `TOPWALL` is defined as silicon with two surface species. However, the reactions consist only of non-site specific neutralization reactions of positive ions with electrons.

5 Chemical Mechanism Analysis

5.1 Mechanism Analyzer

In the CHEMKIN software, the specification of the chemical reaction rates and thermochemical data is necessarily very compact and efficient. As a result, however, the information that might be most useful to a user in developing or analyzing a reaction mechanism is often not readily available because it is “hidden” in the terse Pre-processor input files. One example is rate information about the reverse rate of a reversible reaction, which is not easily determined by examining the chemistry input or output files. Other examples would be the free energy or enthalpy change associated with a particular reaction, or the relative rates of two reactions for a specific set of conditions. Another category of information that could be useful to extract from a CHEMKIN mechanism are simple measures of transport rates, expressed in terms of dimensionless numbers, or quantities such as the pure species viscosity, pure species thermal conductivity, or binary diffusion coefficient for various gas-phase species in the mechanism.

The Mechanism Analyzer provides a means to obtain this type of information, without requiring the user to do any programming. It presents, in tabular and graphical form, detailed information about the temperature and pressure dependence of chemical reaction rate constants and their reverse rate constants, reaction equilibrium constants, reaction thermochemistry, chemical species thermochemistry and transport properties. In general, the user will want to select only a few of the many types of information to be calculated and output, but there is a great deal of flexibility in specifying the desired output. The current version does not, however, handle all of the special rate options available in GAS-PHASE KINETICS and SURFACE KINETICS. Specifically, it does not consider: (1) user-provided rate routines, (2) rate-order

changes, (3) options associated with modeling plasma reactions, (4) the Chebyshev polynomial option for describing pressure-dependent gas-phase reactions, the (5) Landau-Teller rate formulation used for energy transfer processes, or (6) multiple materials. If such options are included in a reaction mechanism, they will be ignored.

5.1.1 Background Information

5.1.1.1 Bath Gas and Carrier Gas

The concept of a “bath gas” is used throughout the Mechanism Analyzer. The specification of a bath gas consists of a characteristic temperature, pressure, and composition at which quantities are to be evaluated by default. Composition, here, refers to the default composition for all phases defined in the mechanism. Reaction rate information is evaluated at the bath gas conditions, unless it is tabulated as a function of a system parameter, such as temperature. In this case, all other parameters are fixed at the bath gas conditions in the table. The default temperature for the bath gas is 298.15 K. The default pressure is 1 atmosphere, and the default composition is an equimolar composition in each phase. All defaults can be overridden by selections in the CHEMKIN Interface input panels.

The concept of a “carrier gas” is also used in the Mechanism Analyzer. Unless overridden, the carrier gas is assumed to be the gas component having the largest mole fraction. CHEMKIN calculates a single number for the characteristic time scale of diffusion (to be compared with the characteristic time scale of reaction). To make this comparison, the diffusion coefficient is calculated for a specified “major” species in the carrier gas. For example, the diffusion of the major species CH_4 in the carrier gas H_2 is used to calculate the characteristic diffusion time scale. Unless overridden, the major species in the gas phase is assumed to be the gas component having the second largest mole fraction.

5.1.1.2 Uniform-dimensional and Non-dimensional Reaction Rate Information

It is often useful to know, in some sense, which reactions in a mechanism are “fast” and which are “slow.” It is difficult or misleading to simply compare rate constants, which can have different units depending on the molecularity of the reaction. In order to compare the rates of reactions in the mechanism, we define a quantity

Equation 5-1

$$k_f^* = k_f [G]^g \prod_n [S_n]^{s_n}$$

which we call the “uniform-dimensional” rate constant. Regardless of the order of reaction, it will have units of mole • cm⁻³ • sec⁻¹ for a gas-phase reaction or mole • cm⁻² • sec⁻¹ for a surface reaction. In this expression, k_f is the rate constant for the forward reaction, $[G]$ is the total concentration of gas-phase species determined at the bath gas conditions (in mole • cm⁻³), g is the sum of the stoichiometric coefficients of all gas-phase species appearing as reactants in the reaction, $[S_n]$ is the total site density of surface phase n determined at the bath gas conditions, S_n is the sum of the stoichiometric coefficients of all surface species in phase n participating as reactants in this reaction.

Using the usual rate constant, one calculates the forward reaction rate as k_f times the product of the concentrations of the reactant species (in mole • cm⁻³ for gas species, or mole • cm⁻² for surface species) raised to the power of their stoichiometric coefficients. With the uniform-dimensional rate constant, one calculates the same reaction rate as k_f^* multiplied by the (dimensionless) species mole fractions (gas-phase reactants) or site fractions (surface species) raised to the power of their stoichiometric coefficients. Thus, independent of the molecularity of the reaction, the reaction rate is k_f^* times quantities that have maximum values on the order of unity (the mole and site fractions), and it is easier to compare one reaction to another.

The quantity k_f^* just discussed can point out which reactions are fast relative to one another. It can also be of interest to know if a reaction is “fast” relative to a competing process like molecular transport. The Damköhler number for gas-phase reactions, Da , allows for such a comparison.

Equation 5-2

$$Da = \frac{k_f^*}{D[G]/L^2}$$

In [Equation 5-2](#), D is a diffusion coefficient and L is a characteristic length scale for diffusion; for example, a boundary-layer thickness or a characteristic reactor dimension. The Damköhler number is a dimensionless number that is a measure of the relative importance of gas-phase kinetics versus molecular mass transport. If Da is much greater than 1, then a reaction is fast relative to transport; if it is much less than 1, then transport processes occur on a shorter time scale than kinetic processes.

One must supply a diffusion coefficient in [Equation 5-2](#) to evaluate Da . To do this, THE Mechanism Analyzer requires the user to name a “major species” and a “carrier gas species.” Through internal calls to the TRANSPORT Subroutine Library, CHEMKIN evaluates the binary diffusion coefficient between these two species at the specified bath temperature and pressure. The user may also specify the length scale L . The default value for L is 1 cm.

For each gas-phase reaction, a report is generated of k^* and Da for the forward and reverse directions. In some cases, the input CHEMKIN reaction mechanism specifies the reaction to be irreversible. In these cases, the quantities k^* and Da are still calculated for the reverse direction, but the numbers are enclosed in square brackets [] to flag these reactions as not being part of the mechanism.

A uniform-dimensional rate constant of [Equation 5-1](#) is also calculated for surface reactions. In this case, k_f^* has units of mole • cm⁻² • sec⁻¹. Thus, one can make a comparison between reaction rates for surface reactions. The surface Damköhler number is defined to be

Equation 5-3

$$Da = \frac{k_f^*}{D[G]/L}$$

The equation for the surface Damköhler number differs from the equation for the gas-phase Damköhler number by a factor of the length scale L . As before, it provides a measure of the relative speed of the surface reaction rate versus the molecular mass transport rate.

5.1.2 Reaction Mechanism for Diamond CVD

5.1.2.1 Project Description

This user tutorial demonstrates the use of the Mechanism Analyzer model to extract a wider variety of detailed thermodynamic, chemical kinetic, and transport data from a CHEMKIN reaction mechanism. The chemistry set nominally describes a diamond CVD process and is a subset of a published mechanism,⁴² but one that has now been superseded by the authors.⁴³ The reactions in this example, especially the surface reactions, have been contrived to demonstrate the capabilities of the Mechanism Analyzer and should not be used as a source of kinetic data for diamond deposition.

42.“Analysis of diamond growth in subatmospheric dc plasma-gun reactors.” Michael E. Coltrin and David S. Dandy, *Journal of Applied Physics*, **74**(#9):5803 (1993).

5.1.2.2 Project Setup

The project file is called *mechanism_analyzer__diamond_cvd.ckprj*. The data files used for this sample are located in the *samples\mechanism_analyzer\diamond_cvd* directory. This reactor diagram contains only the Mechanism Analyzer.

[Section 5.1.2.3](#) illustrates which sections of the output result from which choices on the input panels, so only brief usage instructions are provided here.

The Output Control tab of the Output Control panel contains a number of selections that determine the kinds of information that will be put into the output file and XML Solution File (*XMLdata.zip*). At the top of the Output Control tab, there is a choice to turn All Tables On or Off. Turning All Tables On will result in a very large output file, so this is generally **not** recommended, except for the smallest reaction mechanisms. The usage of these controls is as follows. To obtain All output of a certain type, turn it On at the highest level. To limit the output of a certain type to specific species or reactions, turn it Off at the higher level(s), then On for the class (gas, surface or bulk) of species/reactions or by listing the specific species/reactions of interest.

As an illustration of how to use the levels of choices to specify data types, consider the case of thermodynamic data tables. There are two types of data tables available: summary tables which are given at the bath gas conditions, and detailed tables which cover a range of temperatures. In this example, the Summary Thermo Tables are turned Off in general, but then back On for Species, but not for Reactions. Turning All Summary Thermo Tables On is equivalent to checking all three boxes, but is simpler. In the case of the more detailed Species Thermo Tables, they are turned Off in general, and On for the Bulk species only. In addition, on the Species-specific Data panel, Species Thermo Tables are specified for two gas phase species, CH₃ and CH₄, plus two surface species, CH₂(S) and CH(S). The results of these selections are shown in [Section 5.1.2.3](#). For reaction information, most of the output types are turned On at the general level, so there are no entries on the Reaction-specific Data tab of the Output Control panel.

The C1_ Mechanism Analyzer panel allows specification of the physically based parameters that affect the output file. The Reactor Physical Property tab allows the user to override the default values for pressure and temperature of the bath gas, as well as the ranges used for the thermodynamics and kinetics tables. The Species-specific Data tab allows specification of the composition of the bath gas, as well as overriding the default definitions for the carrier gas and major species. No entries are made on the Cluster Properties, Solver, or Continuations panels for this problem.

43. The authors now prefer the mechanism in: "A simplified analytical model of diamond growth in direct current arcjet reactors." David S. Dandy and Michael E. Coltrin, *Journal of Materials Research*, **10**(#8):1993 (1995). Private communication, M. E. Coltrin, Feb. 1998.

5.1.2.3 Project Results

Although an XML Solution File is created and the graphical CHEMKIN Post-Processor can be used for viewing the results, the output file is generally the more useful form of output for this application, as the user is generally looking for values of specific chemical or transport parameters. This section reproduces the Mechanism Analyzer diagnostic output file, which has been augmented in a number of places by comments in larger font. The information in the tables is generally self-explanatory, so these comments general deal with the input controls that produce that section of output.



The output file first echoes the input file created by the CHEMKIN Interface.

```
*****
*                   CHEMKIN Release 4.0                   *
*                   SURFTHERM Application                 *
*                   REACTION MECHANISM ANALYSIS          *
* Copyright(c) 1997-2004 Reaction Design. All Rights Reserved. *
*****
```

Command File = surftherm.inp

WORKING SPACE REQUIREMENTS		
	PROVIDED	REQUIRED
LOGICAL	57	57
INTEGER	995	995
REAL	3525	3525
CHARACTER*16	43	43
CHARACTER*48	4	4
CHARACTER*64	10	10

Initializing CHEMKIN Gas-phase Library, a component of CHEMKIN Release 4.0. Build date: May 7, 2004
This and All Other CHEMKIN(R) Libraries are Copyright (c) 1997-2004 Reaction Design. All rights reserved.

LICENSE INFORMATION:

No Information Provided

Initializing SURFACE CHEMKIN Library, a component of CHEMKIN Release 4.0.

Initializing TRANSPORT Library, a component of CHEMKIN Release 4.0.

Command lines read:

```
KEYWORD INPUT
NONE
GEN ALL
GRXN ALL
GTHB ALL
NDIM ALL
PFAL ALL
SCOV ALL
SRXN ALL
STCK ALL
TFAL ALL
THRM NONE
TRAN ALL
TSUM NONE
CARR H2
LSCL 1.3
MAJ CH4
PBTH 20.0
PHIG 700.0
FLOW 100.0
PNUM 3
TBTH 1100.0
```

```
TDEL 400.0
THIG 1200.0
TLOW 300.0
THRM BULK
THRM CH(S)
THRM CH2(S)
THRM CH3
THRM CH4
TSUM SPECIES
XBTH CH3 0.03
XBTH CH4 0.05
XBTH H 0.02
XBTH H2 0.9
END
```



The **Turn On General Tables** button in the Output Control tab gives the following general information about the elements, species, phases, and reactions in the mechanism.

=====

GENERAL INFORMATION CONCERNING THE SURFACE CHEMKIN PROBLEM:

```
Total number of elements declared = 2 ( H C )
Total number of species = 12
Total number of phases = 3
Total number of gas-phase reactions = 5
Total number of surface-phase reactions = 4
Universal gas constant = 8.3145100E+07 ergs/(mole*K)
Universal gas constant used for activation energies = 1.987216 cal/(mole*K)
Pressure of one standard atmosphere = 1013250. dynes/cm**2
```

GAS phase (Always phase # 1, with the name, "GAS"):

```
Number of species = 5
Number of surface reactions where the # of gas products is different than the # of gas reactants = 2
Number of elements in the phase = 2 ( H C )
```

SURFACE PHASES:

Phase Number	Name of Phase	SS Site Density (moles/cm**2)	Number of Species	Number of Elements	Site_changing Surf_rxns	Elements:
2	DIAMOND	5.2200E-09	6	2	0	(H C)

Tot SS Site Dens= 5.2200E-09 (mole/cm**2) (used in sticking coefficient express)

BULK PHASES:

Phase Number	Name of Phase	Number of Species	Number of Elements	Mole_changing Surf_rxns	Elements:
3	BULK1	1	1	1	(C)



The **Turn On General Tables** button in the Output Control tab gives the following table of conditions. The bath gas conditions are set in the Reactor Physical Property tab. The bath gas composition, carrier gas and major species are set in the Species-specific Data tab.

=====

SUMMARY OF SPECIES IN THE MECHANISM with a DESCRIPTION OF BATH GAS COMPOSITION:

```
Total pressure = 20.0 torr
Temperature (where needed) = 1100.E+00 Kelvin
Carrier Gas (used in diff. calcs) = H2
Major Gas Species (used in nondim calcs) = CH4
```

Number	Name	Mole_fraction	Concentration
1.	CH3	0.3000E-01	0.8747E-08 mole/cm**3
2.	C2H6	0.0000E+00	0.0000E+00 mole/cm**3
3.	CH4	0.5000E-01	0.1458E-07 mole/cm**3
4.	H	0.2000E-01	0.5831E-08 mole/cm**3
5.	H2	0.9000	0.2624E-06 mole/cm**3
6.	CH(S)	0.1667	0.8700E-09 mole/cm**2
7.	C(S,R)	0.1667	0.8700E-09 mole/cm**2
8.	CH3(S)	0.1667	0.8700E-09 mole/cm**2
9.	CH2(S)	0.1667	0.8700E-09 mole/cm**2
10.	CH2(S,R)	0.1667	0.8700E-09 mole/cm**2
11.	CH(S,R)	0.1667	0.8700E-09 mole/cm**2
12.	D	1.000	activity(unitless)



The Turn On Summary Tables for Species checkbox gives the following table of thermochemical data.

=====

SUMMARY OF STANDARD STATE THERMODYNAMIC FUNCTIONS FOR SPECIES AT BATH GAS CONDITIONS:

Bath Gas Temperature = 1100. Kelvin

Number	Name	H(298 K) (kcal/mole)	H(T_bath) (kcal/mole)	Cp(T_bath) (cal/moleK)	S(T_bath) (cal/moleK)	G(T_bath) (kcal/mole)
1.	CH3	34.823	44.555	14.636	61.467	-23.058
2.	C2H6	-20.673	-2.1376	30.891	82.903	-93.331
3.	CH4	-17.900	-6.9967	18.069	60.837	-73.917
4.	H	52.099	56.082	4.9680	33.877	18.818
5.	H2	5.85489E-04	5.6660	7.3196	40.393	-38.766
6.	CH(S)	-1.85943E-04	4.8351	8.7997	7.1576	-3.0383
7.	C(S,R)	43.365	46.634	5.2414	5.1549	40.964
8.	CH3(S)	17.301	26.175	16.043	16.567	7.9503
9.	CH2(S)	-11.490	-4.6306	12.687	10.129	-15.773
10.	CH2(S,R)	50.665	57.524	12.687	10.129	46.382
11.	CH(S,R)	31.878	36.713	8.7997	7.1576	28.839
12.	D	0.45379	3.7231	5.2414	5.1549	-1.9472

=====



The Turn On General Tables button in the Output Control tab gives the following general information about reactions in the mechanism.

=====

SHORT DESCRIPTION OF GAS-PHASE REACTIONS

Number	Description	Gas_Mole Change	Gas_Mole Reactants
1.	2CH3(+M) <=> C2H6(+M)	-1.00	2.00
2.	CH4+H <=> CH3+H2	0.00	2.00
3.	CH3+H(+M) <=> CH4(+M)	-1.00	2.00
4.	2H+M <=> H2+M	-1.00	2.00
5.	2H+H2 <=> 2H2	-1.00	3.00

=====

SHORT DESCRIPTION OF SURFACE-PHASE REACTIONS

Number	Description	Gas Mole Change	Surf Mole Change	Bulk Mole Change	Surf_Site Change
1.	CH(S)+H <=> C(S,R)+H2	0.00	0.00	0.00	0.00
2.	C(S,R)+H <=> CH(S)	-1.00	0.00	0.00	0.00
3.	C(S,R)+CH3 <=> D+CH3(S)	-1.00	0.00	1.00	0.00
4.	CH2(S,R)+CH(S,R) <=> CH2(S)+CH(S)	0.00	0.00	0.00	0.00

=====



The Turn On Uni-dimensional Rate Tables button in the Output Control panel gives the following tables of "uniform-dimensional" rates that allow comparisons between reactions of different orders. The length scale used for evaluating the relative importance of kinetics to transport is set on the Reactor Physical Property tab.

=====

NON-DIMENSIONAL GAS REACTION RATE CONSTANTS
AT THE BATH GAS CONDITIONS
Total Pressure = 20.0 torr
Temperature = 1100.E+00 Kelvin

Number	Description	k_star (mole/cm**3 sec)	k_star_rev (mole/cm**3 sec)	Gas_Da_For	Gas_Da_Rev
1.	2CH3(+M) <=> C2H6(+M)	0.270	4.280E-09	6.113E+03	9.677E-05
2.	CH4+H <=> CH3+H2	4.546E-02	2.096E-03	1.028E+03	47.4
3.	CH3+H(+M) <=> CH4(+M)	2.813E-02	1.534E-14	636.	3.469E-10

=====

4.	2H+M<=>H2+M	2.253E-06	5.666E-20	5.094E-02	1.281E-15
5.	2H+H2<=>2H2	3.412E-05	8.583E-19	0.772	1.941E-14

NOTE ON THE ABSOLUTE NUMBERS IN THIS TABLE:

The rate constants (mole/cm**3*sec) should be compared to rate of mass transport in order to characterize their values as being fast or slow. The nondimensionalization of the mass transport involves the following multiplicative factor, which also has the units of mole/cm**3*sec:

$$\text{Total_Concentration} * \text{Diffusivity} / \text{Length_scale}^{**2}$$

Using the binary diffusion coefficient between H2

and CH4, the following factors are calculated at bath gas conditions:

$$\text{Total Concentration} = 2.915E-07 \text{ mole/cm}^{**3}$$

$$\text{Binary Diffusion Coefficient} = 256. \text{ cm}^{**2}/\text{sec}$$

$$\text{Length scale} = 1.30 \text{ cm}$$

Therefore, the non-dimensionalization factor for gas reactions becomes:

$$\text{Conc} * \text{Diff} / \text{Length}^{**2} = 4.423E-05 \text{ mole/cm}^{**3} * \text{sec}$$

Note that this number is independent of pressure

NON-DIMENSIONAL SURFACE REACTION RATE CONSTANTS

AT THE BATH GAS CONDITIONS

Total Pressure = 20.0 torr

Temperature = 1100.E+00 Kelvin

Number	Description	k_star (mole/cm**2 sec)	k_star_rev (mole/cm**2 sec)	Surf_Da_For	Surf_Da_Rev
1.	CH(S)+H<=>C(S,R)+H2	2.871E-03	5.750E-06	49.9	0.100
2.	C(S,R)+H=>CH(S)	1.237E-02	[1.553E-13]	215.	[2.701E-09]
3.	C(S,R)+CH3<=>D+CH3(S)	3.516E-03	54.6	61.2	9.504E+05
4.	CH2(S,R)+CH(S,R)<=>CH2(S)+CH(S)	655.	1.362E-16	1.139E+07	2.369E-12

[] indicates that this reaction is not in mechanism

NOTE ON THE ABSOLUTE NUMBERS IN THIS TABLE:

The rate constants (mole/cm**2*sec) should be compared to rate of mass transport to the surface in order to characterize their values as being fast or slow. The nondimensionalization of the mass transport involves the following multiplicative factor, which also has the units of mole/cm**2*sec:

$$\text{Total_Concentration} * \text{Diffusivity} / \text{Length_scale}$$

Using the binary diffusion coefficient between H2

and CH4, the following factors are calculated at bath gas conditions:

$$\text{Total Concentration} = 2.915E-07 \text{ mole/cm}^{**3}$$

$$\text{Binary Diffusion Coefficient} = 256. \text{ cm}^{**2}/\text{sec}$$

$$\text{Length scale} = 1.30 \text{ cm}$$

Therefore, the non-dimensionalization factor for surface reactions becomes:

$$\text{Conc} * \text{Diff} / \text{Length} = 5.749E-05 \text{ mole/cm}^{**2} * \text{sec}$$

Note that this number is independent of pressure



Listing these species on the Species-specific Data tab, combined with the Turn On Bulk Species Thermo Tables checkbox in the Output Control panel gives the following tables of thermodynamic data for two gas-phase species, two surface species and the one bulk species. The **Turn On Transport Tables** button adds the table of Viscosity, Thermal Conductivity and Binary Diffusion Coefficients to the tables for the gas-phase species. The temperature intervals are set on the Reactor Physical Property tab.

THERMO TABLE FOR MOLECULE "CH3" IN PHASE "GAS"

Overall, this is the 1th species in the mechanism

It is the 1th species in phase GAS

Elemental Composition:

H : 3

C : 1

L-J Potential well depth = 144. K

L-J collision diameter = 3.80 Angstroms

Dipole Moment = 0.000E+00 Debye

Polarizability = 0.000E+00 Angstroms**3

Rotational Collision number at 298K = 0.000E+00

This molecule is linear

Heat of Formation at 298 = 34.823 kcal/mole

Molecular Weight = 15.035 gm/mole

Temp (K)	(H-H298) (kcal/mole)	(G-H298) (kcal/mole)	Cp (cal/mole*K)	S (cal/mole*K)	Viscosity (gm/cm*sec)	Therm_Cond (erg/cm*sec*K)	Dif_Co_with_H2 (cm**2/sec)
298.15	0.0000E+00	-13.828	9.2147	46.380	1.069E-04	3.556E+03	28.0
300.00	1.70635E-02	-13.914	9.2323	46.437	1.074E-04	3.581E+03	28.3
700.00	4.3363	-34.452	12.199	55.412	2.032E-04	9.207E+03	119.
1100.00	9.7317	-57.882	14.636	61.467	2.767E-04	1.486E+04	253.

[Pressure for binary diffusion coeff. calc. = 20.0 torr]

THERMO TABLE FOR MOLECULE "CH4" IN PHASE "GAS"

Overall, this is the 3th species in the mechanism
 It is the 3th species in phase GAS
 Elemental Composition:
 H : 4
 C : 1
 L-J Potential well depth = 141. K
 L-J collision diameter = 3.75 Angstroms
 Dipole Moment = 0.000E+00 Debye
 Polarizability = 2.60 Angstroms**3
 Rotational Collision number at 298K = 13.0
 This molecule is non-linear
 Heat of Formation at 298 = -17.900 kcal/mole
 Molecular Weight = 16.043 gm/mole

Temp (K)	(H-H298) (kcal/mole)	(G-H298) (kcal/mole)	Cp (cal/mole*K)	S (cal/mole*K)	Viscosity (gm/cm*sec)	Therm_Cond (erg/cm*sec*K)	Dif_Co_with_H2 (cm**2/sec)
298.15	0.00000E+00	-13.259	8.3994	44.470	1.143E-04	3.406E+03	28.4
300.00	1.55651E-02	-13.341	8.4277	44.522	1.148E-04	3.436E+03	28.7
700.00	4.4636	-33.081	13.703	53.636	2.167E-04	1.092E+04	121.
1100.00	10.904	-56.017	18.069	60.837	2.950E-04	1.879E+04	256.

[Pressure for binary diffusion coeff. calc. = 20.0 torr]

 THERMO TABLE FOR MOLECULE "CH(S)" IN PHASE "DIAMOND"
 Overall, this is the 6th species in the mechanism
 It is the 1th species in phase DIAMOND
 Elemental Composition:
 H : 1
 C : 1
 Number of surface sites occupied by the species = 1
 Heat of Formation at 298 = 0.000 kcal/mole
 Molecular Weight = 13.019 gm/mole

Temp (K)	(H-H298) (kcal/mole)	(G-H298) (kcal/mole)	Cp (cal/mole*K)	S (cal/mole*K)
298.15	0.00000E+00	-0.10647	1.4451	0.35709
300.00	2.70072E-03	-0.10714	1.4746	0.36612
700.00	1.6957	-0.85821	6.5209	3.6485
1100.00	4.8353	-3.0381	8.7997	7.1576

 THERMO TABLE FOR MOLECULE "CH2(S)" IN PHASE "DIAMOND"
 Overall, this is the 9th species in the mechanism
 It is the 4th species in phase DIAMOND
 Elemental Composition:
 H : 2
 C : 1
 Number of surface sites occupied by the species = 1
 Heat of Formation at 298 = -11.490 kcal/mole
 Molecular Weight = 14.027 gm/mole

Temp (K)	(H-H298) (kcal/mole)	(G-H298) (kcal/mole)	Cp (cal/mole*K)	S (cal/mole*K)
298.15	0.00000E+00	-0.15233	2.0387	0.51091
300.00	3.80910E-03	-0.15329	2.0792	0.52365
700.00	2.3780	-1.2093	9.1983	5.1248
1100.00	6.8591	-4.2830	12.687	10.129

 THERMO TABLE FOR MOLECULE "D" IN PHASE "BULK1"
 Overall, this is the 12th species in the mechanism
 It is the 1th species in phase BULK1
 Elemental Composition:
 C : 1
 Bulk Density = 3.5150 gm/cm**3
 Activity (bath gas dependent) = 1.0000
 Heat of Formation at 298 = 0.454 kcal/mole
 Molecular Weight = 12.011 gm/mole

Temp (K)	(H-H298) (kcal/mole)	(G-H298) (kcal/mole)	Cp (cal/mole*K)	S (cal/mole*K)
298.15	0.00000E+00	-0.11273	1.4405	0.37811
300.00	2.68420E-03	-0.11344	1.4613	0.38708
700.00	1.2898	-0.76152	4.4759	2.9304
1100.00	3.2693	-2.4010	5.2414	5.1549



The **Turn On Gas Reaction Tables** button in the Output Control tab gives the following tables of high-pressure rates constants as a function of temperature for the gas-phase reactions. Reactions 1 and 3 have (+M), so for these reactions, the **Turn On Pressure Tables** button adds a table of rate constants as a function of pressure at the bath-gas temperature, and the **Turn On Temperature Tables** buttons add a table of rate constants as a function of temperature at the bath-gas pressure. Reaction 4 has +M, so for this reaction, the Turn On 3rd Body Reaction Tables button adds a table where the effect of the third body is lumped into the rate constants. The bath gas conditions and temperature/pressure intervals are set on the Reactor Physical Property tab.

```
=====
Gas Reaction # 1          2CH3(+M)<=>C2H6(+M)
```

```
Change in moles in the reaction = -1.00
This reaction does have third body effects. 1 modified enhanced third body efficiencies were input
Species "H2", modified enhanced third body efficiency for the reaction = 2.000
This is a reversible reaction, having 2.00 reactant species
and 1.00 product species
```

```
k (cm**3/(mole sec)) = 9.0300E+16 T**(-1.180) exp(-0.6540 kcal/mole / RT)
```

```
Reaction has a pressure-dependent behavior with a 6 parameter Troe function form:
klow (cm**6/(mole**2 sec)) = 3.180E+41 T**(-7.030) exp(-2.76 kcal/mole / RT)
a = 0.6041
T*** = 6927.E+00 Kelvin
T* = 132. Kelvin
```

```
-----
HIGH PRESSURE GAS REACTION RATE CONSTANTS AS A FUNCTION OF TEMPERATURE
```

T (K)	k (cm**3/(mole sec))	A_factor	Ea (kcal/mol)	DeltaG (kcal/mol)	DeltaH (kcal/mol)	DeltaS (cal/moleK)	k_rev (sec-1)	A_factor_rev	Ea_rev (kcal/mol)	UnifDimensnl k_star (mole/cm**3*sec)	Rate_Const k_star_rev (mole/cm**3*sec)
298.15	3.60E+13	3.34E+13	-4.5136E-02	-79.16	-90.32	-37.42	1.38E-49	7.55E+16	89.68	39.	1.38E-55
300.00	3.60E+13	3.31E+13	-4.9474E-02	-79.09	-90.33	-37.45	3.52E-49	7.59E+16	89.69	38.	3.50E-55
700.00	2.48E+13	1.22E+13	-0.9874	-63.31	-91.52	-40.30	7.41E-12	5.02E+16	89.14	2.8	1.85E-18
1100.00	1.73E+13	7.15E+12	-1.925	-47.21	-91.25	-40.03	7.96E-02	1.63E+16	87.14	0.27	4.28E-09

```
-----
PRESSURE-DEPENDENT BEHAVIOR AS A FUNCTION OF TEMPERATURE: Reaction # 1
Bath Gas Pressure = 20.0 torr
```

Temperature (K)	k (cm**3/(mole sec))	A_factor	Ea (kcal/mole)	k/kinf	klow	Reduc_Press	FC	Eff_Conc (mole/cm**3)	k_rev (sec-1)	A_factor_rev	Ea_rev (kcal/mole)
298.	3.3497E+13	2.644E+13	-0.1402	0.930	1.209E+22	686.	0.931	2.04E-06	1.2870E-49	5.983E+16	89.59
300.	3.3447E+13	2.615E+13	-0.1467	0.929	1.192E+22	672.	0.931	2.03E-06	3.2699E-49	5.991E+16	89.59
700.	1.3481E+13	1.279E+12	-3.276	0.544	4.356E+20	15.3	0.579	8.70E-07	4.0298E-12	5.264E+15	86.85
1100.E+00	3.1806E+12	7.839E+10	-8.095	0.184	3.738E+19	1.20	0.338	5.54E-07	1.4680E-02	1.790E+14	80.97

```
-----
PRESSURE-DEPENDENT BEHAVIOR AS A FUNCTION OF PRESSURE: Reaction # 1
Bath Gas Temperature = 1100.E+00 K
Low Pressure Limiting Reaction Rate = klow = 3.7385E+19 (cm**6/(mole**2 sec))
```

Pressure (torr)	k (cm**3/(mole sec))	A_factor	Ea (kcal/mole)	k/kinf	klow*Eff_Conc	Reduc_Press	FC	Eff_Conc (mole/cm**3)	k_rev (sec-1)	A_factor_rev	Ea_rev (kcal/mole)
700.	1.1510E+13	1.447E+12	-4.532	0.667	7.248E+14	42.0	0.683	1.94E-05	5.3124E-02	3.306E+15	84.53
265.	9.1067E+12	5.942E+11	-5.967	0.528	2.739E+14	15.9	0.561	7.33E-06	4.2031E-02	1.357E+15	83.10
100.	6.4507E+12	2.165E+11	-7.420	0.374	1.035E+14	6.00	0.436	2.77E-06	2.9772E-02	4.944E+14	81.64

```
=====
Gas Reaction # 2          CH4+H<=>CH3+H2
```

```
Change in moles in the reaction = 0.00
This reaction does not have any third body effects
This is a reversible reaction, having 2.00 reactant species
and 2.00 product species
```

```
k (cm**3/(mole sec)) = 2.2000E+04 T**(-3.000) exp(-8.750 kcal/mole / RT)
```

```
-----
HIGH PRESSURE GAS REACTION RATE CONSTANTS AS A FUNCTION OF TEMPERATURE
```

T (K)	k (cm**3/(mole sec))	A_factor	Ea (kcal/mol)	DeltaG (kcal/mol)	DeltaH (kcal/mole)	DeltaS (cal/moleK)	k_rev (cm**3/(mole sec))	A_factor_rev	Ea_rev (kcal/mol)	UnifDimensnl k_star (mole/cm**3*sec)	Rate_Const k_star_rev (mole/cm**3*sec)
298.15	2.25E+05	1.17E+13	10.53	-1.084	0.6253	5.732	3.61E+04	6.55E+11	9.902	2.60E-07	4.18E-08
300.00	2.51E+05	1.19E+13	10.54	-1.094	0.6304	5.749	4.00E+04	6.61E+11	9.908	2.87E-07	4.58E-08
700.00	1.40E+10	1.52E+14	12.92	-3.810	1.310	7.314	9.04E+08	3.82E+12	11.61	2.94E-03	1.90E-04
1100.00	5.35E+11	5.88E+14	15.31	-6.726	1.135	7.146	2.47E+10	1.61E+13	14.17	4.55E-02	2.10E-03

Gas Reaction # 3 CH3+H(+M)<=>CH4(+M)

Change in moles in the reaction = -1.00
 This reaction does have third body effects. 1 modified enhanced third body efficiencies were input
 Species "H2", modified enhanced third body efficiency for the reaction = 2.000
 This is a reversible reaction, having 2.00 reactant species
 and 1.00 product species

$$k \text{ (cm**3/(mole sec))} = 6.0000E+16 T^{**}(-1.000) \exp(-0.0000E+00 \text{ kcal/mole} / RT)$$

Reaction has a pressure-dependent behavior with a Lindeman function form:
 $k_{low} \text{ (cm**6/(mole**2 sec))} = 8.000E+26 T^{**}(-3.000) \exp(-0.000E+00 \text{ kcal/mole} / RT)$

HIGH PRESSURE GAS REACTION RATE CONSTANTS AS A FUNCTION OF TEMPERATURE

T (K)	k (cm**3/(mole sec))	A_factor	Ea (kcal/mol)	DeltaG (kcal/mol)	DeltaH (kcal/mole)	DeltaS (cal/moleK)	k_rev (sec-1)	A_factor_rev	Ea_rev (kcal/mol)	UnifDimensnl k_star (mole/cm**3*sec)	Rate_Const k_star_rev (mole/cm**3*sec)
298.15	2.01E+14	7.40E+13	-0.5925	-96.09	-104.8	-29.30	3.05E-61	2.82E+15	103.6	55.	7.69E-68
300.00	2.00E+14	7.36E+13	-0.5962	-96.03	-104.8	-29.34	8.96E-61	2.84E+15	103.6	53.	2.22E-67
700.00	8.57E+13	3.15E+13	-1.391	-83.31	-106.7	-33.41	1.46E-17	4.04E+15	103.9	0.42	1.55E-25
1100.00	5.45E+13	2.01E+13	-2.186	-69.68	-107.6	-34.51	8.67E-06	2.84E+15	103.3	2.81E-02	1.53E-14

PRESSURE-DEPENDENT BEHAVIOR AS A FUNCTION OF TEMPERATURE: Reaction # 3
 Bath Gas Pressure = 20.0 torr

Temperature (K)	k (cm**3/(mole sec))	A_factor	Ea (kcal/mole)	k/kinf (cm**6/(mole**2 sec))	klow (cm**6/(mole**2 sec))	Reduc_Press (sec)	FC	Eff_Conc (mole/cm**3)	k_rev (sec-1)	A_factor_rev	Ea_rev (kcal/mole)
298.	4.7215E+13	1.748E+12	-1.953	0.235	3.018E+19	0.307	1.00	2.04E-06	7.1494E-62	6.659E+13	102.3
300.	4.6261E+13	1.696E+12	-1.971	0.231	2.963E+19	0.301	1.00	2.03E-06	2.0728E-61	6.536E+13	102.3
700.	1.9833E+12	3.894E+10	-5.468	2.314E-02	2.332E+18	2.369E-02	1.00	8.70E-07	3.3858E-19	4.990E+12	99.83
1100.E+00	3.3092E+11	6.172E+09	-8.704	6.067E-03	6.011E+17	6.104E-03	1.00	5.54E-07	5.2628E-08	8.751E+11	96.74

PRESSURE-DEPENDENT BEHAVIOR AS A FUNCTION OF PRESSURE: Reaction # 3
 Bath Gas Temperature = 1100.E+00 K
 Low Pressure Limiting Reaction Rate = klow = 6.0105E+17 (cm**6/(mole**2 sec))

Pressure (torr)	k (cm**3/(mole sec))	A_factor	Ea (kcal/mole)	k/kinf (cm**3/(mole sec))	klow*Eff_Conc (cm**3/(mole sec))	Reduc_Press (sec)	FC	Eff_Conc (mole/cm**3)	k_rev (sec-1)	A_factor_rev	Ea_rev (kcal/mole)
700.	9.6017E+12	2.982E+11	-7.589	0.176	1.165E+13	0.214	1.00	1.94E-05	1.5270E-06	4.228E+13	97.86
265.	4.0753E+12	9.340E+10	-8.254	7.471E-02	4.404E+12	8.075E-02	1.00	7.33E-06	6.4812E-07	1.324E+13	97.19
100.	1.6154E+12	3.234E+10	-8.550	2.962E-02	1.665E+12	3.052E-02	1.00	2.77E-06	2.5691E-07	4.584E+12	96.90

Gas Reaction # 4 2H+M<=>H2+M

Change in moles in the reaction = -1.00
 This reaction does have third body effects. 1 modified enhanced third body efficiencies were input
 Species "H2", modified enhanced third body efficiency for the reaction = 0.0000E+00
 This is a reversible reaction, having 3.00 reactant species
 and 2.00 product species (including the third body)

$$k \text{ (cm**6/(mole**2 sec))} = 1.0000E+18 T^{**}(-1.000) \exp(-0.0000E+00 \text{ kcal/mole} / RT)$$

HIGH PRESSURE GAS REACTION RATE CONSTANTS AS A FUNCTION OF TEMPERATURE

T (K)	k (cm**6/(mole**2 sec))	A_factor	Ea (kcal/mol)	DeltaG (kcal/mol)	DeltaH (kcal/mole)	DeltaS (cal/moleK)	k_rev (cm**3/(mole sec))	A_factor_rev	Ea_rev (kcal/mol)	UnifDimensnl k_star (mole/cm**3*sec)	Rate_Const k_star_rev (mole/cm**3*sec)
298.15	3.35E+15	1.23E+15	-0.5925	-97.17	-104.2	-23.57	8.16E-61	2.63E+15	103.0	4.17E-04	9.44E-74
300.00	3.33E+15	1.23E+15	-0.5962	-97.13	-104.2	-23.59	2.38E-60	2.62E+15	103.0	4.07E-04	2.72E-73
700.00	1.43E+15	5.26E+14	-1.391	-87.12	-105.4	-26.09	1.58E-17	1.70E+15	102.6	1.37E-05	3.31E-31
1100.00	9.09E+14	3.34E+14	-2.186	-76.40	-106.5	-27.36	6.67E-06	1.30E+15	102.1	2.25E-06	5.67E-20

ANALYSIS OF THIRD BODY REACTIONS: LUMPING [M] WITH RATE CNST

Reaction # 4
 Bath Gas Pressure = 20.0 torr

Temperature (K)	k (cm**3/(mole sec))	A_factor (kcal/mole)	Ea (kcal/mole)	Concentration (mole/cm**3)	C_eff (mole/cm**3)	k_rev (sec-1)	A_factor_rev (kcal/mole)	Ea_rev (kcal/mole)
298.15	3.6077E+08	4.882E+07	-1.185	1.076E-06	1.076E-07	8.7732E-68	1.040E+08	102.4
300.00	3.5633E+08	4.822E+07	-1.192	1.069E-06	1.069E-07	2.5474E-67	1.030E+08	102.4
700.00	6.5449E+07	8.857E+06	-2.782	4.582E-07	4.581E-08	7.2209E-25	2.861E+07	101.2
1100.00	2.6504E+07	3.587E+06	-4.372	2.916E-07	2.915E-08	1.9435E-13	1.395E+07	99.94

```

Gas Reaction # 5      2H+H2<=>2H2

Change in moles in the reaction =-1.00
This reaction does not have any third body effects
This is a reversible reaction, having 3.00 reactant species
and 2.00 product species

k (cm**6/(mole**2 sec)) = 9.2000E+16 T**(-0.6000 ) exp( -0.0000E+00 kcal/mole / RT)

```

HIGH PRESSURE GAS REACTION RATE CONSTANTS AS A FUNCTION OF TEMPERATURE

T (K)	k (cm**6/(mole**2 sec))	A_factor (kcal/mol)	Ea (kcal/mol)	DeltaG (kcal/mol)	DeltaH (kcal/mole)	DeltaS (cal/moleK)	k_rev (cm**3/(mole sec))	A_factor_rev (kcal/mol)	Ea_rev (kcal/mol)	UnifDimensnl k_star (mole/cm**3*sec)	Rate_Const k_star_rev
298.15	3.01E+15	1.65E+15	-0.3555	-97.17	-104.2	-23.57	7.33E-61	3.52E+15	103.2	3.75E-03	8.48E-73
300.00	3.00E+15	1.65E+15	-0.3577	-97.13	-104.2	-23.59	2.15E-60	3.52E+15	103.2	3.67E-03	2.45E-72
700.00	1.81E+15	9.91E+14	-0.8346	-87.12	-105.4	-26.09	1.99E-17	3.20E+15	103.2	1.74E-04	4.18E-30
1100.00	1.38E+15	7.56E+14	-1.312	-76.40	-106.5	-27.36	1.01E-05	2.94E+15	103.0	3.41E-05	8.58E-19



The **Turn On Surface Reaction Tables** button in the Output Control tab gives the following tables of information about surface reactions in the mechanism. The first two surface reactions were input as sticking coefficients, and the third reaction can be described that way, so for these reactions, the Turn On Sticking Coefficient Tables button adds tables of sticking coefficients as a function of temperature. The first reaction also has a surface coverage dependence, so the **Turn On Surface Coverage Dependence Tables** button adds a table of rate constants that include the effect of the surface coverage at bath-gas conditions for that reaction.

```

-----
Surface Reaction # 1      CH(S)+H<=>C(S,R)+H2

Change in gas      moles in the reaction = 0.00
Change in surface  moles in the reaction = 0.00
Change in bulk     moles in the reaction = 0.00

This reaction has 1 species whose surface coverage modify the rate constant
Each of these species has three parameters that multiplicatively modify the rate constant as follows:
k_prime = k * 10**(Z_k*nu_ki) * Z_k**mu_ki * exp[ - eps_ki*Z_k / RT ]
where Z_k = Site Fraction of species k
Species = CH(S)
nu_ki = 0.1000
mu_ki = 0.0000E+00
eps_ki = -2.5000E-04 (Kcal/mole)

This is a reversible surface reaction, having the following types of reactant species:
1.00 gas-phase species
1.00 surface-phase species
0.00 bulk-phase species
and the following types of product species:
1.00 gas-phase species
1.00 surface-phase species
0.00 bulk-phase species
The reaction rate constant was input via a sticking coefficient in the interpreter input file
Motz-Wise Correction factor is used

Sticking Coeff = MIN( 2.140 exp( - 7.300 kcal/mole / RT) , 1 )

It can be fit to the following general rate constant form:

k (cm**3/mol sec) = 5.3961E+11 T**( 0.6423 ) exp( - 7.180 kcal/mole / RT)

The reverse rate constant can be fit to the following form:

```

$k(\text{rev}) \text{ (cm}^3/\text{mol sec)} = 1.4817\text{E}+11 \text{ T}^{**}(0.5045) \exp(- 15.83 \text{ kcal/mole / RT)}$

The reverse rate constant can also be expressed in a sticking coefficient form:

$\text{Sticking Coeff}(\text{rev}) = 0.3030 \text{ T}^{**}(4.0223\text{E}-03) \exp(- 15.83 \text{ kcal/mole / RT)}$

FORWARD AND REVERSE SURFACE REACTION RATE CONSTANTS											Bath Gas Dependent	
T (K)	k (cm**3/mol sec)	A_factor	Ea (kcal/mol)	DeltaG (kcal/mol)	DeltaH (kcal/mole)	DeltaS (cal/moleK)	k_rev (cm**3/mol sec)	A_factor_rev	Ea_rev (kcal/mol)	k_star	k_star_rev	
											UnifDimensnl	Rate_Const
											(mole/cm**2*sec)	
298.15	1.14E+08	4.23E+13	7.596	-9.879	-8.733	3.843	6.6	6.12E+12	16.33	6.67E-07	3.83E-14	
300.00	1.24E+08	4.24E+13	7.598	-9.886	-8.730	3.855	7.8	6.10E+12	16.33	7.18E-07	4.51E-14	
700.00	2.08E+11	6.71E+13	8.037	-11.70	-8.328	4.819	4.62E+07	5.94E+12	16.36	5.17E-04	1.15E-07	
1100.00	1.82E+12	9.63E+13	8.681	-13.58	-8.618	4.513	3.64E+09	9.94E+12	17.30	2.87E-03	5.75E-06	

ANALYSIS OF FORWARD AND REVERSE COVERAGE DEPENDENT
SURFACE RATE CONSTANTS AT BATH GAS CONDITIONS:

T (K)	k_prime (cm**3/mol sec)	A_factor	Ea (kcal/mole)	k (cm**3/mol sec)	Cov_fac (cgs)	k_rev (cm**3/mol sec)	krev_prime (cm**3/mol sec)	A_factor_rev	Ea_rev (kcal/mole)
298.15	1.188E+08	4.395E+13	7.596	1.1433E+08	1.039	6.558	6.816	6.3547E+12	16.33
300.00	1.286E+08	4.408E+13	7.598	1.2374E+08	1.039	7.773	8.078	6.3364E+12	16.33
700.00	2.160E+11	6.975E+13	8.037	2.0785E+11	1.039	4.6192E+07	4.8001E+07	6.1703E+12	16.36
1100.00	1.887E+12	1.001E+14	8.681	1.8155E+12	1.039	3.6355E+09	3.7778E+09	1.0328E+13	17.30

BREAKDOWN OF FORWARD REACTION'S STICKING COEFFICIENT

Surface site density divisor = 5.2200E-09 mole** 1.00/cm** 2.00

T (K)	Stck_Coeff (unitless)	A_factor	Ea	Eff_Veloc (cm/sec)	Veloc_Corr	Sden_Ratio	k* (cm/sec)	k (cm**3/mol sec)
298.15	9.5391E-06	2.140	7.300	6.2564E+04	1.000	1.000	0.5968	1.1433E+08
300.00	1.0292E-05	2.140	7.300	6.2757E+04	1.000	1.000	0.6459	1.2374E+08
700.00	1.1254E-02	2.140	7.300	9.5864E+04	1.006	1.000	1085.	2.0785E+11
1100.00	7.5871E-02	2.140	7.300	1.2017E+05	1.039	1.000	9477.	1.8155E+12

BREAKDOWN OF REVERSE REACTION'S STICKING COEFFICIENT

Surface site density divisor = 5.2200E-09 mole** 1.00/cm** 2.00

T (K)	Stck_Coeff (unitless)	A_factor	Ea	Eff_Veloc (cm/sec)	Veloc_Corr	Sden_Ratio	k* (cm/sec)	k (cm**3/mol sec)
298.15	7.7387E-13	0.4377	16.03	4.4239E+04	1.000	1.000	3.4235E-08	6.558
300.00	9.1439E-13	0.4351	16.03	4.4376E+04	1.000	1.000	4.0577E-08	7.773
700.00	3.5571E-06	0.2773	15.67	6.7786E+04	1.000	1.000	0.2411	4.6192E+07
1100.00	2.2330E-04	0.3700	16.20	8.4974E+04	1.000	1.000	18.98	3.6355E+09

Surface Reaction # 2 C(S,R)+H=>CH(S)

Change in gas moles in the reaction = -1.00
Change in surface moles in the reaction = 0.00
Change in bulk moles in the reaction = 0.00

This is an irreversible surface reaction, having the following types of reactant species:

1.00 gas-phase species
1.00 surface-phase species
0.00 bulk-phase species

and the following types of product species:

0.00 gas-phase species
1.00 surface-phase species
0.00 bulk-phase species

The reaction rate constant was input via a sticking coefficient in the interpreter input file
Motz-Wise Correction factor is used

$\text{Sticking Coeff} = \text{MIN}(0.3000 \exp(-0.0000\text{E}+00 \text{ kcal/mole / RT}) , 1)$

It can be fit to the following general rate constant form:

$k \text{ (cm}^3/\text{mol sec)} = 2.4498\text{E}+11 \text{ T}^{**}(0.5000) \exp(-487.64\text{E}-14 \text{ kcal/mole / RT)}$

Even though this reaction is IRREVERSIBLE, the reverse rate constant will also be analysed:

The reverse rate constant can be fit to the following form:

$k(\text{rev}) \text{ (1 / sec)} = 9.0322\text{E}+10 \text{ T}^{**}(1.096) \exp(- 94.69 \text{ kcal/mole / RT)}$

FORWARD AND REVERSE SURFACE REACTION RATE CONSTANTS											Bath Gas Dependent	
T	k	A_factor	Ea	DeltaG	DeltaH	DeltaS	k_rev	A_factor_rev	Ea_rev	k_star	k_star_rev	
(note: reverse rate constant is not in mechanism)											UnifDimensnl	Rate_Const
											(mole/cm**2*sec)	

(K)	(cm**3/mol sec)	(kcal/mol)	(kcal/mol)	(kcal/mole)	(cal/moleK)	(1 / sec)	(kcal/mol)	(mole/cm**2*sec)			
298.15	4.23E+12	6.97E+12	0.2962	-87.29	-95.46	-27.41	1.79E-56	1.03E+14	95.17	2.38E-02	9.36E-65
300.00	4.24E+12	7.00E+12	0.2981	-87.24	-95.47	-27.44	4.83E-56	1.04E+14	95.17	2.37E-02	2.52E-64
700.00	6.48E+12	1.07E+13	0.6955	-75.41	-97.05	-30.91	3.22E-16	3.90E+14	96.36	1.55E-02	1.68E-24
1100.00	8.13E+12	1.34E+13	1.093	-62.82	-97.88	-31.87	2.98E-05	5.05E+14	96.79	1.24E-02	1.55E-13

BREAKDOWN OF FORWARD REACTION'S STICKING COEFFICIENT

Surface site density divisor = 5.2200E-09 mole** 1.00/cm** 2.00

T (K)	Stck_Coeff (unitless)	A_factor	Ea	Eff_Veloc (cm/sec)	Veloc_Corr	Sden_Ratio	k* (cm/sec)	k (cm**3/mol sec)
298.15	0.3000	0.3000	0.0000E+00	6.2564E+04	1.176	1.000	2.2081E+04	4.2301E+12
300.00	0.3000	0.3000	0.0000E+00	6.2757E+04	1.176	1.000	2.2150E+04	4.2432E+12
700.00	0.3000	0.3000	0.0000E+00	9.5864E+04	1.176	1.000	3.3834E+04	6.4816E+12
1100.00	0.3000	0.3000	0.0000E+00	1.2017E+05	1.176	1.000	4.2413E+04	8.1252E+12

Surface Reaction # 3 C(S,R)+CH3<=>D+CH3(S)

Change in gas moles in the reaction = -1.00

Change in surface moles in the reaction = 0.00

Change in bulk moles in the reaction = 1.00

This is a reversible surface reaction, having the following types of reactant species:

1.00 gas-phase species
 1.00 surface-phase species
 0.00 bulk-phase species

and the following types of product species:

0.00 gas-phase species
 1.00 surface-phase species
 1.00 bulk-phase species

A sticking coefficient was not used though the forward reaction could have used one

$$k \text{ (cm**3/mol sec)} = 4.0000E+12 \exp(-1.200 \text{ kcal/mole} / RT)$$

The forward rate constant (with Motz-Wise correction) can be fit to the following sticking coefficient expression:

$$\text{Sticking Coeff} = 13.56 \exp(-0.4622 / T) \exp(-1.082 \text{ kcal/mole} / RT)$$

The reverse rate constant can be fit to the following form:

$$k(\text{rev}) \text{ (1 / sec)} = 1.0000E+13 \exp(-8.9265E-12 / T) \exp(-15.00 \text{ kcal/mole} / RT)$$

$$k(\text{rev}) \text{ (1 / sec)} = 1.0000E+13 \exp(-15.00 \text{ kcal/mole} / RT)$$

FORWARD AND REVERSE SURFACE REACTION RATE CONSTANTS

T (K)	k (cm**3/mol sec)	A_factor	Ea (kcal/mol)	DeltaG (kcal/mol)	DeltaH (kcal/mole)	DeltaS (cal/moleK)	k_rev (1 / sec)	A_factor_rev	Ea_rev (kcal/mol)	Bath Gas Dependent	
										k_star	k_star_rev
298.15	5.28E+11	4.00E+12	1.200	-47.78	-60.43	-42.43	1.01E+02	1.00E+13	15.00	2.96E-03	5.28E-07
300.00	5.34E+11	4.00E+12	1.200	-47.70	-60.44	-42.46	1.18E+02	1.00E+13	15.00	2.98E-03	6.17E-07
700.00	1.69E+12	4.00E+12	1.200	-29.94	-61.58	-45.19	2.07E+08	1.00E+13	15.00	4.04E-03	1.1
1100.00	2.31E+12	4.00E+12	1.200	-11.90	-61.29	-44.90	1.05E+10	1.00E+13	15.00	3.52E-03	55.

BREAKDOWN OF FORWARD REACTION'S STICKING COEFFICIENT

Surface site density divisor = 5.2200E-09 mole** 1.00/cm** 2.00

T (K)	Stck_Coeff (unitless)	A_factor	Ea	Eff_Veloc (cm/sec)	Veloc_Corr	Sden_Ratio	k* (cm/sec)	k (cm**3/mol sec)
298.15	0.1567	0.6393	0.8329	1.6199E+04	1.085	1.000	2755.	5.2779E+11
300.00	0.1581	0.6368	0.8306	1.6249E+04	1.086	1.000	2790.	5.3442E+11
700.00	0.3015	0.4102	0.4284	2.4821E+04	1.178	1.000	8812.	1.6882E+12
1100.00	0.3247	0.3382	8.9653E-02	3.1115E+04	1.194	1.000	1.2059E+04	2.3102E+12

Surface Reaction # 4 CH2(S,R)+CH(S,R)<=>CH2(S)+CH(S)

Change in gas moles in the reaction = 0.00

Change in surface moles in the reaction = 0.00

Change in bulk moles in the reaction = 0.00

This is a reversible surface reaction, having the following types of reactant species:

0.00 gas-phase species
 2.00 surface-phase species
 0.00 bulk-phase species

and the following types of product species:

0.00 gas-phase species
 2.00 surface-phase species

0.00 bulk-phase species

k (cm**2/mol sec) = 6.0000E+19 exp(- 2.000 kcal/mole / RT)

The reverse rate constant can be fit to the following form:

$k(\text{rev})$ (cm**2/mol sec) = 5.9991E+19 T**(2.0901E-05) exp(- 96.02 kcal/mole / RT)

FORWARD AND REVERSE SURFACE REACTION RATE CONSTANTS										Bath Gas Dependent	
T (K)	k (cm**2/mol sec)	A_factor	Ea (kcal/mol)	DeltaG (kcal/mol)	DeltaH (kcal/mole)	DeltaS (cal/moleK)	k_rev (cm**2/mol sec)	A_factor_rev	Ea_rev (kcal/mol)	UnifDimensnl	Rate_Const
										k_star	k_star_rev
										(mole/cm**2*sec)	
298.15	2.05E+18	6.00E+19	2.000	-94.03	-94.03	5.5511E-17	2.44E-51	6.00E+19	96.03	56.	6.64E-68
300.00	2.10E+18	6.00E+19	2.000	-94.03	-94.03	0.0000E+00	6.62E-51	6.00E+19	96.03	57.	1.80E-67
700.00	1.42E+19	6.00E+19	2.000	-94.03	-94.03	*****	6.26E-11	6.00E+19	96.03	3.88E+02	1.71E-27
1100.00	2.40E+19	6.00E+19	2.000	-94.03	-94.03	8.8818E-16	5.0	6.00E+19	96.03	6.55E+02	1.36E-16

Total CPUtime: 1 second or less

Index

A

adiabatic flame temperature 17
 A-factors 109
 aftertreatment 91
 aftertreatment, engine exhaust 101
 ALD 134
 ALD processes 134
 alumina 156
 alumina, ALD of 156
 ammonia 154
 approximations, cylindrical channel flow 122
 Arrhenius pre-exponential factors 109
 atomic layer deposition 134, 156
 autoignition for hydrogen/air 24
 autoignition, ignition times for propane 27
 axisymmetric results visualization 75

B

bath gas 162, 163
 burner-stabilized laminar premixed flame 32

C

C1_Inlet1 panel 34
 calculation, equilibrium 17, 116
 carrier gas 162, 164
 catalytic combustors 91
 catalytic converters 91
 catalytic oxidation 108
 Center for Energy Research 87
 Chapmen-Jouguet detonation 56
 chemical mechanism analysis 161
 chemical vapor deposition 115
 chemistry sets 85, 112, 154
 alumina ALD 156
 chlorine plasma 158
 ethylene/air combustion 87
 fluorocarbon plasma 159

GRMech 3.0 86
 hydrogen/air 85
 methane air 86
 methane oxidation on Pt 112
 methane/air 86
 methane/air reduced mechanism 86
 propane/air 87
 Pt/Rh three-way catalyst 113
 reduced mechanism 86
 silicon deposition from silane 155
 silicon deposition from trichlorosilane 155
 silicon nitride CVD 154

CHEMKIN

 format 56
 reactor models 13
 chlorine plasma 158
 spacial 145
 steady-state 141
 chlorosilane CVD 116
 closed homogeneous panel 24, 28
 coefficients, normalized sensitivity 48
 colorbar property panel 76
 combustion 79
 combustion in complex flows 57
 combustion, hydrogen 22
 combustion, propane 27
 combustion, steady-state gas-phase 22
 combustor, gas turbine 57
 combustor, homogeneous 96
 combustor, two stage catalytic 91
 continuations panel 18, 23, 38, 116, 119, 124, 127, 150
 CRUPROF subroutine 74
 Curl's model, modified 66
 CVD 115
 chlorosilane 116
 diamond 164
 steady-state thermal 118
 trichlorosilane 131
 CVD reactor 118

cylindrical channel flow 122
 cylindrical shear flow panel 123
 cylindrical shear flow reactor 115, 122

D

Damköhler number 163, 164
 DDASPK solver 66
 deposition in a rotating disk 126
 detonation, Chapmen-Jouguet 56
 diagnostic output file 166
 diamond CVD 164
 DVODE solver 66

E

engine exhaust aftertreatment, transient flow 101
 engineout 102
 equilibrium analysis 20, 116
 equilibrium calculation 17, 116
 equilibrium panel 18, 116
 equivalence ratio 17
 etching, fluorocarbon plasma 149
 etching, plasma 141

F

files
 diagnostic output 166
 XML solution 25, 119, 165, 166
 flame speed panel 36
 flame speed, laminar 36
 flames 22
 burner-stabilized premixed laminar 32
 hydrogen/air 46
 methane/air premixed 36
 non-premixed jet 60
 opposed-flow diffusion 46
 flammability 22
 fluorocarbon plasma 159
 etching 149
 FORTRAN subroutine 101

G

gas inlet panel 136
 Gas Research Institute 86
 gas turbine combustor 57
 gas turbine network 57
 gas, bath 162, 163
 gas, carrier 162, 164
 gas-phase combustion, steady-state 22
 GRImech 3.0 86

H

HCCI 49
 heat-transfer correlation 52
 homogeneous charge compression ignition 49
 homogeneous combustor 96
 honeycomb monolith panel 95
 honeycomb monolith reactor 94
 hydrogen combustion 22
 hydrogen/air chemistry set 85
 hydrogen/air flame 46
 hydrogen/air system 17
 hydrogen/air, autoignition for 24

I

IC engine panel 50
 IC engine, single-zone 50
 ignition 22
 ignition time, defining 28
 ignition times for propane autoignition 27
 inlet panel 40
 internal combustion engine 49

J

jet flame network 60
 JSR/PFR system, soot formation 78

L

laminar flame speed 36
 low-pressure plasma reactor 141

M

mechanism analysis, chemical 161
 mechanism analyzer panel 165
 mechanism analyzer tool 161
 methane oxidation on Pt 112
 methane/air chemistry set 86
 methane/air, partially stirred reactor for 64
 modified Curl's model 66
 Monte Carlo mixing model 66
 multiple reactor models 135

N

networks
 gas turbine 57
 jet flame 60
 PSR 57, 60, 123
 PSR-PFR hybrid 57
 non-dimensional reaction rate 162
 non-premixed jet flame 60

normalized sensitivity coefficients 48
number, Damköhler 163, 164

O

opposed-flow diffusion flame 46
opposed-flow flame panel 46
output control panel 23, 25, 47, 119, 123, 150, 165, 168, 169

P

panel
 reactor properties 67
panels
 C1_Inlet1 34
 closed homogeneous 24, 28
 continuation 18, 23, 38, 116, 119, 124, 127, 150
 cylindrical shear flow 123
 equilibrium 18, 116
 flame speed 36
 gas inlet 136
 honeycomb monolith 95
 IC engine 50
 inlet 40
 mechanism analyzer 165
 opposed-flow flame 46
 output control 23, 25, 47, 119, 123, 150, 165, 168, 169
 PFR 123
 planar shear flow 131
 plasma PFR 145
 plasma PSR 142, 149
 preferences 73
 pre-mixed burner 33, 34
 PSR 22, 102, 119, 123, 136
 R1_IN 36
 recycling 61
 rotating disk 127
 run model 67
 select results to load from solution file 109
 solver 23, 25, 29, 34, 47, 103, 123, 131, 136, 137, 142, 150
 stagnation flow 136
panels (Post-Processor)
 colorbar property (Post-Processor) 76
Parameter Study 39, 108
partially stirred reactor 64
PaSR 65
perfectly stirred reactor 93, 118, 122, 135, 141
PFR panel 123
planar channel flow 131
planar shear flow panel 131
planar shear flow reactor 115
plasma chlorine 141

plasma etching 141
 silicon dioxide 149
plasma PFR panel 145
plasma plug flow reactor 145
plasma PSR panel 142, 149
plasma, fluorocarbon 159
plug flow
 side inlet 69
plug flow reactor 93, 94, 115, 122
Post 68
power profile, with spacial chlorine plasma 145
preferences panel 73
pre-mixed burner panel 33, 34
probability density functions 66
propane
 ignition times for autoignition 27
PSR analysis 118
PSR network 57, 60
PSR panel 22, 102, 119, 123, 136
PSR-PFR network 57
Pt/Rh three-way catalyst 113

R

R1_IN panel 36
rate constant, uniform-dimensional 163
Rate-Of-Production analysis 83
rate-of-production analysis 144
rate-of-production options 118
reaction mechanism for diamond CVD 164
reaction rates 162
reactor properties panel 67
recycling panel 61
reduced mechanism, methane/air 86
ROP 118
ROP analysis 83
rotating disk panel 127
rotating disk reactor 115, 126
run model panel 67

S

sample problems, models used 14
select results to load from solution file panel 109
shock-heated air 55
shock-tube experiment 27, 55
side inlet on plug flow reactor 69
silane 155
silicon deposition from silane 155
silicon deposition from trichlorosilane 155
silicon dioxide 159
silicon nitride CVD 154
silicon tetrafluoride 154
single-zone IC engine 50

solver panel 23, 25, 29, 34, 47, 103, 123, 131, 136, 137,
142, 150
solvers
 DDASPK 66
 DVODE 66
 transient 102
soot formation 78
soot nucleation reaction 79
spacial chlorine plasma 145
stagnation flow panel 136
stagnation flow reactor 115
steady-state gas-phase combustion 22
steady-state thermal CVD 118
stoichiometric hydrogen/air mixture 24
stoichiometric methane/air premixed flame 36
sub-projects 135
subroutine library
 TRANSPORT 164
surface chemistry analysis 108

T

temperature, adiabatic flame 17
time-dependent simulations of ALD process 135
TMA 156
transient inlet flow 101
transient solver 102
TRANSPORT subroutine library 164
trichlorosilane CVD 131
trichlorosilane, silicon deposition from 155
trimethylaluminum 156
TRIT 91
turbine rotor inlet temperature 91
two stage catalytic combustor 91

U

uniform-dimensional rate constant 163
uniform-dimensional reaction rate 162
UPROF keyword 74
user-defined subroutine 101
USRINLET 101
USRINLET subroutine 104

V

vapor deposition, chemical 115

W

Woschni correction 52

X

XML solution file 25, 119, 165, 166

XMLdata.zip 66, 165